IDENTIFICATION OF SYNAPTOTAGMIN XIII AS A LIVER TUMOR SUPPRESSOR GENE

Jennifer Elizabeth Jahn

A dissertation submitted to the faculty of the University of North Carolina at Chapel Hill in partial fulfillment of the requirements for the degree of Doctor of Philosophy in the Department of Pathology and Laboratory Medicine.

Chapel Hill
2007

Approved by:

William B. Coleman, Ph.D.

Frank C. Church, Ph.D.

David A. Gerber, M.D.

Wendell D. Jones, Ph.D.

Gloria A. Preston, Ph.D.

ABSTRACT

Jennifer E. Jahn: Identification of Synaptotagmin XIII as a Liver Tumor Suppressor Gene

(Under the direction of William B. Coleman, Ph.D.)

The molecular pathogenesis of hepatocellular carcinoma is well-studied but not completely understood. We utilized a microcell-hybrid model approach to facilitate the identification of novel liver tumor suppressor genes located on human chromosome 11. These investigations confirmed a liver tumor suppressor locus at human chromosome 11p11.2, and subsequently identified *SYT13* as the gene responsible for the suppression of tumorigenicity in rat liver tumor cell lines. Complementary approaches involving both silencing SYT13 in suppressed microcell-hybrid cell lines and expressing SYT13 in tumor cell lines showed that this gene is both required and sufficient for 11p11.2-mediated suppression of tumorigenicity in the GN6TF rat liver tumor cell line. Furthermore, the results strongly suggest that the dimerized form of the SYT13 protein is necessary for tumor suppressor function and that tumor suppression may be affected through pathways implicated in epithelial to mesenchymal transition. These observations also suggest that the deficit in GN6TF that leads to the tumorigenic phenotype involves loss of the ability of the endogenous Syt13 to dimerize, perhaps through protein misfolding or loss of post-translational processing.

ACKNOWLEDGEMENTS

First and foremost, I must thank my parents, Tom and Sandy Jahn, for their unconditional support, encouragement, and love. To my advisor, Bill, I owe gratitude for impartially providing wisdom, guidance, autonomy, and opportunity throughout my graduate school training. Additionally, my dissertation committee members—Dr. Frank Church, Dr. David Gerber, Dr. Wendell Jones, and Dr. Gloria Preston—have been instrumental in the successful completion and refinement of this document. To Frank, I am especially grateful not only professionally for his insight and input regarding my dissertation project, but also personally for his advice and moral support throughout the past five and a half years. In the Department of Pathology and Laboratory Medicine, I would like to thank Dr. Jennette for his support of the Graduate Program, Dr. Bagnell for help with all things regarding microscopy, Dr. Kim for assistance with implementation and interpretation of real-time RT-PCR data, and Ms. Poteat for meticulous and critical attention to logistical "i" dotting and "t" crossing.

I must also acknowledge the people I am grateful to who have provided the network of moral support that has been crucial for my success as well as the maintenance of my sanity. In addition to Mom and Dad, I thank my brothers, Mike and Chris, and their families for continued support throughout the years. To my lifelong friends—Jamie, Nicole, Brooke, Meg, and Morgan—thanks for keeping me grounded, proud, and young. To others who have provided support along the journey—Mary Beth, Velez, Alberto, Ruffin, Holly, Zar, Josh, Joe, and Bubba—thank you. Finally, to Roscoe, Kristi, and Hunter, you have been through every step of this journey with me, lifting me up from the trenches, talking me down from the

ledges, and saving me from myself. I will never be able thank you enough or begin to tell you how much your contributions have meant to me. I will be forever grateful.

TABLE OF CONTENTS

LIST OF TABLES

LIST OF FIGURES

LIST OF ABBREVIATIONS

$\Delta\Delta C_T$	Comparative Method for real-time RT-PCR analysis
5-aza	5-aza-2'-deoxycytidine
ANOVA	analysis of variance
ATP	adenosine triphosphate
BLAST	basic local alignment search tool
bp	basepairs
BSA	bovine serum albumin
C2	protein kinase C conserved region 2
cDNA	complememtary DNA
CEL	cell intensity file
CFE	colony forming efficiency
cRNA	complementary RNA
DAVID	Database for Annotation, Visualization, and Integrated Discovery
DMSO	dimethyl sulfoxide
DNA	deoxyribonucleic acid
dNTP	deoxynucleotide-triphosphate
DTT	dithiothreitol
ECL	enhanced chemiluminescence
EDTA	ethylenedinitrilotetraacetic acid
EMT	epithelial to mesenchymal transition
EST	expressed sequence tag

GAPDH	glyceraldehyde 3-phosphate dehydrogenase
GeneNote	gene normal tissue expression
GenMAPP	Gene Map Annotator and Pathway Profiler
GFP	green fluorescent protein
GO	gene ontology
HBV	Hepatitis B virus
HCC	hepatocellular carcimona
HCV	Hepatitis C virus
HEPES	4-(2-hydroxyethyl)-1-piperazineethanesulfonic acid
IgG	immunoglobulin G
ISS	inferred from sequence similarity
KLH	keyhole limpet hemocyanin
LOH	loss of heterozygosity
Mbp	mega base pairs
MCH	microcell hybrid
MET	mesenchymal to epithelial transition
miRNA	microRNA
MMCT	microcell-mediated chromosome transfer
MMLV	Moloney murine leukemia virus
mRNA	messenger RNA
MTT	methylthiazolyldiphenyl-tetrazolium bromide
NCBI	National Center for Biotechnology Information
OD	optical density

OMIM	Online Mendelian Inheritance in Man
ORF	open reading frame
PAGE	polyacrylamide gel electrophoresis
PCR	polymerase chain reaction
PDNN	Positional Dependent Nearest Neighbor
PSS	Potocki-Shaffer syndrome
qPCR	quantitative polymerase chain reaction
RISC	RNA-induced silencing complex
RNA	ribonucleic acid
RNAi	RNA-interference
RT-PCR	reverse transcription polymerase chain reaction
SDS	sodium dodecyl sulfate
shRNA	small hairpin RNA
SREBP	sterol responsive element-binding protein
siRNA	small interfering RNA
TBE	Tris/Borate/EDTA
TBST	Tris buffered saline w/ Tween-20
TMR	transmembrane region
UTR	untranslated region

NOMENCLATURE FOR RAT LIVER CELL LINES

CELL LINE	ABBREVIATION	DERIVATION
WB-F344	n/a	normal rat liver epithelial cell line
GN6 GP10 GN3	n/a	*in vitro*-transformed cell lines derived from WB-F344 cells
GN6TF GN3TF GP10TA	n/a	tumor cell lines derived from GN6, GN3, and GP10
GN6TF-11^{neo}C1	C1 (distint from *SYT13*-transfected cell line)	suppressed MCH cell lines derived from GN6TF
GN6TF-11^{neo}CX2	CX2	
GN6TF-11^{neo}CX4	CX4	
GN6TF-11^{neo}CX2T1*	n/a	tumor cell lines (*) derived from GN6TF-derived MCH cell line
GN6TF-11^{neo}CX4T3*	n/a	
GN3TG-11^{neo}C2 GN3TG-11^{neo}C3 GN3TG-11^{neo}C4 GN3TG-11^{neo}C5 GN3TG-11^{neo}C7	n/a	suppressed MCH cell lines derived from GN3TG
GN3TG-11^{neo}C4T3*		tumor cell line derived from GN3TG-11^{neo}C4
GP10TA-11^{neo}C7 GP10TA-11^{neo}C11 GP10TA-11^{neo}C12	n/a	suppressed and non-suppressed (*) MCH cell lines derived from GP10TA
GP10TA-11^{neo}C6* GP10TA-11^{neo}C7T3**		tumor cell line (**) derived from GP10TA-11^{neo}C7
CX4^{SYT13}i3	*SYT13*i3 or i3	GN6TF-11^{neo}CX4-derived cell lines transfected with the *SYT13*-targeting psiRNA vector
CX4^{SYT13}i5	*SYT13*i5 or i5	
CX4^{SYT13}i6	*SYT13*i6 or i6	
CX4^{SYT13}i8	*SYT13*i8 or i8	
CX4^{SYT13}i12	*SYT13*i12 or i12	
CX4^{SYT13}s1	*SYT13*s1 or s1	GN6TF-11^{neo}CX4-derived cell lines transfected with the scrambled-control psiRNA vector
CX4^{SYT13}s7	*SYT13*s7 or s7	
CX4^{SYT13}s8	*SYT13*s8 or s8	
CX4^{SYT13}i5t2	i5t2	tumor cell lines derived from *SYT13*i and *SYT13*s cell lines
CX4^{SYT13}i6t1	i6t1	
CX4^{SYT13}i12t4	i12t4	
CX4^{SYT13}s8t1	s8t1	
GN6TF^{neo}SYT13-B3	B3	GN6TF-derived cells transfected with the ORF of *SYT13*
GN6TF^{neo}SYT13-C1	C1 (distinct from the MCH)	
GN6TF^{neo}SYT13-C2	C2	
GN6TF^{neo}SYT13-E2	E2	
GN6TF^{neo}SYT13-F3	F3	
GN6TF^{neo}SYT13-J1	J1	
GN6TF^{neo}GFP	GFP	GN6TF-derived cell population transfected with GFP

INTRODUCTION

HEPATOCELLULAR CARCINOMA

Hepatocellular carcinoma (HCC) is a vicious neoplasm with a global incidence that ranks fifth among all cancers and a poor prognosis that results in a survival rate of 3-5% (1). Eighty-five percent of cases worldwide occur in Asia and Africa, with high concentrations of affected individuals in Southeast Asia and sub-Saharan Africa (1). The incidence of HCC is much lower in developed countries, such as the United States. The geographic disparity in HCC incidence reflects varying exposures to different environmental factors that promote chronic liver disease (including hepatitis and cirrhosis), which represents a precursor of HCC. Important etiological factors in hepatocarcinogenesis include hepatitis B virus (HBV) and hepatitis C virus (HCV) infection and/or exposure to aflatoxin B_1 (2). HBV is the primary risk factor in many areas, especially in Asia and Africa (3). Mechanisms involved in HBV-related hepatocarcinogenesis include chronic viral-associated inflammation and cellular proliferation as well as HBV-DNA integration into the host genome and interactions of HBV-specific proteins with liver genes (4). The molecular mechanisms of HCV-associated hepatocarcinogenesis are less well understood although it is not considered a directly cytotoxic virus (5). Hepatitis associated with HCV occurs as a result of the reaction of the host immune system against virus-infected cells, and it is thought that the core protein of HCV is a likely candidate oncogene (6). Aflatoxin B_1 is a highly mutagenic toxin produced by fungus that grows on improperly stored grains. Not only is it a potent direct-

acting liver carcinogen, but it can also cause *p53* mutations leading to HCC and may have a synergistic interaction with HBV in hepatocarcinogenesis (2, 7). Other factors contributing to HCC development include various metabolic/genetic abnormalities (i.e. hemochromatosis, tyrosinemia, Wilson's disease, α-1 antitrypsin deficiency, and others), excessive alcohol consumption, non-alcoholic fatty liver disease, radiation, some therapeutic drugs, and certain chemicals in the workplace or environment (2). All of these agents cause damage to hepatocytes, promote proliferative regeneration, and give rise to the preneoplastic liver pathologies which provide settings from which HCC commonly arises.

MOLECULAR PATHOGENESIS OF HUMAN HEPATOCELLULAR CARCINOMA

The majority of human hepatocellular carcinomas arise from the preneoplastic conditions of either chronic hepatitis or cirrhosis. Because the liver has great regenerative capacity in response to cellular damage, the persistent proliferation of surviving hepatocytes provides the setting for the acquisition of genomic alterations (DNA damage, chromosomal alterations, gene mutations). Molecular characterization of the tissue lesions that precede HCC, phenotypically altered and dysplastic hepatocytes of chronic hepatitis and cirrhosis, provide some evidence of the temporal genomic events involved in hepatocarcinogenesis. Commonly documented genetic events involve alterations in gene expression (proto-oncogenes, growth factors, growth factor receptors), epigenetic modification of DNA (aberrant DNA methylation), mutations (in tumor suppressor genes and oncogenes), and chromosomal alterations (large-scale deletions, rearrangements) (2). Interestingly, the majority of these molecular lesions have been found in dysplastic hepatocytes of chronic hepatitis or cirrhosis. However, HCC develops in only a subset of patients with chronic liver

disease. This suggests that more frequently recognized genetic lesions may provide a selective growth advantage for these hepatocytes, but that these alterations are not sufficient to drive neoplastic transformation. Furthermore, these observations suggest additional alterations are required for acquisition of tumorigenic potential of dysplastic hepatocytes in preneoplastic lesions. It is clear that development of HCC requires a number of genomic changes, involving both epigenetic and genetic alterations, and that several different molecular pathways can lead to development of HCC (8-10). This possibility is reflected in the observation that there is considerable genomic heterogeneity among HCCs, and this heterogeneity remains even when consideration is given to size, histological grade, and clinical stage of the tumors being studied (10).

CHROMOSOMAL ABERRATIONS IN HUMAN HEPATOCELLULAR CARCINOMA

Recurring allelic losses have been documented for 11 chromosome arms affecting more than 30% of all HCC examined, including 1p, 1q, 4q, 5q, 6q, 8p, 9p, 13q, 16p, 16q, and 17p (10). However, the frequency of LOH involving loci on these chromosome arms is rarely observed in >60% of HCCs examined. Other chromosomal arms demonstrate LOH with less frequency, including chromosome 11p (11-14). The significance of alterations involving chromosome 11 in HCC depends upon the specific study evaluated. Some investigators have implicated chromosome 11 as a frequent alteration in human HCC (12), while other investigators noted these changes less frequently (15-17), at very low levels (18), or not at all (19). These studies combine to suggest a possible role for genetic loci carried on chromosome 11 in the molecular pathogenesis of some subsets of HCC. In theory, deleted chromosomal regions may harbor genes with tumor suppressor-like activity. In fact, several

well known tumor suppressor genes reside on chromosome arms that are frequently affected by regional chromosomal deletion, such as *p53* at 17p and *Rb1* at 13q (11, 13, 14). These observations suggest that chromosomal losses can be effectively exploited to infer the location of important tumor suppressor genes that are subject to inactivation through this molecular mechanism. Furthermore, the diversity of chromosomal aberrations among HCCs supports the suggestion that several molecular pathways contribute to the development of HCC, and that these pathways may involve any of several chromosomal regions and/or genes (8-10).

COMPARATIVE MAPPING OF CHROMOSOMAL ALTERATIONS IN HUMANS AND RODENTS

Comparative mapping studies of human and rodent genomes suggest that common loci may be involved in hepatocellular carcinogenesis in these species. Rat chromosomes 1, 4, 7, and 10 are often observed to be structurally abnormal in rat liver tumor cells, as are chromosomes 2, 3, 6, 8, and 11 less frequently (20-33). Various karyotypic analyses of murine liver tumors have revealed LOH in chromosomes 1, 2, 4, 5, 6, 7, 8, 9, 12, 13, 14, and 18 (34, 35). These studies predict that alterations in orthologous regions of synteny in the human, rat, and murine genomes may be relevant in the development of a subset of HCC in each species. One conserved gene cluster is a 27-Mbp syntenic region located on chromosome 11 (11q11-11p14.2), rat chromosome 3 (3q24-3q33), and mouse chromosome 2 (2E1-2E3) (FIGURE 1.1). Some studies have found frequent, nonrandom aberrations on human 11 and rat 3 in HCC (12, 36, 37), while mouse 2 has not been as widely implicated (38). The observation that deletions in these orthologous regions may be causally related to liver tumor formation in each species strongly suggests that a subset of neoplasms may

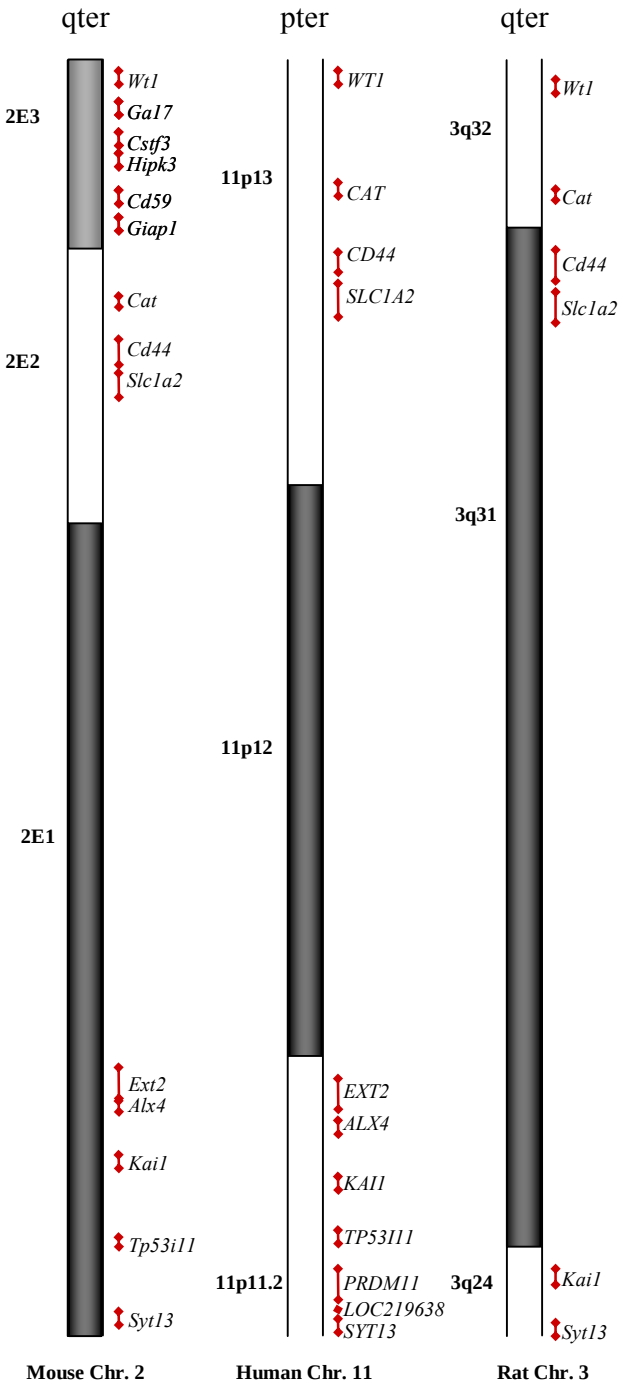

FIGURE 1.1. *Comparative mapping of 27-Mb regions of mouse chromosome 2, human chromosome 11, and rat chromosome 3.* The relative locations of several gene contained within mouse 2E1-E3, human 11p11.2-p13, and rat 3q24-q32 are shown. These regions contain a cluster of syntenic genes including *Syt13*, *Kai1*, *Cd44*, *Cat*, and *Wt1*.

involve common genetic mechanisms, possibly involving the same gene(s) (34).

MICROCELL HYBRID MODEL OF TUMOR SUPPRESSION

Microcell-mediated chromosome transfer (MMCT) is a commonly utilized technique in which a microcell, containing single or small numbers of chromosomes, is fused with a whole cell. Generally, the genetic information contained in the microcell is expected to complement a defect in the recipient cell line, and the resulting microcell hybrid (MCH), displaying an altered phenotype, is then characterized. This system has been successfully used to identify and characterize several genes involved in normal cellular activities such as the regulation of telomerase activity, genomic stability, chromatin modification, genomic methylation, X-inactivation, mitochondrial function, and cellular proliferation (39). Using this method, tumor suppressor genes or loci have been identified on human chromosomes 1, 3-13, 17-19, 22, and X (39). Based upon the observation that several chromosomal regions altered in neoplasms of humans, rats, and other mammals contain syntenic clusters of genes that may harbor common loci involved in carcinogenesis, it was proposed that chromosome transfer studies utilizing human chromosomes and rat liver cell lines may facilitate the identification and localization of human genes responsible for liver tumor suppression (40).

A model has been established and characterized for the functional identification of human tumor suppressor genes which employs microcell-mediated transfer of human chromosomes into rat liver tumor cell lines (FIGURE 1.2). Because human chromosome 11 has been implicated in the pathogenesis of several human tumors and is orthologous to commonly implicated regions in the rat and mouse genomes, MMCT was employed to transfer an intact copy of human chromosome 11 into a highly aggressive rat liver tumor cell

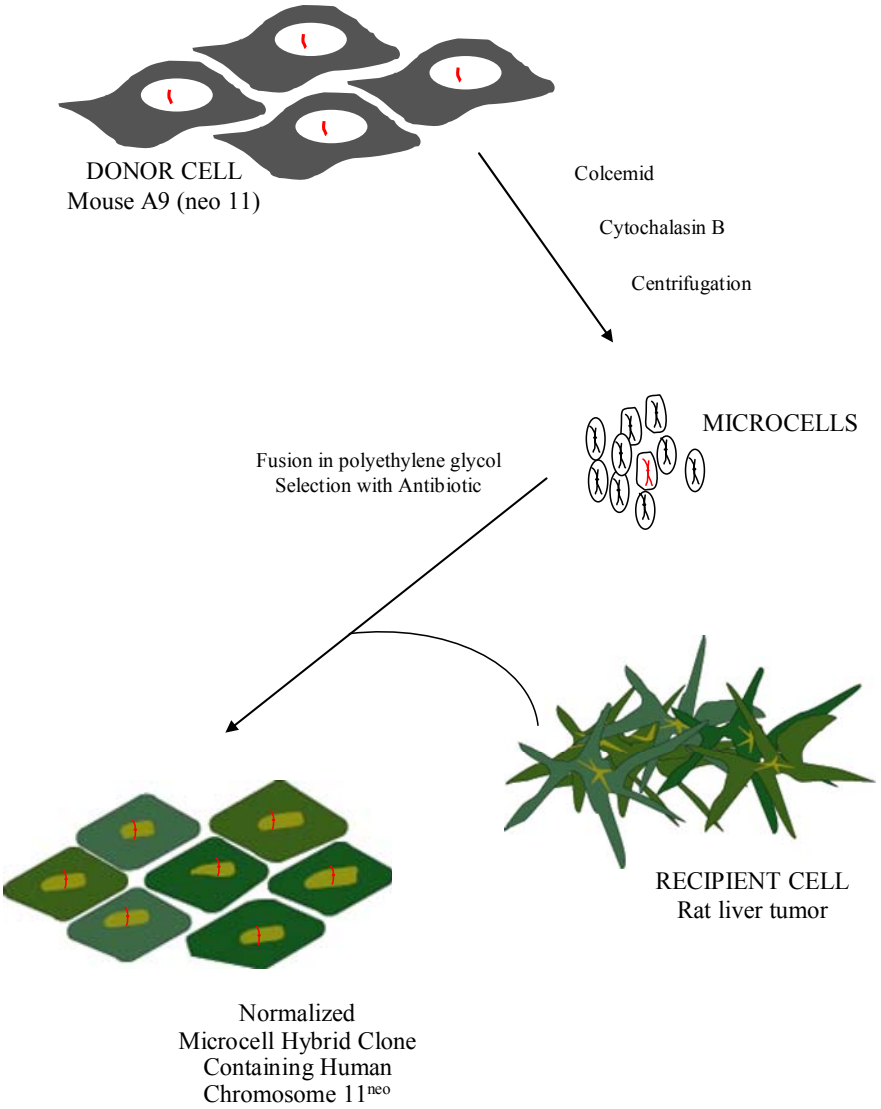

FIGURE 1.2. *Microcell hybrid model of tumor suppression.* The general methodology for production of MCH cell lines is shown. Donor cells containing a Neo^R-tagged human chromosome 11 (shown in red) are used to produce microcells, which are fused to recipient rat liver tumor cells. Neomycin-resistant MCH cell lines are then selected and characterized.

line (GN6TF) and to examine the possibility that this chromosome may contain a liver tumor suppressor locus (40). This study demonstrated that human chromosome 11 suppresses the tumorigenic potential of some rat liver tumor cell lines (40). Suppressed MCH cell lines exhibit normalized cellular morphology (FIGURE 1.3), reexpression of contact inhibition, complete loss of anchorage-independent growth potential, and decreased tumorigenic potential *in vivo* and/or significantly elongated latency for tumor formation following transplantation into syngeneic hosts (TABLE 1.1). Subsequent studies demonstrated suppression of tumorigenicity in other rat liver epithelial tumor cell lines after MMCT of human chromosome 11 (TABLE 1.1), providing additional evidence for the presence of a liver tumor suppressor gene on this human chromosome (41).

MOLECULAR MAPPING OF THE 11P11.2 TUMOR SUPPRESSOR LOCUS IN SUPPRESSED MICROCELL HYBRID CELL LINES

Several suppressed and non-suppressed MCH cell lines were derived from GN6TF, GP10TA, and GN3TG tumor cell lines (TABLE 1.1) (40, 41). Because human chromosomes are unstable on the rodent genomic backgrounds, spontaneous deletions occurred in the introduced chromosome in some of these MCH cell lines. Molecular mapping (by PCR with template MCH cell line DNA), using human chromosome 11-positioned markers, was employed to discern which region(s) of the introduced chromosome remained intact among suppressed and non-suppressed MCH cell lines. The minimal inclusive liver tumor suppressor region was defined by correlating molecular mapping data with information on the phenotypic characteristics of each MCH cell line. Through the screening of >200 human markers localized to chromosome 11 by early investigations of the Human Genome Project, the minimal inclusive tumor suppressor region was reduced to a <1-Mbp region (*D11S1344*-

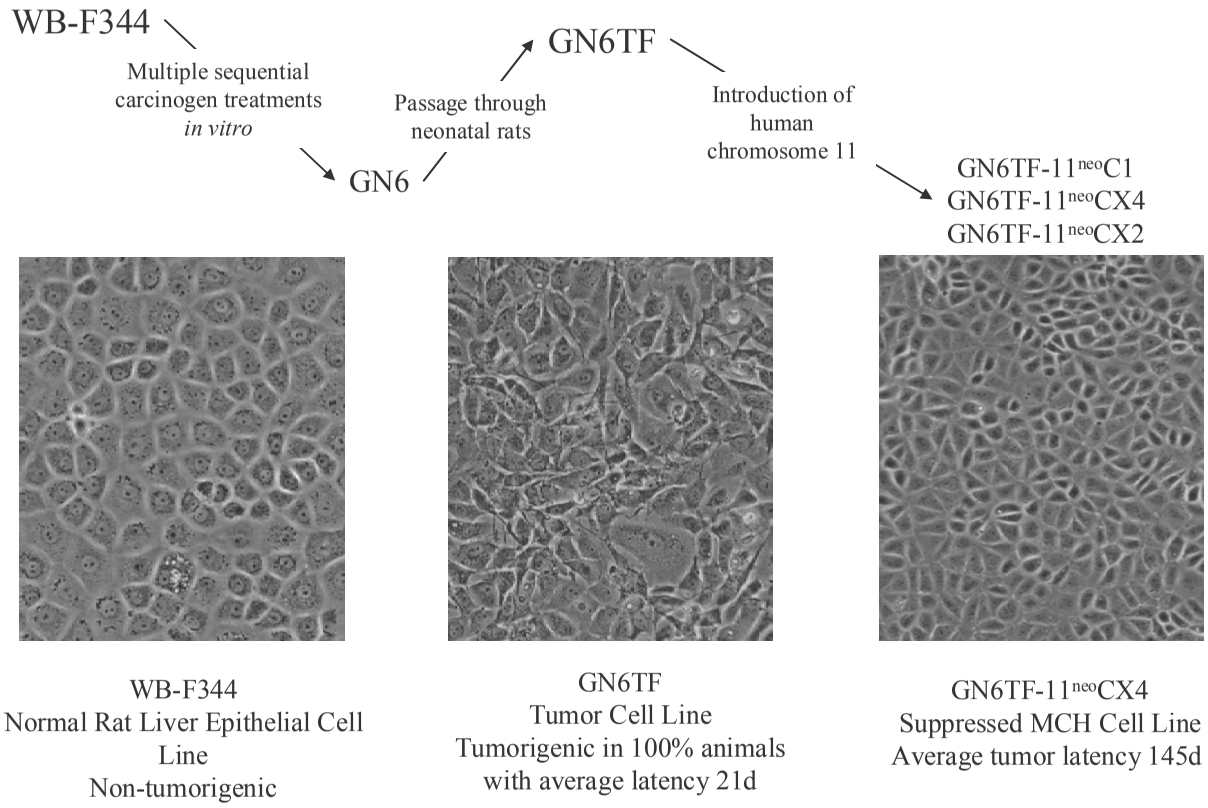

FIGURE 1.3. *Microcell-mediated introduction of human chromosome 11 into the GN6TF tumor cell line.* The experimental derivation of GN6TF tumor cells and GN6TF-derived MCH cell lines is shown. Phase contrast micrographs of WB-F344, GN6TF and CX4 cells are shown for comparison of cellular morphology and growth patterns. Information related to the tumorigenic potential of these cell lines is also provided.

TABLE 1.1. *Phenotypic characteristics of GN6TF-11^{neo}, GN3TG-11^{neo} and GP10TA-11^{neo} microcell hybrid cell lines**

Cell Line	Saturation Density (Cells/cm^2)	Soft Agar Growth (%CFE)	Tumorigenicity (%)	Latency (Days)
GN6TF	2.83 x 10^5	13.1 ± 1.4	21/21 (100%)	21 ± 1
GN6TF-11^{neo} C1	3.00 x 10^4	0	8/10 (80%)	152 ± 16
GN6TF-11^{neo} CX2	3.36 x 10^4	0	9/9 (100%)	164 ± 19
GN6TF-11^{neo} CX4	1.44 x 10^4	0	7/7 (100%)	145 ± 18
GN3TG	1.75 x 10^5	6.8 ± 0.6	15/15 (100%)	18 ± 2
GN3TG-11^{neo}C3	3.1 x 10^4	0	8/9 (89%)	45 ± 1
GN3TG-11^{neo}C4	5.1 x 10^4	3.5 ± 0.1	6/6 (100%)	46 ± 2
GN3TG-11^{neo}C5	7.9 x 10^4	3.1 ± 0.3	ND	NA
GN3TG-11^{neo}C7	4.1 x 10^4	0	7/8 (88%)	46 ± 2
GP10TA	1.69 x 10^5	13.3 ± 1.1	13/13 (100%)	75 ± 5
GP10TA-11^{neo}C6**	1.3 x 10^5	12.8 ± 0.5	9/9 (100%)	99 ± 6
GP10TA-11^{neo}C7	7.1 x 10^4	3.6 ± 0.3	5/12 (100%)	182 ± 5
GP10TA-11^{neo}C11	5.0 x 10^4	3.9 ± 0.3	ND	NA
GP10TA-11^{neo}C12	5.1 x 10^4	3.6 ± 0.5	ND	NA

* Derived from Coleman *et al*. *Molecular Carcinogenesis*. 1995. *13*:220 and Mahon *et al*. *International Journal of Oncology*. 1999. *14*:337.
** non-suppressed MCH cell line.

D11S436) centered at 11p11.2 (41, 42) (FIGURE 1.4). These studies, in addition to efforts by the Human Genome Project, provided the foundation, biological reagents, and bioinformatic tools to identify and characterize the tumor suppressor gene(s) from this region of human chromosome 11p11.2.

A PUTATIVE ROLE FOR *WT1* IN LIVER TUMOR SUPPRESSION

Having identified and mapped a locus within human chromosome 11p11.2 that suppresses the tumorigenic potential of some rat liver tumor cell lines, possible molecular mechanisms of tumor suppression were examined by examining gene expression patterns in suppressed MCH cell lines (43). The parental GN6TF rat liver tumor cells express moderate levels of *p53* mRNA and protein, overexpress mRNAs for c-H-*ras*, c-*myc*, and *TGFα*, and does not express detectable levels of *Wt1* mRNA or protein. Suppression of tumorigenicity by human chromosome 11p11.2 was not accompanied by significant alterations in the levels of expression of *p53*, c-*myc*, or *TGFα*. Expression of c-H-*ras* was decreased significantly in both suppressed and nonsuppressed MCH cell lines, suggesting that down-regulation of c-H-*ras* is not directly responsible for tumor suppression. In contrast, the level of expression of *Wt1* correlated precisely with tumor suppression in this model system (43). All suppressed MCH cell lines expressed *Wt1* mRNA and protein at levels comparable to that of normal rat liver epithelial cells (WB-F344) (FIGURE 1.5). PCR analysis demonstrated that 2/3 of the suppressed MCH cell lines do not carry the human *WT1* gene, indicating that *Wt1* expression in these lines originates from the rat locus. Reexpression of tumorigenicity by suppressed MCH cell lines was accompanied by the coordinate loss of human chromosome 11p11.2 and of *Wt1* gene expression, suggesting that one or more human 11p11.2 genes

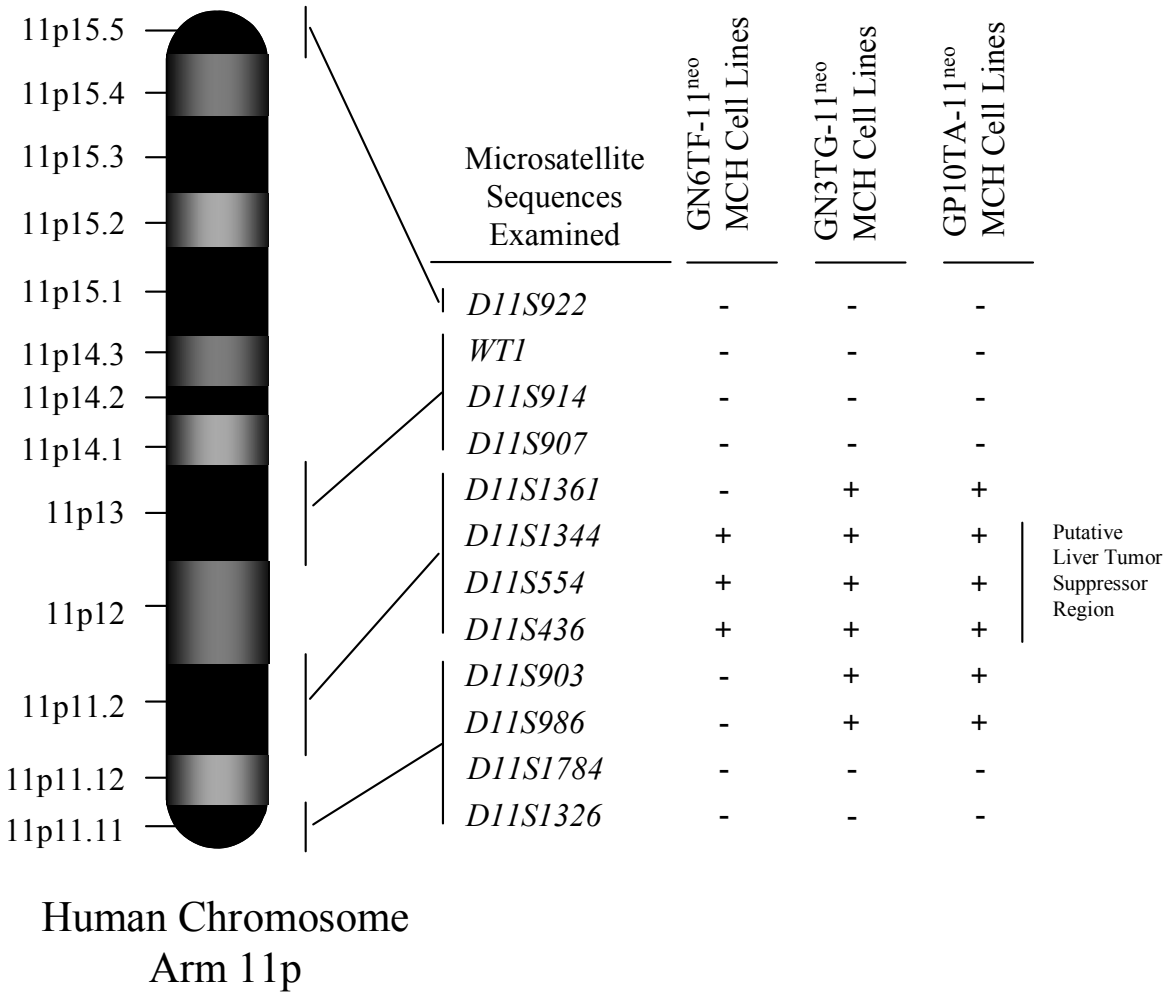

FIGURE 1.4. *Molecular mapping of the 11p11.2 tumor suppressor locus among suppressed MCH cell lines.* A representative panel of microsatellite/EST markers localized to human chromosome 11p is shown (of >200 that were analyzed) and a line connects the markers to their relative chromosomal location. The positive signs (+) in the columns indicate the smallest region of overlapped markers contained in each of the suppressed GN6TF, GN3TG, and GP10TA-derived MCH cell lines. The smallest common tumor suppressor locus retained in all suppressed MCH cell lines (*D11S1344-D11S436*) is shown (adapted from Mahon *et al. International Journal of Oncology*. 1999. *14*:337).

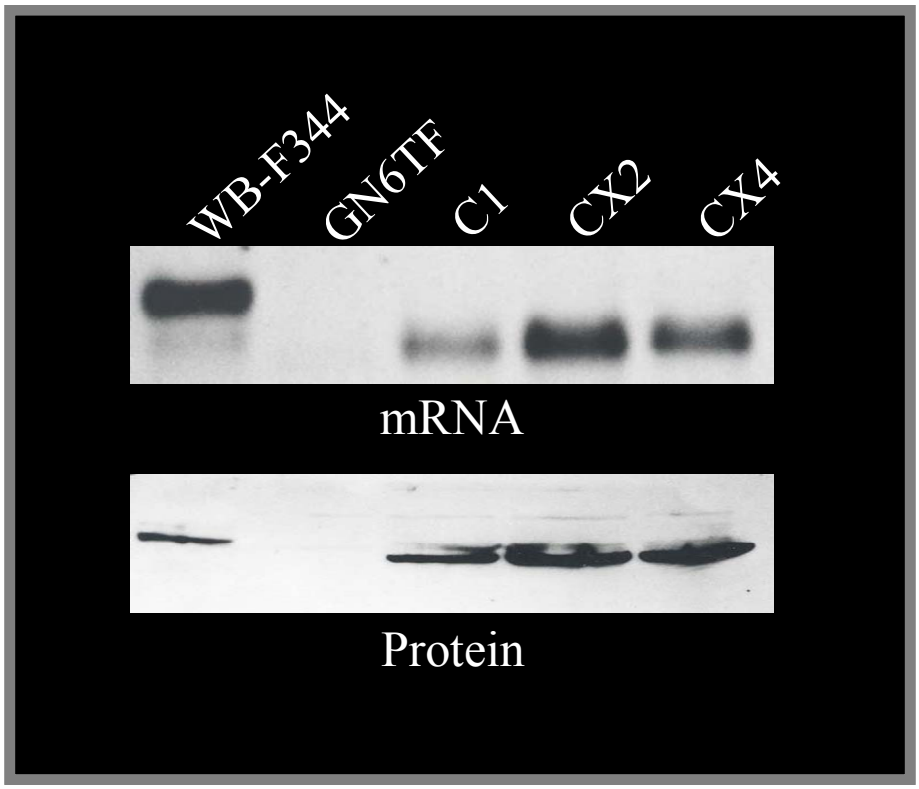

FIGURE 1.5. *Expression of* Wt1 *in GN6TF-derived MCH Cell Lines.* A representative autoradiogram and fluorogram are shown for northern and western analysis of *Wt1* mRNA and protein among MCH cell lines. The approximate size of the *Wt1* mRNA is 3 Kbp and the MCH cell lines (C1, CX2, and CX4) express an approximately 2.8 Kbp *Wt1* mRNA. The molecular weight of the Wt1 protein is approximately 50 kDa. GN6TF tumor cells are negative for both gene and protein Wt1 products (adapted from Coleman *et al. International Journal of Oncology*. 1999. *14*:957)

are required for sustained expression of *Wt1* in these cell lines. Together, these results suggest that the molecular mechanism governing human chromosome 11p11.2-mediated liver tumor suppression may involve induction of rat *Wt1* gene expression under the direct or indirect transcriptional regulation of a genetic locus (or loci) on human 11p11.2 (43).

OBJECTIVES OF THIS DISSERTATION RESEARCH

Strong evidence suggests the presence of a previously unidentified liver tumor suppressor gene in a <1-Mbp region on human chromosome 11p11.2. The overall objectives of this research were to (i) identify the gene responsible for suppression of the neoplastic phenotype of rat liver tumor cells, (ii) characterize the involvement of this gene in tumor suppression, (iii) determine the ability of this gene to individually express tumor suppressor activity *in vivo*, and (iv) identify molecular targets and pathways in liver tumor cell lines that are subject to direct or indirect modification in response to the expression of the human chromosome 11p11.2 liver tumor suppressor gene.

EXPERIMENTAL PROCEDURES

CELL LINES AND CELL CULTURE

Rat Liver Epithelial Tumor Cell Lines

The rat liver epithelial tumor cell lines (44) used in these studies (GN6TF, GN3TG, and GP10TA) were derived from a normal rat liver epithelial cell line (WB-F344) that has been described (45). Phenotypically distinct clonal cell lines were established from a tumorigenic population of WB-F344 cells transformed *in vitro* by 11 consecutive brief treatments with 5.0 μg/ml *N*-methyl-*N*'-nitro-*N*-nitrosoguanidine (46, 47). Tumor cell lines that expressed altered phenotypic properties and produced subcutaneous tumors in 100% of animals after a short latency period were established from tumors that formed in syngeneic animals after transplantation of the transformed cell lines (44). WB-F344 cells and parental tumor cell lines were cultured on plastic in Richter's Improved Minimal Essential Medium (prepared by the UNC Lineberger Comprehensive Cancer Center Tissue Culture Facility) supplemented with 10% fetal bovine serum (Hyclone, Logan, UT), and Antibiotic-Antimycotic (Gibco/Invitrogen Life Technologies, Carlsbad, CA) (48).

Microcell Hybrid Cell Lines

MCH cell lines were established from GN6TF, GN3TG, and GP10TA liver tumor cell lines after the introduction of human chromosome 11 by microcell-mediated chromosome transfer (40, 41), using established methods (40). The derivation of individual

MCH cell lines and MCH-derived tumor cell lines is outlined in FIGURE 2.1. The GN6TF-derived MCH cell lines used included GN6TF-11^{neo}CX2 (designated CX2, which contains an intact copy of human chromosome 11), GN6TF-11^{neo}C1 (designated C1, which contains a portion of 11p11.2 bounded by, but not including, *D11S1361-D11S1357*), and GN6TF-11^{neo}CX4 (designated CX4, which contains the *D11S1361-D11S1357* interval) (40). In addition, two MCH-derived tumor cell lines were used (GN6TF-11^{neo}CX2T1 and GN6TF-11^{neo}CX4T3). These cell lines were established in culture from tumors that formed at least four months after the transplantation of GN6TF-11^{neo} MCH cell lines into syngeneic host rats (40). The GN3TG-derived MCH cell lines included five suppressed MCH cell lines (GN3TG-11^{neo}C2, GN3TG-11^{neo}C3, GN3TG-11^{neo}C4, GN3TG-11^{neo}C5, and GN3TG-11^{neo}C7), and one MCH-derived tumor cell line (GN3TG-11^{neo}C4T3) (41). The GP10TA-derived cell lines included a non-suppressed MCH cell line (GP10TA-11^{neo}C6), three suppressed MCH cell lines (GP10TA-11^{neo}C7, GP10TA-11^{neo}C11, and GP10TA-11^{neo}C12), and one MCH-derived tumor cell line (GP10TA-11^{neo}C7T3) (41). All MCH cell lines were cultured in Richter's Improved Minimal Essential Medium supplemented as described (48) with 800 μg/ml G418 (Gibco) (40). MCH-derived tumor cell lines were cultured in the same growth medium, but without the addition of G418.

Human Hepatocellular Carcinoma Cell Lines

The human HCC cell lines used in this study were generously provided by Dr. Snorri S. Thorgeirsson (NCI, National Institutes of Health, Bethesda, MD). This group of cell lines included nineteen human hepatoma cell lines (18 HCC and 1 hepatoblastoma) established from patients in North America, Japan, China, South Africa, and South Korea (49, 50) (TABLE 2.1). Non-neoplastic control cell lines included Chang and WRL-68 were obtained

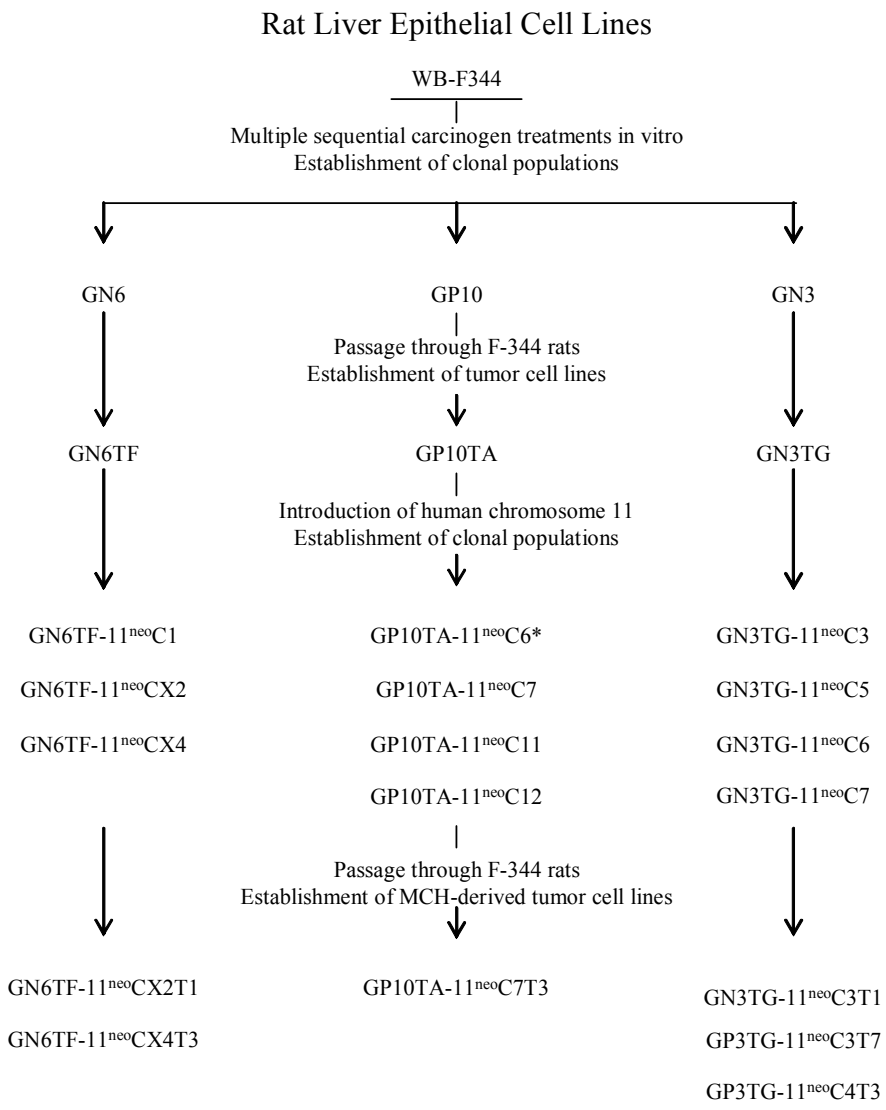

FIGURE 2.1. *Derivation of rat liver epithelial tumor cell lines and microcell hybrid cell lines.* The normal rat liver epithelial cell line WB-F344 was neoplastically transformed by 11 sequential carcinogen treatments resulting in the growth of clonal cell lines (including GN6, GP10, and GN3) with varying tumorigenic potential. These cloned cell lines were passaged through neonatal rats resulting in tumors and tumor cell lines. MCHs were clonally isolated after microcell-mediated chromosome transfer of human chromosome 11 into tumor cell lines, and MCH-derived tumor cell lines were established after transplantation of MCHs into neonatal rats. * Denotes a non-suppressed MCH cell line.

TABLE 2.1. *Human hepatocellular carcinoma cell lines**

Cell Line	Origin	HBV-DNA
HepG2	Argentina	Negative
Sk-Hep1	United States	Negative
Focus	United States	Positive
Hep3B	United States	Positive
Hep3B-TR	United States	ND
PRF/PLC/5	South Africa	Positive
HLE	Japan	Negative
HLF	Japan	Negative
Huh-1	Japan	Positive
Huh-6	Japan	Negative
Huh-7	Japan	Negative
Hep40	China	Positive
7703	China	Negative
SNU182	Korea	Positive
SNU387	Korea	Positive
SNU398	Korea	Positive
SNU423	Korea	Positive
SNU449	Korea	Positive
SNU475	Korea	Positive

* Provided by Dr. Snorri S. Thorgeirsson (NCI, National Institutes of Health, Bethesda, MD)

from American Type Culture Collection (ATCC, Manassas, VA). Chang (CCL-13), is a normal human liver cell line (51), and WRL-68 (CL-48) is a human fetal liver cell line (52). All human HCC cell lines and non-neoplastic control cell lines were grown on plastic in Dulbecco's Modified Eagle Medium/Nutrient Mixture F-12 (1:1) mix supplemented with 15 mM HEPES, 2 mM L-glutamine (Gibco/Invitrogen), 10% fetal bovine serum (Hyclone), and Antibiotic-Antimycotic (Gibco/Invitrogen).

Treatment with 5-aza-2'-deoxycytidine

To examine the possibility of epigenetic silencing (through promoter hypermethylation) of several 11p11.2 candidate tumor suppressor genes in human liver tumors, HCC cell lines (FOCUS, SNU475, SNU398, Huh-1, SNU449, Hep3B, PRF/PLC/5, and HepG2) were plated at densities between $5x10^5$ and $1.8x10^6$ cells/150 mm culture dish in normal growth medium. The demethylating agent 5-aza-2'-deoxycytidine (5-aza, Sigma, St. Louis, MO) was dissolved in DMSO prior to addition to growth medium. HCC cells lines were treated with 5 μM 5-aza for 7 days, with refeeding of fresh culture medium on days 3 and 5. Control cultures of HCC cells were grown in culture medium containing DMSO vehicle control only. RNA was isolated on day 7 for gene expression analysis.

SYT13-targeted and SYT13-transfected Cell Lines

Transfection: Plasmid DNA to be transfected into CX4 (for *SYT13*-targeted cell lines) or GN6TF (for *SYT13*-transfected cell lines) was linearized with the appropriate restriction enzymes. Linearized plasmid DNA (5 μg) and Lipofectamine 2000 (12.5 μl) (Invitrogen, Carlsbad, CA) were incubated separately in 1.5 ml Opti-MEM I Reduced Serum Medium (Invitrogen), for 5 minutes at room temperature. The DNA and Lipofectamine were

then mixed and incubated at room temperature for 20 minutes. This mixture was added to 90-95% confluent cells in a 100 mm tissue culture dish and incubated at 37° overnight. Complete growth medium was replaced the next day, and 24 hours after transfection, cells were passaged 1:10 into 150 mm tissue culture dishes. Successfully transfected cells were selected with the appropriate antibiotic (G418 or zeocin), and after approximately 2 weeks in culture with medium changes 3 times per week, individual clones were identified, isolated using cloning rings, and established as individual cell lines.

Transfected cell lines: Twelve *SYT13*-targeted cell lines [$CX4^{SYT13}$i (designated i1, i2, i3…i12)] were established from the suppressed MCH cell line CX4 by transfection with the psiRNA-hH1zeo vector (FIGURE 2.2.A; InvivoGen, San Diego, CA) containing a *SYT13*-targeted ds-RNA hairpin (shRNA). Eight control cell lines [$CX4^{SYT13}$s (designated s1, s2, s3…s8)] were established by transfecting CX4 cells with the same vector containing a scrambled-sequence shRNA. These cell lines were cultured on plastic and maintained in Richter's Improved Minimal Essential Medium containing 800 μg/ml G418 and 360 μg/ml Zeocin (InvivoGen) supplemented as described (48). GN6TF tumor cells were transfected with either SYT13-pReceiver-m11 or a GFP-pReceiver empty vector control (FIGURE 2.2.B.; GeneCopoeia, Germantown, MD). The resulting cell lines, $GN6TF^{neo}$SYT13- (designated B3, C1, C2, E2, F3, J1) and $GN6TF^{neo}$GFP (designated GFP) were cultured on plastic in Dulbecco's Modified Eagle Medium/Nutrient Mixture F-12 (1:1) mix (Gibco/Invitrogen) supplemented with 10% fetal bovine serum (Hyclone), Antibiotic-Antimycotic (Gibco/Invitrogen), 3.2 g/L sodium bicarbonate, and 800 μg/ml G418.

A.

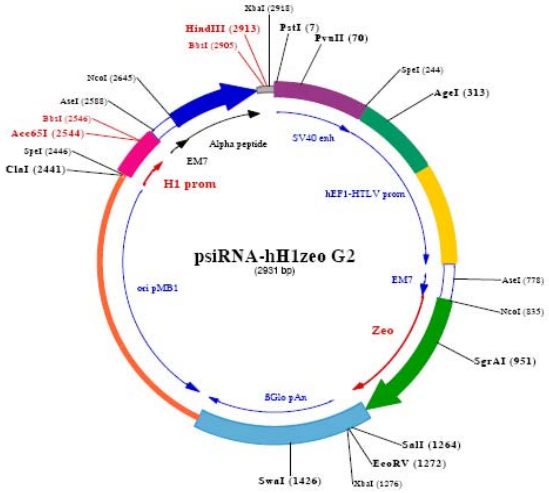

B.

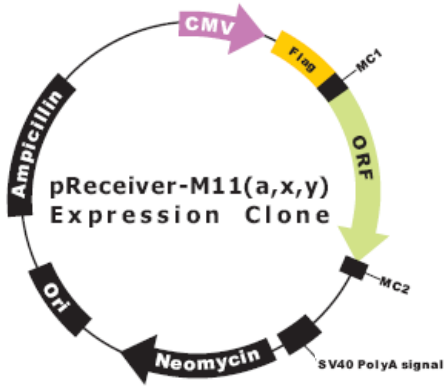

FIGURE 2.2. *Plasmid maps.* (A) The vector used to silence SYT13 (psiRNA-hH1zeo G2) contains the Zeocin resistance gene and utilizes an H1 promoter to drive expression of the dsRNA hairpin. (B) *SYT13* was cloned into the pReceiver-M11 expression vector which contains a neomycin resistance cassette and uses a CMV promoter to drive expression of a FLAG-tagged (N-terminus) SYT13 (adapted from www.invivogen.com and www.genecopoeia.com).

Phenotypic Characterization of SYT13-Targeted and SYT13-Transfected Cell Lines In Vitro

Morphology: The morphologies of experimental cell lines were evaluated by phase contrast microscopy. Cells were examined for nuclear/cytoplasmic ratio, shape, and contact inhibition during both growth phase and at confluency. Photographs of cells in culture were taken at the UNC Microscopy Services Laboratory with the Olympus IMT2 inverted microscope (Center Valley, PA).

Saturation density: For determination of saturation density in monolayer cultures, cells were plated at a density of 1.25×10^5 cells/60-mm dish (or 6.25×10^4 cells/well in a 6-well plate) and maintained in culture with medium changes every 3 days. At the end of 14 days, cells were harvested, counted using a Model ZM particle counter (Coulter Electronics, Hialeah, FL). Saturation densities for individual cell lines were calculated and expressed as total cells/cm^2.

Anchorage-independent growth in soft agar: Anchorage-independent growth was assayed essentially as described (53). The soft agarose medium consisted of Seaplaque GTG low melting point agarose (FMC Bioproducts, Rockville, ME) in Richter's Improved Minimal Essential Medium. Cells suspended in 0.5% agarose were plated (1.0×10^4 cells/60-mm dish or 5.0×10^3 cells/well in a 6-well plate) between layers of agarose medium containing 1% agarose. Soft agarose cultures were maintained for four weeks with weekly feeding of fresh medium. Viable soft agar colonies were identified by overnight staining with 0.05 mg/ml MTT [3-(4,5-Dimethylthiazol-2-yl)-2,5-diphenyl-2H-tetrazolium bromide] (Sigma) (54). MTT-stained colonies were counted for each replicate dish (n=5) in five random fields on an inverted microscope (12.6 mm^2/field). Total colonies per plate were calculated by averaging the number of colonies/field and extrapolating on to the growth area

of the dish. Colony forming efficiency (CFE) was determined by dividing the total colonies/plate by the total number of cells plated.

Tumorigenicity of Cell Lines In Vivo *and Characterization of Tumor Revertants*

Cells intended for transplantation (*SYT13*-targeted, *SYT13*-transfected, and appropriate controls) were trypsinized, rinsed in PBS (1.54 mM KH_2PO_4, 155.17 mM NaCl, 2.71 mM NaH_2PO_4-$7H_2O$; pH 7.2) (Gibco/Invitrogen), resuspended in PBS at a density of 1 x 10^6 cells/0.10 ml, and held on ice until transplanted. Cell suspensions containing 1 x 10^6 cells were injected into the dorsal subcutaneous tissue of 1-day-old Fisher 344 rats (Charles River Laboratories, Inc., Wilmington, MA). Tumor growth was monitored and interim tumor measurements were taken with calipers *in vivo* 10 days after transplantation. Animals were euthanized when tumors reached an approximate diameter of 1 cm, or after 10 months. Tumor tissue was harvested aseptically and used for cell culture or histology. Tissue for histology was fixed in 10% formalin, and processed by Histo-Scientific Research Laboratories (Woodstock, VA) for paraffin embedding, sectioning, and staining with hematoxylin and eosin. Tumor cell lines were established from freshly harvested tumor tissue essentially as described previously (44). Tissue was washed in Ca^{2+}- and Mg^{2+}- free red Hank's Balanced Salt Solution (Cellgro #21-021-CV, Mediatech Inc., Herndon, VA), placed in a tissue culture plate, and minced finely with a scalpel. The culture was incubated in Richter's Improved Minimal Essential Medium (supplemented as described) overnight at 37°C. On the following day, growth medium and solid tissue remnants were removed completely to discourage outgrowth of fibroblasts. After 2 weeks in culture, individual clones were isolated with cloning rings and established as tumor revertant cell lines.

GENERAL METHODS

Nucleic Acid Preparation and Quantitation

DNA isolation from cultured cells: High molecular weight DNA was isolated from cultured cells using the Puragene DNA Purification Kit (Gentra Systems, Minneapolis, MN). Briefly, 1-2 million cells were lysed in 300 µl Cell Lysis Solution and incubated overnight with 1.2 U Proteinase K (Gentra Systems). Subsequently, the lysate was treated with 0.12 U RNase A (Gentra Systems), 100 µl Protein Precipitation Solution was added, and the precipitate was allowed to form for 5 minutes on ice. After centrifugation at 15,000 x g for 1 minute, the supernatant containing DNA was transferred to a new microfuge tube containing 300 µl 100% isopropanol. Tubes were inverted 50 times and centrifuged at 15,000 x g for 1 minute. The DNA pellet was dried briefly and resuspended in DNA Hydration Solution.

DNA isolation from tissue: Paraffin-embedded tissue sections were deparaffinized with xylene and subsequently rehydrated using a gradient of ethanol solutions (100%, 95%, 70%). DNA was then extracted from the tissue using the Puragene DNA Purification Kit (Gentra Systems).

RNA isolation: Total cellular RNA was isolated from cultured cells using the RNeasy® Mini Kit (Qiagen, Valencia, CA). Cells were lysed in Buffer RLT, homogenized by vortexing for 1 minute, and 70% ethanol was added before addition to the RNA binding column. After RNA was absorbed by the membrane, contaminants were removed, and total RNA was washed on the column with Buffers RW1 and RPE. RNA was eluted with RNase-Free H_2O.

Nucleic acid quantitation: Concentrations of isolated DNA and RNA were determined by analyzing UV absorbance (OD at 260nm) using the SmartSpec™ 3000

spectrophotometer (Bio-Rad, Hercules, CA), and purity was assessed by OD260/OD280 ratios.

Nucleic Acid Amplification

Reverse transcription: Total RNA (1-2 μg) was reverse-transcribed for 1 hour at 42°C using MMLV reverse transcriptase (Ambion, Austin, TX) in a buffer consisting of 100 mM Tris-HCl (pH 8.3), 500 mM KCl, 15 mM $MgCl_2$, 0.25 mM of each dNTP, 1 μM cDNA synthesis primer (RETROscript™ First-Strand Synthesis Kit, Ambion, Austin, TX), in a total volume of 20 μl. Newly synthesized cDNA was used as the template for PCR.

Polymerase chain reaction: PCR reactions consisted of 50 ng of template DNA or 2 μl RT-reaction mixture (cDNA) in 50 μl total of a buffer consisting of 50 mM KCl, 20 mM Tris-HCl (pH 8.4), 2 mM $MgCl_2$, 200 μM of each dNTP (EasyStart PCR Mix-in-a-Tube, Molecular Bio-Products, San Diego, CA), 0.4 μM of each primer, and 2.5 U AmpliTaq enzyme (Perkin Elmer, Boston, MA). Amplifications were carried out in a Perkin Elmer Thermocycler using a step-cycle program consisting of 35 cycles of 94°C for denaturing (1 minute), 55-65°C for annealing (1 minute), and 72°C for extension (2 minutes). TABLE 2.2 contains the list of genes and corresponding oligonucleotide primers utilized for deletion and transcription mapping of the human 11p11.2 tumor suppressor locus.

Agarose and polyacrylamide gel electrophoresis: PCR products were either fractionated on a 2% agarose gel containing 40 mM Tris-acetate/1 mM EDTA (pH 8.0), or an 8% polyacrylamide gel in TBE [89 mM Tris-borate, 89 mM boric acid, 2 mM EDTA (pH 8.0)] and visualized by ethidium bromide staining.

TABLE 2.2. *Oligonucleotide PCR primers for deletion and transcription mapping of the 11p11.2 liver tumor suppressor locus*

Gene	Forward Primer	Reverse Primer	Amplicon Size (bp)
ALX4	CTCTTGTTTGGTTCAACCATTGG	TGCTTTACCAGCCTCACTCCC	400
AP15	TTTCAAAAGCATAAGGGGACA	CCCCTTCCCTTTCCTAAGG	152
BHC80	CCAGTTCTGACACCTTTTTAATAGA	CGGGCACTGTTTTTTTATGC	210
C1QTNF4	GGCGCCTACTTCTTCTCCTT	TACTTGCCGTGGTTGCTGTA	231
ch-TOG	CCTGCTGAGGCCATTTTTAA	AGAATAAAGAGCAGCCGCAA	105
DEPC-1	GCGCCTTCCTGACTTACTGC	CTGAGCCCCAGTTTTTCCTC	241
DKFZp779M0652	CACCCTGGAAGGTAGCACAT	AAGGAACTCTGGCGAGTCAA	215
FLJ10450	CTATTTTCTGGCTTACCCCTTGG	CCTTTTCTCAGACCTTAGGCACA	337
FLJ10890	GCACCTGTTATAAGGGGCTG	AAACTTCAAAATCAAGTGCCA	234
FLJ11320	GGATTCTTTATTCAATCACA	CTATATAGTGAAAAGCTACCCA	132
FLJ12827	CTGGCTTCCCTACACTCTCG	GCCACACTCAGTGCAAAGAA	173
FLJ14213	TGTTGTTTATTGAATCCATTTTGG	TTTTTCTCTCCTAGATTCATTTTCA	147
FLJ14576	CAAACAGTCCAGAAAGAAAG	TTGGGTTGTAGGTTGGGCTC	90
FLJ1904	CCTCGTGCTGATAGATGG	AGAGTGTCTTGTTGTATTTACTGCC	170
FLJ20294	AGCAGAAGAGGCAAAAGAGTCA	TGAGAGCAACCTTCTTTTGGACT	303
FLJ23598	TGGGCATGTGGTCAAGATGC	GAGCAAACCTGACATACAGC	303
FLJ25785	CTGCCCAATACGTGGCATGC	GGGAGCAGATCCAGGTGTCC	230
FLJ32675	GTTTCCACGGCAGTTCATTT	GACATTGGCAACACAACGAC	202
FLJ35207	CGTCTGACCTCAAGGTGATC	GGGGCAGGAAAGTGACATGC	270
FLJ41423	CTCTGAGGCCAAGACCTGAC	CTGCATTCTCCTTCCTCCTG	172
HSA249128	CAGGAAGAAGGGTTCTGGTC	CCATGTGTTCTGAATTCAGC	78
HSD17B12	AATGATGCTGATAGCAGATGGCT	TGAAATATGCAGCAAGAAGATTGG	193
HSPC166	GGGAACACTCTGGATGGAC	TGGAGGGAATCGGACAGG	95
KIAA1580	TCTCCTCGCAGAGGACTAGC	ATCGCTGGCTCTTCTCATCC	140
LOC120297	GTGTCTTTTGGTGCCTCACC	GCCAAACATACCCCACAACC	162
LOC399888	AGGAGTGGGCACAGAGCTAA	GGGATGCTCAGCACCTAGAG	239
LOC90139	ATTTCCCTCATTGGTCCTCATTT	TGGTTTCTCTTCTGATAGGCAGG	305
MAPK8IP1	GACTCTGTCAAGTACACGCTGG	TCATATTCCTCTCCGATGGC	167
NDUFS3	TTAAGTCATTGTCTTCTGAAGATGG	CCTTAACCATAATGTCTTTTGATGG	102
NR1H3	GACAGAACAGTCATTCGTGCA	ATGCCTACGTCTCCATCCAC	184
NUP160	GTGCTTGCTGGTGGTGCTAAC	TACAACAAGCCAACAACCCT	185
OASIS	GCAATTAAAAAGGCCCAGC	AAATCTCCCTCTTCCCTTCG	150
PEX16	TTCAAGAGATGGGGTGAAGG	CACAGAAGGACCGTACGACA	156
PHACS	GTATCTGGCTGTGGATTCGC	TTCTGGAGCATTCTCCTTCC	260
PRDM11	CTTGGGGATGACCTCGTTTA	AAAGCTTCCAGCAAGTGGAC	218/729
RAG1	ACCATGAACCCTCAGGCAAG	CCCCATACACAGCAGTAAAG	178
SPI1	ACCAGTTCCTGTTGGACCTG	CTTCACCTTCTTGACCTCGC	218
SYT13	TTAACAATGTGGACATCTGTTTAGA	TTAGTCTATGACATCTGGCTACATG	177
TBP1	TCAGCCGTGAGACTGG	AAGGCATCCTGGAGGTG	88
TP53I11	TGTGGAACGCTCTCTACACG	TTCGGCCGACTTGGTAATAG	204/747
TRAF6	TTTTTATGTTGCTGATTGTATGTGT	TTGTTATGCTATGTAACCCTTTTTG	125
TYRL	AGCCATCTGCGTTTGAGC	GGGCATGTTAATGCACTTTG	175
β-ACTIN	AGAGATGGCCACGGCTGCTT	ATTTGCGGTGGACGATGGAG	605/810

Real-time reverse transcription-polymerase chain reaction: Oligonucleotides and fluorescently labeled probes were designed around intron-exon boundaries using Primer Express software (Applied Biosystems, Foster City, CA) (TABLE 2.3). Additional real-time probe/primer sets were purchased directly from Applied Biosystems and supplied in a 20X mix containing both primers and the FAM-labeled probe. These TaqMan assays included *Cdh1* (Rn00580109_m1), *Gapdh* (Rn99999916_s1), *Pawr/Par4* (Rn00583738_m1), *Snail* (Rn00441533_g1), *SYT13* (Hs00951871_m1), and *Wt1* (Rn00580566_m1). Each RT-PCR was carried out in triplicate in a 30 µl volume [2X ABsolute™ QPCR ROX Mix (ABgene, Rochester, NY), 0.1 µg/µl of each primer, 20 µM TaqMan probe, 5 U Reverse-iT™ Rtase Blend (ABgene), 100 ng total RNA] for 30 minutes at 48°C for reverse transcription, 10 minutes at 95°C for initial denaturing, followed by 40 cycles of 95°C for 15 seconds and 60°C for 1 minute in the ABI 7700 Prism Sequence Detection System. Values for expression levels (C_T) were normalized to the expression of glyceraldehyde-3-phosphate dehydrogenase (GAPDH) and relative quantitation of the multiplex reactions was compared to a reference sample mRNA using the Comparative ($\Delta\Delta C_T$) Method described in User Bulletin #2: ABI Prism 7700 Sequence Detection System. In this method, the number of PCR cycles is recorded when the fluorescence intensity of excited PCR probes exceeds a pre-determined threshold (the cycle threshold or C_T). A C_T which exceeds the maximum limit of 40 cycles is equivalent to zero expression. It is therefore critical to note that quantitation of a fold-increase from zero expression to any discernable level is a mathematical impossibility. However, to facilitate the analysis of quantitative increases in gene expression, a C_T of 40 was assigned to genes with zero expression. Thus, the fold-change values for expression of these genes correspond to the value that would be expected if expression of the control were

TABLE 2.3. *Real-time RT-PCR primers and probes**

Gene	Forward Primer	Taqman Probe	Reverse Primer	Amplico Size (bp
PRDM11	TATGGCCAGCCCTGCTCTA	CCGGACTCCTCGGCCATGGA	TGAGCCCAAGAAACTGAAGG	67
SYT13	CCTGGTGGTGCTGATTAAAG	ACCAGTCCAAGGAGCTCCTGGGGA	TGTCTCTGTCAAGGTGACCT	86
TP53I11	GCAGTTCGTCTCTGCTGTG	TCTCCGGCATTGCCATCATGGCG	GACCAGCTCTATGATGCGG	77
WT1	GCTATTCGCAATCAGGGTTAC	TCACCTTCGACGGGACGCCCAG	GCACCATGCGGCGCAGTT	86
GAPDH	ACCTCAACTACATGGTTTAC	CAAGCTTCCCGTTCTCAGCC	GAAGATGGTGATGGGATTTG	116

* synthesized by the UNC Oligonucleotide Core Facility

detected at a C_T of 40. The ΔC_T represents the C_T normalized to the endogenous *GAPDH* housekeeping gene [$\Delta C_T = C_{T\ (GENE)} - C_{T\ (GAPDH)}$]. To calculate expression fold-change relative to a reference calibrator, the equation $2^{-\Delta\Delta CT}$ is used where $\Delta\Delta C_T = \Delta C_{T\ (5\text{-aza TREATED})} - \Delta C_{T\ (DMSO)}$.

Protein Analysis

Whole cell lysate preparation and protein quantitation: Cells intended for western blot analysis were lysed in ice-cold RIPA buffer [50 mM Tris-HCl (pH 8), 150 mM NaCl, 1% NP-40, 0.5% sodium deoxycholate, 0.1% SDS], and protein concentrations were determined with the bicinchoninic acid protein assay (Pierce, Rockford, IL) using bovine serum album (BSA) as the protein standard.

Western analysis: Lysates (30-80 μg protein) were boiled for five minutes in sample buffer (125 mM Tris-HCl, 4% SDS, 20% glycerol, 10% 2-mercaptoethanol, 0.004% bromophenol blue) and fractioned by SDS-PAGE on 10% polyacrylamide resolving gels [0.375 M Tris-HCl (pH 8.8), 1.6% SDS] and transferred to nitrocellulose membrane [BA85 (0.45 μm), Schleicher & Schuell, Keene, NH], as previously described (55). After transfer, the gel and blot were stained with Coomassie Blue (0.1% Coomassie Blue R250, 20% methanol, and 10% acetic acid) (Sigma) or PonceauS (0.1% in 5% acetic acid) (Sigma), respectively, to assess successful transfer and equal loading. Blots were rinsed briefly with TBST [10 mM Tris-HCl (pH 8.0), 0.15 M NaCl, 8 mM sodium azide, 0.05% Tween-20] and blocked for 1 hour at room temperature in 5% milk/TBST. Primary antibodies were used at a dilution of 1:500-1:1000 in 5% milk/TBST. Bound primary antibody was detected using the appropriate peroxidase-conjugated secondary antibody and visualized by chemiluminescence using the Amersham ECL kit (GE Healthcare, Buckinghamshire, UK) and Kodak BioMax

Light Film (Eastman Kodak Company, Rochester, NY). For quantitation of immunoreactive protein bands, exposed films were scanned and analyzed by densitometry using ImageJ software (v1.37, http://rsb.info.nih.gov/ij/).

Development of a polyclonal antibody to SYT13: A rabbit polyclonal antibody directed against human SYT13 was generated by Anaspec (San Jose, CA). The antibody was raised against a 14 amino acid sequence (RDQDPDLEKAKPSL) located in the linker region between the transmembrane (TMR) and C2A domains of human SYT13, corresponding to amino acids 41-57 (FIGURE 2.3.A). This peptide target was chosen based on its antigenicity and divergence from the rat Syt13 homolog [57% similarity (8/14aa)] (FIGURE 2.3.B). Rabbits (n=2) were immunized with 4 mg KLH-conjugated peptide in Complete Freund's Adjuvant, and subsequently immunized at 3, 6, and 10 weeks with the KLH-conjugated peptide in incomplete Freund's Adjuvant. Serum was collected 7 and 11 weeks after the initial immunization. The serum was used directly without antibody purification at a dilution of 1:1000 for western blotting (suggested from ELISA analysis performed by Anaspec).

Additional antibodies: Rabbit polyclonal antibody directed against E-cadherin (H-108) and rabbit polyclonal antibody directed against WT1 (C-19) (Santa Cruz Biotechnology, Santa Cruz, CA) were used at a dilution of 1:500 for western blotting. Goat polyclonal antibody directed against the FLAG antigen DDDDK (anti-FLAG, ab1238; 1:1000) and rabbit polyclonal directed against GAPDH (ab9385; 1:1000) were both primary antibodies conjugated to horseradish peroxidase (Abcam, Cambridge, MA). A donkey anti-rabbit IgG horseradish peroxidase-conjugated secondary antibody was used to detect primary antibodies raised in rabbits (NA 934, GE Healthcare; 1:10,000).

A.

B.

```
Human: 1   MVLSVPVIALGATLGTATSILALCGVTCLCRHMHPKKGLLPRDQDPDLEKAKPSLLGSAQ 60
           MVLSVPVIALGATLGTATSILALCGVTCLCRHMHPKKGLLPRD++PD EKA+P +L +AQ
  Rat: 1   MVLSVPVIALGATLGTATSILALCGVTCLCRHMHPKKGLLPRDREPDPEKARPGVLQAAQ 60

Human: 61  QFNVKKSTEPVQPRALLKFPDIYGPRPAVTAPEVINYADYSLRSTEEPTAPASPQPPNDS 120
           QFNVKKSTEPVQPR LLKFPDIYGPRPAVTAPEVINYADY+L +TEE  APASPQ  +DS
  Rat: 61  QFNVKKSTEPVQPRPLLKFPDIYGPRPAVTAPEVINYADYTLGTTEESAAPASPQAQSDS 120

Human: 121 RLKRQVTEELFILPQNGVVEDVCVMETWNPEKAASWNQAPKLHYCLDYDCQKAELFVTRL 180
           RLKRQVTEELFILPQNGVVEDVCVMETWNPEKAASWNQAPKLH+ LDYD +KAELFVT L
  Rat: 121 RLKRQVTEELFILPQNGVVEDVCVMETWNPEKAASWNQAPKLHFRLDYDQKKAELFVTSL 180

Human: 181 EAVTSNHDGGCDCYVQGSVANRTGSVEAQTALKKRQLHTTWXXXXXXXXXXXXXXXXXXX 240
           EAVTS+H+GGCDCY+QGSVA +TGSVEAQTALKKRQLHTTW
  Rat: 181 EAVTSDHEGGCDCYIQGSVAVKTGSVEAQTALKKRQLHTTWEEGLALPLGEEELPTATLT 240

Human: 241 XXXXXCDRFSRHSVAGELRLGLDGTSVPLGAAQWGELKTSAKEPSAGAGEVLLSISYLPA 300
                CDRFSRHSV GELRLGL+G SVPLG AQWGELKT+AKEPSAG GEVLLSISYLPA
  Rat: 241 LTLRTCDRFSRHSVIGELRLGLNGASVPLGTAQWGELKTTAKEPSAGTGEVLLSISYLPA 300

Human: 301 ANRLLVVLIKAKNLHSNQSKELLGKDVSVKVXXXXXXXXXXXXXXXXXXXXINPVWNEMI 360
           ANRLLVVLIKAKNLHSNQSKELLGKDVSVKV                    INPVWNEMI
  Rat: 301 ANRLLVVLIKAKNLHSNQSKELLGKDVSVKVTLKHQAQKLKKKQTKRAKHKINPVWNEMI 360

Human: 361 MFELPDDLLQASSVELEVLGQDDSGQSCALGHCSLGLHTSGSERSHWEEMLKNPRRQIAM 420
           MFELPDDLLQASSVELEVLGQ + G SC LG CSLGLH SGSERSHWEEMLKNPRRQIAM
  Rat: 361 MFELPDDLLQASSVELEVLGQGEEGPSCELGRCSLGLHASGSERSHWEEMLKNPRRQIAM 420

Human: 421 WHQLHL 426
           WHQLHL
  Rat: 421 WHQLHL 426
```

FIGURE 2.3. *Polyclonal SYT13 antibody peptide selection.* (A) The SYT13 protein contains an N-terminal transmembrane region (TMR, in blue) followed by a cytoplasmic linker region (in white) and two tandem C2 domains (C2A and C2B, in red). (B) The SYT13 antibody was raised against a 14 amino acid sequence (green) with 57% (8/14) homology to the rat Syt13 protein. Amino acids in blue correspond to the TMR and in red correspond to the individual C2 domains.

Statistical Analysis

Data in the text, tables, and figures represent mean values ± the standard error of the mean. Statistical analysis of real-time PCR data was accomplished using one-way ANOVA (Kaleidagraph, Reading, PA). The statistical significance of data from densitometry, saturation density, and anchorage-independent growth assays was assessed using the Student's t-Test for unpaired data with unequal variance. Statistical significance associated with Kaplan-Meier survival analysis was determined using the Log-Rank test (Lifetest Procedure, SAS System, SAS Institute, Cary, NC).

STUDY-SPECIFIC METHODS

Methods Specific to Loss of Heterozygosity Study

Patients and tumor specimens: Forty-seven hepatocellular carcinomas were selected for this study. DNA corresponding to tumor and matched non-tumor tissue were provided by Dr. Snorri S. Thorgeirsson (NCI, National Institutes of Health, Bethesda, MD). All HCC tumors were from patients in China. The majority of patients were male (75%) and HBV^+ (76%). These HCCs occurred in the setting of cirrhosis in slightly less than half the patients (42%) and in non-cirrhotic patients in the remainder (58%). HCC stage II disease and stage III disease were detected in 33% and 42% of the samples respectively.

Microsatellite markers: Deletions involving chromosome 11 were examined by PCR utilizing two markers from 11q13 (*D11S1777*, *D11S4076*), seven markers from 11p11.2 (*D11S1344*, *D11S436*, *D11S4174*, *D11S1290*, *D11S1361*, *D11S554*, *D11S4103*), seven markers from 11p12 (*D11S4102*, *D11S4083*, *D11S4185*, *D11S935*, *D11S4203*, *D11S907*, *D11S4200*), two markers from 11p13 (*WT1*, *D11S914*), and two markers from 11p15.5

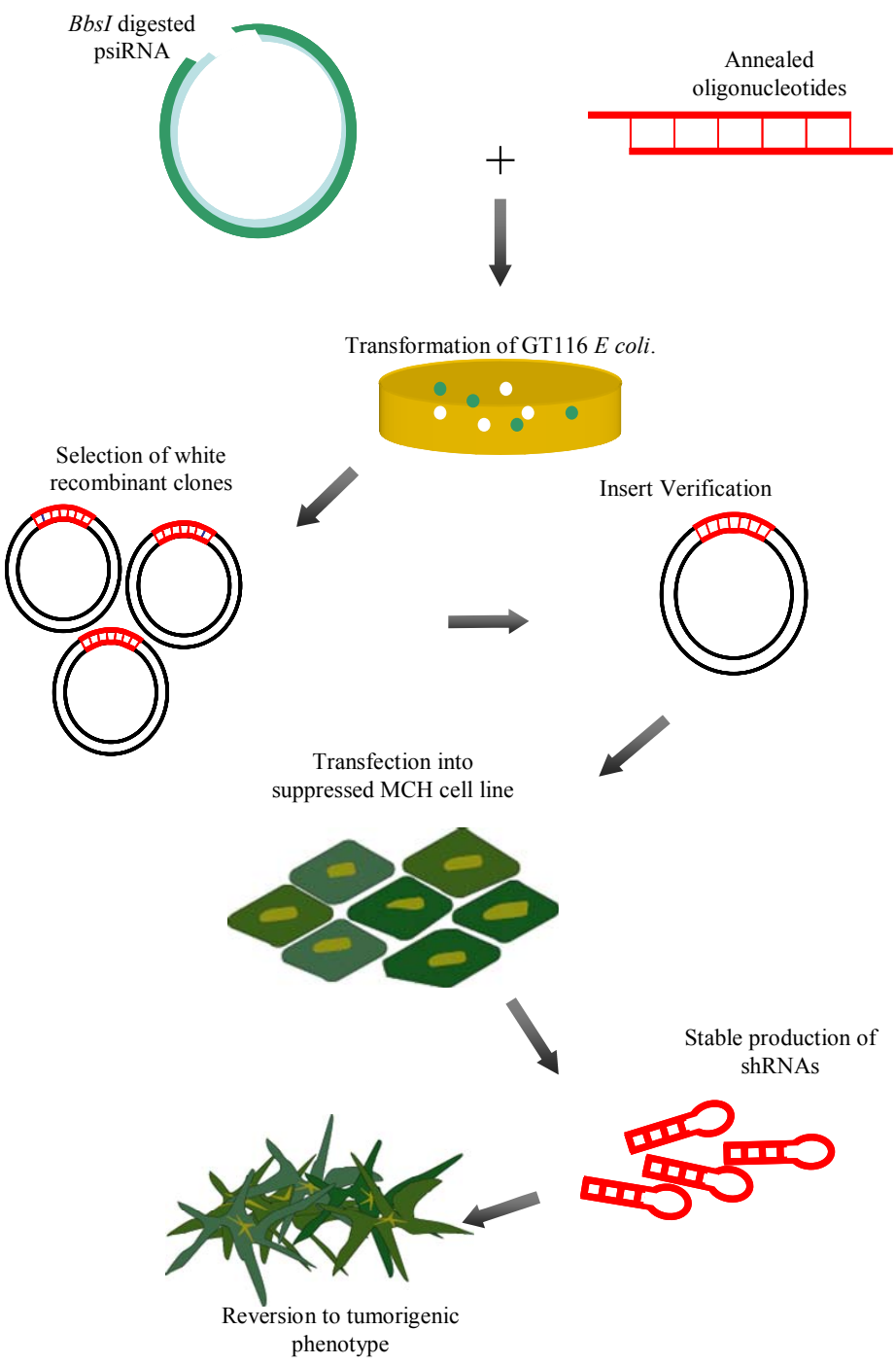

FIGURE 2.4. *Experimental design of the SYT13-silencing study.* Annealed oligonucleotides are ligated into the psiRNA vector and transformed into competent GT116 *E. coli*. Plasmids with proper inserts were transfected into suppressed MCH cells, and stable production of targeted shRNAs silence SYT13.

(*D11S922*, *D11S3806*). The majority of these were MapPairs microsatellite markers purchased from Invitrogen (formerly Research Genetics). Others (*D11S4203*, *D11S935*, *D11S4185*, *D11S4083*, *D11S4102*, *D11S907*, and *D11S4200*) were synthesized by the UNC Oligonucleotide Core Facility based on sequences obtained from the UniSTS Database on the NCBI website (www.ncbi.nlm.nih.gov).

Methods Specific to RNAi Study

Stable silencing system: Stable knock-down of SYT13 was accomplished using a system from InvivoGen (San Diego, CA) that is summarized in FIGURE 2.4. The psiRNA-hH1zeo expression vector was obtained from InvivoGen (FIGURE 2.2.A). It utilizes the human H1 RNA Pol III promoter. The message is transcribed into a short dsRNA with a hairpin structure (shRNA) which is recognized and cleaved by the endogenous Dicer complex into a 21nt double-stranded siRNA that directs the RISC complex toward cleavage of target *SYT13* mRNA (56-58).

Design of shRNA oligonucleotides: Several guidelines for choosing RNAi target regions have been published (59-62). An ideal target region was identified in exon 2 of h*SYT13* (FIGURE 2.5.A) using the following guidelines suggested by literature and customer support from InvivoGen: (i) the sequence should be 19-21 nucleotides within the coding region of the gene of interest; (ii) it should begin with an A and should not contain 3 repeating nucleotides, especially TTT; (iii) the G/C content should be ≤50%; (iv) palendromic sequences should be avoided; and (v) the sequence should not be homologous to other genes within the genome. Additional considerations for target design in this unique MCH system were that the selected sequence would not interfere with the expression of other human 11p11.2 genes or other genes in the rat genome, including rat *SYT13* (FIGURE 2.5.B).

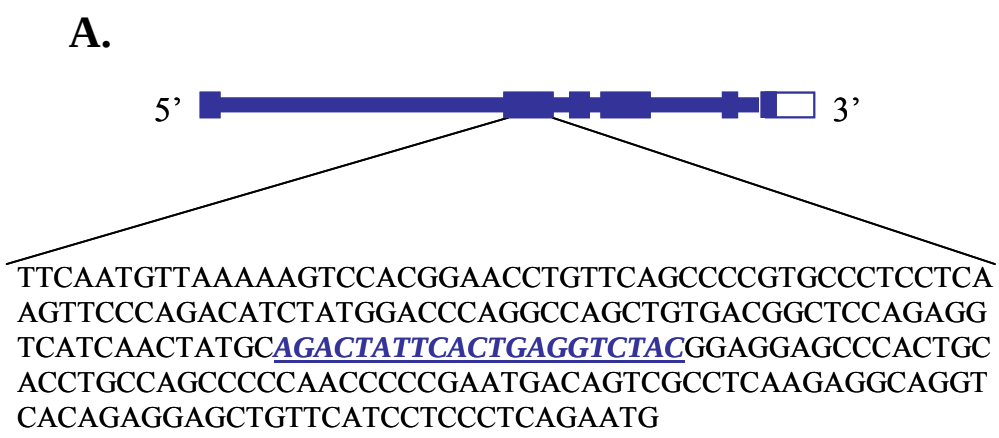

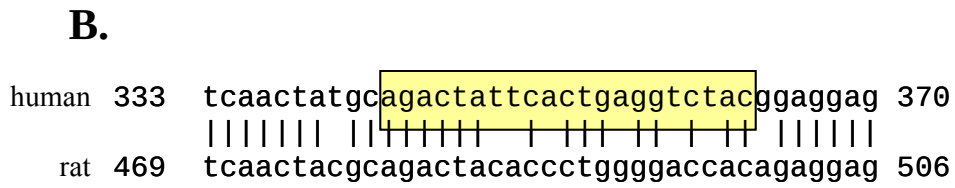

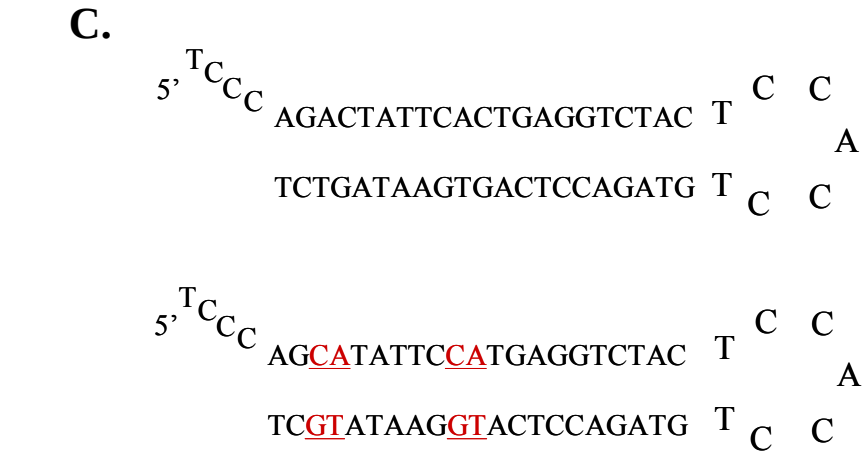

FIGURE 2.5. *Design of the* SYT13*i and* SYT13*s shRNAs.* (A) The *SYT13* gene is comprised of 6 exons depicted by blue boxes. The 21nt *SYT13* target (indicated in blue/underlined) localizes to the coding sequence of exon 2. (B) The target sequence has 71% (15/21) homology to the rat *Syt13* gene. (C) Sequence and structure of *SYT13*i and *SYT13*s shRNAs. The four scrambled nucleotides of *SYT13*s are shown in red/underlined.

Oligonucleotides (53-mers) were designed that encode a 4 nucleotide *BbsI*-compatible overhang and two complementary 21 nucleotide sequences separated by a 7 nucleotide spacer (this targeting sequence is referred to as *SYT13*i) (FIGURE 2.5.C). A matched control RNAi oligonucleotide was also constructed that encodes siRNA of the same basic design as the silencing vector and contains the identical nucleotide composition, but the sequence has been scrambled (*SYT13*s) (FIGURE 2.5.C). The scrambled-control sequence was confirmed to contain low sequence homology to other genes in the rat genome.

Synthesis, annealing, and ligation of shRNA oligonucleotides: Two DNA oligonucleotide strands (sense and antisense) for both the *SYT13*i and *SYT13*s sequences were synthesized by the UNC Oligonucleotide Core Facility. To anneal, the complimentary oligonucleotides were dissolved to a concentration of 1.7 μM in 10 mM NaCl and incubated at 80°C for 2 minutes. Power was removed from the heating block and the samples were maintained in the block until the temperature reached 35°C. 100 ng of *BbsI*-linearized psiRNA vector (obtained from InvivoGen) and 1 μl of the annealed siRNA insert reaction were ligated at 16°C overnight in a reaction containing 1 U T4 DNA Ligase (New England BioLabs, Beverly, MA) and T4 DNA Ligase Reaction Buffer (50 mM Tris-HCl, 10 mM $MgCl_2$, 10m M DTT, 1 mM ATP, 25 μg/ml BSA, pH 7.5 at 25°C) (New England BioLabs, Beverly, MA) (Figure 2.6).

Preparation of chemically competent GT116 cells: The *E. coli* GT116 strain, a *sbcCD* deletion mutant, was provided with the psiRNA-hH1zeo kit (InvivoGen). Hairpin structures are known to be unstable in *E. coli* due to their elimination by a protein complex called SbcCD that recognizes and cleaves hairpins (63). The *sbcCD* gene deletion in the GT116 strain supports the growth of plasmid DNAs carrying hairpin structures.

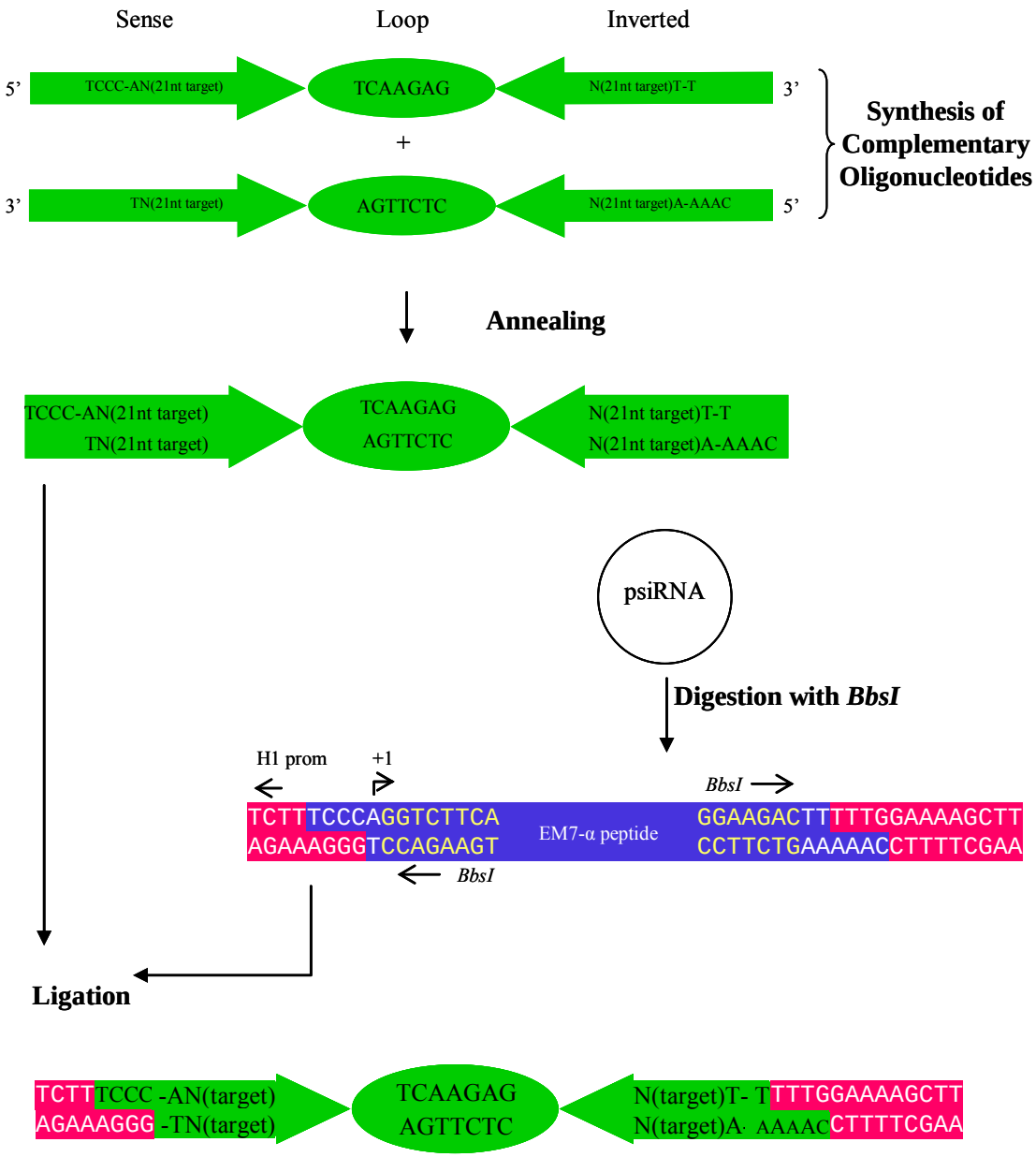

FIGURE 2.6. *Cloning of the* SYT13*i and* SYT13*s shRNAs.* Two complementary oligonucleotides were synthesized with overhangs to correspond with the asymmetrical overhangs of the *BbsI* cloning site. Annealed oligonucleotides were cloned into the *BbsI* cloning site disrupting the EM7-α peptide and allowing blue/white selection after ligation and transformation.

A GT116/LB broth suspension was streaked on an LB agar plate and placed in a 37°C incubator overnight. A single colony was picked from the plate and grown for 2 hours in 5 ml of LB broth. This culture was transferred to 100 ml LB broth and shaken until OD600=0.5 (approximately 5 hours). Bacteria were collected by centrifugation at 700 x g for 5 minutes, gently resuspended in 25 ml ice cold TFB1 solution (30 mM $C_2H_3KO_2$, 50 mM $MnCl_2$, 100 mM KCl, 10 mM $CaCl_2$, pH 5.8), and kept on ice for 1 hour. After being pelleted at 450 x g for 5 minutes, the bacteria were resuspended in 4 ml ice cold TFB2 solution [10 mM Na-MOPS (pH 7.0), 75 mM $CaCl_2$, 10 mM KCl, 20% glycerol], and incubated on ice for 1 hour. 100 µl aliquots were then snap frozen in liquid N_2 and stored at -80°C.

Bacterial transformation and culture: Ten µl ligated psiRNA was transformed into 100 µl chemically competent GT116 bacteria. The DNA/bacteria mixture was incubated on ice for 30 minutes and heat-shocked at 42°C for 90 seconds. After a brief cooling on ice, 900 µl warm LB broth (1% bacto-tryptone, 0.5% bacto-yeast extract, 0.5% NaCl) was added, and the transformation mixture was incubated 1 hour at 37°C with gentle agitation. 100 µl of transformed cells were spread on Fast-Media Zeo XGal agar plates (InvivoGen) and incubated at 37°C overnight. Fifty ml ImMedia Zeo Liquid (Invitrogen, Carlsbad, CA) medium was used to culture white recombinant clones picked from psiRNA-transformed bacteria overnight at 37°C. Overnight cultures were pelleted at 10,000 x g for 10 minutes and used for plasmid preparation.

Plasmid preparation: Plasmid DNA was extracted from bacterial clones using the Wizard® Plus Midipreps DNA Purification System (Promega, Madison, WI). The cell pellet was resuspended in 3 ml Cell Resuspension Solution (50 mM Tris-HCl, pH 7.5; 10 mM

EDTA; 100 μg/ml RNase A). Three ml Cell Lysis Solution (0.2 M NaOH, 1% SDS) was added followed by neutralization with 3 ml Neutralization Solution (1.32 M $C_2H_3KO_2$, pH 4.8). Cellular debris was pelleted at 14,000 x g for 30 minutes and the DNA-containing supernatant was collected. Ten ml Wizard® Midiprep DNA Purification Resin was added to the supernatant and the mixture was applied to a column. After the sample passed through the column, the resin was washed twice with 15 ml Column Wash Solution (80 mM $C_2H_3KO_2$; 8.3 mM Tris-HCl, pH 7.5; 40 μM EDTA). The resin was dried briefly by centrifugation and eluted with 300 μl Nuclease-Free water.

Digestion mapping of psiRNA-transformed plasmids and DNA sequencing: After plasmid preparation, successful siRNA insert verification was accomplished by digesting 1 μg of the psiRNA plasmid with the *SpeI* restriction enzyme (New England BioLabs, Beverly, MA) for 2 h at 37°C in a reaction consisting of 100 μg/ml BSA, 50 mM NaCl, 10 mM Tris-HCl (pH 7.9), 10 mM $MgCl_2$, and 1 mM DTT. Plasmids with siRNA inserts yielded 2 restriction digestion products of 2208 and 425 base pairs. Additional insert verification was obtained by DNA sequencing. Purified plasmid DNA was sequenced at the UNC-CH Genome Analysis Facility using a 3100 Genetic Analyzer (Applied Biosystems). Template DNA (1.5 μg plasmid) was sequenced using the ABI PRISM BigDye Terminator Cycle Sequencing Ready Reaction Kit with AmpliTaq DNA Polymerase FS (Applied Biosystems) and 10 pmoles of either the OL381 reverse primer or OL178 forward primer supplied with the psiRNA kit (InvivoGen).

Plasmid restriction digestion: Prior to transfection into CX4 cells, cloned plasmids were linearized to direct insertion into the host genome. psiRNA-hH1-derived vectors with

verified shRNA inserts were linearized by digestion for 1 h at 25°C with *SwaI* [10 U enzyme, 100 mM NaCl, 50 mM Tris-HCl (pH 7.9), 10 mM $MgCl_2$, 1 mM DTT, 100 μg/ml BSA].

Methods Specific to SYT13 Transfection

The open reading frame of human *SYT13* (1281/5108) bp was cloned into the pReceiver-M11x vector by GeneCopoeia (FIGURE 2.2.B), and the GFP-pReceiver was utilized as an empty vector control (not shown). Thirty ng of the *SYT13*-pReceiver-M11 or GPF-pReceiver vector control were transformed into 100 μl competent JM109 cells (Promega, Madison, WI). Transformed bacteria were streaked on LB-ampicillin agar plates (1.5% bacto-agar, 1% bacto-tryptone, 0.5% bacto-yeast, 0.5% NaCl, and 0.1 mg/ml ampicillin) and cultured overnight in 50 ml LB broth with 0.1 mg/ml ampicillin. Plasmids were prepared with the Wizard Plus Midipreps DNA Purification System (Promega) and linearized by digestion overnight at 37°C with *ScaI* [10 U enzyme, 50 mM 100 mM NaCl, 50 mM Tris-HCl (pH 7.9), 10 mM $MgCl_2$, 1 mM DTT] before transfection into GN6TF tumor cells.

Methods Specific to Large-Scale Gene Expression Analysis

Affymetrix gene array: The Affymetrix GeneChip Rat Genome 230 2.0 Array (Affymetrix, Santa Clara, CA) was used in this study. The array chip contains 31,042 probe sets that analyze the expression level of >30,000 transcripts and variants from >28,000 genes corresponding to the rat genome. In addition, this microarray contains 100 normalization control probe sets and hybridization controls.

RNA processing for microarray hybridization: RNA for microarray analysis was processed by Expression Analysis (Research Triangle Park, NC) according to the Affymetrix

Technical Manual (Affymetrix). Briefly, total RNA (10 μg) was converted into cDNA using Superscript II Reverse Transcriptase (Invitrogen) and a modified oligo(dT)24 primer that contains T7 promoter sequences (GenSet, Evry, France). After first strand synthesis, residual RNA was degraded by the addition of RNaseH, and a double-stranded cDNA molecule was generated using DNA Polymerase I and DNA Ligase (Invitrogen). The cDNA was purified and concentrated using a standard phenol:chloroform extraction, followed by ethanol precipitation. Labeled cRNA products were generated from the purified cDNAs by incubation with T7 RNA Polymerase and biotinylated ribonucleotides using an In Vitro Transcription kit (Enzo Diagnostics, Farmingdale, NY). cRNA products were purified on an RNeasy column (Qiagen) and quantified spectrophotometrically.

Microarray hybridization and analysis: Microarray hybridization and analysis was performed by investigators at Expression Analysis (Durham, NC). Purified cRNA target (20 μg) was incubated at 94°C for 35 minutes in fragmentation buffer [200 mM Tris-acetate (pH 8.1), 500 mM potassium acetate, and 50 mM magnesium acetate], and then diluted into hybridization buffer [100 mM 2-(N-morpholino) ethanesulfonic acid, 20 mM EDTA, and 0.1% Tween 20] containing biotin-labeled OligoB2 and Eukaryotic Hybridization Controls (Affymetrix). The hybridization cocktail was denatured at 99°C for 5 minutes, incubated at 45°C for 5 minutes, and then injected onto a Rat Genome 230 2.0 Array cartridge (Affymetrix). The Rat Genome 230 2.0 Array was incubated at 42°C for at least 16 hours in a rotating oven at 60 rpm. Subsequently, the hybridized GeneChips were washed under nonstringent conditions at 25°C in a buffer consisting of 0.9 M NaCl, 70 mM sodium phosphate (pH 7.4), 6 mM EDTA, and 0.01% Tween 20, and stringent conditions at 50°C in a buffer consisting of 100 mM 2-(N-morpholino) ethanesulfonic acid, 100 mM NaCl, and

0.01% Tween 20. The microarrays were then stained with Streptavidin Phycoerythrin, and the fluorescent signal was amplified using a biotinylated antibody solution. Fluorescent images were detected in an Agilent GeneArray Scanner (Agilent Technologies, Santa Clara, CA). After probe-level data was extracted from the MicroArray Suite-derived CEL files, the probes were normalized using quantile probe normalization (64). Signal was computed using the Positional Dependent Nearest Neighbor (PDNN) method (65), and scaled by Expression Analysis proprietary methods to mitigate bias in fold change underestimation. Microarray hybridizations were performed in duplicate for each cell line and the final values for (log) signal for all graphs are expressed as averages of the duplicates (equivalent to geometric averages of signal).

Gene expression analyses and web-based bioinformatics: Gene expression profiles generated by the microarray analysis were mined and manipulated using Data Desk software (Data Descriptions, Ithaca, NY), GenMAPP (v.2, www.genmapp.org) (66), and the DAVID and EASE 2006 Bioinformatic Resources (http://david.abcc.ncifcrf.gov/) (67, 68).

RESULTS

LOSS OF HETEROZYGOSITY IN HUMAN LIVER TUMORS

We have identified, using a MCH model system, a tumor suppressor locus on human chromosome 11p11.2, and studies from other groups suggest that aberrations of human 11p may play a role in the carcinogenesis of a subset of HCC. While numerous allelotyping studies of human HCC have appeared, a detailed allelotype of human 11p11.2 has not been reported. Therefore, we analyzed 47 primary HCCs and their corresponding non-tumor DNA for LOH on chromosome arm 11p.

Loss of Heterozygosity of Chromosome 11 Microsatellite Markers in Human Hepatocellular Carcinoma

A map of the 11p11.2 polymorphic microsatellite markers that were used in this study is shown in FIGURE 3.1. FIGURE 3.2.A shows representative results of this LOH analysis at polymorphic loci on human chromosome 11 in our HCC tumor samples, and FIGURE 3.2.B summarizes these findings. 15/47 (32%) HCCs showed LOH of $\geq$1 marker corresponding to chromosome 11. Furthermore, 10/47 (21%) HCCs exhibited LOH of $\geq$1 marker within the 11p11.2 liver tumor suppressor region (*D11S4103-D11S1344*). Other deletions were noted in 11p13-pter (4/47, 9%) or involving markers on 11q (1/47, 2%). The greatest frequency of loss involving individual markers was observed with D11S1290 (5/47, 11%) and D11S554 (4/47, 9%). These results indicate that chromosomal deletions involving the 11p11.2 liver

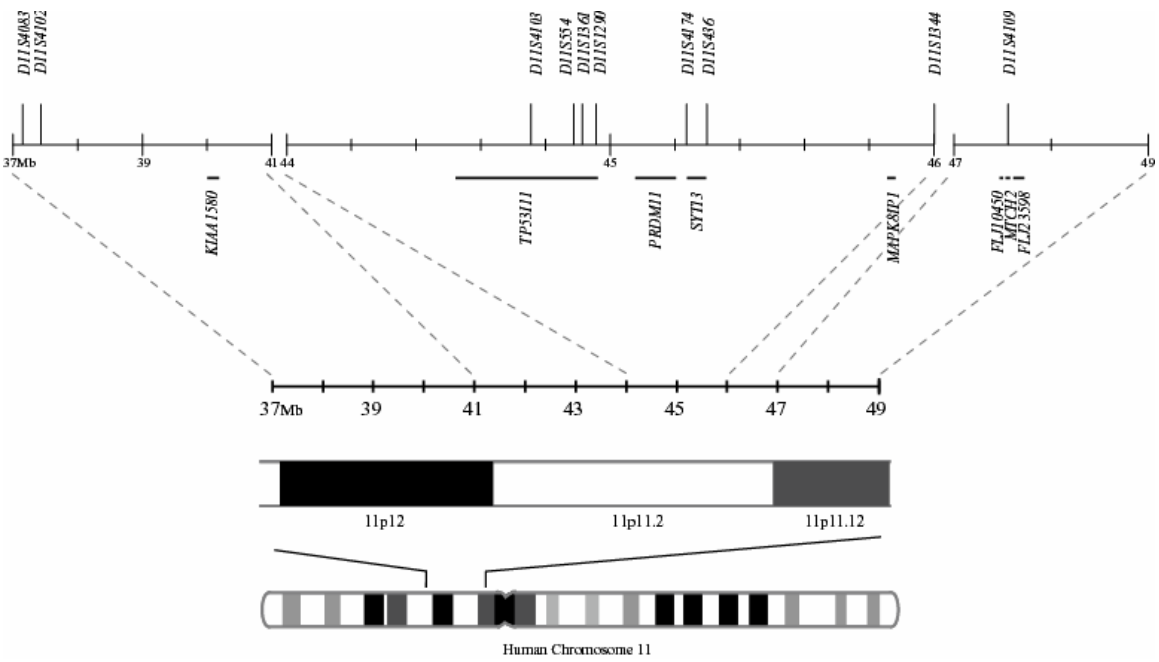

FIGURE 3.1. *Integrated map of the human chromosome 11p11.2 liver tumor suppressor region.* An integrated microsatellite marker/gene map of the region of human 11p11.2-p12 (corresponding to a 37-49 Mbp interval of human 11p) is shown. The relative location of microsatellite markers is depicted by tick marks above the line. The location of *SYT13* and other genes in this region is depicted by dashes parallel to the chromosome.

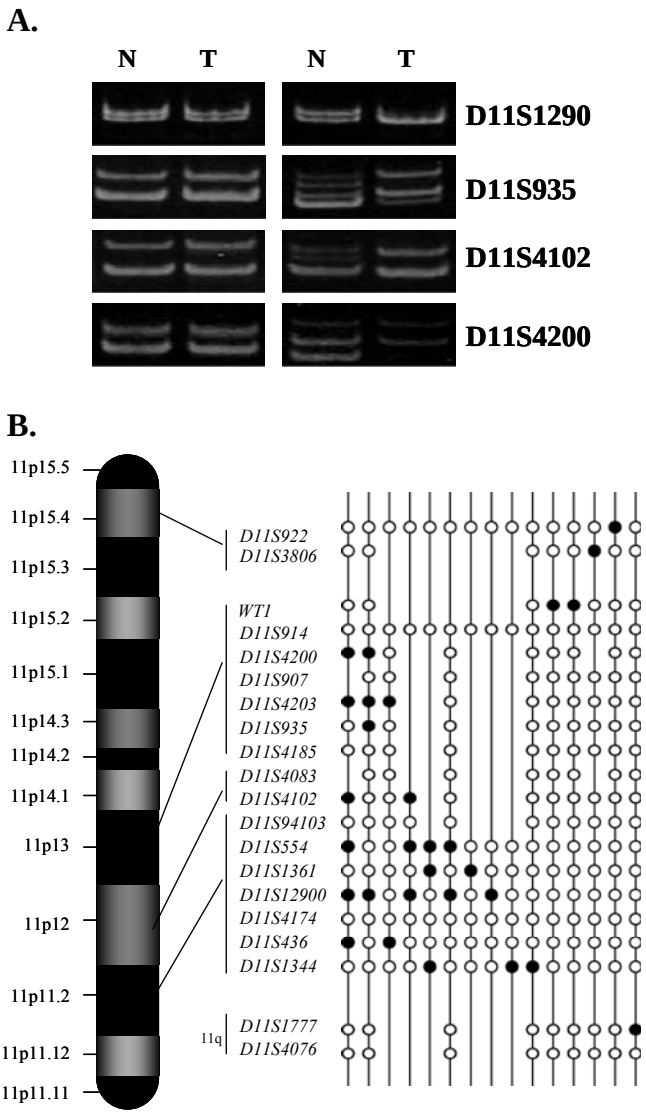

FIGURE 3.2. *Analysis of LOH at polymorphic loci on human chromosome 11 in HCC tumor samples.* (A) Representative gels demonstrating loss of heterozygosity in HCC samples. The patient on the left retains both alleles of the markers shown in both the tumor (T) and non-neoplastic (N) tissue, whereas the patient on the right demonstrates LOH in the tumor tissue. (B) Diagrammatic summary of LOH on chromosome 11 in 15 HCC tumor samples. The relative loci of the molecular markers examined are indicated on the ideogram of 11p. Closed circles designate LOH, open circles designate no loss, and the absence of a circle indicates that the locus was not tested for LOH.

tumor suppressor region occur in a subset of human HCCs, suggesting that loss of one or more genes in this region may be important in human hepatocarcinogenesis.

Correlation of LOH with Patient or Clinicopathological Characteristics

To determine if human 11p11.2 loss tends to correlate with specific patient or clinico-pathological characteristics, we examined the frequency of 11p11.2 LOH among subsets of HCC. In our HCC sample set, loss of 11p11.2 occurred more frequently among female patients (35% show loss) than males patients (15% show loss). HCC tends to affect men much more frequently than women (8), leading to the suggestion that hormonal differences may protect from or contribute to development of HCC. Our observation suggests that 11p11.2 loss may be more important in hepatocarcinogenesis in females, perhaps by contributing to the abrogation of protective factors. LOH of markers within the 11p11.2 liver tumor suppressor region occurred with similar frequency among grade II HCC (26% show loss) and grade III HCC (26% show loss). This observation suggests that 11p11.2 loss may be an early alteration (required for tumorigenesis) in the subset of tumors that are affected by such loss, rather than a late change associated with progression of the neoplastic phenotype. In a similar manner, 11p11.2 loss was documented with similar frequency among patients with cirrhosis (21% show loss) and patients without cirrhosis (19% show loss). This observation suggests that 11p11.2 loss may not be a general characteristic of cirrhotic liver, but that these deletions may occur in the early lesions that characterize hepatocarcinogenesis, such as focal proliferative phenotypically altered hepatocytes, hyperplastic hepatocytes, or dysplastic hepatocytes. In this subset of HCC patients, loss of 11p11.2 markers occurred more frequently in HBV-negative samples (30% show loss) than in HBV-positive patients (16% show loss), although this trend did not reach statistical significance probably due to

small sample size. Human chromosome 11p11.2 has been suggested as a preferential site for HBV insertion (15, 69, 70), possibly causing disruption of genes in that chromosomal region, producing a selective growth advantage in affected cells. Our observation suggests that LOH of 11p11.2 might account for disruption of critical target genes in this region in the absence of HBV insertional mutagenesis, producing a similar selective growth advantage in affected cells.

IDENTIFICATION OF CANDIDATE LIVER TUMOR SUPPRESSOR GENES FROM HUMAN CHROMOSOME 11P11.2

MCH cell lines were utilized in a candidate gene approach to identify genes from human chromosome 11p11.2 that were differentially expressed in the suppressed versus the non-suppressed cell lines. Our criteria for the best candidate(s) for the 11p11.2 tumor suppressor gene dictated that the gene(s) be present and expressed in suppressed MCH cell lines and absent/silent in non-suppressed MCH cell lines.

Deletion Analysis of Candidate Tumor Suppressor Genes from Human 11p11.2 in GN6TF-Derived Microcell Hybrid Cell Lines

Using DNA samples from an index panel of suppressed MCH cell lines (C1, CX2, and CX4) each of 39 genes, ESTs, and predicted genes positioned by the Human Genome Project within human 11p11.2 (TABLE 2.2) were analyzed by PCR to determine which ESTs/genes map to the human 11p11.2 liver tumor suppressor region. The suppressed GN6TF-11^{neo} MCH cell lines each contain a different, but overlapping, fraction of human chromosome 11 (40, 42). CX2 contains an intact copy of human chromosome 11 based upon fluorescence *in situ* hybridization chromosomal analysis (40), and extensive PCR mapping

studies (40, 42, 71). C1 and CX4 contain only a portion of the short arm of the chromosome, including 11p11.2-p12 (40, 42). Thus, ESTs/genes detected in the DNA from each of these cell lines reside in the minimal liver tumor suppressor region of 11p11.2 and are considered potential candidate liver tumor suppressor genes. These selection criteria for identification of candidate liver tumor suppressor genes have been described (71). Seven of the 39 ESTs/genes evaluated mapped to the human 11p11.2 liver tumor suppressor region defined by the index panel of suppressed GN6TF-derived MCH cell lines (FIGURE 3.3 and data not shown). These 7 ESTs/genes include *ALX4*, *FLJ10450*, *FLJ23598*, *KIAA1580*, *LOC399888*, *LOC90139*, *MAPK8IP1*, and *SYT13*. The majority of the remaining ESTs/genes (31/32, 97%) were positive in DNA samples from CX2, indicating a localization to chromosome 11, but outside of the minimal liver tumor suppressor region of 11p11.2. One gene, *BHC80*, was detected in CX2 and CX4, indicating localization to a chromosomal site that is proximal to the minimal liver tumor suppressor region, but not contained within it (FIGURE 3.3). These results suggest that *ALX4*, *FLJ10450*, *FLJ23598*, *KIAA1580*, *LOC399888*, *LOC90139*, *MAPK8IP1*, and *SYT13* are potential candidates for the human 11p11.2 liver tumor suppressor gene based upon their localization to the minimal tumor suppressor region of human 11p11.2.

Transcription Analysis of Candidate Tumor Suppressor Genes from Human 11p11.2 in GN6TF-Derived Microcell Hybrid Cell Lines

The expression levels of *ALX4*, *FLJ10450*, *FLJ23598*, *KIAA1580*, *LOC399888*, *LOC90139*, *MAPK8IP1*, and *SYT13* were examined among the index panel of suppressed MCH cell lines (C1, CX2, and CX4) using RT-PCR. *FLJ10450*, *FLJ23598*, *KIAA1580*, *MAPK8IP1*, and *SYT13* were absent in GN6TF tumor cells but expressed uniformly among

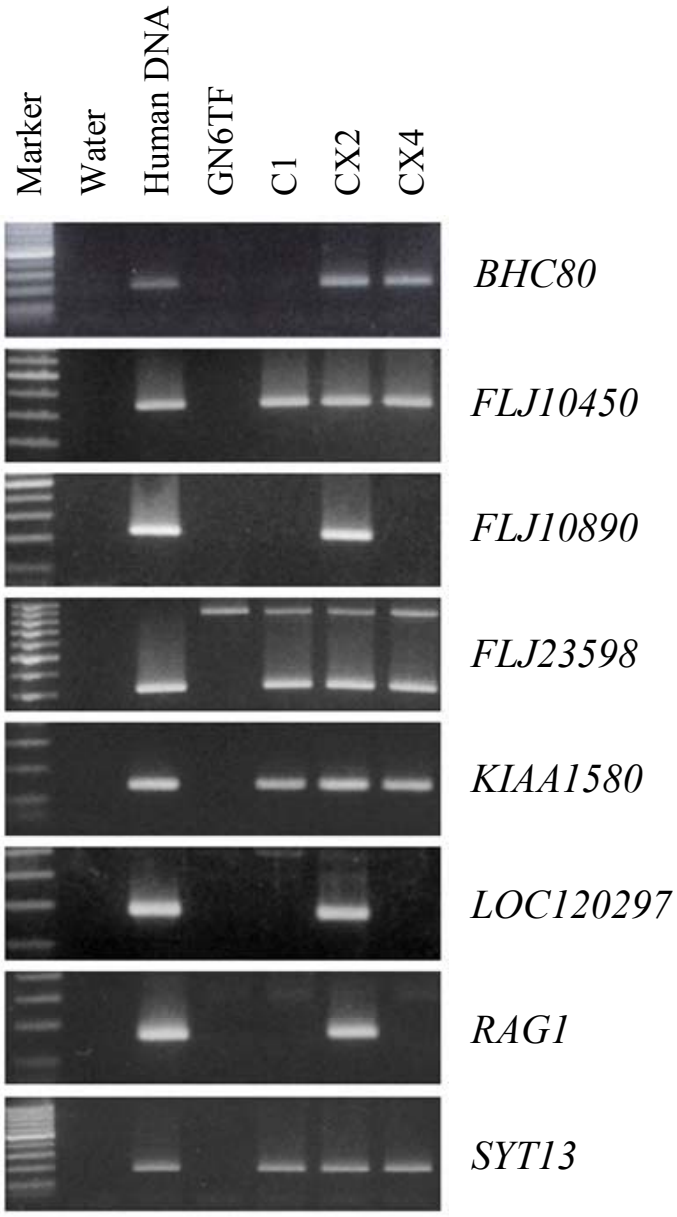

FIGURE 3.3. *Chromosome 11p11.2 deletion analysis of GN6TF-derived MCH cell lines*. Representative gels from deletion mapping of 11p11.2 with ESTs/genes that are positioned within human 11p11.2 are shown. ESTs/genes that map to the minimal tumor suppressor region are amplified in each MCH cell line (C1, CX2, and CX4).

the GN6TF-derived MCH cell lines (FIGURE 3.4). *ALX4* was expressed in CX2 and CX4 only, LOC90139 was found in CX2, and expression of LOC399888 was not detected in any of the GN6TF-derived MCHs (data not shown). Our previously established criteria for candidate liver tumor suppressor genes (71) dictate that candidate genes be expressed by each of these GN6TF-derived MCH cell lines. This result suggests that these five ESTs/genes represent good candidates for the human 11p11.2 liver tumor suppressor gene. Additional expression analyses of these ESTs/genes were conducted using RNA samples from GN6TF-derived MCH-derived tumor cell lines (GN6TF-11^{neo}CX2T1 and GN6TF-11^{neo}CX4T3). These tumor cell lines were established in cell culture from tumors that formed in syngeneic rats following transplantation of the GN6TF-11^{neo} MCH cell lines (40). In each case, the MCH-derived tumors developed with long latency compared to the parental GN6TF tumor line (40), indicative of tumor suppression. Molecular characterization of these MCH-derived tumor cell lines provided evidence that reexpression of tumorigenicity by these cells is accompanied by significant (if not complete) deletion of the introduced (suppressive) human chromosome (40). It is expected that the tumor suppressor gene that is active in this model system is lost in conjunction with these chromosomal deletions that result in restoration of the tumorigenic phenotype. In fact, no detectable level of expression of *FLJ10450*, *FLJ23598*, *KIAA1580*, and *SYT13* was observed in the MCH-derived tumor cell lines evaluated (data not shown), consistent with our expectations of a tumor suppressor gene. These results combine to suggest that *FLJ10450*, *FLJ23598*, *KIAA1580*, and *SYT13* are potential candidates for the human 11p11.2 liver tumor suppressor gene based upon their expression in GN6TF-derived MCH cell lines and loss of their expression in GN6TF-derived

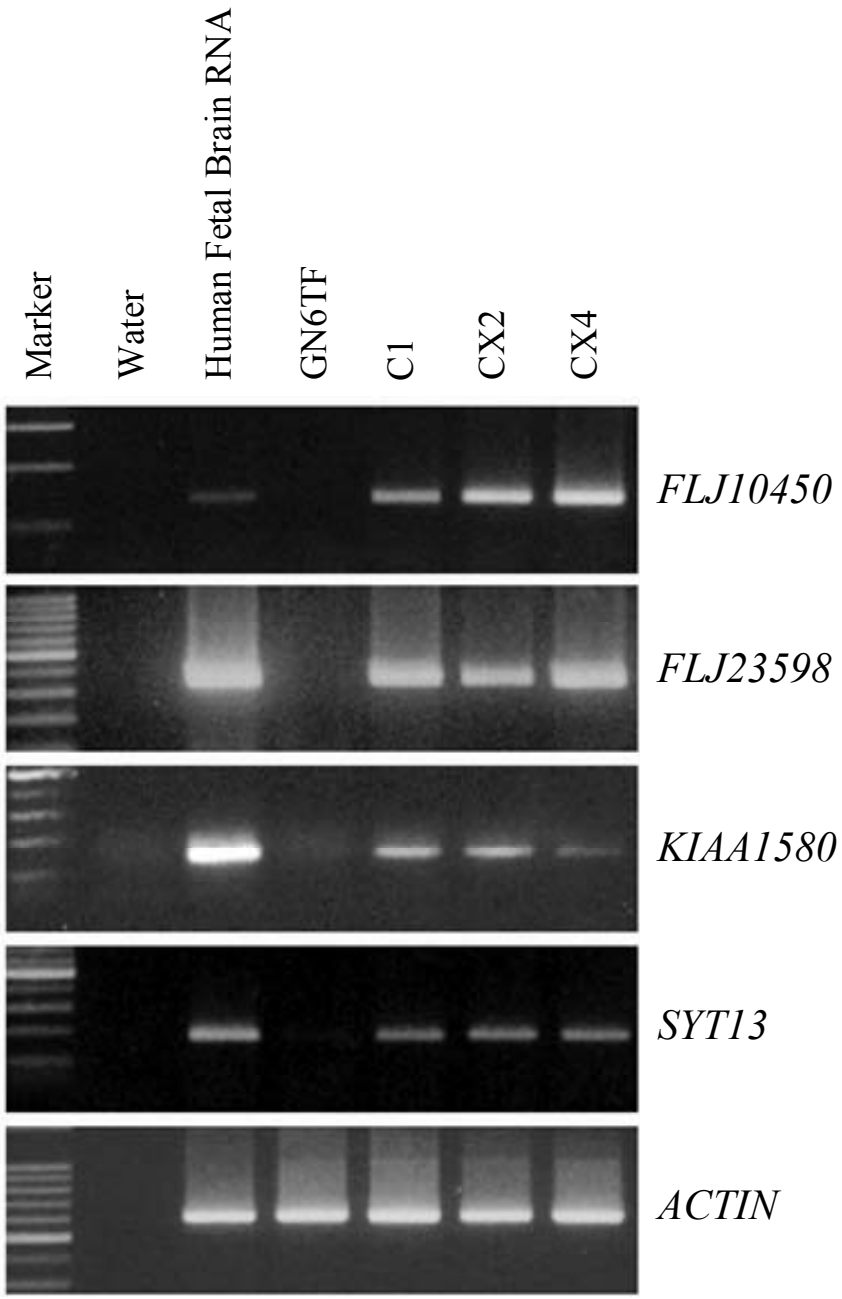

FIGURE 3.4. *Transcription analysis of GN6TF-derived MCH cell lines.* Representative gels showing expression patterns of the genes that were amplified in the GN6TF-derived cell lines. *β-actin* was amplified as a control for quality of the RT template.

MCH-derived tumor cell lines.

Deletion Analysis of Candidate Tumor Suppressor Genes from Human 11p11.2 in GN3TG and GP10TA-Derived Microcell Hybrid Cell Lines

The candidate ESTs/genes identified using GN6TF-derived MCH cell lines were further evaluated using two additional panels of MCH cell lines and MCH-derived tumor cell lines (41). Eight suppressed MCH cell lines derived from GN3TG (GN3TG-11^{neo} clones C2, C3, C4, C5, and C7) and GP10TA (GP10TA-11^{neo} clones C7, C11, and C12) were utilized, as well as four MCH-derived tumor cell lines (GN3TG-11^{neo} C3T1, C3T7, C4T3, and GP10TA-11^{neo} C7T3). Our previous studies implicated the human 11p11.2 liver tumor suppressor locus in the suppression of GN3TG-11^{neo} and GP10TA-11^{neo} MCH cell lines (41), suggesting that the same tumor suppressor gene(s) will be active (expressed in common) between these suppressed MCH cell lines and the suppressed GN6TF-derived MCH cell lines. In addition, GP10TA-11^{neo} C6 was analyzed. This MCH cell line is not suppressed for tumorigenicity and other para-neoplastic phenotypic traits (41). The lack of suppression in this MCH cell line is due to an interstitial deletion of the introduced human chromosome 11 that involves the 11p11.2 liver tumor suppressor region (41). Combined, these suppressed MCH, nonsuppressed MCH, and MCH-derived tumor cell lines represent excellent reagents for examination of candidate liver tumor suppressor genes.

Using DNA samples from the GN3TG-11^{neo} MCH, GP10TA-11^{neo} MCH, and MCH-derived tumor cell lines, *FLJ10450*, *FLJ23598*, *KIAA1580*, *MAPK8IP1*, and *SYT13* were analyzed by PCR to determine if each of these ESTs/genes is retained by these cells that differ in tumorigenic potential. PCR for *MAPK8IP1* was uninformative due to its non-species-specific expression in the parental GN3TG and GP10TA cell lines (data not shown).

FLJ10450 and *FLJ23598* were detected in DNA samples from 7/8 (88%) suppressed MCH cell lines evaluated (FIGURE 3.5), and were lost from each of the MCH-derived tumor cell lines analyzed (FIGURE 3.5 and data not shown). Furthermore, both of these ESTs were detected in DNA from the nonsuppressed GP10TA-11^{neo}C6 cell line (FIGURE 3.5). The loss of *FLJ10450* and *FLJ23598* from the suppressed GN3TG-11^{neo}C5 cell line, combined with their retention in the nonsuppressed MCH line, suggest that neither of these genes are required/sufficient for suppression of the tumorigenic phenotype in this model system. *KIAA1580* was detected in each of the 8 suppressed GN3TG-11^{neo} and GP10TA-11^{neo} MCH cell lines (FIGURE 3.5), and was lost from each of four MCH-derived tumor cell lines (FIGURE 3.5 and data not shown). These results are consistent with the pattern that we expect for a tumor suppressor gene. However, retention of *KIAA1580* in the non-suppressed GP10TA-11^{neo}C6 cell line (FIGURE 3.5) argues against this EST being a strong candidate tumor suppressor gene. *SYT13* was detected in the DNA of 8/8 (100%) suppressed MCH cell lines (FIGURE 3.5), was lost from the DNA of 4/4 (100%) MCH-derived tumor cell lines ((FIGURE 3.5) and data not shown), and was not found in the DNA of the non-suppressed GP10TA-11^{neo}C6 cell line (FIGURE 3.5). These results combine to suggest that *SYT13* is a strong candidate for the 11p11.2 liver tumor suppressor gene.

Transcription Analysis of Candidate Tumor Suppressor Genes from Human 11p11.2 in GN3TG and GP10TA-Derived Microcell Hybrid Cell Lines

The expression of *FLJ10450*, *FLJ23598*, *KIAA1580*, and *SYT13* was examined among the GN3TG-11^{neo} MCH, GP10TA-11^{neo} MCH, and MCH-derived tumor cell lines using RT-PCR to determine patterns of expression of these ESTs/genes for cell lines with

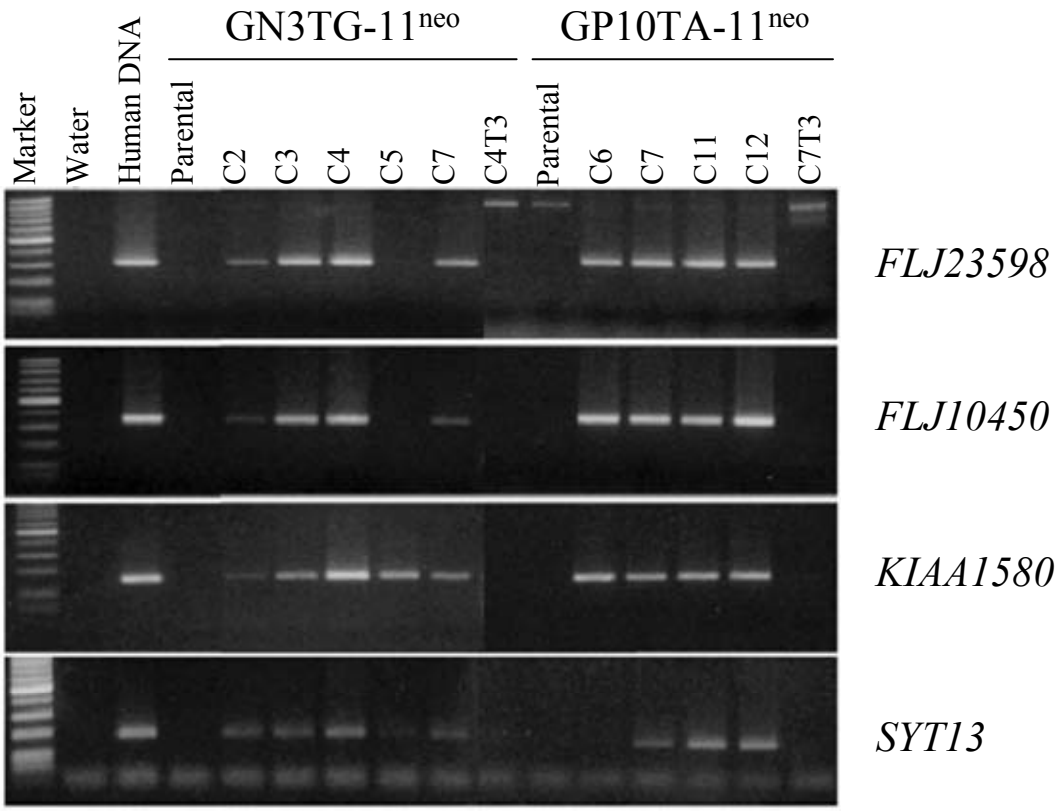

FIGURE 3.5. *Deletion analysis of GN3TG- and GP10TA- derived MCH cell lines.* Representative gels from PCR analysis of ESTs/genes representing potential candidate liver tumor suppressor genes among GN3TG-derived and GP10TA-derived MCH and MCH-derived tumor cell lines are shown.

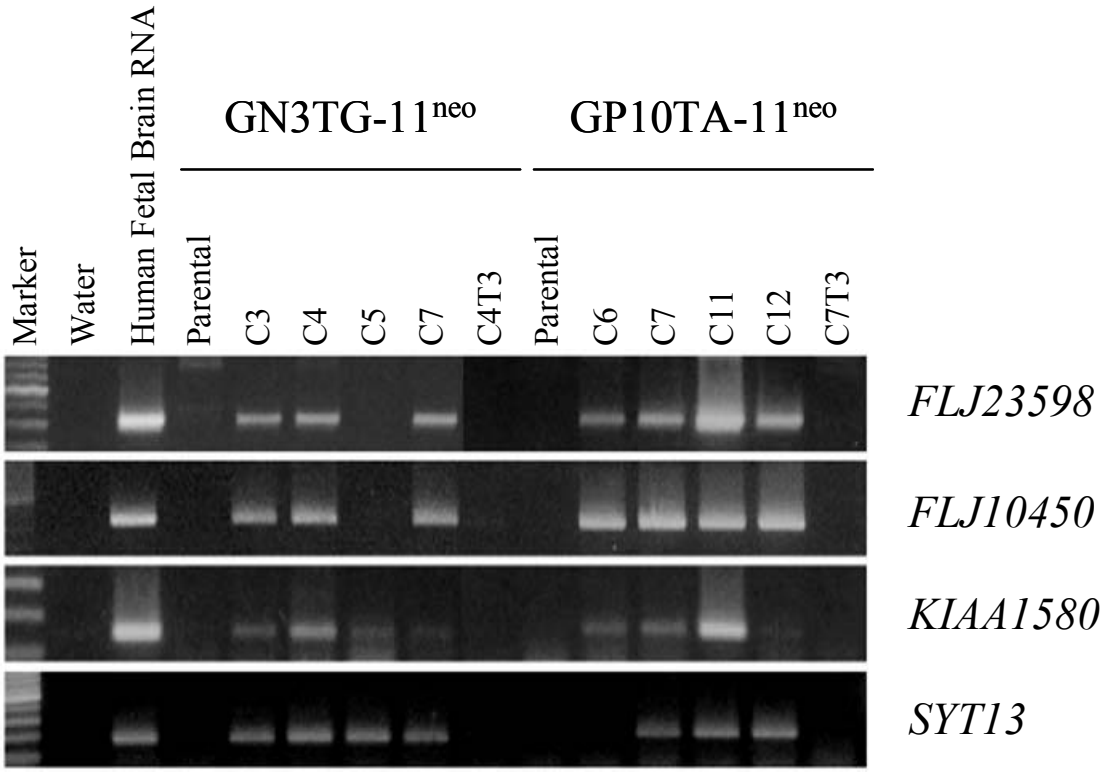

FIGURE 3.6. *Transcription analysis of GN3TG- and GP10TA- derived MCH cell lines.* Four of the genes that amplified in GN6TF-derived cell lines were evaluated by RT-PCR among the suppressed GN3TG- and GP10TA-derived MCH and MCH-derived tumor cell lines. *β-actin* was amplified as a control for quality of the RT template (data not shown).

known phenotype/genotype. *FLJ10450* and *FLJ23598* were expressed at easily detectable levels by 6/7 (86%) suppressed MCH cell lines (FIGURE 3.6), and this expression was extinguished in the MCH-derived tumor cell lines (FIGURE 3.6 and data not shown). As expected, GN3TG-11^{neo} C5 did not express mRNA for either *FLJ10450* or *FLJ23598* (FIGURE 3.6). *KIAA1580* was expressed by each of the suppressed MCH cell lines, although the levels of expression varied (FIGURE 3.6). Expression of *KIAA1580* was not detected in MCH-derived tumor cell lines (FIGURE 3.6 and data not shown). *FLJ10450*, *FLJ23598*, and *KIAA1580* were expressed by the nonsuppressed GP10TA-11^{neo}C6 MCH cell line (FIGURE 3.6). These results combine to suggest that *FLJ10450*, *FLJ23598*, and *KIAA1580* are not good candidates for the human 11p11.2 liver tumor suppressor gene based upon their lack of consistent expression among suppressed MCH cell lines and/or their expression in a non-suppressed MCH cell line. In contrast, robust expression of *SYT13* was detected in 7/7 (100%) suppressed MCH cell lines (FIGURE 3.6), and was not detected in 4/4 (100%) of MCH-derived tumor cell lines (FIGURE 3.6 and data not shown). Furthermore, expression of *SYT13* was not detected in GP10TA-11^{neo} C6 (FIGURE 3.6), as expected. These results suggest that *SYT13* is a strong candidate for the human 11p11.2 liver tumor suppressor gene.

EXPRESSION OF 11P11.2 CANDIDATE TUMOR SUPPRESSOR GENES IN HUMAN HEPATOCELLULAR CARCINOMA CELL LINES

Using specific criteria requiring differential expression of human 11p11.2 candidate tumor suppressor genes in a panel of suppressed and nonsuppressed MCHs, we identified *SYT13* as a strong tumor suppressor candidate. In parallel studies with identical selection criteria, we additionally identified the *SYT13*-proximal genes *TP53I11* and *PRDM11* as putative 11p11.2 tumor suppressor genes (72). To investigate if one or more of these genes

play a role in the pathogenesis of human HCC we examined the expression of candidate genes in a series human hepatocellular carcinoma cell lines.

Deletion and Transcription Analysis of 11p11.2 Candidate Tumor Suppressor Genes in Human Hepatocellular Carcinoma Cell Lines

The HCC cell lines used in this study (TABLE 2.1) were established from patients in North America, Japan, China, South Africa, and South Korea (49). We expected that candidate genes with tumor suppressor function would be down-regulated or extinguished in some portion of HCC cell lines, consistent with the elimination of a specific tumor suppressor function in these cells. The expression levels of *TP53I11, PRDM11,* and *SYT13* varied considerably among these cell lines (FIGURE 3.7.A). The expression of *TP53I11* was lost or decreased (<50% relative to mRNA in Chang) in 11/19 (58%) HCC cell lines and *SYT13* was lost or decreased (<50%) in 7/19 (37%) (FIGURE 3.7.B). *PRDM11* was expressed at normal levels in the majority of HCC cell lines, with diminished expression (<50%) noted in only 4/19 (21%) (FIGURE 3.7.B). PCR analysis of template DNA isolated from these cell lines show that the candidate tumor suppressor genes are not deleted (FIGURE 3.7.C), which suggests that gene deletion does not account for the loss of mRNA expression detected in the HCC cell lines. These results demonstrate that these candidate tumor suppressor genes identified in a rat-human MCH model system, are functionally deficient in subsets of human HCC cell lines, consistent with the activity of a liver tumor suppressor gene. Several other genes from 11p11.2 were evaluated for expression in this group of HCC cell lines (FIGURE 3.7.A). *FLJ10450* was expressed in all HCC cell lines, the expression of *FLJ23598* was decreased in only 5/19 (26%) HCC cell lines, and *KIAA1580* was lost or decreased in 8/19 (42%) HCC cell lines (FIGURE 3.7.A). These results demonstrate that several of the genes

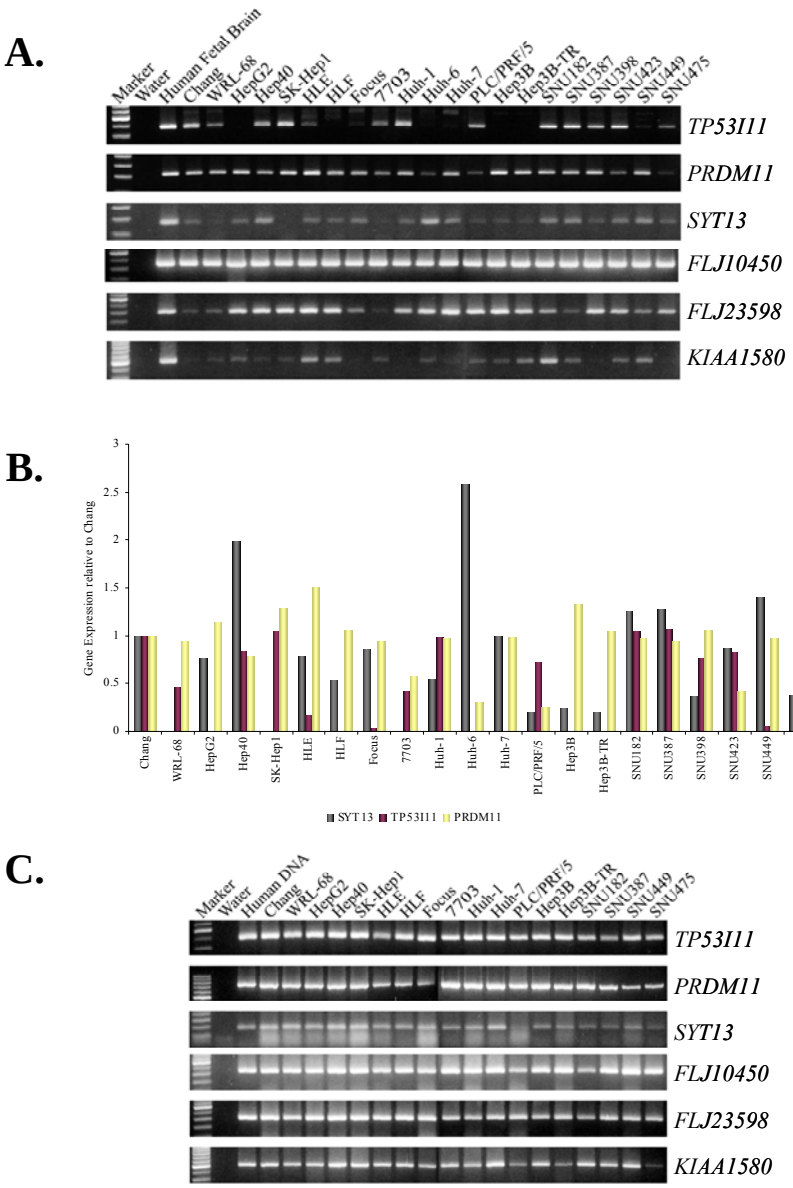

FIGURE 3.7. *Deletion and transcription analysis of candidate 11p11.2 tumor suppressor genes in HCC cell lines.* (A) Semi-quantitative RT-PCR of candidate tumor suppressor genes in HCC cell lines. Human fetal brain RNA was used as a positive control. (B) Densitometry of *SYT13*, *PRDM11*, and *TP53I11* expression from RT-PCR in panel (A) using ImageJ software. Signal strength is expressed relative to the normal liver cell line Chang. (C) PCR of candidate genes using template DNA from HCC cell lines and genomic DNA as a positive control.

from 11p11.2 that are not considered candidate tumor suppressor genes are expressed at normal or near normal levels in HCC cell lines, strengthening the argument for elimination of these genes from further consideration.

Epigenetic Regulation of Candidate Tumor Suppressor Genes in Human Hepatocellular Carcinoma Cell Lines

Because methylation-dependent epigenetic silencing represents a common mechanism for inactivation of tumor suppressor genes in several types of tumors (73-76) (mechanism reviewed in FIGURE 3.8), and our analysis of candidate gene expression in HCC cell lines revealed a loss or reduction of several candidate genes with no clear evidence for gene deletion (FIGURE 3.7), we evaluated the possibility that DNA methylation may be responsible for inactivation of these genes in a subset of HCC cell lines. Inspection of candidate 11p11.2 tumor suppressor genes *TP53I11* and *SYT13* reveals a dense CpG dinucleotide-rich region at the promoter/exon 1 of these genes (but not in *PRDM11*) (FIGURE 3.9), which predicts the potential for methylation-dependent silencing.

After treatment of HCC cell lines (FOCUS, SNU475, SNU398, Huh-1, SNU449, Hep3B, PLC/PRF/5, and HepG2) with 5-aza, TaqMan real-time RT-PCR of treated and DMSO control-treated cells was performed targeting *SYT13*, *TP53I11*, *PRDM11*, and *WT1*. *WT1* has a CpG dinucleotide-rich region at the promoter/exon 1 (FIGURE 3.9), has been identified as a methylation-target in HCC (77), and has been implicated in 11p11.2-mediated tumor suppression (43). The $\Delta\Delta C_T$ method was used to quantitate the fold change in gene expression after 5-aza treatment relative to the vehicle control. Expression of genes in several cell lines after treatment with DMSO only was undetectable at the C_T maximum of 40 cycles [denoted (-) in FIGURE 3.10.B and assigned a C_T of 40 for calculation of fold-change]

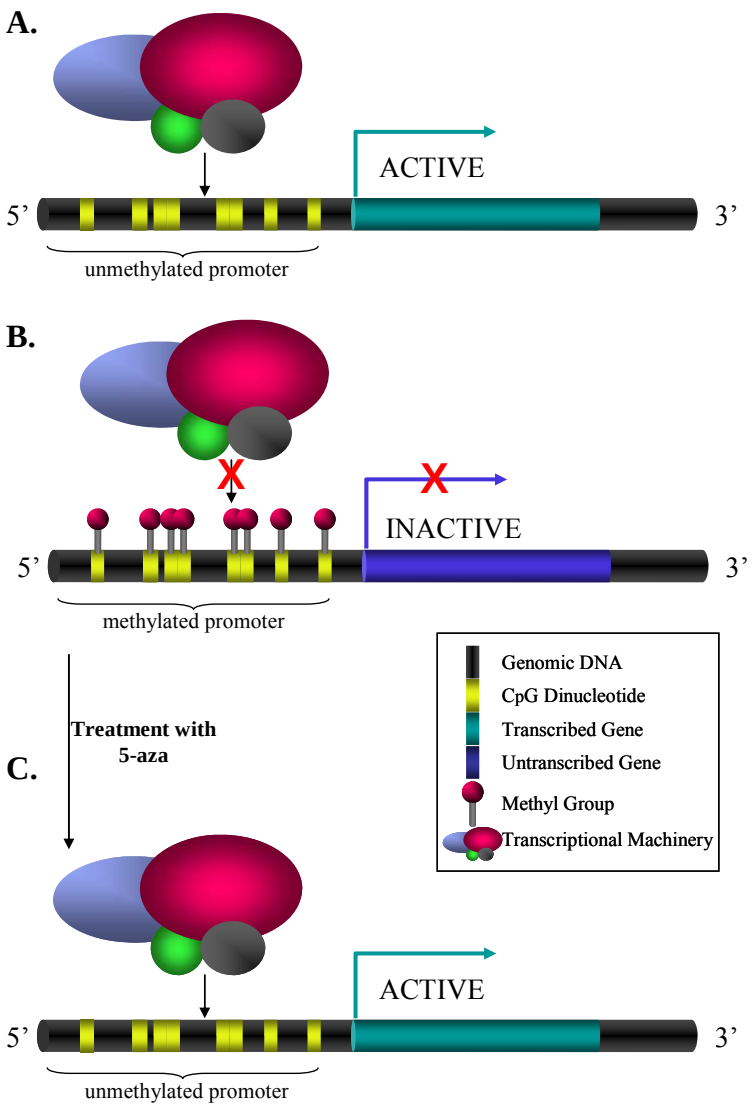

FIGURE 3.8. *Mechanism for methylation-dependent silencing of tumor suppressor genes*. (A) A hypothetical gene containing a promoter CpG island is depicted. Interaction of the transcriptional machinery with the unmethylated promoter results in gene transcription. (B) Methylation (or hypermethylation) of the promoter CpG island directly or indirectly interferes with the interaction between the transcriptional machinery and the promoter sequence, resulting in loss of gene expression. (C) Treatment of cells with demethylating agents (such as 5-aza) results in reexpression of silenced genes in response to promoter demethylation.

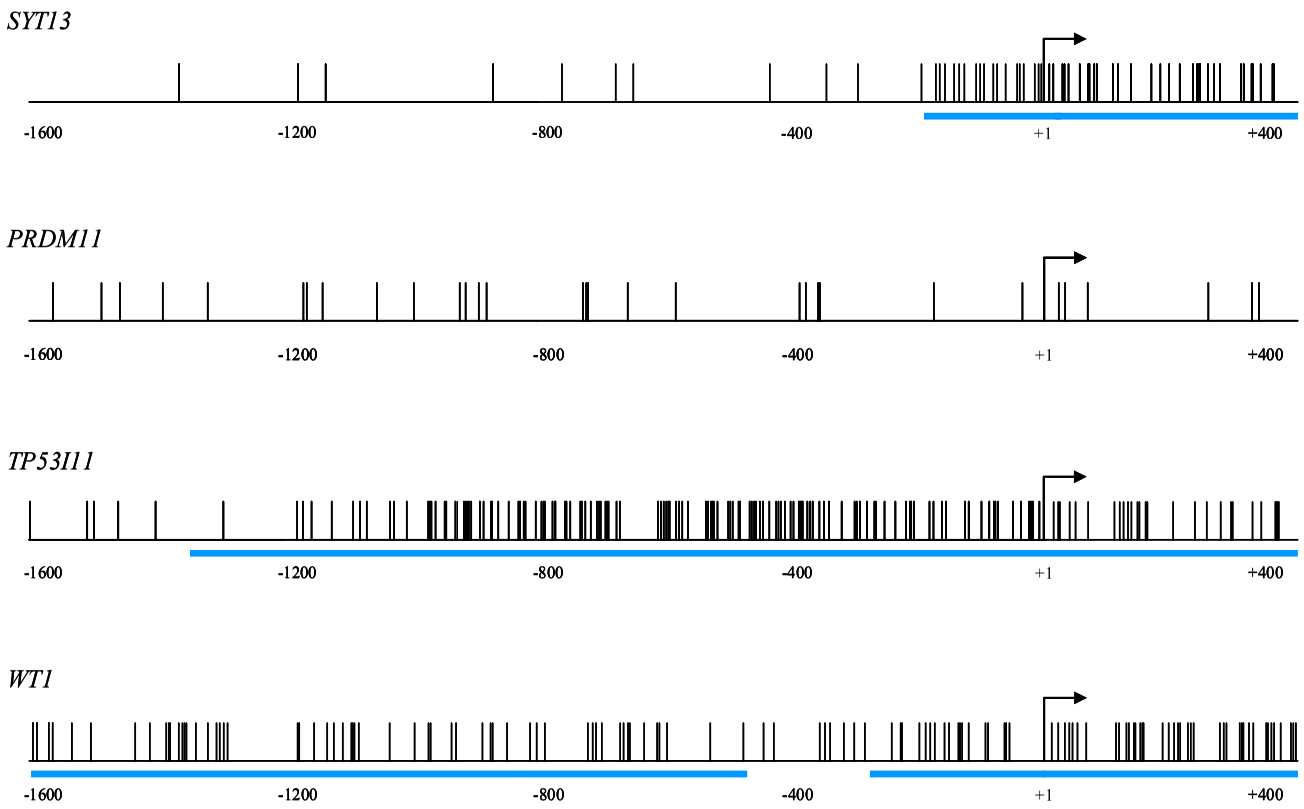

FIGURE 3.9. *CpG dinucleotides in the promoter region of 11p11.2 genes and* WT1. A scaled representation of the promoter regions (-1600 to +400) of *SYT13*, other 11p11.2 genes (*PRDM11* and *TP53I11*), and *WT1* are shown. Tick marks represent CpG dinucleotides and blue lines demarcate CpG islands. The arrow located at +1 indicates the start site for transcription. *PRDM11* does not contain a CpG island in its promoter/exon 1.

A.

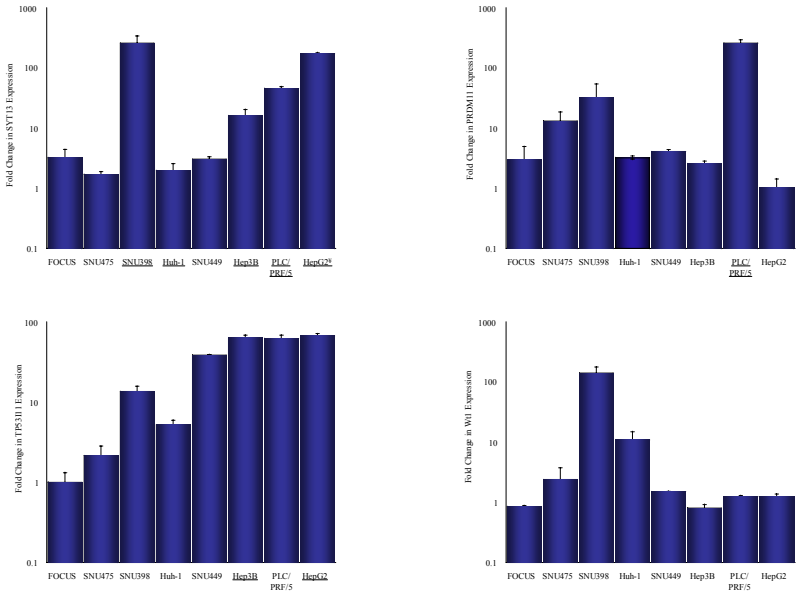

B.

Cell Line	*SYT13*		*PRDM11*		*TP53I11*		*WT1*	
	DMSO	5aza	DMSO	5aza	DMSO	5aza	DMSO	5aza
FOCUS	++	++	+++	+++	++++	++++	-	-
SNU475	++	++	++	+++	+++	++++	++	++
SNU398	-	++	++	+++	+++	++++	+	+++
Huh-1	-	+	++	++	+++	++++	+++	++++
SNU449	+++	++++	++	+++	+	+++	++++	++++
Hep3B	-	+	++	+++	-	++	++++	++++
PLC/PRF/5	-	++	-	++	++	++++	++++	++++
HepG2	-	++	++	++	-	++	++++	++++

FIGURE 3.10. *Expression of candidate 11p11.2 tumor suppressor genes after treatment of HCC cell lines with 5-aza.* (A) Fold-change expression of *SYT13*, *PRDM11*, *TP53I11*, and *WT1* in 5aza-treated compared to DMSO control-treated HCC cell lines using the Comparative $\Delta\Delta C_T$ Method. Average changes determined by assigning a C_T of 40 to DMSO-treated cells are underlined. (B) Qualitative analysis of gene expression using ΔC_T values. - =ΔC_T > 20; + = ΔC_T 15-19; ++ = ΔC_T 12-14; +++ = ΔC_T 8-11; ++++ = ΔC_T <8.

which suggests that DMSO alone may reduce the basal expression levels of the genes depicted in FIGURE 3.7. Nonetheless, strikingly increased expression for *SYT13*, *TP53I11*, *PRDM11*, and *WT1* was observed in several HCC cell lines after treatment with 5-aza (FIGURE 3.10.A). Expression of the 11p11.2 candidate tumor suppressor gene *SYT13* increased greater than 5-fold in 4/8 5-aza treated cell lines including SNU398, Hep3B, PLC/PRF/5, and HepG2 (FIGURE 3.10.A) and *TP53I11* increased >5-fold in 6/8 cell lines, including SNU398, Huh-1, SNU449, Hep3B, PLC/PRF/5, and HepG2 (FIGURE 3.10.A). The expression of *PRDM11* (with no CpG island) exceeded a 5-fold increase in 3/8 HCC cell lines, including SNU475, SNU398, and PLC/PRF/5 (FIGURE 3.10.A). Surprisingly, *WT1* induction exceeded a 5-fold increase in response to 5-aza treatment in only 2/8 HCC cell lines [SNU398 and Huh-1 (FIGURE 3.10.A)]. This may be explained by the robust baseline expression of *WT1* in several of these cell lines as shown in FIGURE 3.10.B. These results indicate that promoter methylation may be directly or indirectly responsible for silencing of the candidate 11p11.2 tumor suppressor genes in a subset of HCC. Additionally, induction of *WT1* in response to treatment with 5-aza in these cell lines does not appear to correlate with 5-aza-mediated induction of *SYT13*, *TP53I11*, or *PRDM11* mRNA. This suggests that the previously observed link between 11p11.2 mediated tumor suppression and Wt1 induction must either involve an indirect pathway or require other mechanisms/modifications that are not represented by absolute steady-state levels of tumor suppressor gene mRNA.

RNAI-MEDIATED SILENCING OF SYT13 IN THE SUPPRESSED CX4 MICROCELL HYBRID CELL LINE

Synaptotagmin XIII (*SYT13*) is an excellent candidate 11p11.2 tumor suppressor gene based on its differential expression in suppressed and non-suppressed MCH cell lines and

loss of expression in several human HCC cell lines. To further characterize a functional role for *SYT13* in the MCH model system, we employed RNA interference to silence this gene in suppressed GN6TF-11^{neo}CX4 MCH cells.

Molecular Analysis of SYT13*i and* SYT13*s Clones*

SYT13 Expression: CX4 cells transfected with the *SYT13*-targeting (designated i1-i12) and scrambled-control (designated s1-s8) psiRNA vectors were expanded and SYT13 knockdown was assessed by western blot. Protein analysis revealed a marked reduction of SYT13 protein in several *SYT13*i cell lines (FIGURE 3.11). The SYT13 protein is approximately 66 kDa in size (78, 79), but synaptotagmin protein family members have been shown to form SDS-resistant dimers (80). We detected both monomer and dimer forms of immunoreactive SYT13 protein using the α-SYT13 antibody. The monomeric and dimeric forms of SYT13 were found at similar levels in *SYT13*-transfected cells relative to the CX4 cells (FIGURE 3.11). The antibody, which was designed for human SYT13 specificity (FIGURE 2.3), recognizes the rat Syt13 (rSyt13) monomer in GN6TF cells. However, the amount of SYT13 detected in CX4 cells exceeds that of GN6TF cells reflecting the contribution of the human allele in the MCH cell line. *SYT13*i3, i5, i6, i12, and the scrambled control-transfected clone s1 express reduced levels of SYT13 protein (less than 50% for both monomer and dimer) compared to CX4 (FIGURE 3.11.B), while the SYT13 monomer in s8 was unaffected. The apparent protein attenuation in these scrambled control-transfected cell lines is an unexpected result. Because the scrambled target differs from the *SYT13* sequence in only 4 of 21 nucelotides (FIGURE 2.5.C), this observation may be explained by inhibition of protein translation which is a poorly-understood mechanism identified in microRNA–mediated (miRNA) gene silencing which requires mismatched

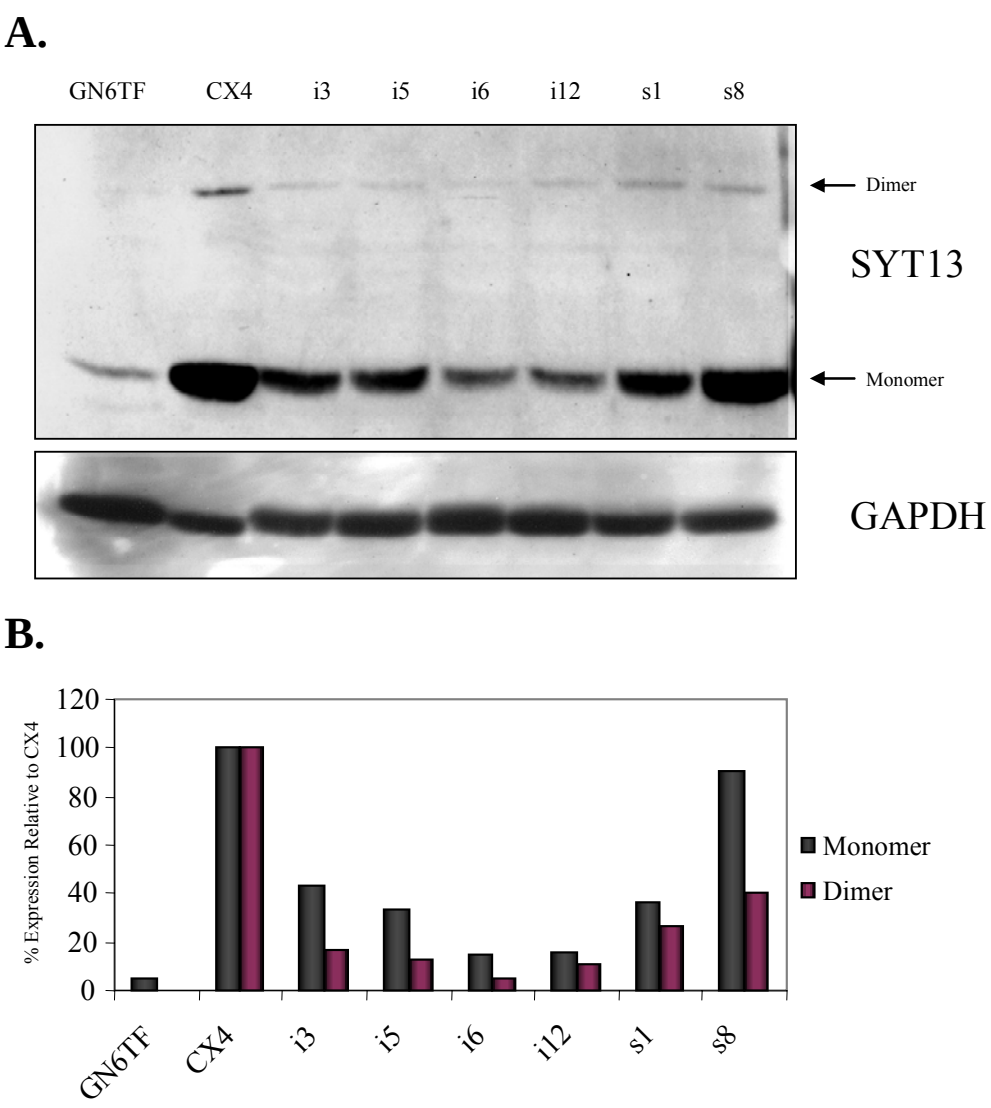

FIGURE 3.11. *Evidence of shRNA-mediated silencing of SYT13.* (A) Western analysis of SYT13 protein expression in GN6TF, CX4, *SYT13*i, and *SYT13*s cell lines. The migration of the monomeric (66 kDa) and dimeric (130 kDa) forms of SYT13 are indicated. This blot shows clear knockdown of both the dimeric and monomeric species of SYT13 among *SYT13*i cell lines. The level of SYT13 is decreased in the SYT13s cell lines, but not eliminated. (B) Quantitation of protein expression level shown in (A) normalized to GAPDH expression in (A) with densitometry.

hybridization to the mRNA target (81-83). Western blot analysis of additional *SYT13*i- (i2, i4, i7, and i9) and *SYT13*s- (s2 and s3) transfected cell lines did not demonstrate any appreciable change in protein levels, therefore providing excellent internal controls for this study. *SYT13* mRNA expression was analyzed by both quantitative and semi-quantitative RT-PCR. Neither measure revealed a change in gene expression (FIGURE 3.12.A and data not shown). Thus, there is a clear lack of correspondence between *SYT13* mRNA levels and SYT13 protein levels in targeted cell lines. This phenomenon has been noted by other investigators using a similar experimental system (84, 85), and these data strongly suggest that the knockdown of SYT13 observed in this model system, using the shRNA target described, is accomplished through a post-transcriptional mechanism, such as inhibition of translation and/or regulation of heterochromatin (81, 86).

shRNA-mediated interferon response and potential off-target effects: Transfection of cells with shRNA can result in an interferon response (87-89) or off-target effects (86). In studies that have shown an interferon response to shRNA transfection, numerous interferon-associated genes were found to be induced 2-fold to 5-fold (89). The gene expression profile of both *SYT13*i and *SYT13*s cell lines (including *SYT13*i3, i5, i12, and s1) were evaluated to determine the levels of expression of 36 interferon-associated genes (TABLE 3.1). There was minimal change in gene expression for these genes among *SYT13*i and *SYT13*s cells when compared to CX4 cells; 35/36 interferon-associated genes were expressed at levels similar to or less than that observed in CX4 cells (TABLE 3.1 and FIGURE 3.13), and the other (*Isg20*, interferon stimulated exonuclease 20) was modestly induced (2-fold). These results suggest that no interferon-associated gene expression changes accompany the transfection of *SYT13*i or *SYT13*s shRNA expression vectors in CX4 cells.

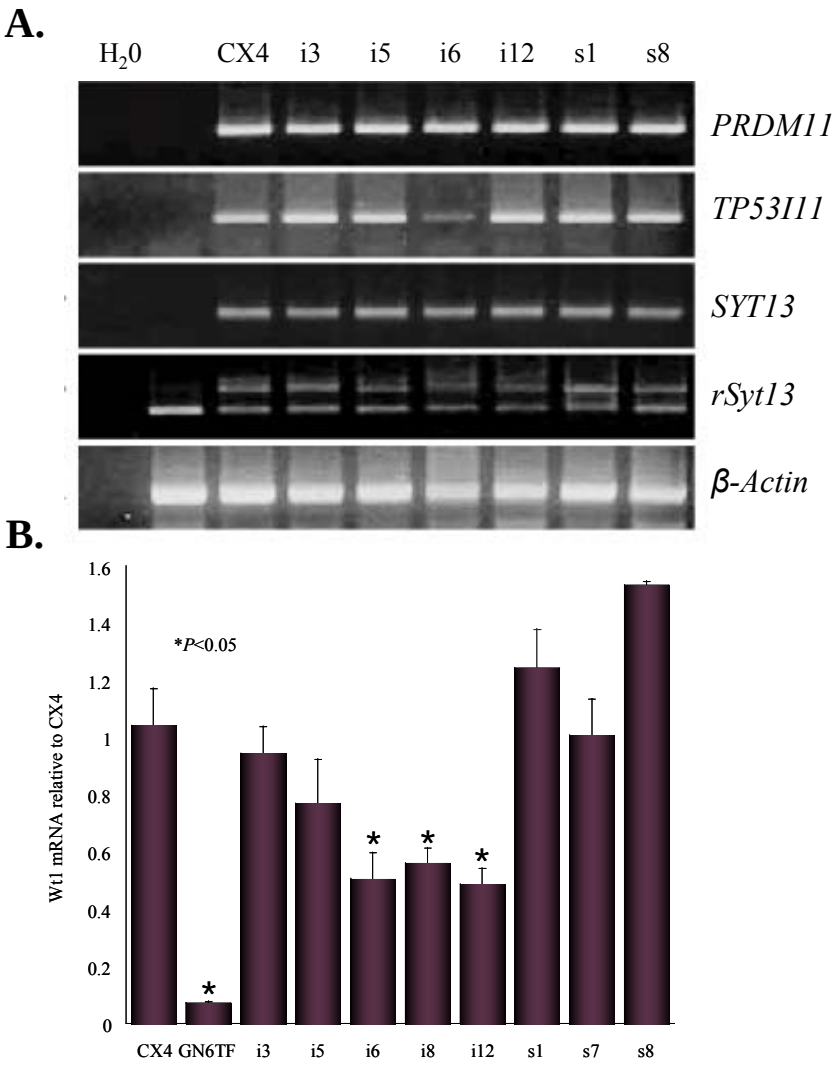

FIGURE 3.12. *Molecular characterization of* SYT13*i- and* SYT13*s-transfected cell lines.* (A) Semi-quantitative RT-PCR of human 11p11.2 genes in *SYT13*i and *SYT13*s clones shows no change in mRNA expression of these genes in most shRNA-transfected cell lines (a decrease of *TP53I11* expression was seen in *SYT13*i6). Primers for r*Syt13* cross-react with the human gene (top band), but no significant change in mRNA for either the human or the rat gene was detected. (B) Quantitative real-time RT-PCR analysis of *Wt1* expression in *SYT13*i and *SYT13*s cell lines expressed relative to CX4 cells. **P*< 0.05 compared to CX4 using the one-way ANOVA.

siRNAs have also been reported to affect translation of unintended transcripts containing partial complementarity to targets (85, 90). A BLAST search (http://www.ncbi.nlm.nih.gov/blast/) of the 21nt sequences of the *SYT13*i target and *SYT13*s scrambled control identified several potential off-target genes in the rat genome. The *SYT13*i target matched 31 potential off-target genes with 14/21 (67%) to 18/21 (86%) sequence identity (67% n=14, 71% n=8, 76% n=5, 81% n=1, 86% n=3) (TABLE 3.2). Likewise, the *SYT13*s control matched 25 potential off-targets with 67%-86% sequence identity (67% n=9, 71% n=5, 76% n=4, 81% n=6, 86% n=1) (TABLE 3.2). Overall, the *SYT13*i and *SYT13*s shRNAs match 33 off target genes with $\geq$15/21 (71%) sequence identity. However, microarray analysis failed to show significant alterations in mRNA levels of these potential off-target genes. No analysis of the corresponding protein products was performed.

Gene expression in SYT13*i and* SYT13*s clones:* RNA samples corresponding to zeocin-resistant *SYT13*i and *SYT13*s clones were analyzed by semi-quantitative and real-time RT-PCR to determine RNAi-mediated alterations in the expression of several genes, including human genes carried on human 11p11.2 and rat *Wt1*, which has been implicated in 11p11.2-mediated tumor suppression in our model system (43). In addition to *SYT13*, FIGURE 3.12.A shows relative expression levels of the human genes *PRDM11* and *TP53I11* which are located within a ~350 Kbp region with *SYT13* on human 11p11.2. The semi-quantitative RT-PCR results do not show any change in expression of these genes between CX4, *SYT13*i-, and *SYT13*s-transfected cell clones, suggesting that knockdown of the SYT13 protein does not result in secondary alterations in the expression of other 11p11.2 genes.

TABLE 3.1. *Expression of interferon-related genes in* SYT13*i and* SYT13*s cell lines relative to CX4*

UniGene Number	*Gene Symbol*	Gene Description	Log Ratio vs. CX4		
			s1	i12	i5
Rn.10089	*Cdkn1a*	cyclin-dependent kinase inhibitor 1A	-0.31	-0.49	-0.30
Rn.48054	*G1p2*	similar to interferon-stimulated protein (LOC298693)	0.82	-0.25	-0.70
Rn.25736	*Gbp2*	guanylate binding protein 2, interferon-inducible	-0.46	-0.73	-0.20
Rn.3765	*Icsbp1*	similar to interferon consensus sequence-binding protein (LOC292060)	-0.21	-0.38	-0.03
Rn.3867	*Ifi27l*	interferon, alpha-inducible protein 27-like	0.14	-0.78	-0.71
Rn.44680	*Ifi35*	similar to Interferon-induced 35 kDa protein homolog (LOC287719)	-0.21	-0.06	-0.42
Rn.22087	*Ifitm1*	similar to interferon induced transmembrane protein 2 like (LOC293618)	0.21	0.12	0.06
Rn.107166	*Ifitm3l*	interferon induced transmembrane protein 3-like	-0.04	-2.23	-1.52
Rn.108174	*Ifitm3l*	interferon induced transmembrane protein 3-like	-0.85	-1.89	-1.61
Rn.105738	*Ifnar1*	similar to interferon alpha/beta receptor (LOC288264)	-0.26	-0.20	-0.32
Rn.119051	*Ifnb1*	interferon, beta 1	0.14	0.20	0.10
Rn.10795	*Ifng*	interferon gamma	0.07	0.10	0.01
Rn.19927	*Ifngr*	interferon gamma receptor	-0.37	-0.43	-0.44
Rn.23305	*Ifngr2*	similar to interferon gamma receptor 2 (LOC360697)	0.08	-1.00	-0.62
Rn.104672	*Ifnk*	similar to interferon kappa precursor (LOC313152)	0.19	0.11	0.16
Rn.3723	*Ifrd1*	interferon-related developmental regulator 1	-0.06	-0.26	-0.26
Rn.20083	*Igifbp*	interferon gamma inducing factor binding protein	0.16	-0.15	-0.16
Rn.6396	*Irf1*	interferon regulatory factor 1	-0.40	-0.58	-0.66
Rn.107887	*Irf2*	similar to interferon regulatory factor 2 (LOC290749)	-0.03	0.26	0.01
Rn.1499	*Irf3*	similar to interferon regulatory factor 3 (LOC292892)	-0.06	-0.11	-0.15
Rn.17870	*Irf5*	similar to interferon regulatory factor 5 (LOC296953)	0.03	0.10	0.15
Rn.101159	*Irf7*	similar to interferon regulatory factor 7 (LOC293624)	-0.37	-0.54	-0.28
Rn.16103	*Isg20*	similar to interferon-stimulated protein; DnaQL protein (LOC293052)	-0.25	1.01	-0.29
Rn.35673	*Isgf3g*	similar to interferon stimulated gene factor 3 gamma (LOC305896)	0.01	0.10	-0.23
Rn.7391	*Mig*	monokine induced by gamma interferon	0.06	0.07	-0.01
Rn.10373	*Mx1*	myxovirus (influenza virus) resistance	0.11	-0.07	0.06
Rn.28882	*Ndufv2*	24-kDa subunit of mitochondrial NADH dehydrogenase	0.00	-0.03	-0.04
Rn.10383	*Oas1*	25 oligoadenylate synthetase	0.01	0.12	0.08
Rn.10022	*Prkr*	protein kinase, interferon-inducible double stranded RNA dependent	-0.06	-0.14	-0.16
Rn.2742	*Psme1*	protease (prosome, macropain) 28 subunit, alpha	-0.08	0.32	-0.19
Rn.109376	*Psme2*	protease (prosome, macropain) 28 subunit, beta	-0.07	-0.08	-0.46
Rn.79620	*Pumag*	interferon-gamma inducible gene, Puma-g	0.04	-0.21	-0.19
Rn.33229	*Stat1*	signal transducer and activator of transcription 1	-0.18	-0.16	-0.33
Rn.2605	*Tmsb4x*	thymosin beta-4 x-linded	-0.12	-0.34	-0.23
Rn.35775	---	ORF homologous to two human interferon-inducible proteins (LOC309526)	-0.04	-0.04	-0.01
Rn.101760	---	similar to interferon-inducible GTPase (LOC307414)	0.00	0.00	-0.07

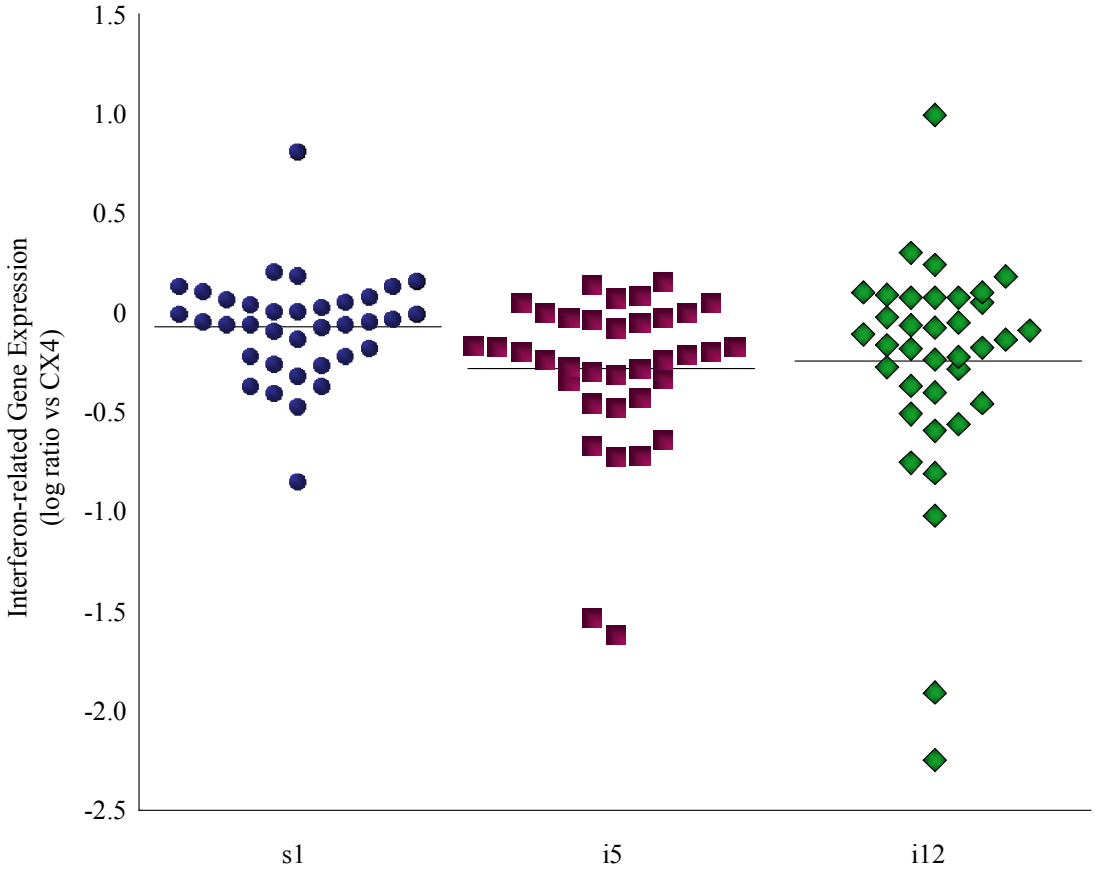

FIGURE 3.13. *Interferon response in* SYT13*i- and* SYT13*s-transfected cell lines.* Log-ratios of interferon-associated gene expression compared to CX4 for s1, i5, and i12 cell lines. Lines represent mean values.

TABLE 3.2. *Rat genes with sequence similarity to the* SYT13*i and* SYT13*s targets*

Gene	% Sequence Identity	Location	Function
***SYT13*i**			
Cnga3	86% (18/21)	2041/2231	olfactory transduction
Cntnap1	86% (18/21)	1055/5379	glial-neuron communication during development
Kcna3	86% (18/21)	1566/2956	delayed rectifier potassium channel activity
RGD1306404	81% (17/21)	2762/376	similar to chondroitin synthase
Camk2d	76% (16/21)	4434/5637	calcium/calmodulin dependent protein kinase
Cgm3	76% (16/21)	427/2761	cytokinin biosynthesis
Kdelc1	76% (16/21)	2405/2463	located in ER, function unknown
LOC686731	76% (16/21)	12020/23862	similar to mucin 17
RGD1308422	76% (16/21)	12311/25273	similar to ovarian cancer related tumor marker CA125
Akap13	71% (15/21)	738/9768	scaffolding proteins for Rho signaling pathway, protein kinase A-anchoring protein
Barhl1	71% (15/21)	1871/2393	DNA-binding transcription regulator
Ddx26	71% (15/21)	4255/4915	3' end processing of snRNAs
Gap	71% (15/21)	178/737	inward-rectifier type potassium channel
Igsf6	71% (15/21)	1742/2244	cell-surface receptor linked signal transduction
Kcnj6	71% (15/21)	3767/16380	potassium channel activity
Lama2	71% (15/21)	9153/9715	laminin alpha 2 subunit
Tra1	71% (15/21)	2328/3215	molecular chaperone protein, histone acetylation
Centb1	67% (14/21)	466/2503	GTPase regulation
Falz	67% (14/21)	4318/8151	transcriptional regulation
Gcn5l2	67% (14/21)	2881/3052	transcriptional activator, histone acetylation
Hdh	67% (14/21)	8225/10295	Huntington disease gene homolog; neuronal development
Kcnab1	67% (14/21)	1554/3522	potassium voltage-gated channel subunit
KIAA0933	67% (14/21)	4965/8940	similar to C21ORF5; unknown function
Kif15	67% (14/21)	522/4214	kinesin family member 15; neural development and migration
LOC287274	67% (14/21)	473/866	unknown function
LOC681610	67% (14/21)	1261/1559	similar to vomeronasal 2
Lrrc42	67% (14/21)	606/1696	leucine rich repeat containing 42; unknown function
Nek6	67% (14/21)	188/1314	serine/threonine kinase
RGD1562451	67% (14/21)	2245/2531	similar to PABPC4; nucleotide metabolism
Tex2	67% (14/21)	3347/5119	testis expressed sequence 2; unknown function
Tpp2	67% (14/21)	1195/4566	tripeptidyl peptidase
***SYT13*s**			
Olr1256	86% (18/21)	670/933	olfactory receptor
Lep7	81% (17/21)	857/921	unknown function
LOC294668	81% (17/21)	601/3765	unknown function
LOC501793	81% (17/21)	84/2619	similar to putative pheromone receptor
LOC681254	81% (17/21)	1430/2036	unknown function
LOC683355	81% (17/21)	1274/1773	monoacylglycerol O-acyltransferase 2
LOC686143	81% (17/21)	767/993	keratinocytes proline-rich protein; unknon function
StARD9	76% (16/21)	858/11587	microtubule-based movement
Ifi44	76% (16/21)	793/1686	interferon-induced; HVB-associated microtubular aggregate protein
RGD1566284	76% (16/21)	1330/1784	similar to heterogeneous nuclear ribonucleoprotein A3; mRNA metabolism and transport
Xpo4	76% (16/21)	632/4957	transport protein
Cap1	71% (15/21)	1926/2584	adenyly cyclase-associated protein; cell polarity maintenance
Dock8	71% (15/21)	3233/7736	guanyl-nucleotide exchange factor activity
Has3	71% (15/21)	576/2465	synthesis of hyaluronan, an extracellular matrix molecule
LOC680422	71% (15/21)	188/3593	unknown function
RGD1304806	71% (15/21)	350/3755	unknown function
Bpgm	67% (14/21)	528/1609	carbohydrate metabolism
Cwf19l2	67% (14/21)	2990/4026	unknown function
Cyb561d1	67% (14/21)	87/686	integral membrane protein; function unknown
Dnahc11	67% (14/21)	7297/11007	microtubule-based movement
LOC679442	67% (14/21)	1454/1818	unknown function
LOC679830	67% (14/21)	1454/1818	unknown function
Phca	67% (14/21)	838/2390	glycosphingolipid metabolism; protein biosynthesis
Tex2	67% (14/21)	3347/5119	testis expressed sequence 2; unknown function
Zfyve9	67% (14/21)	3915/3928	Tgf-β receptor complex assembly

Our previous studies identified a correlation between human 11p11.2-mediated rat liver tumor suppression and induction of rat *Wt1* (43). Based on this observation we hypothesized that the molecular mechanism governing rat liver tumor suppression by human 11p11.2 may directly or indirectly involve this previously identified tumor suppressor gene (43). Thus, if the microcell-mediated introduction of *SYT13* into the cells is responsible for the induction of *Wt1*, we expect the expression of *Wt1* to be diminished in *SYT13*-silenced cell lines. The parental GN6TF tumor cells express *Wt1* at a significantly lower level than the suppressed CX4 cells (FIGURE 3.12.B). *Wt1* was decreased in several *SYT13*i-transfected clones but was unchanged (or higher) in *SYT13*s-transfected cell lines (FIGURE 3.12.B). These data (i) support our previous hypothesis that expression of *Wt1* is directly or indirectly induced in response to h*SYT13* in this model system, and (ii) suggest strongly that *Wt1* is an important down-stream effecter of *SYT13*-mediated tumor suppression.

Phenotypic and Growth Characteristic Analysis of SYT13*i and* SYT13*s Clones* In Vitro

Analysis of morphology, contact inhibition, and anchorage-dependent growth in CX4 cells, revealed that human 11p11.2 normalizes the aggressive phenotype of the GN6TF cells *in vitro* (41, 43). After targeting human *SYT13* in CX4 cells with shRNAs, we re-examined these characteristics to assess the contribution of SYT13 to the suppression of the neoplastic cell phenotype of GN6TF cells *in vitro*. GN6TF cells are spindle-shaped and grow in multiple layers, whereas CX4 cells exhibit a flattened and polygonal cell morphology and produce a contact-inhibited growth pattern (FIGURE 3.14.A). *SYT13*i cell lines retain some polygonal features similar to CX4 cells, but exhibit a multilayer growth pattern after reaching confluence in culture (FIGURE 3.14.A). The morphology of control-transfected cell lines (*SYT13*s) was similar to that of the parental suppressed cell line CX4 (FIGURE 3.14.A).

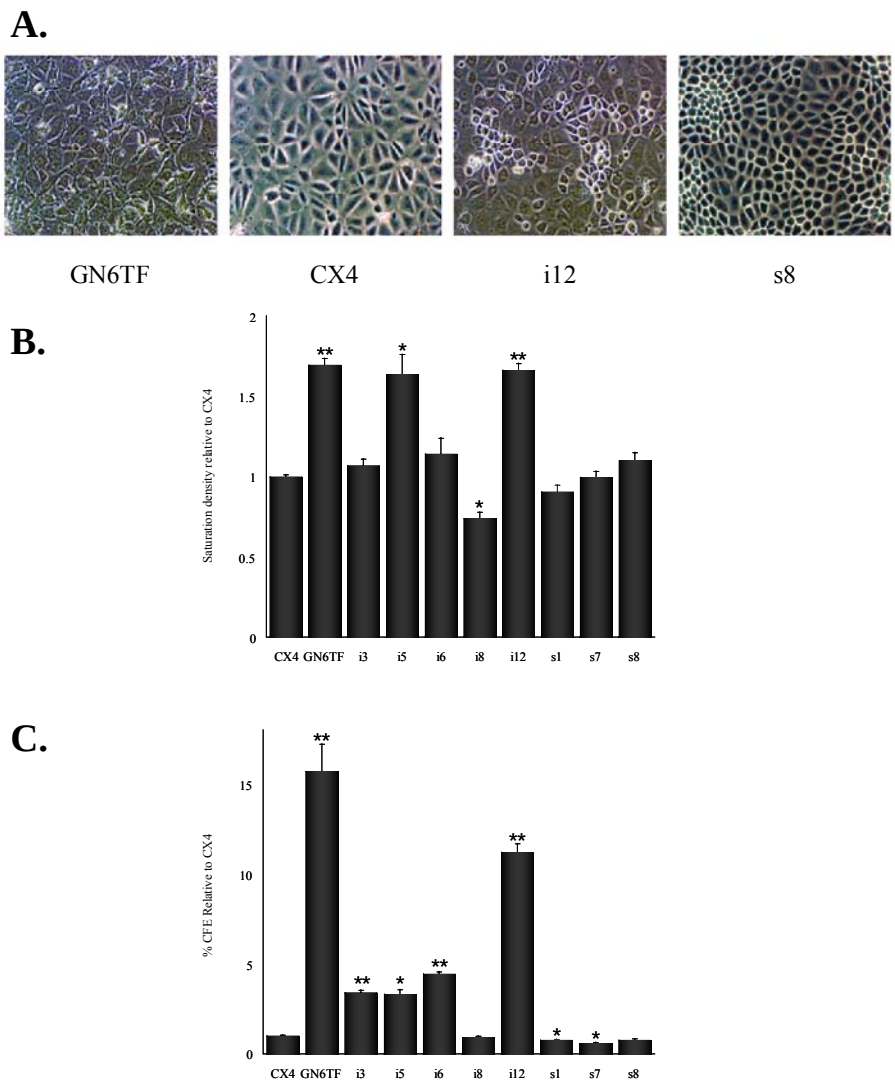

FIGURE 3.14. *Phenotypic characterization of* SYT13*i and* SYT13*s–transfected cell lines.* (A) Phase contrast microscopy of GN6TF tumor cells, CX4 MCH cells, and representative derived *SYT13*i and *SYT13*s transfected cell lines. (B) Saturation densities of GN6TF tumor cells, CX4 MCH cells, and representative derived *SYT13*i and *SYT13*s transfected cell lines (expressed relative to CX4 cells). (C) Anchorage-independent growth of GN6TF cells, CX4 MCH cells, and representative *SYT13*i and *SYT13*s transfected cell lines (expressed relative to CX4 cells). **P*< 0.05 and ***P*<0.001 compared to CX4 using Student's t-Test.

Saturation densities of each of the 12 *SYT13*i- and 8 *STY13*s-transfected cell lines were measured. FIGURE 3.14.B shows a representative panel of these cell clones (saturation densities of cell lines not shown did not significantly differ from CX4). *SYT13*i5 and *SYT13*i12 grow to an elevated saturation density that is indistinguishable from GN6TF, reflecting multilayer growth. *SYT13*i3, i5, i6, and i12 cells efficiently produced colonies in soft agarose, indicative of the restoration of anchorage-independent growth potential (FIGURE 3.14.C). *SYT13*s1, s7, and s8 cells formed few or zero colonies in soft agarose (FIGURE 3.14.C), similar to CX4 cells, and the remainder of the colonies were unable to form any colonies in soft agarose. These results combine to suggest that several cellular features of suppressed CX4 MCH cells (including growth pattern, contact inhibition, and anchorage-dependent growth) may be directly regulated by expression of *SYT13*.

Tumorigenicity of SYT13*i and* SYT13*s Clones* In Vivo

Several *SYT13*-targeted and scrambled control cell lines were selected for analysis of tumorigenicity *in vivo*. *SYT13*i5 and i12 cells displayed the greatest tumorigenic potential with 86% and 80% of syngeneic animals developing tumors with short latency (TABLE 3.3). In contrast, the suppressed parental CX4 cells developed fewer tumors with a much longer average latency, consistent with previous studies (40). The average latency for tumor formation for s1 and s8 control cells in the 50% (4/8) of animals which developed tumors was 226±31 days, similar to the CX4 cells (TABLE 3.3). The increased aggressiveness of *SYT13*i cell lines was evident from a Kaplan-Meier analysis of survival after transplantation of *SYT13*i (FIGURE 3.15) and *SYT13*s cell lines. This analysis revealed a statistically significant survival disadvantage for animals transplanted with *SYT13*i5 cells compared to CX4 cells (FIGURE 3.15).

TABLE 3.3. *Tumorigenic potential of CX4 and derived* SYT13*i and* SYT13*s cell lines*

Cell Line	Tumorigenicity (%)	Latency Range (d)	Average Latency (d)	Latency Significance (*P*)*	Survival Significance (*P*)†
CX4	4/6 (67%)	256 – 293	274 ± 11	--	--
i3	1/5 (20%)	NA	201	N/A	0.10 (NS)
i5	6/7 (86%)	110 – 201	144 ± 14	<0.0001	0.04
i6	1/8 (12%)	NA	201	N/A	0.07 (NS)
i12	8/10 (80%)	87 – 293	164 ± 25	0.002	0.15 (NS)
s1	1/4 (25%)	NA	256	N/A	0.28 (NS)
s8	3/4 (75%)	153 – 293	216 ± 41	0.28 (NS)	0.48 (NS)

*Significance of average latency is compared to CX4 cells using the Student's *t*-Test
†Significance of survival is compared to CX4 cells using the Log-Rank test

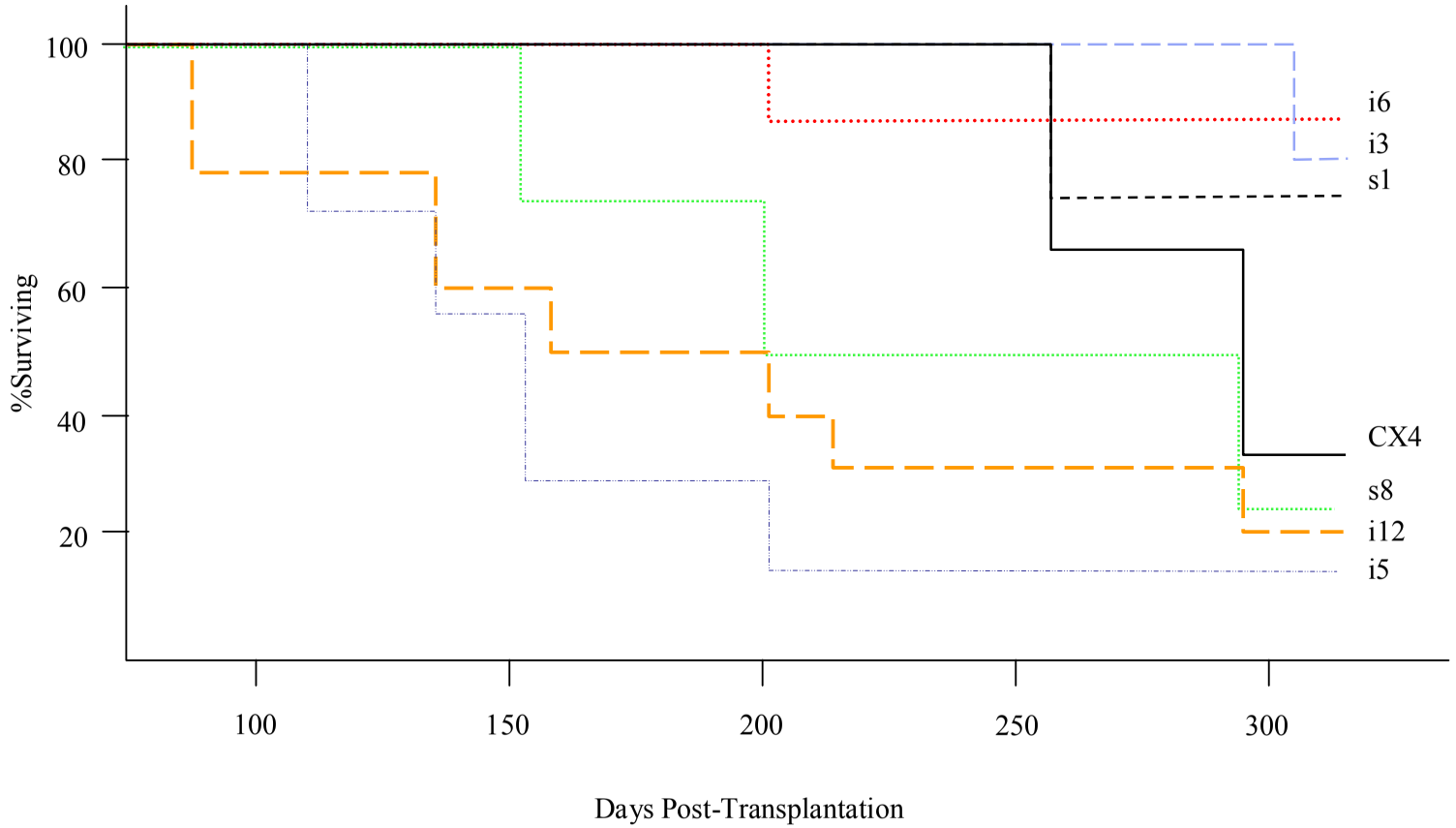

FIGURE 3.15. *Survival analysis for animals transplanted with* SYT13*i- and* SYT13*s-transfected cell lines.* Kaplan-Meier analysis of survival for animals transplanted with CX4, i3, i5, i6, i12, s1, and s8 cell lines. *P* values are found in TABLE 3.3 and were generated by comparison to CX4 using the Log-Rank test. Refer to TABLE 3.3 for number of animals.

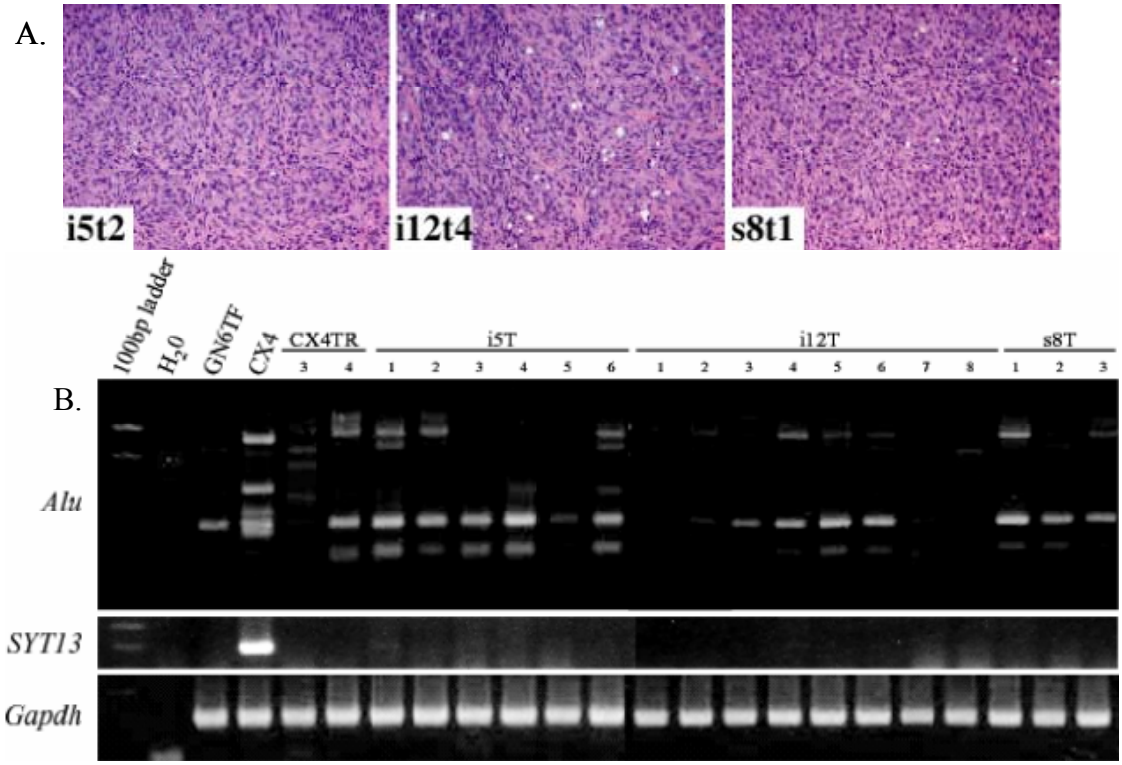

FIGURE 3.16. *Characterization of tumor revertants after transplantation into host animals.* (A) Representative tissue sections corresponding to tumors generated after transplantation of i5, i12, and s8 cells. All tumors were classified as undifferentiated, spindle cell carcinomas regardless of the nature of the transplanted cell line. (B) PCR analysis of tumor cell lines derived from *SYT13*i and *SYT13*s cell clones. The human specific repeating element *Alu* was amplified by PCR in tumor revertants to assess the extent of loss of the suppressive human chromosome. None of the tumor revertants retained the human *SYT13* allele. CX4-derived tumor cell lines are designated CX4TR (3 and 4). Likewise, tumor cell lines derived from *SYT13*i cell lines are designated i5T (tumors 1-6), and i12T (tumors 1-8), and tumor cell lines derived from *SYT13*s8 are designated S8T (tumors 1-3).

Morphological and Molecular Characterization of SYT13i- and SYT13s- derived Tumor Cell Lines

Tumors arising in syngeneic rats after subcutaneous transplantation of *SYT13*i and *SYT13*s cell lines were poorly differentiated carcinomas that were indistinguishable from tumors arising after transplantation of the parental GN6TF tumor cells or the CX4 MCH cell line (FIGURE 3.16.A). Molecular characterization of tumor cell lines derived from *SYT13*i and *SYT13*s clones revealed that the neomycin resistance gene (located on the suppressive human chromosome 11) (40, 91) was not retained in any of the tumor forming cells (data not shown). However, *Alu*-PCR of genomic DNA isolated from these tumor cell lines indicated the presence of human chromosomal DNA (FIGURE 3.16.B). The *Alu*-PCR amplicon patterns generated for individual tumor cell lines suggested that portions of the human chromosome had been lost during tumorigenesis (FIGURE 3.16.B). None of the tumor cell lines analyzed contain h*SYT13*, suggesting that loss of human 11p11.2 occurs coordinate with reexpression of tumorigenicity (FIGURE 3.16.B). The psiRNA vector remained intact in all of the tumor revertant cell lines (data not shown).

EXOGENOUS EXPRESSION OF HUMAN SYT13 IN THE GN6TF TUMOR CELL LINE

Introduction of human chromosome 11 into the GN6TF tumor cell line resulted in the suppression of tumorigenicity in GN6TF-derived MCH cell lines, and mapping of the tumor suppressor locus identified *SYT13* as a strong candidate for the 11p11.2 tumor suppressor gene. Therefore, *SYT13* was ectopically expressed in GN6TF tumor cells in order to directly investigate its tumor suppressive function in this model system.

Molecular Analysis of SYT13-Transfected Clones

SYT13 expression: FLAG-tagged-SYT13-transfected GN6TF clones B3, C1, C2, E2, F3, and J1, as well as the FLAG-tagged-GFP vector control were examined by western blot for SYT13 expression. The SYT13 antibody recognized a 66 kDa protein monomer and the a 130 kDa SDS-resistant dimer, consistent with previous reports (80). In addition, an intermediate species was identified that may represent a SYT13 degradation product or a non-specific binding reaction (FIGURE 3.17.A). CX4, a positive control for SYT13, shows strong expression of the 66 kDA species compared to the other cell lines. Relative to expression in the parental GN6TF tumor cell line, the SYT13 monomer is slightly increased in C1 and reduced in C2. The other cell lines (GFP, B3, E2, F3, and J1) exhibit no real change in the expression of the SYT13 monomer compared to GN6TF. The SYT13 dimer is absent in GN6TF, GFP, C1, and B3 and appears at low, but similar expression levels in the CX4, C2, E2, F3, and J1 cell lines. (FIGURE 3.17.A).

SYT13 mRNA was measured by real time RT-PCR with human specific probes (FIGURE 3.17.B). Levels for GN6TF were essentially zero (10^{-5} times expression in the CX4 MCH). *SYT13*-transfected cell lines C2, F3, C1, and B3 expressed *SYT13* similar to levels found in CX4. Interestingly, *SYT13* mRNA levels in E2 and J1 were found at the same level (essentially zero) seen in GN6TF cells (FIGURE 3.17.B). These data, combined with protein/mRNA data from SYT13-silencing studies (FIGURES 3.11 AND 3.12), suggest that steady state levels of the protein (SYT13) do not necessarily correspond to steady state levels of the gene transcript (*SYT13*). The implications of this finding are (i) although *SYT13* is a strong candidate for the human 11p11.2 tumor suppressor gene, it may unlikely be identified by large-scale expression analysis in cancer research, and (ii) post-transcriptional and post-

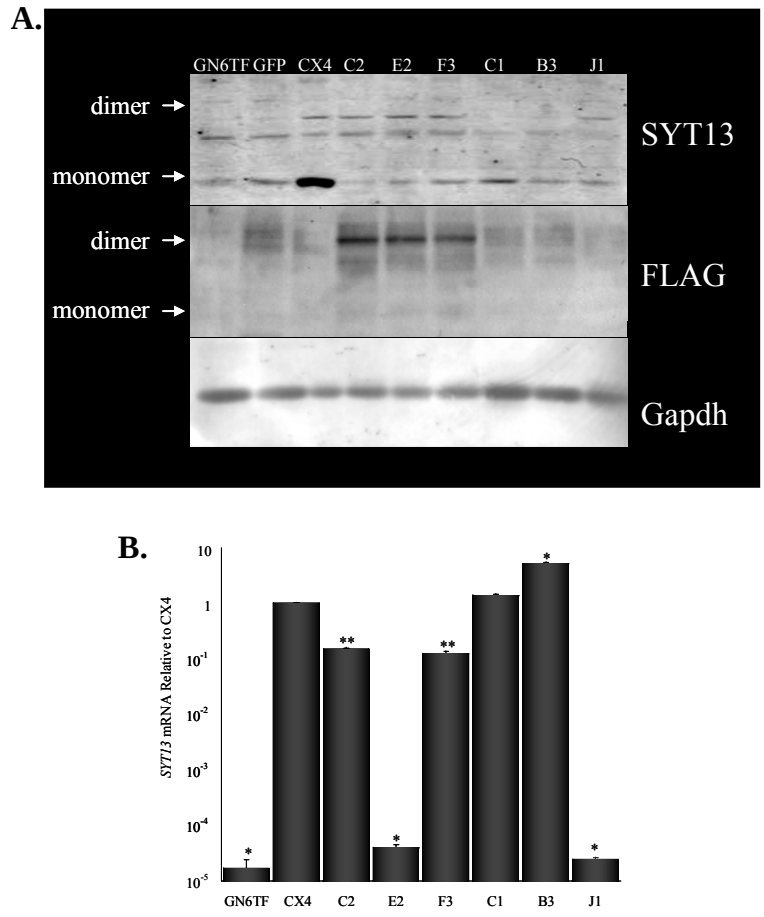

FIGURE 3.17. *Molecular characterization of* SYT13- *and* GFP-*transfected GN6TF cell lines.* (A) Western analysis shows an induction of the expression of the SYT13 dimer in several (but not all) SYT13-transfected cell lines and slight alterations in the SYT13 monomer which do not correlate with increases in the dimer. Analysis with the α-FLAG antibody shows no immunoreactive monomeric species and increases in several (but not all) of the SYT13 dimer in *SYT13*-transfected cells. Gapdh protein expression was utilized as a control to verify equal protein loading. (B) Quantitative real-time RT-PCR analysis of *SYT13* mRNA expression in GN6TF and *SYT13*-transfected cell lines expressed relative to CX4 cells (*SYT13* mRNA was not measured in GFP-transfected cells). **P*<0.05 compared to GN6TF using the Student's t-Test.

translational modifications may be very important in the regulation and function of SYT13.

Exogenous protein expression: The ectopically expressed SYT13 carries a FLAG tag which facilitates discrimination of the exogenous protein from the endogenous protein by western blot using an α-FLAG antibody. The FLAG immunoreactive protein migrates at 130 kDa and corresponds to the SDS-resistant dimer observed on the α-SYT13 immunoblot (FIGURE 3.17.A). No FLAG-positive SYT13 monomer protein is observed in any of the transfected cell lines. Likewise, it is found only in SYT13-transfected cell lines C2, E2, and F3 coordinate with expression of the SYT13 dimer, but it does not recognize the SYT13 dimer in J1 (FIGURE 3.17.A). The α-FLAG antibody also decorates the 30 kDa FLAG-tagged GFP protein expressed in the GFP vector control cell population (data not shown). The lack of α-FLAG immunoreactivity with the 66 kDa SYT13 monomer suggests that either the antibody is unable to recognize the FLAG epitope on the monomeric species or that exogenously expressed SYT13 uniquely produces the SDS-resistant protein dimer. If the latter is true, then only C2, E2, and F3 cells express exogenous SYT13, and the acquisition of the neomycin-resistance phenotype after transfection does not necessarily correspond to coordinate production of SYT13 (as in C1 and B3).

Expression of rat Wt1 in transfected clones: Transfected cell lines were analyzed by real-time RT-PCR for expression of the rat *Wt1* tumor suppressor gene. In our previous studies, *Wt1* was implicated in the suppression of tumorigenicity in GN6TF-derived MCH cell lines as a potential effecter of 11p11.2-mediated tumor suppression (43). Real-time RT-PCR analysis revealed a significant increase in *Wt1* mRNA in SYT13 dimer-positive cell lines C2, E2, F3, and J1 compared to GN6TF (FIGURE 3.18.). Although CX4 displays the most robust expression of SYT13 (the monomeric species; FIGURE 3.18.A), expression of

Wt1 mRNA is greater (2-4-fold) in the SYT13-transfected cell lines C2, E2, F3, and J1 (FIGURE 3.18.B). *Wt1* expression in neomycin-resistant, SYT13 dimer-negative cell lines (C1 and B3) was low and similar to the GN6TF cell line (FIGURE 3.18). Expression of *Wt1* in the GFP-control cell line was similar to GN6TF (FIGURE 3.18). This result (i) provides evidence that SYT13 may directly or indirectly regulate expression of *Wt1*, and (ii) suggests that the SYT13 dimer may be a more important downstream effecter than the monomeric species.

Phenotypic and Growth Characteristics of SYT13-Transfected Clones In Vitro

Cellular morphology of transfected clones: GN6TF tumor cells display a spindly morphology with multiple cellular extensions (FIGURE 3.19), and after reaching confluency in culture, the cells continue to proliferate and exhibit multi-layered growth. Microcell-mediated introduction of human chromosome 11 into these cells resulted in MCHs (i.e. CX4, FIGURE 1.3) that grow in a contact-inhibited monolayer with an epithelioid, cobblestone morphology. SYT13 dimer-positive (and *Wt1*-positive) GN6TF transfectants (C1, E2, F3 and J1; FIGURE 3.19) display a flattened, epithelioid, monolayer—similar to the suppressed MCH cell lines. By contrast, the neomycin-resistant, SYT13 dimer-negative (and *Wt1*-negative) cell lines (C1 and B3, FIGURE 3.19) display a spindly morphology that is indistinguishable from the parental GN6TF tumor cells and the GFP-vector control (FIGURE 3.19).

Contact-inhibition of SYT13-transfected cell lines: Loss of contact inhibition is one measure of neoplastic growth in culture which can be visually observed in culture (FIGURE 3.20.A) and can be assessed quantitatively by the saturation density assay. SYT13 dimer-positive (and *Wt1*-positive) cell lines C2, E2, and J1 produced saturation densities that were

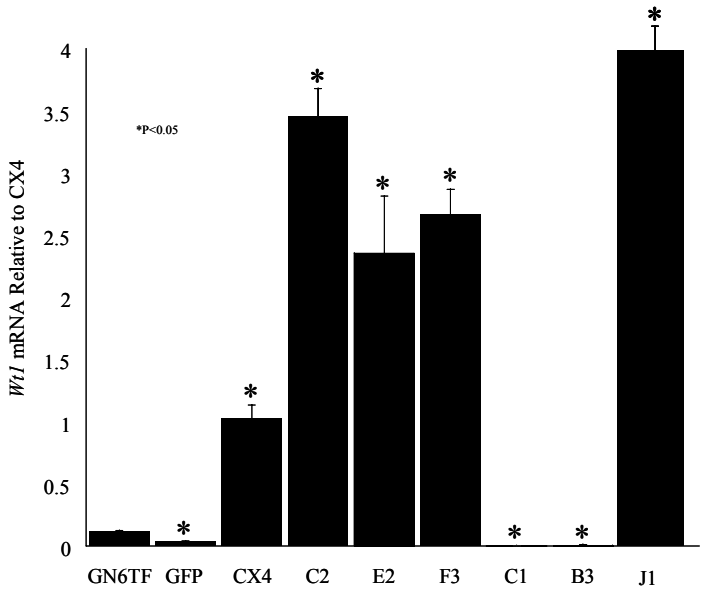

FIGURE 3.18. Wt1 *expression in* SYT13- *and* GFP- *transfected cell lines.* Quantitative real-time RT-PCR analysis of *Wt1* mRNA expression in GN6TF, *SYT13*-, and GFP-transfected cell lines expressed relative to CX4 cells. **P*<0.05 compared to GN6TF using the Student's t-Test.

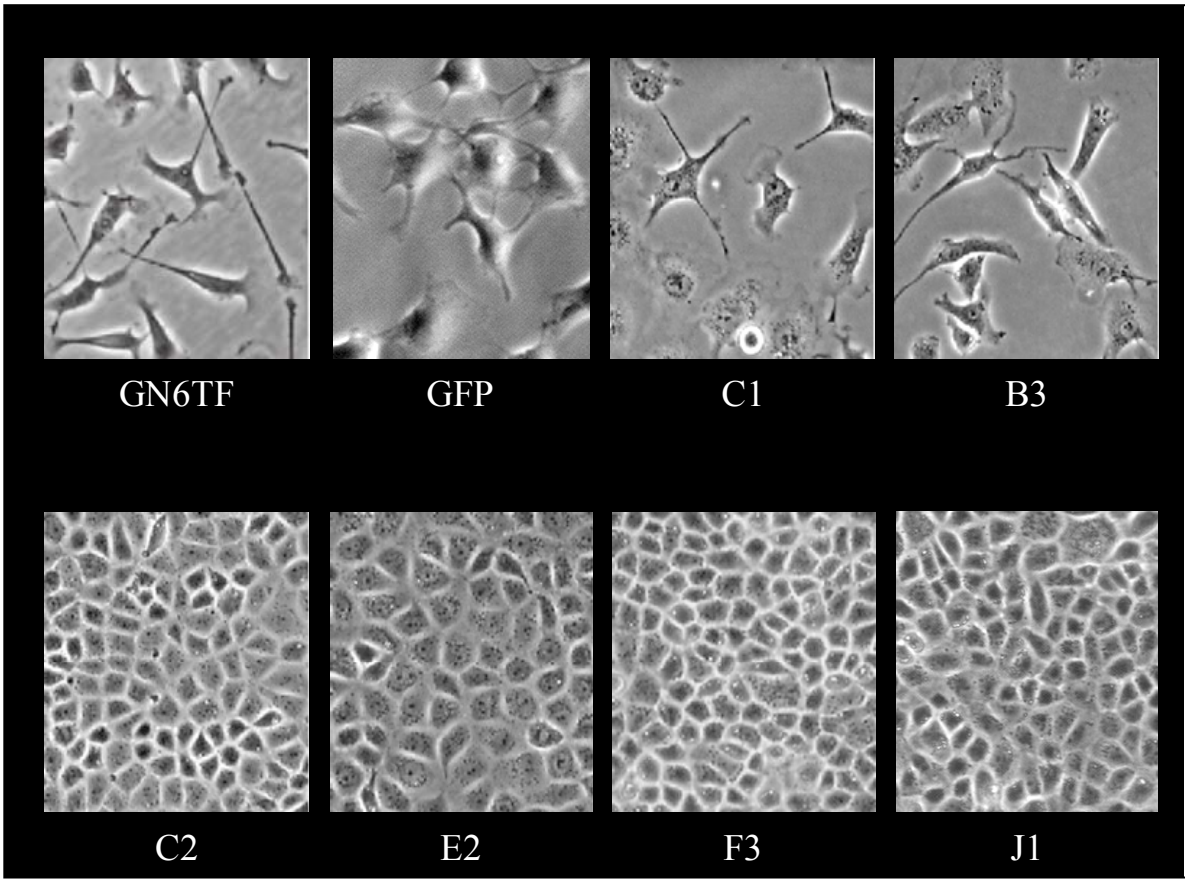

FIGURE 3.19. *Phenotypic characterization of* SYT13- *and* GFP-*transfected cell lines.* Phase contrast microscopy of GN6TF tumor cells, GFP-transfected cells (GFP), and *SYT13*-transfected cell lines (C1, B3, C2, E2, F3, and J1).

>50% reduced from that of the parental GN6TF tumor cell line (FIGURE 3.20.B). This result strongly suggests that establishment of contact inhibition accompanies the expression of the SYT13 dimer (and *Wt1*) in GN6TF transfectants. Conversely SYT13 dimer-negative (and *Wt1*-negative) cell lines (GFP control and B3) displayed no change in contact inhibition compared to GN6TF (FIGURE 3.20.B) and maintained the ability to grow in multi-layered cultures. These results suggest that the cell lines expressing the exogenous SYT13 dimer have acquired the ability to recognize and/or process extracellular stimuli for growth arrest, a pathway which appears to be disrupted in GN6TF tumor cells.

Anchorage-dependent growth in SYT13-transfected cell lines: Anchorage-independent growth represents another measure of neoplastic growth *in vitro*. Colony forming efficiencies relative to GN6TF are graphically represented in FIGURE 3.21.A and viable, MTT-stained colonies are displayed both macroscopically and microscopically in FIGURES 3.21.B. and C respectively. SYT13-dimer positive cell lines C2, E2, and J1 have completely lost the ability to form colonies in soft agar. Likewise, the CFE of SYT13 dimer-positive cell line F3 was significantly attenuated, and the average size of the colonies formed was smaller than GN6TF colonies. SYT13 dimer-negative cell lines C1 and B3 expressed reduced CFEs relative to GN6TF (63% and 43%, respectively), and the average colony size of C1 clones appeared to be smaller than GN6TF. The CFE of the GFP vector control cell line did not significantly differ from that of GN6TF (FIGURE 3.21.B) and the average colony size appeared to be similar. Although SYT13 dimer-negative (Wt1-negative) cell lines C1 and B3 expressed reduced CFEs, they maintain a significant capacity for anchorage-independent growth compared to the virtually ablated potential that accompanied SYT13 expression in C2, E2, F3, and J1 cells. This suggests that exogenous expression of SYT13,

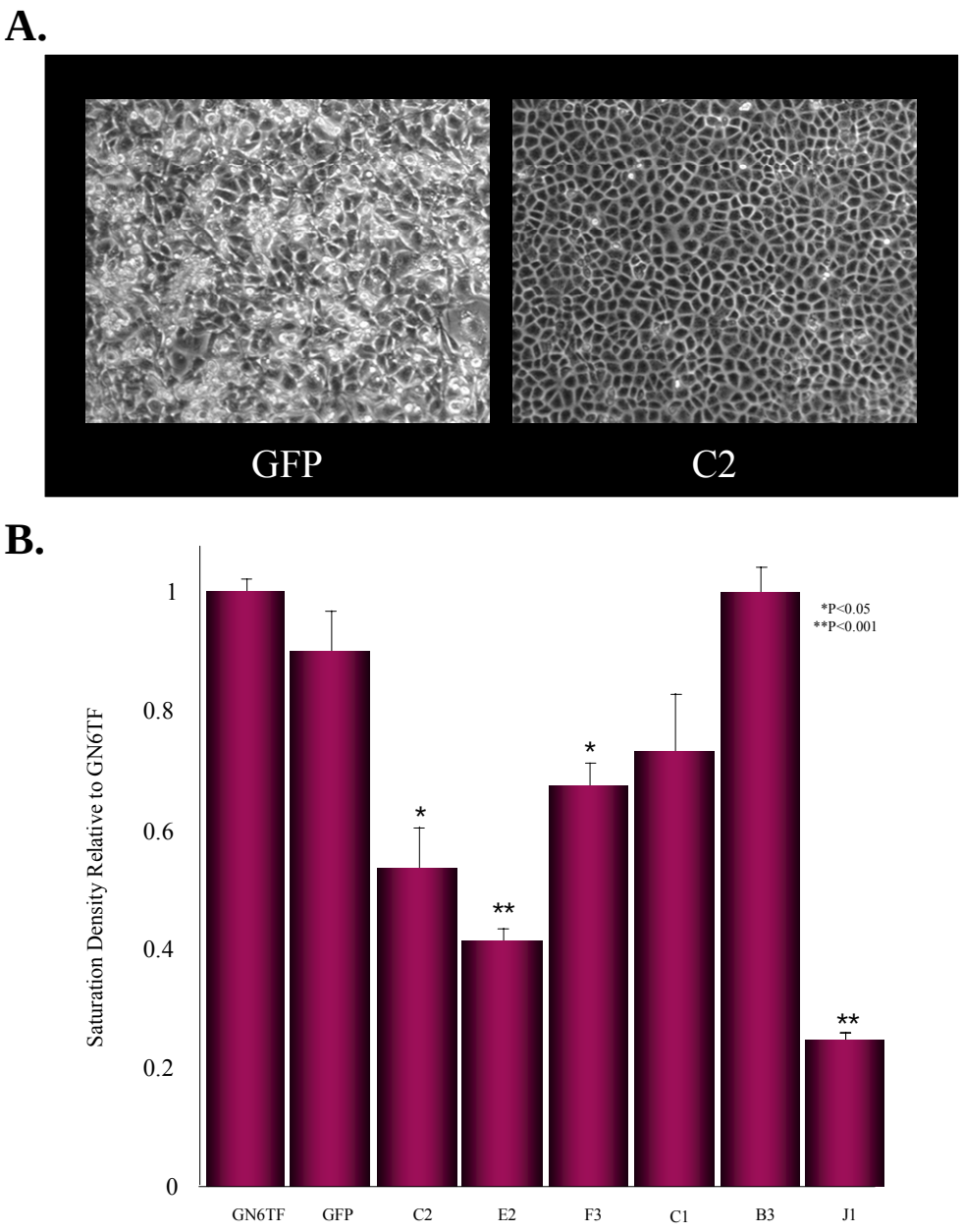

FIGURE 3.20. *Contact inhibition of* SYT13- *and* GFP-*transfected cell lines.* (A) Phase contrast microscopy of representative GFP-transfected and SYT13-transfected cells after 14 days in culture. (B) Saturation densities of GN6TF tumor cells, GFP-transfected cells, and *SYT13*-transfected cell lines (expressed relative to GN6TF cells). **P*<0.05 and ***P*<0.001 compared to GN6TF using the Student's t-Test.

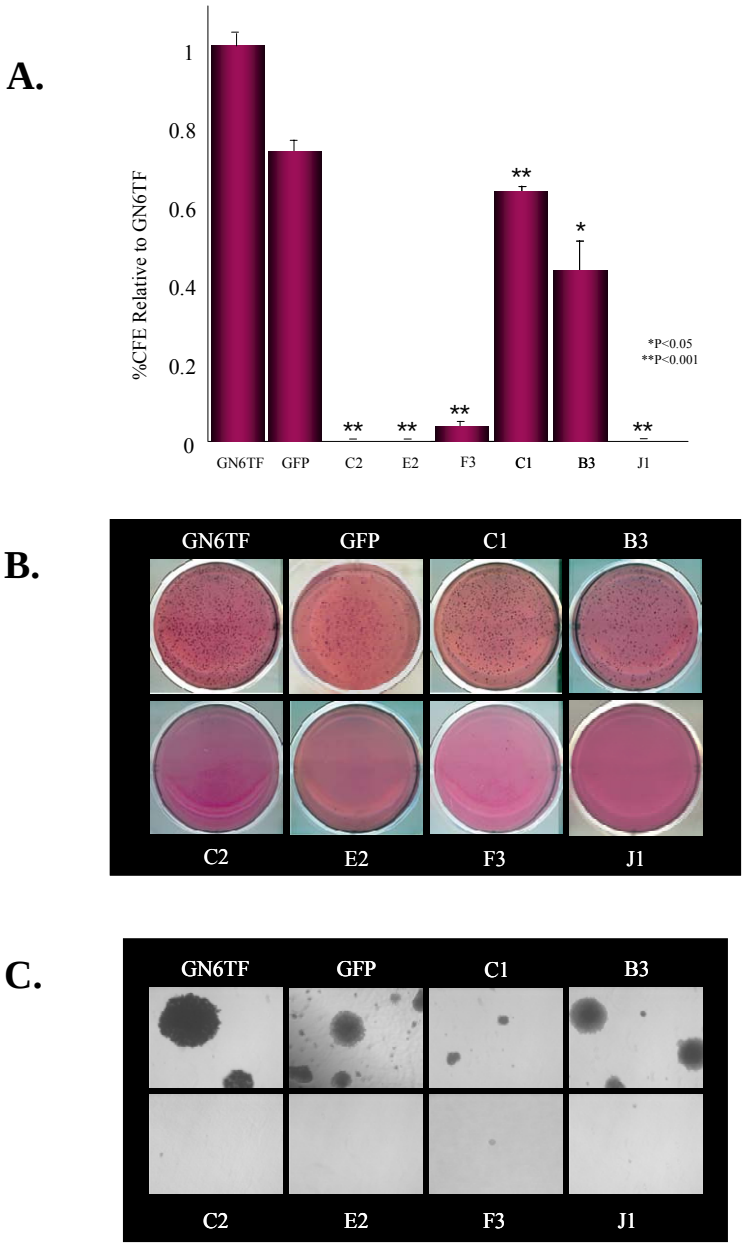

FIGURE 3.21. *Anchorage-independent growth of* SYT13- *and* GFP-*transfected cell lines.* (A) Colony forming efficiency (CFE) of GN6TF, GFP-transfected cells, and *SYT13*-transfected cell lines (expressed relative to GN6TF cells). **P*<0.05 and ***P*<0.001 compared to GN6TF using the Student's t-Test. (B) and (C) Macroscopic and microscopic (obj. x20) views of MTT-stained colonies of GN6TF tumor cells, GFP-transfected cells, and *SYT13*-trasfected cells in soft agar.

specifically the SYT13 dimeric species, is able to significantly attenuate the neoplastic growth of GN6TF cells *in vitro*.

Tumorigenicity of SYT13-*Transfected Cell Lines* In Vivo

GN6TF tumor cells are highly aggressive *in vivo* and have been documented to form tumors in syngeneic hosts with an average latency of 21d (40). SYT13-transfected GN6TF clones were transplanted into syngeneic neonatal rats to assess the ability of exogenously expressed SYT13 to alter tumorigenicity. Ten days after transplantation, tumors were palpable and macroscopically visible in 100% of the animals transplanted with the SYT13 dimer-negative cell lines GN6TF, GFP, C1, and B3. At this time point after transplantation, there was no indication of tumor formation in animals transplanted with SYT13-positive cell lines C2, E2, F3, and J1 (FIGURE 3.22.A). Tumor diameters in the remaining animals were measured (*in vivo*) 20 days post-transplantation, and at this time, there was still no palpable tumor formation in animals transplanted with the SYT13 dimer-positive cell lines C2, E2, and J1 (diameters of tumors that were harvested previous to 20 days post-transplantation were measured as 1 cm) (FIGURE 3.22.B). By 30 days post-transplantation, 1 cm tumors had formed in 100% of the animals with each of the SYT13 dimer-negative cell lines GN6TF, GFP, C1, and B3 (TABLE 3.5 AND FIGURE 3.23). There was no significant difference in average latency of tumor formation between these cell lines. At the conclusion of the study (120 days), 20% (2/10) of the animals transplanted with the E2 cell line had formed 1 cm tumors. Of the animals remaining, 29% (2/7) transplanted with J1, 9% (1/11) transplanted with C2, and 50% (4/8) of the remaining animals transplanted with E2 had formed palpable tumors of less than 1 cm. FIGURE 3.23 depicts a survival analysis among

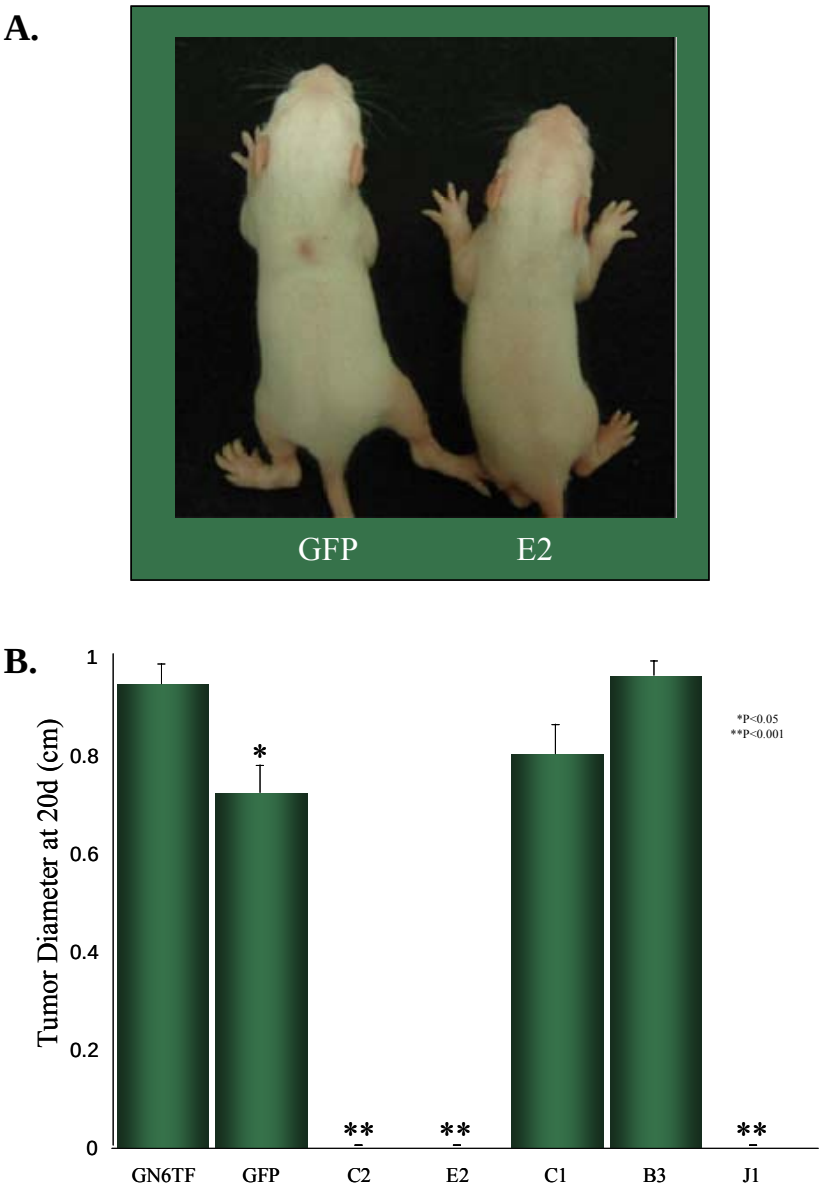

FIGURE 3.22. *Early indications of tumorigenicity* in vivo. (A) Tumor formation in representative GFP and E2 syngeneic host animals of identical age 10 days after subcutaneous (on back) transplantation of GFP or E2 cells. No tumor formation is noted at the transplantation site of animals injected with E2 cells. (B) Average diameter of tumors formed in syngeneic host animals 20 days post- transplantation with parental GN6TF tumor cells, GFP-transfected, and *SYT13*-transfected cell lines. **P*<0.05 and ***P*<0.001 compared to GN6TF using the Student's t-Test.

TABLE 3.4. *Tumorigenic potential of GN6TF cells and* GFP-*transfected and* SYT13-*tranfected GN6TF cells*

Cell Line	Tumorigenicity (%)	Latency Range (d)	Average Latency (d)	Latency Significance (*P*)*	Survival Significance (*P*)†
GN6TF	5/5 (100%)	18 - 25	20 ± 1.	--	--
GFP	7/7 (100%)	18 - 25	23 ± 1	0.13 (NS)	0.24 (NS)
B3	7/7 (100%)	18 - 22	19 ± 1	0.58 (NS)	0.55 (NS)
C1	9/9 (100%)	18 - 30	25 ± 1	0.06 (NS)	0.08 (NS)
C2	0/11 (0%)	--	--	N/A	<0.0001
E2	2/10 (20%)	107 - 109	108 ± 1	<0.0001	<0.0001
J1	0/7 (0%)	--	--	N/A	0.0003

*Significance of average latency is compared to GN6TF cells using the Student's *t*-Test
†Significance of survival is compared to GN6TF cells using the Log-Rank test

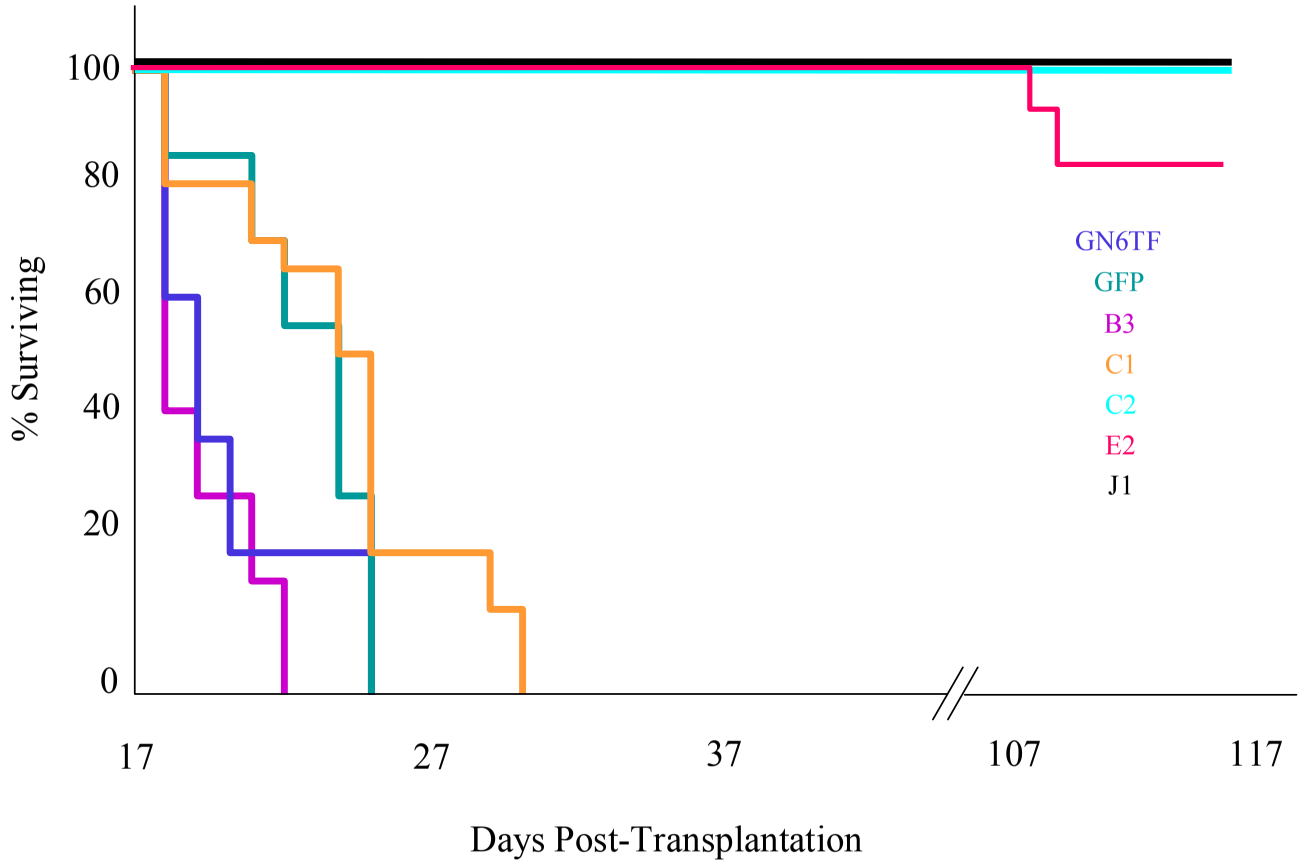

FIGURE 3.23. *Tumorigenicty of* SYT13- *and* GFP-*transfected cell lines* in vivo. Kaplan-Meier analysis of survival for animals transplanted with GN6TF, GFP, and *SYT13*-transfected cell lines. *P* values comparing data to GN6TF using the Log-Rank test are located on TABLE 3.4. Refer to TABLE 3.4 for number of animals.

animals transplanted with each individual cell line and indicates statistically powerful suppression of tumorigenicity in animals transplanted with SYT13 dimer-positive cell lines C2, E2, and J1. The significant results of this study provide very strong evidence that SYT13, specifically as a protein dimer, is able to complement a molecular deficiency in GN6TF and suppress the tumorigenic phenotype of this cell line.

LARGE-SCALE GENE EXPRESSION ANALYSIS OF SYT13-POSITIVE AND SYT13-NEGATIVE CELL LINES

RNA isolated from several cell rat liver cell lines was subjected to large-scale gene expression analysis to identify specific genes and pathways that mediate SYT13-dependent tumor suppression.

Affymetrix Microarray Analysis and Validation

RNA from CX4, GN6TF, *SYT13*i5, *SYT13*i12, and *SYT13*s1 was isolated in duplicate and individually hybridized to gene arrays. Expression analyses based on log signal values for duplicate hybridizations showed a Pearson correlation coefficient $\geq$0.995, demonstrating the reproducibility of data between duplicates. FIGURES 3.24.A and B compare gene expression profiles between duplicate hybridizations of CX4 and GN6TF. A log ratio plot showing gene expression in CX4 cells relative to expression in GN6TF cells is shown in (FIGURE 3.24.C). Real-time RT-PCR was used to validate expression changes of *Cdh1*, *Pawr*, and *Snail* in the CX4 cell line relative to GN6TF cells (FIGURE 3.35). Expression of these genes was also measured in *SYT13*-transfected cell lines to compare the gene expression patterns in 11p11.2-mediated (CX4) and SYT13-mediated (C2, E2, F3, and J1) tumor suppression (FIGURE 3.25).

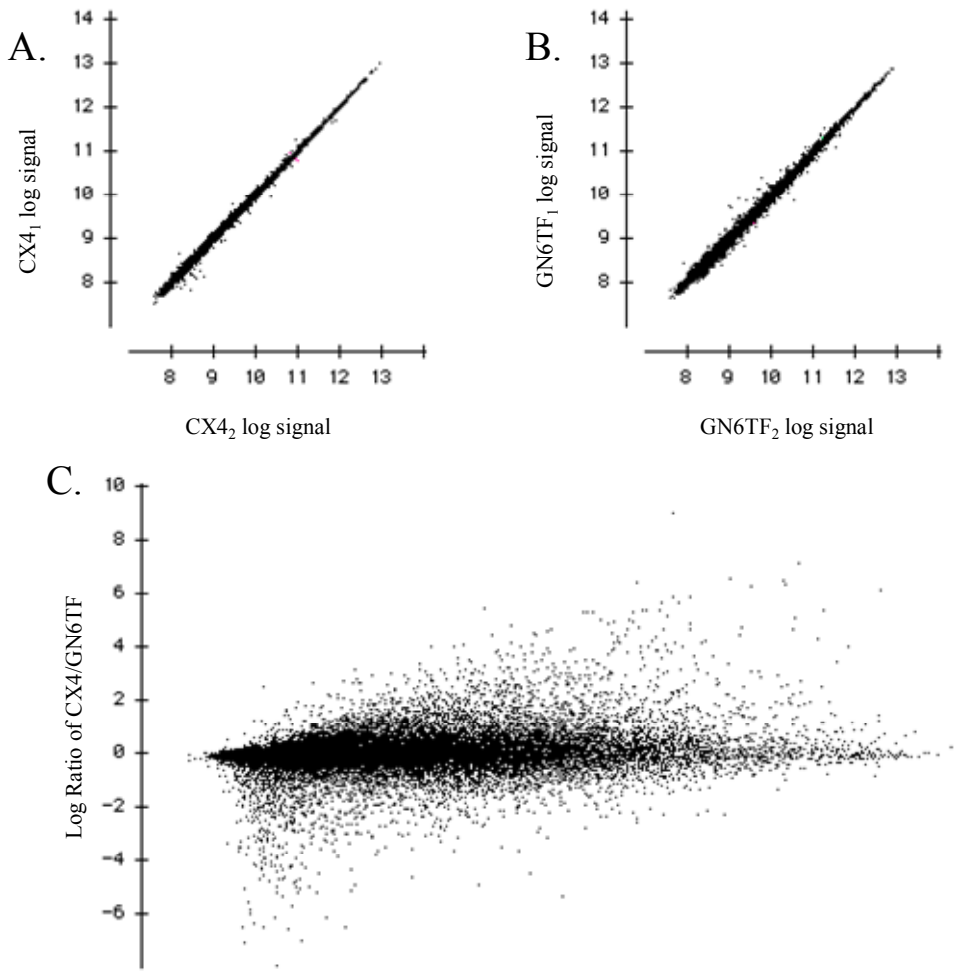

FIGURE 3.24. *Scatterplot representation of microarray data.* (A) Scatterplot of log signal values for duplicate hybridizations of CX4 and (B) GN6TF cRNA. Subscripts represent 1st and 2nd hybridization experiments for CX4 (A) and GN6TF (B). The Pearson correlation coefficient for replicate hybridizations of CX4 is 0.999 and is 0.997 for GN6TF. (C) Scatterplot of the ratio of log signal values for CX4/GN6TF. Each dot represents a transcript (gene) on the microarray. Y values represent $\log_2$(CX4/GN6TF). Therefore, a point (transcript) that falls at 2 on the vertical axix is equal to a 4-fold (2^2) increase of expression in CX4 cells compared to expression in GN6TF.

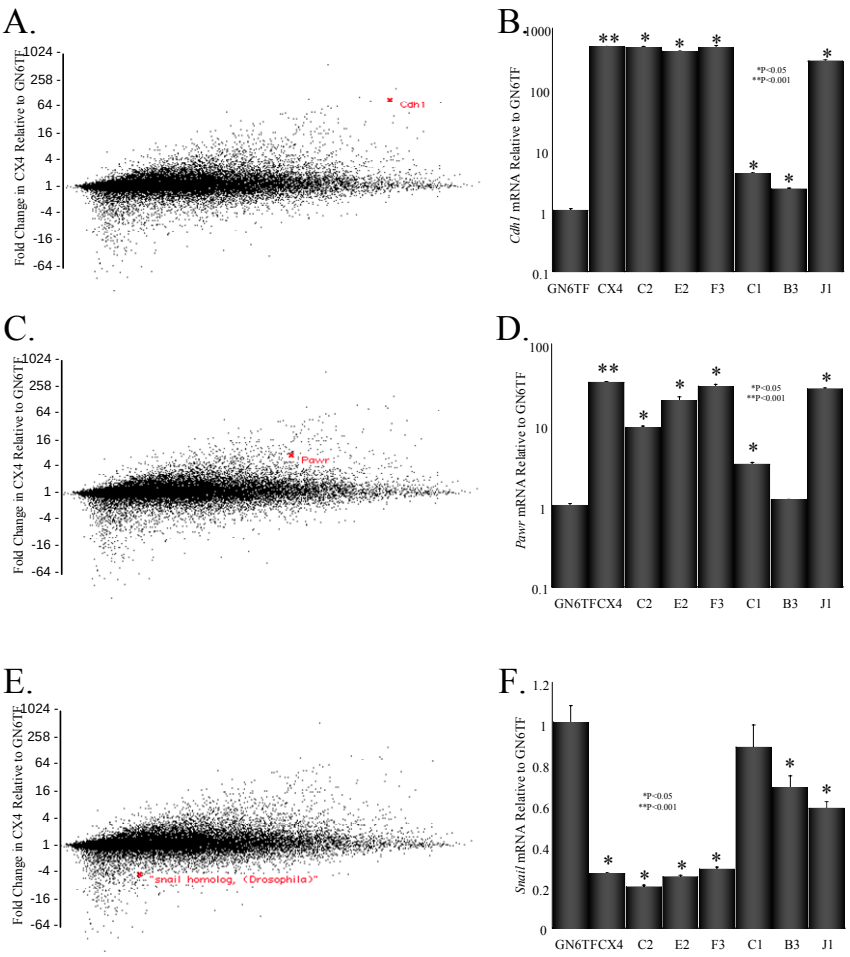

FIGURE 3.25. *Validation of microarray results by quantitative RT-PCR.* Microarray results were validated by measuring mRNA levels of several genes (including *Pawr/Par4*, *Cdh1*, and *Snail*). (A), (C), and (E) depictF microarray output on scatterplots of the ratio of log signal values for the CX4 cell line compared to GN6TF. Y values of these data points (or genes, highlighted in red) correspond to fold change increases or decreases (designated by the negative signs) of the genes in CX4 compared to GN6TF cells. (B), (D), and (F) demonstrate real-time RT-PCR analysis of these genes in GN6TF, CX4, and SYT13-transfected cell lines. **P*<0.05 and ***P*<0.001 compared to GN6TF using the Student's t-Test. (B) and (D) are depicted on log scale and (F), on linear scale.

Differentially Expressed Genes Revealed by Microarray Analysis

The expression output was queried for genes with ≥2-fold increased expression in the CX4 cell line compared to GN6TF and a corresponding list of genes with decreased expression levels ≥2-fold in the CX4 cell line compared to GN6TF. This analysis resulted in the identification of 2,742 transcripts with increased and 1,397 with reduced expression. The 2,742 transcripts expressed at least ≥2-fold higher in CX4 cells corresponded to a total of 1,662 known or predicted genes in the *R. norvegicus* genome (APPENDIX A). The 1,397 unique Affymetrix Probe IDs that reflected ≥2-fold decreased expression in CX4 relative to GN6TF corresponded to 168 known or predicted genes in the *R. norvegicus* genome (APPENDIX B).

To more closely examine the specific effects mediated by SYT13 expression, a comparison was made between the expression profiles of three tumorigenic cell lines (GN6TF, *SYT13*i5 and *SYT13*i12) and two suppressed cell lines (CX4 and *SYT13*s1). Genes identified using these stringent criteria must be expressed at ≥2-fold above or below the expression levels in *each* of the tumorigenic cell lines (GN6TF, *SYT13*i5 and *SYT13*i12) compared to *both* of the suppressed (CX4 and *SYT13*s1) control cell lines (TABLE 3.5). This analysis resulted in the identification of 22 transcripts (corresponding to 11 known or predicted genes) with ≥2-fold decreased expression in each of the aggressive cell lines compared to both of the suppressed cell lines (TABLE 3.5). Only 3 genes were expressed at ≥2-fold greater in each of the suppressed cell lines (TABLE 3.5).

Differentially Expressed Biological Themes Revealed by Microarray Analysis

DAVID Bioinformatics 2006 [http://david.abcc.ncifcrf.gov, (67)] was utilized to identify enriched biological themes present in the gene lists generated by comparative

TABLE 3.5. *Genes differentially expressed in aggressive SYT13-negative and suppressed SYT13-positive cell lines*

Affymetrix ID	Gene Name
INCREASED	
APOE	APOLIPOPROTEIN E
AUTS2	AUTISM SUSCEPTIBILITY CANDIDATE 2 (PREDICTED)
CD59	CD59 ANTIGEN
EPHB6	EPH RECEPTOR B6
FNDC1	FIBRONECTIN TYPE III DOMAIN CONTAINING 1 (PREDICTED)
GOLPH4	GOLGI PHOSPHOPROTEIN 4
SCIN	SCINDERIN
LOC263543	SIMILAR TO RIKEN CDNA 4930429H24 (PREDICTED)
SLIT2	SLIT HOMOLOG 2 (DROSOPHILA)
SULF2	SULFATASE 2
TM4SF1	TRANSMEMBRANE 4 SUPERFAMILY MEMBER 1 (PREDICTED)
DECREASED	
CA3	CARBONIC ANHYDRASE 3
ESP8	EPIDERMAL GROWTH FACTOR RECEPTOR PATHWAY SUBSTRATE 8
NRN1	NEURITIN

analysis of transcript expression in suppressed and non-suppressed cell lines. The Functional Annotation Tool of DAVID converts gene lists to associated biological themes based on gene-annotation enrichment analysis using the Fisher's Exact Test to determine *P* values. Gene ontology (GO) terms (or biological themes) associated with genes showing decreased expression following introduction of chromosome 11 into GN6TF cells (CX4 versus GN6TF, APPENDIX A) are shown in TABLE 3.6. A complete list of statistically significant ($P<0.05$) biological themes can be found in APPENDIX C. The most enriched theme in this list involves lipid metabolism/biosynthesis, and differentially expressed genes associated with this are listed in TABLE 3.7. Expression values from the microarray analysis were extracted and uploaded into GenMapp software (66) to visualize the alterations of expression in genes associated with cholesterol biosynthesis. The pathway generated by GenMapp is reproduced in FIGURE 3.25. Expression of 8/10 genes in the cholesterol biosynthesis pathway is attenuated in the suppressed CX4 cell line compared to GN6TF cells. This finding is consistent with the well documented observation that elevations in cholesterol/isoprenoid biosynthesis is commonly associated with a neoplastic phenotype (92, 93), and suggests a putative mechanism for SYT13-mediated tumor suppression. Another statistically enriched biological theme that was decreased in CX4 cells compared to GN6TF cells is genes associated with the extracellular matrix. A list of these matrix-associated genes is shown in TABLE 3.8.

The same annotation tool was used to identify enriched biological themes in the list of genes up-regulated in the suppressed CX4 cell line relative to the tumorigenic GN6TF cell line (APPENDIX B). A complete list of statistically significant biological themes is provided in APPENDIX D. Several of the most significant themes are presented in TABLE 3.9.

TABLE 3.6. *Gene ontology terms associated with genes down-regulated ≥2-fold in the CX4 cell line relative to GN6TF cells.*

Gene Ontology Term	*P*Value
cellular lipid metabolism	2.6×10^{-6}
lipid biosynthesis	8.7×10^{-6}
lipid synthesis	1.2×10^{-5}
cytoplasm	2.1×10^{-5}
nadp	2.6×10^{-5}
biosynthesis of steroids	3.2×10^{-5}
lipid metabolism	4.7×10^{-5}
Golgi-associated vesicle	9.0×10^{-5}
coenzyme metabolism	1.0×10^{-4}
extracellular matrix (sensu Metazoa)	1.1×10^{-4}
cholesterol biosynthesis	1.1×10^{-4}
organelle membrane	1.3×10^{-4}
cofactor metabolism	1.3×10^{-4}
extracellular matrix	1.4×10^{-4}
catalytic activity	1.6×10^{-4}
cholesterol metabolism	1.7×10^{-4}
isoprenoid biosynthesis	2.5×10^{-4}
sterol biosynthesis	2.5×10^{-4}
oxidoreductase activity,	2.6×10^{-4}
fatty acid metabolism	2.6×10^{-4}
Golgi apparatus	2.8×10^{-4}
oxidoreductase activity, acting on CH-OH group of donors	3.0×10^{-4}
integrin binding	3.1×10^{-4}
cell adhesion	3.1×10^{-4}
oxidoreductase activity	3.5×10^{-4}
organic acid metabolism	3.6×10^{-4}
Golgi membrane	3.7×10^{-4}
sterol metabolism	4.0×10^{-4}
cholesterol biosynthesis	4.5×10^{-4}
organ morphogenesis	4.7×10^{-4}
endoplasmic reticulum	5.7×10^{-4}
peroxisome	6.3×10^{-4}
collagen	7.0×10^{-4}
microbody	7.1×10^{-4}
peroxisome	7.1×10^{-4}
sterol biosynthesis	7.6×10^{-4}
carboxylic acid metabolism	7.9×10^{-4}
homophilic cell adhesion	7.9×10^{-4}
alcohol metabolism	8.0×10^{-4}
lipid metabolism	8.8×10^{-4}
endomembrane system	0.001
Golgi vesicle transport	0.001
steroid biosynthesis	0.001
isoprenoid metabolism	0.001

TABLE 3.7. *Genes decreased ≥2-fold in CX4 cells compared to GN6TF cells associated with the cholesterol/steroid/mevalonate biosynthesis/metabolism*

24-dehydrocholesterol reductase	*DHCR24*
3-hydroxy-3-methylglutaryl-coenzyme a reductase	*HMGCR*
3-hydroxy-3-methylglutaryl-coenzyme a synthase 1	*HMGCS1*
acetyl-coenzyme a synthetase 2 (adp forming) (predicted)	*ACAS2*
acyl-coa synthetase long-chain family member 1	*ACSL1*
acyl-coa synthetase long-chain family member 3	*ACSL3*
acyl-coa synthetase long-chain family member 4	*ACSL4*
acyl-coenzyme a dehydrogenase, short/branched chain	*ACADSB*
acyl-coenzyme a dehydrogenase, very long chain	*ACADVL*
acyl-coenzyme a oxidase 1, palmitoyl	*ACOX1*
adiponectin receptor 2	*ADIPOR2*
adipose differentiation-related protein	*ADRP*
alcohol dehydrogenase 1	*ADH1*
aldo-keto reductase family 1, member b8	*AKR1B8*
alkylglycerone phosphate synthase	*AGPS*
alpha-fetoprotein	*AFP*
atp citrate lyase	*ACLY*
carnitine o-octanoyltransferase	*CROT*
caveolin	*CAV*
cd36 antigen	*CD36*
crystallin, lamda 1	*CRYL1*
cytochrome p450, subfamily 51	*CYP51*
diacylglycerol o-acyltransferase homolog 2 (mouse)	*DGAT2*
diazepam binding inhibitor	*DBI*
dodecenoyl-coenzyme a delta isomerase	*DCI*
dolichol-phosphate (beta-d) mannosyltransferase 1 (predicted)	*DPM1*
electron-transfer-flavoprotein, beta polypeptide	*ETFB*
elovl family member 6, elongation of long chain fatty acids (yeast)	*ELOVL6*
enoyl coenzyme a hydratase 1, peroxisomal	*ECH1*
farensyl diphosphate synthase	*FDPS*
farnesyl diphosphate farnesyl transferase 1	*FDFT1*
fatty acid binding protein 5, epidermal	*FABP5*
fatty acid desaturase 1	*FADS1*
fatty acid synthase	*FAS*
ferredoxin reductase	*FDXR*
glutathione peroxidase 4	*GPX4*
glyceronephosphate o-acyltransferase	*GNPAT*
high density lipoprotein binding protein	*HDLBP*
hydroxysteroid (17-beta) dehydrogenase 7	*HSD17B7*
hydroxysteroid 11-beta dehydrogenase 1	*HSD11B1*
isopentenyl-diphosphate delta isomerase	*IDI1*
l-3-hydroxyacyl-coenzyme a dehydrogenase, short chain	*HADHSC*
lanosterol synthase	*LSS*
leukotriene b4 12-hydroxydehydrogenase	*LTB4DH*
lipin 1	*LPIN1*
lipoprotein lipase	*LPL*
low density lipoprotein receptor	*LDLR*
low density lipoprotein receptor-related protein 1	*LRP1*
membrane-bound transcription factor protease, site 1	*MBTPS1*
mevalonate (diphospho) decarboxylase	*MVD*
mevalonate kinase	*MVK*
microsomal glutathione s-transferase 3 (predicted)	*MGST3*
mitochondrial acyl-coa thioesterase 1	*MTE1*
nad(p) dependent steroid dehydrogenase-like	*NSDHL*
notch1-induced protein	*LOC493574*
nuclear receptor subfamily 0, group b, member 1	*NR0B1*
nuclear receptor subfamily 1, group h, member 3	*NR1H3*
nuclear receptor subfamily 2, group f, member 2	*NR2F2*
peroxisomal trans-2-enoyl-coa reductase	*PECR*
peroxisome proliferator activated receptor, gamma	*PPARG*
phosphatidylcholine transfer protein	*PCTP*
phosphatidylinositol 3-kinase, c2 domain containing, alpha polypeptide	*PIK3C2A*
phosphatidylinositol 3-kinase, regulatory subunit, polypeptide 1	*PIK3R1*
phosphatidylinositol-4-phosphate 5-kinase, type 1 alpha	*PIP5K1A*
phosphatidylserine synthase 2 (predicted)	*PTDSS2*
phospholipase a2, group iva (cytosolic, calcium-dependent)	*PLA2G4A*
phospholipase c, beta 1	*PLCB1*
phospholipase c, delta 4	*PLCD4*
phosphorylase kinase alpha 1	*PHKA1*
phytanoyl-coa hydroxylase	*PHYH*
prostaglandin-endoperoxide synthase 1	*LOC497767*
prostaglandin-endoperoxide synthase 2	*PTGS1*
protein kinase, camp dependent regulatory, type ii beta	*PTGS2*
sialyltransferase 7f	*PRKAR2B*
sialyltransferase 9	*SIAT7F*
similar to acetyl coa transferase-like	*SIAT9*
cholinephosphotransferase 1 alpha	*MGC95138*
similar to chromosome 20 open reading frame 155	*RGD1311037*
solute carrier family 27 (fatty acid transporter), member 3 (predicted)	*SLC27A3*
sphingomyelin phosphodiesterase 1, acid lysosomal	*SMPD1*
stearoyl-coenzyme a desaturase 1	*SCD1*
stearoyl-coenzyme a desaturase 2	*SCD2*
steroid sulfatase	*STS*
steroidogenic acute regulatory protein	*STAR*
sterol regulatory element binding factor 1	*SREBF1*
tumor necrosis factor receptor superfamily, member 1a	*TNFRSF1A*

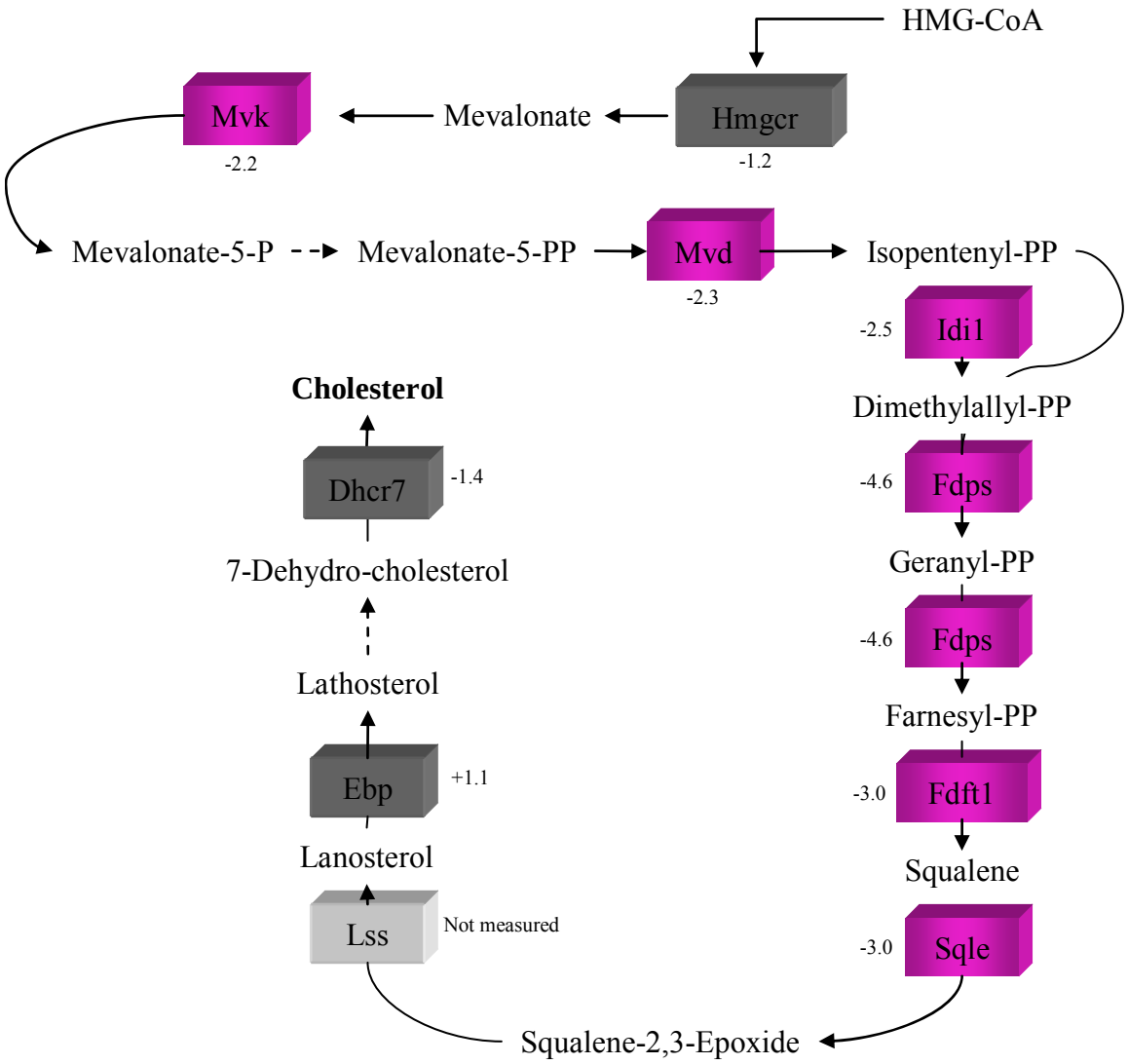

FIGURE 3.26. *Expression changes of genes involved in the cholesterol biosynthesis pathway in CX4 cells compared GN6TF cells.* Expression of genes in this pathway were measured by microarray analysis and loaded into GenMapp for visualization of the results. Genes in pink represent a ≥2-fold reduction of gene expression in suppressed CX4 compared to GN6TF. The adjacent numbers represent fold-change and the sign designates the direction of the change. *Hmgcr*, *Dhcr7* and *Ebp* were decreased, but did not meet the ≥2-fold criterion, and *Lss* was not measured.

TABLE 3.8. *Genes decreased ≥2-fold in CX4 cells compared to GN6TF cells associated with the extracellular matrix*

a disintegrin-like and metalloproteasewith thrombospondin type 1	*ADAMTS1*
biglycan	*BGN*
chondroitin sulfate proteoglycan 2	*CSPG2*
collagen, type 1, alpha 1	*COL1A1*
collagen, type iii, alpha 1	*COL3A1*
collagen, type v, alpha 1	*COL5A1*
collagen, type v, alpha 2	*COL5A2*
collagen, type v, alpha 3	*COL5A3*
craniofacial development protein 1	*CFDP1*
egf-containing fibulin-like extracellular matrix protein 2	*EFEMP2*
fibrillin 1	*FBN1*
fibromodulin	*FMOD*
glypican 1	*GPC1*
matrix extracellular phosphoglycoprotein with asarm motif (bone)	*MEPE*
matrix metallopeptidase 13	*MMP13*
matrix metallopeptidase 3	*MMP3*
matrix metalloproteinase 14 (membrane-inserted)	*MMP14*
nidogen 1	*NID1*
periostin, osteoblast specific factor (predicted)	*POSTN*
pleiotrophin	*PTN*
procollagen, type vi, alpha 3 (predicted)	*COL6A3*
procollagen, type xii, alpha 1	*COL7A1*
procollagen, type xv	*COL15A1*
procollagen, type xvi, alpha 1	*COL16A1*
procollagen, type xxvii, alpha 1	*COL27A1*
sarcoglycan, alpha (dystrophin-associated glycoprotein) (predicted)	*SGCA*
sarcoglycan, beta (dystrophin-associated glycoprotein) (predicted)	*SGCB*
sarcoglycan, epsilon	*SGCE*
secreted acidic cysteine rich glycoprotein	*SPARC*
secreted phosphoprotein 1	*SPP1*
sialophorin	*SPN*
similar to glypican 4	*LOC317322*
spondin 1	*SPON1*
superoxide dismutase 3, extracellular	*SOD3*
tenascin c	*TNC*
transforming growth factor, beta induced	*TGFBI*
vascular endothelial growth factor a	*VEGF1*

is

Cluster analysis of these GO terms reveals enriched biological themes associated with nucleotide binding (specifically RNA-associated) and cell junction molecules (TABLE 3.10 and TABLE 3.11 respectively). These data suggest that introduction of a gene on chromosome 11 may be responsible for the transcriptional regulation of genes with RNA binding motifs (RRM, TABLE 3.10). Consistent with the flattened cellular morphology and contact inhibition that accompanies suppression of the neoplastic phenotype in CX4 MCH cells, there is an up-regulation of cellular adhesion/junction genes (TABLE 3.11) that may account for the restored ability of these suppressed cells to recognize and/or process extracellular stimuli for growth arrest.

These analyses provide a statistically relevant indication of groups of genes which may be directly or indirectly causative or affected by introduction of human chromosome 11 into the tumorigenic rat liver tumor cell line GN6TF. In order to understand more directly the effects of SYT13 in this system, the short list of genes that follows strict differential expression guidelines in suppressed and non-suppressed cell lines (TABLE 3.5) was submitted to the DAVID Functional Annotation Tool. Several gene ontology terms were statistically associated with the short list of genes that were 2-fold down-regulated in all aggressive (i5, i12, and GN6TF) cell lines versus suppressed (CX4 and *SYT13*s1) (TABLE 3.12). Enriched themes in this table include development and differentiation, specifically the regulation of neurogenesis. No GO terms were associated with the 4 genes up-regulated in the aggressive cell lines. This analysis suggests novel information regarding both the biological relevance/function of SYT13 as well as an indication on the potential mechanism of SYT13-mediated tumor suppression through a re-establishment of target cell differentiation.

TABLE 3.9. *Gene ontology terms associated with genes up-regulated in the CX4 cell line relative to GN6TF*

Gene Ontology Term	*P*Value
nucleus	2.5×10^{-8}
intracellular	1.4×10^{-7}
nuclear protein	2.7×10^{-7}
cell	1.1×10^{-6}
cell junction	1.2×10^{-6}
cell organization and biogenesis	2.2×10^{-6}
intercellular junction	2.5×10^{-6}
rna-binding	3.8×10^{-6}
intracellular signaling cascade	6.6×10^{-6}
cellular localization	7.3×10^{-6}
establishment of cellular localization	7.8×10^{-6}
intracellular transport	8.9×10^{-6}
cytoskeleton	1.1×10^{-5}
protein binding	2.0×10^{-5}
phosphorylation	2.8×10^{-5}
RNA-binding region RNP-1 (RNA recognition motif)	7.5×10^{-5}
apical part of cell	9.3×10^{-5}
organelle	1.0×10^{-4}
intracellular organelle	1.1×10^{-4}
cytoskeletal protein binding	1.2×10^{-4}
adherens junction	1.2×10^{-4}
protein amino acid dephosphorylation	1.4×10^{-4}
non-membrane-bound organelle	1.5×10^{-4}
intracellular non-membrane-bound organelle	1.5×10^{-4}
Nucleotide-binding, alpha-beta plait	1.5×10^{-4}
actin binding	1.5×10^{-4}
RRM domain	1.8×10^{-4}
dephosphorylation	2.1×10^{-4}
cell-cell adherens junction	2.4×10^{-4}
regulation of cellular physiological process	2.4×10^{-4}
regulation of biological process	2.4×10^{-4}
adherens junction	2.6×10^{-4}
transforming protein	2.7×10^{-4}
positive regulation of apoptosis	3.8×10^{-4}
tight junction	4.4×10^{-4}
positive regulation of programmed cell death	4.9×10^{-4}
focal adhesion	5.1×10^{-4}
regulation of physiological process	5.2×10^{-4}
programmed cell death	5.2×10^{-4}
cell death	6.0×10^{-4}
regulation of cellular process	6.3×10^{-4}
zinc-finger	6.4×10^{-4}
apicolateral plasma membrane	6.4×10^{-4}
apical junction complex	6.4×10^{-4}
proto-oncogene	6.8×10^{-4}
biopolymer metabolism	6.9×10^{-4}
mRNA processing	7.0×10^{-4}
establishment of protein localization	7.1×10^{-4}
apoptosis	7.4×10^{-4}
nucleic acid binding	7.5×10^{-4}
DNA binding	7.7×10^{-4}
GTP binding	8.0×10^{-4}
guanyl nucleotide binding	8.5×10^{-4}
death	9.7×10^{-4}
Tyrosine specific protein phosphatase	0.001
chromosome	0.001
protein transport	0.001
phosphoprotein phosphatase activity	0.001
actin filament binding	0.001
regulation of programmed cell death	0.001
small GTPase mediated signal transduction	0.001

TABLE 3.10. *Genes increased ≥2-fold in CX4 cells compared to GN6TF associated with RNA-binding*

atp-dependent, rna helicase	*DDX52*
cell division cycle 5-like	*CDC5L*
cleavage and polyadenylation specific factor 6, 68kda	*CPSF6*
cold inducible rna binding protein	*CIRBP*
cytochrome p450, family 2, subfamily s, polypeptide 1	*CYP2S1*
cytotoxic granule-associated rna binding protein 1	*TIA1*
ddx5 gene	*DDX5*
down syndrome critical region homolog 1 (human)	*DSCR1*
elav (embryonic lethal, abnormal vision, drosophila)-like 2 (hu antigen b)	*ELAVL2*
eukaryotic translation initiation factor 2, subunit 1 alpha	*EIF2S1*
eukaryotic translation initiation factor 4b	*EIF4B*
exportin 1, crm1 homolog (yeast)	*XPO1*
fibrillarin	*FBL*
fus interacting protein (serine-arginine rich) 1	*FUSIP1*
fusion (involved in t(12;16) in malignant liposarcoma)	*FUS*
heterogeneous nuclear ribonucleoprotein a/b	*HNRPAB*
heterogeneous nuclear ribonucleoprotein a1	*HNRPA1*
heterogeneous nuclear ribonucleoprotein a3	*HNRPA3*
heterogeneous nuclear ribonucleoprotein d-like	*HNRPDL*
heterogeneous nuclear ribonucleoprotein k	*HNRPK*
heterogeneous nuclear ribonucleoprotein r	*HNRPR*
high density lipoprotein binding protein	*HDLBP*
hla-b-associated transcript 1a	*BAT1A*
hnrnp-associated with lethal yellow	*RALY*
hypothetical gene supported by nm_173309	*LOC497806*
hypothetical gene supported by y16641	*RGD1564920*
hypothetical rna binding protein rgd1359713	*RGD1359713*
iron responsive element binding protein 2	*IREB2*
matrin 3	*MATR3*
nucleophosmin 1	*NPM1*
pai-1 mrna-binding protein	*PAIRBP1*
paraspeckle protein 1	*PSPC1*
protein phosphatase 1, regulatory subunit 10	*PPP1R10*
ras-gtpase-activating protein sh3-domain binding protein	*G3BP*
ribosomal protein l22	*RPL22*
rna binding motif protein 16	*RBM16*
rna binding motif protein 24 (predicted)	*RBM24*
rna binding motif protein 27 (predicted)	*RBM27*
rna binding motif protein 8 (predicted)	*RBM8*
rna helicase	*DDX46*
rna-binding region (rnp1, rrm) containing 2	*RNPC2*
siah binding protein 1;ribonucleoprotein-binding protein 1	*SIAHBP1*
signal recognition particle 54	*SRP54*
similar to 2810036l13rik protein (predicted)	*RGD1305861*
similar to chromosome 20 open reading frame 6	*RGD1306067*
similar to dj862k6.2.2 (splicing factor, arginine/serine-rich 6 (srp55-2)(isoform 2))	*LOC362264*
similar to heterogeneous nuclear ribonucleoprotein a0	*RGD1563684*
similar to heterogeneous nuclear ribonucleoprotein g - human	*LOC302855*
similar to hnrpa3 protein	*RGD1563768*
similar to hnrpa3 protein	*RGD1562688*
similar to igf-ii mrna-binding protein 2 (predicted)	*RGD1305614*
similar to msx-2 interacting nuclear target protein	*RGD1564662*
similar to riken cdna 1700025b16 (predicted)	*RGD1308015*
similar to riken cdna 3110010f15	*RGD1308378*
similar to riken cdna g430041m01	*RGD1562563*
similar to rna binding motif protein 25	*RGD1565486*
similar to rna binding protein gene with multiple splicing	*RGD1561067*
similar to rna-binding protein isoform g3bp-2a	*RGD1309571*
similar to rna-binding protein musashi2-s	*RGD156039*
small nuclear ribonucleoprotein polypeptides b and b1	*SNRPB*
splicing factor proline/glutamine rich (polypyrimidine tract binding protein associated)	*SFPQ*
splicing factor, arginine/serine-rich 10 (transformer 2 homolog, drosophila)	*SFRS10*
splicing factor, arginine/serine-rich 12	*SFRS12*
splicing factor, arginine/serine-rich 3 (srp20) (predicted)	*SFRS3*
splicing factor, arginine/serine-rich 5	*SFRS5*
src associated in mitosis, 68 kda	*KHDRBS1*
synaptojanin 1	*SYNJ1*
synaptotagmin binding, cytoplasmic rna interacting protein	*SYNCRIP*
tho complex 1	*THOC1*
tial1 cytotoxic granule-associated rna binding protein-like 1 (mapped)	*TIAL1*
vascular endothelial zinc finger 1 (predicted)	*VEZF1*
zinc responsive protein zd7	*LOC474154*

TABLE 3.11. *Genes increased ≥2-fold in CX4 cells compared to GN6TF cells associated with cell adhesion.*

a disintegrin and metalloproteinase domain 15 (metargidin)	*ADAM15*
afadin	*AF6*
ahnak nucleoprotein (desmoyokin)	*AHNAK*
ajuba homolog (xenopus laevis)	*JUB*
angiomotin like 2	*AMOTL2*
ash1 (absent, small, or homeotic)-like (drosophila) (predicted)	*ASH1L*
cadherin 1	*CDH1*
catenin (cadherin-associated protein), alpha 1, 102kda	*CATNA1*
coxsackie virus and adenovirus receptor	*CXADR*
desmoplakin	*DSP*
dipeptidylpeptidase 4	*DPP4*
discs, large homolog 5 (drosophila) (predicted)	*DLG5*
envoplakin (predicted)	*EVPL*
fat tumor suppressor homolog (drosophila)	*FATH*
filamin, beta (predicted)	*FLNB*
gap junction membrane channel protein alpha 4	*GJA4*
gap junction membrane channel protein beta 3	*GJB3*
gap junction membrane channel protein beta 5	*GJB5*
junction plakoglobin	*JUP*
junctional adhesion molecule 1	*F11R*
laminin, alpha 3	*LAMA3*
lim domain only protein 7	*LMO7*
myosin, heavy polypeptide 9	*MYH9*
p21 (cdkn1a)-activated kinase 1	*PAK1*
par-6 (partitioning defective 6) homolog beta (c. elegans) (predicted)	*PAR6B*
parvin, alpha	*PARVA*
plakophilin 1 (predicted)	*PKP1*
plakophilin 2	*PKP2*
plakophilin 3 (predicted)	*PKP3*
plakophilin 4 (predicted)	*PKP4*
poliovirus receptor-related 2 (herpesvirus entry mediator b)	*PVRL2*
procollagen, type xvii, alpha 1 (predicted)	*COL17A1*
protein kinase c, zeta	*PRKCZ*
protein kinase, lysine deficient 4	*PRKWNK4*
protocadherin 1 (cadherin-like 1) (predicted)	*PCDH1*
similar to claudin-18a1.2	*LOC315953*
similar to hypothetical protein mgc33926	*MGC94782*
thiopurine methyltransferase	*TPMT*
tight junction protein 1 (predicted)	*TIP1*
tight junction protein 2	*TIP2*
tight junction protein 3 (predicted)	*TIP3*
transforming growth factor beta 1 induced transcript 1	*TGFB1I1*
transglutaminase 1	*TGM1*
vinculin (predicted)	*VCL*

TABLE 3.12. *Gene ontology terms associated with genes down-regulated in* SYT13*i5,* SYT13*i12, and GN6TF compared to CX4 and* SYT13*s1*

Gene Ontology Term	***P*Value**
regulation of development	0.002
signal	0.003
regulation of axonogenesis	0.009
response to external stimulus	0.011
regulation of neurogenesis	0.013
extracellular space	0.014
signal peptide	0.022
extracellular region	0.023
positive regulation of development	0.025
axon guidance	0.025
cell differentiation	0.029
positive regulation of biological process	0.030
phospholipid binding	0.037
wound healing	0.040
axonogenesis	0.046

DISCUSSION

IDENTIFICATION OF *SYT13* AS A CANDIDATE 11P11.2 TUMOR SUPPRESSOR GENE

The studies presented herein were initiated January of 2001, approximately one year after the first version of the annotated genome by the International Human Genome Sequencing Consortium was published in *Nature* (94). By April of 2003, 50 years after the description of the double helix structure of DNA (95), 99% of the gene-containing portion of the human genome had been sequenced with 99.99% accuracy (96). The resources provided by the Human Genome Project, including the placement of genes and ESTs on human chromosome 11, facilitated a candidate gene approach to identification of putative liver tumor suppressor genes using our MCH model system. Synaptotagmin XIII was identified as the strongest candidate for the 11p11.2 tumor suppressor gene based on its differential expression among a panel of several suppressed and MCH cell lines. Additional evidence that suggested *SYT13* as a novel tumor suppressor gene was its apparent methylation-dependent attenuation in several human HCC cell lines. However, as far as we know, SYT13 has been implicated as a tumor suppressor only by its differential expression in two genome-wide expression analyses of colorectal (97) and pancreatic (84) neoplasms, and its biological functions are unknown.

CHARACTERIZATION OF *SYT13* AS A CANDIDATE TUMOR SUPPRESSOR GENE

Subsequent to the identification of *SYT13* as a strong candidate tumor suppressor

gene, it was essential to characterize its involvement and function in suppression of the neoplastic phenotype of rat liver tumor cell lines in our model system. A complementary approach was utilized to silence SYT13 in a suppressed MCH cell line and to introduce SYT13 into a rat liver tumor cell line. Specific silencing of the SYT13 protein in CX4 cells resulted in significant alterations of both the suppressed phenotype *in vitro* (FIGURE 3.15) and the average latency of tumor formation *in vivo* (TABLE 3.3), suggesting that SYT13 is necessary for 11p11.2-mediated tumor suppression in the CX4 MCH cell line. SYT13 was exogenously expressed in GN6TF tumor cells to determine if SYT13 could independently effect the same level of tumor suppression seen in the MCH cell lines in response to human 11p11.2. Tumorigenicity was significantly reduced in transfected cell lines that expressed the dimeric form of SYT13 (TABLE 3.4). The summation of these studies revealed that SYT13 is both necessary and sufficient for human chromosome 11p11.2-mediated suppression of tumorigenicity in GN6TF tumor cells.

The current investigation has characterized several tumor-suppressive functions of SYT13, including (i) normalization of tumor cell morphology, (ii) restoration of contact inhibition, (iii) reestablishment of anchorage-dependent growth, and (iv) suppression of tumorigenic potential *in vivo*. However, other functional characteristics ascribed to classic tumor suppressor genes have not been directly evaluated. Thus, it remains to be determined if SYT13 possesses additional tumor suppressor functions. Other measurable down-stream effects attributed to specific tumor suppressor genes (in culture and/or *in vivo*) include regulation of cellular proliferation/cell-cycle progression, inhibition of cell invasion and migration, reestablishment of tumor cell mortality, and restoration of sensitivity to pro-apoptotic stimuli, among others (98). Although not measured in the SYT13-transfected cells

described here, the potential effects of SYT13 on some of these characteristics can be extrapolated from previous studies and general observation. Population doubling times for suppressed GN6TF-derived MCH cell lines were not significantly affected by introduction of human chromosome 11 (40). Therefore, given that the suppressive effects of human chromosome 11 are SYT13-mediated, we can infer that SYT13 has minimal or no effect on the regulation of cellular proliferation or cell cycle control as they impact on the kinetics of cellular proliferation. Likewise, neither the suppressed MCH cell lines nor the SYT13-transfected cell lines senesce in culture. Thus, SYT13-mediated tumor suppression des not simply reflect a reestablishment of cellular mortality. Further, no appreciable level of apoptosis occurs in SYT13-expressing cells growing in culture at various densities, suggesting that direct induction of apoptosis is not a downstream effect of SYT13. The abilities of SYT13-negative and SYT13-positive cells to invade and migrate *in vitro* were not measured. Complete characterization of the tumor suppressor functions of SYT13 will require further investigation of these (and possibly other) tumor suppressive functions.

THE SYNAPTOTAGMIN PROTEIN FAMILY

Synaptotagmins are a family of membrane-associated synaptic vesicle transport proteins which largely serve as Ca^{2+} sensors in vesicular trafficking and exocytosis (78, 99). SYT1 was the first identified and most well characterized (100) and 14 other family members have been identified based on similar structural characteristics. All synaptotagmins display type I membrane topology with a single transmembrane region (TMR) of varying lengths and two distinct tandem C2 domains (C2A and C2B) in the cytoplasmic C terminus (101). The C2 domain forms an eight-stranded beta sandwich around a 4-stranded motif (101).

Common functions among synaptotagmin family members are calcium-dependent phospholipid binding in vesicle transport and calcium-independent binding to target SNARE (tSNARE) heterodimers during calcium-triggered membrane fusion (102).

Synaptotagmin XIII is an atypical synaptotagmin (78, 79). Perhaps the most conserved function across the protein family is calcium-independent binding to tSNARE heterodimers during membrane fusion, and SYT13 is one of the only two synaptotagmins (along with SYT12) that do not bind to this complex (102). Additionally, SYT13 lacks the calcium-dependent phospholipid binding properties conserved in several of the family members. The disparity between the functional roles of SYT13 and its family members most likely reflects the atypical characteristics of the SYT13 protein. It displays less than 35% sequence similarity (at the amino acid level) with its closest relative among synaptotagmin family members, SYT1 (FIGURE 4.1). SYT13 lacks an N-terminal intravesicular (extracellular) sequence that precedes the TMR, and the linker region between the TMR and first C2 domain is much longer in SYT13 than in any other synaptotagmin. This proline-rich linker in SYT13 contains conserved PxxP motifs which von Poser *et al.* predict may be SH3-domain binding regions (79). In addition, the calcium-binding residues common in most synaptotagmins are not conserved in SYT13 (78, 79) which accounts for the absence of calcium-dependent functions. Even the features that distinguish this synaptotagmin as such (the TMR, connecting sequence, C2A and C2B domains) are dissimilar from SYT1 (30%, 0.0%, 22.7%, and 34.5% identity respectively) at the amino acid level (79).

Possibly the most informative comparisons between SYT13 and typical synaptotagmin family members are the properties that are selectively conserved. The C2B domains of synaptotagmins differ from C2A domains by a C-terminal sequence that

corresponds to an extra α-helix (FIGURE 4.1) (103). Despite the lack of calcium binding sites and the absence of the calcium-dependent phospholipid binding properties of SYT13, it retains this differentiating α-helix at the end of the C2B domain (FIGURE 4.1) (79). The function of this secondary structure is not fully understood, but is likely responsible for several of the calcium–independent functions of the C2B domain (103). An additionally conserved feature among all synaptotagmins is the size of the linker sequence between the two C2 domains (6-7 amino acid residues) (FIGURE 4.1) (79), which suggests that the tertiary structure of the tandem C2 domains (C2A-linker-C2B) may be important for the conserved function of synaptotagmins. SYT13 also retains the WHXL motif found at the C-terminus of all synaptotagmins (FIGURE 4.1). This sequence is responsible for association with neurexins and the docking of vesicles to plasma membranes (104). Neurexins are structural cell adhesion molecules and plasma membrane receptors that are responsible for cell recognition, axonal guidance, and epithelial cell polarity (105). While describing SYT13 in mouse, Fukuda and Mikoshiba confirmed an association between SYT13 and neurexin 1α (78). Finally, a conserved cluster of cysteine residues reside at the cytoplasmic border between the TMR and the linker sequence of most synaptotagmins, including SYT13 (FIGURE 4.1). These cysteine residues are palmitoylated and are essential for SDS-resistant oligomerization of synaptotagmins (80). This fatty acylation and subsequent oligomerization is critical for calcium-independent association with the plasma membrane which is necessary for several of the synaptotagmin functions (106).

Temporal and spatial bio-availability of SYT13 has been, for the most part, determined by mRNA analysis. A multiple tissue northern blot analysis performed by von Poser and Südhof found expression of a single species in rat brain (highest expression),

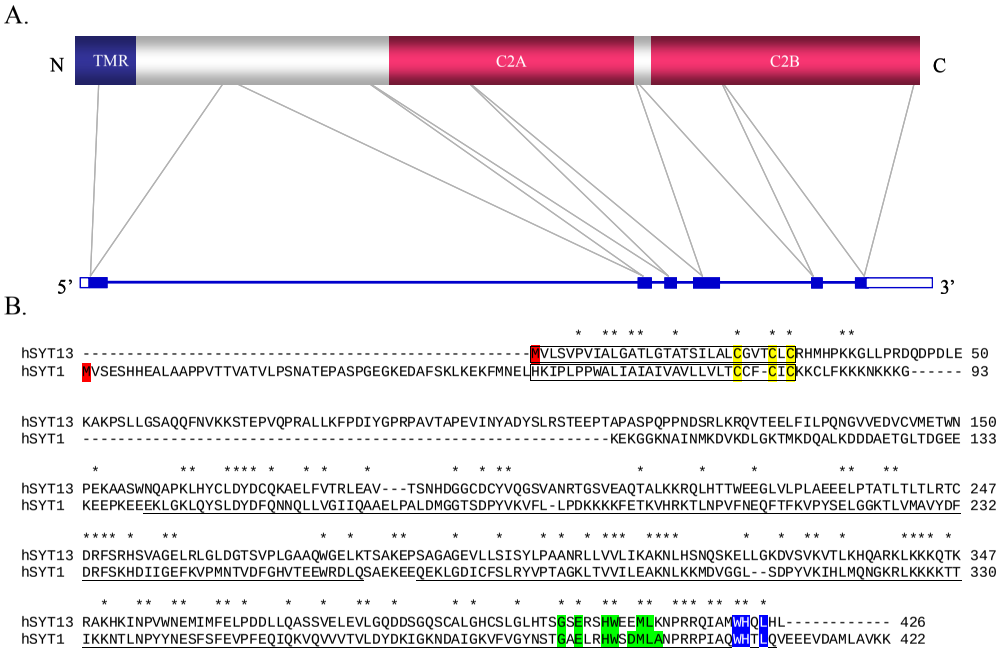

FIGURE 4.1. *Synaptotagmin XIII.* (A) Exon-coding regions of *SYT13*, identified by blue boxes, are mapped with lines directed to their corresponding regions on the SYT13 protein. TMR=transmembrane region. C2A and C2B=tandem C2 domains. (B) Human SYT13 is aligned with human SYT1. Asterisks denote conserved residues. The TMR is boxed and the two C2 domains are underlined. Methionine start sites are highlighted in pink and conserved cysteine residues (putative palmitoylation sites) are highlighted in yellow. Residues differentiating the C2B domain from the C2A domain are shown in green, and the WHXL motif is highlighted in blue.

spleen, kidney, and testis (79). Fukuda and Mikoshiba used RT-PCR to identify mRNA expression in mouse heart, brain, spleen, lung, skeletal muscle, kidney and testis (highest in brain, lung, and testis) (78). Additionally, they found expression to peak on embryonic day 7 of mouse development (78). A genome wide expression analysis of normal human tissue provided by GeneNote (http://bioinfo2.weizmann.ac.il/cgi-bin/genenote/home_page.pl) found the highest expression of *SYT13* in brain, spinal cord, heart, pancreas, prostate, and kidney (107). However, several lines of evidence suggest that mRNA expression is an inappropriate measure of SYT13 protein expression, and that the expression of the protein may be regulated post-transcriptionally. von Poser and Südhof used a polyclonal antibody raised to recombinant C2-domains from SYT13 in rat brain homogenates and subcellular fractions from rat brains and failed to detect a protein band of the appropriate size (79). Another indication of the inappropriate use of mRNA detection for measuring SYT13 protein production is the discrepancy of tissue-specific expression between human, mouse, and rat in these afore mentioned studies (78, 79, 107). A study that compared a genomic and proteomic approach to identifying genes and proteins differentially secreted between cancerous and normal pancreatic cells showed a lack of correlation between *SYT13* and the corresponding protein (84). In fact, they found a correlation coefficient (r) of 0.28 between proteomic and transcriptomic studies (84). Finally, the protein recognized by the polyclonal antibody utilized in these studies (for both silencing and transfection of SYT13) did not correlate with mRNA expression (FIGURES 3.11, 3.12 and 3.17), adding significantly to the argument that SYT13 protein expression is regulated at the posttranscriptional level.

The human *SYT13* gene is composed of 6 coding exons and 5 gt-ag introns distributed over 42 kb of genomic DNA [FIGURE 4.1; (79) and AceView

(http://www.ncbi.nlm.nih.gov/IEB/Research/Acembly/index.html; (108)]. The complete coding sequence mRNA is 5,265 bp long. The 3' UTR contains 3,874 bp—among 5% of the longest 3' UTRs recorded (AceView). There appears to be no splice variants of the *SYT13* gene (AceView). *SYT13* homologs have been confirmed in *P. troglodytes*, *C. familiaris*, *M. musculus*, *R. norvegicus*, and *G. gallus* (NCBI). The long 3' UTR is conserved in each of these homologs, and is likely important for a conserved regulatory function which has not yet been elucidated.

KNOWN AND INFERRED FUNCTIONS OF SYT13

We are the first to functionally characterize *SYT13* as a tumor suppressor gene. The tumorigenic rat liver cell line GN6TF expresses both the endogenous *Syt13* mRNA and protein (FIGURES 3.11 AND 3.12). However, we have clearly shown that exogenous expression of human SYT13 is able to suppress the tumorigenic phenotype of this cell line. Specifically, suppression is rigorously associated with the expression of the SDS-resistant dimeric form of the protein. Despite the presence of the endogenous protein and transcript, the suppressive dimeric species is not detected in GN6TF cells (FIGURES 3.11 and 3.17), nor is it detected in tumorigenic *SYT13*-transfected cell lines (FIGURE 3.17). This strongly suggests that the suppressive function of SYT13 is restricted to the dimeric form of the protein. It is known that the SDS-resistant, calcium-independent oligomerization of synaptotagmins is mediated by palmitoylation of the cysteine residues that cluster at the carboxyl-terminus of the TMR (80). This fatty acylation and dimerization is critical for the calcium-independent membrane association of many synaptotagmins (80). It is unclear if the structure of the dimeric form of the protein itself is critical for tumor suppressor function or if

its membrane localization is important for its downstream effects. Nonetheless, these data provide strong evidence for a tumor suppressive function of the SYT13 dimer.

Several additional studies have characterized functional properties of the SYT13 protein. These studies have identified calcium independent association of the C2B with phospholipids (78) and the absence of calcium-mediated association of the C2A domain with phospholipids (78). Additionally, the role of vesicle trafficking has been attributed to SYT13 based on its (i) multiple tissue expression, (ii) peri-nuclear compartmentalization (presumably in the Golgi), (iii) docking with the membrane receptor neurexin, and (iv) punctate cytosolic staining, apparently indicating transport from the Golgi to the plasma membrane (78). Additional resources outline proposed or inferred biological functions of SYT13. The GO biological process terms associated with SYT13 by the Gene Ontology Consortium [www.geneontology.org, (109)] are "transport" and "vesicle-mediated transport." However the evidence for these terms is "ISS" (inferred from sequence similarity) which is a code for predictions based on sequence alignment, structure comparison, or evaluation of sequence features such as composition (www.geneontology.org).

Another potential source for information about the function of SYT13 is from deletion analyses in other diseases states. Recent studies provide evidence that SYT13 may have other diseases implications. Potocki-Shaffer syndrome (PSS) is a contiguous gene syndrome that results from haploinsufficiency of at least two genes on human chromosome 11p11.2 (ALX4 and EXT2) and can manifest in multiple congenital anomalies and mental retardation (OMIM #601224; NCBI). Wakui *et al*. constructed a panel of 11p11.2 deletions in several of these patients to identify 11p11.2 genes that are responsible for specific disease

traits (110). They identified a 1.1 Mbp region (D11S554-D11S1385) that was necessarily deleted for the impaired cognitive function/mental retardation phenotype in the patients. These results were later confirmed by another group in a 3-generation patient subset lacking the mental retardation phenotype (111). This region contains nine genes (including *SYT13*), and considering the implication for a neuronal development function of *SYT13* in our microarray study (TABLE 3.9), it is a very likely candidate for the mental retardation phenotype seen in Potocki-Shaffer syndrome.

Inferences of biological function may also be made by analyzing available microarray data which has identified differential expression of the *SYT13* in various experimental settings (although it is important to recall that *SYT13* mRNA and protein levels do not necessarily correlate). TABLE 4.1 outlines several studies in which differential expression of *SYT13* has been documented. The studies presented in this table reiterate a potential function for *SYT13* in neuronal development and differentiation (112-115), suggest different transcription factors and repressors that may be important in *SYT13* regulation (116-118), and implicate loss of *SYT13* in the progression of colorectal and pancreatic neoplasia (97, 119).

Considering the variety of biological implications for *SYT13* inferred from sequence similarity to other synaptotagmins, functional properties of the protein product, electronic annotation, and differential expression in various experimental settings, it will be essential to complete additional functional studies, similar to the ones presented here, to grasp a better understanding of the conserved biological functions of SYT13 in both disease and normal physiology. The studies herein appear to be the first and only studies to experimentally describe a biological function for SYT13, the function of a tumor suppressor gene.

TABLE 4.1. *Differential expression of* SYT13 *in various experimental settings*.

Tissue	*SYT13* Context	Implication	Reference
murine tissue	highly expressed in a pool of 10 nervous tissues compared to a pool of 72 peripheral tissues representing 30 organs	although *SYT13* is expressed in various tissues, its expression may be enriched in the neural system	(120)
cultured murine airway smooth muscle cells	decreased in cells with persistant β-adrenergic receptor signaling compared to wild type	*SYT13* may be regulated by receptor signaling	(121)
rat inner ear	elevated in rat vestibular inner ear hair cells compared to adjacent supporting hair cells	*SYT13* may be involved in the differentiation of these cell types or contribute to the different functions	(112)
murine pancreas	decreased in transcription factor Ngn3-deficient pancreatic tissue compared to wild type	*SYT13* may be directly or indirectly regulated by Ngn3—a transcription factor required for differentiation of pancreatic endocrine (vs. exocrine) cells	(118)
neuronally differentiated PC12 cells	elevated in ceramide-dependent apoptosis	may be directly or indirectly be regulated by ceramide-dependent signaling and/or involved in apoptosis	(122)
murine primary visual cortex	increased in dark rearing animals (DR) vs normal reared	(i) may be important in aspects of activity-dependent plasticity in the visual cortex (ii) may be regulated by enriched CREB pathway in DR	(114)
rat pancreas	(i) decreased in fatty rat islets overexpressing SREBP-1c (ZDF) compared to lean controls (ii) increased in both ZDF and controls after treatment with dominant negative SREBP-1c	SREBP may regulate *SYT13* expression even under basal conditions	(117)
cultured human pancreatic ductal adenocarcinoma and non-neoplastic human pancreatic duct epithelial cell line	(i) decreased in pancreatic cancer secretome compared to normal (ii) protein is down, but transcript is not detected on microarray (iii) correlation coefficient of 0.28 between proteomic data and transcriptomic data	(i) SYT13 may be directly or indirectly involved in tumor suppression (ii) SYT13 protein and transcript do not necessarily correlate (iii) genomic microarray data may not always identify important and relevant proteins	(84)
PC12 cells	(i) SYT13 contains a cAMP response element that associates with the transcription factor CREB which regulates differentiation, survival, and synaptic plasticity (ii) elevated expression in response to forskolin stimulation	(i) may be a CREB transcriptional target (ii) may be a cAMP-regulated gene	(116)
human colorectal carcinoma	decreased in lyphatically metastasized compared to locally restricted colorectal carcinoma	may be important for suppression of the invasive and metastatic progression of colorectal carcinoma	(97)
human brain	increased in the brain of suicide victims and depressed suicide victims compared to psychiatrically normal controls	SYT13 may be involved in the neurobiology and predisposition to suicide	(123)
rat lung	elevated expression in adult rat lung tissue compared to both fetal and newborn lung	may be important of normal lung function in adulthood	(124)
murine retinal ganglion cell	down when the transcription factor Brn3b is deleted compared to wild type	may be involved in establishment of axonal cytoskeletal network and axon guidance	(113)
human prostate cancer	elevated in small-cell neuroendocrine carcinoma compared to prostate adenocarcinoma	reflects the neuroendocrine origin of prostate small cell carcinoma	(119)

POTENTIAL MECHANISMS OF SYT13-MEDIATEDTUMOR SUPPRESSION

Our previous studies have implicated the induction of Wt1 in human chromosome 11p11.2-mediated tumor suppression, and studies presented here further characterize the putative association between *Wt1* expression and SYT13-mediated tumor suppression. Additional evidence used to delineate potential mechanisms of tumor suppression includes information generated by microarray analysis and comparisons between the phenotypic characteristics of aggressive SYT13-dimer-negative and suppressed SYT13-dimer-positive cell lines. Coordinate with SYT13 expression in GN6TF tumor cells, we have observed: an induction of *Wt1* (FIGURE 3.18); the morphological organization of a polarized, contact-inhibited epithelial sheet (FIGURE 3.19); the establishment of contact inhibition (FIGURE 3.20); decreased expression of several genes associated with both the extracellular matrix and cholesterol/mevalonate biosynthesis (TABLE 3.7 AND TABLE 3.8); and elevated expression of genes associated both with development/differentiation and cellular adhesion (TABLE 3.5 AND TABLE 3.11). A potential link between several or all of these observations is the phenotypic and functional differences between the mesenchymal and epithelial cell type, and the requirements and manifestations of a physiological switch (transdifferentiation) between the two.

WT1 is a tumor suppressor gene implicated in hereditary and sporadic Wilms' tumor and is required for normal renal development. Based on several observations, including the temporal-spatial expression of *Wt1* during renal development (125) and the correlation of *Wt1* expression with the degree of epithelial differentiation of Wilm's tumor (126), *Wt1* has been implicated in mesenchymal-epithelial transition (MET, a process important in cellular differentiation and development) in both disease and normal states (127). Luo *et al*. showed

that *WT1* could slow the growth of both non-transformed and *ras*-transformed NIH3T3 fibroblasts, and cells expressing *WT1* were characterized by a flattened morphology (128). The group later demonstrated the ability of WT1 to induce features of epithelial differentiation in a mesenchymal cell line (127). MET is characterized by changes in various markers including a flattened, contact inhibited cellular morphology; a decrease in extracellular matrix proteins; and an increase in cellular adhesion molecules. Consistent with the *WT1*-associated induction of MET, our studies demonstrate a coordinate expression of *Wt1* with the expression of an epithelioid cellular morphology (FIGURE 3.19), a reduction of several extracellular matrix proteins (TABLE 3.7), and an increase in cellular adhesion molecules (TABLE 3.11). The adhesion molecule E-cadherin (*CDH1*) is an epithelial marker and tumor suppressor gene important in the maintenance of epithelial intracellular contact. Because *CDH1* is absent in mesenchymal cells and consistently activated in MET events, *CDH1* expression is commonly measured to identify the differentiation of cells from a mesenchymal to epithelial phenotype and signal MET. *WT1* directly transactivates *CDH1* through a *WT1*-response element in the promoter (129). Consistent with this, our microarray data demonstrate an 84-fold increase in *Cdh1* expression in CX4 cells compared to GN6TF cells (FIGURE 3.25.A). *Cdh1* levels were also measured in *SYT13*-transfected cell lines (FIGURE 3.25.B). Expression levels of *Cdh1* in the tumor suppressed and morphologically normal cell lines that express the SYT13 dimeric species (and *Wt1*) (C2, E2, F3, and J1) were greater than 100-fold elevated compared to GN6TF (FIGURE 3.25.B). Furthermore, microarry data presented here (TABLE 3.12) and generated in additional studies [TABLE 4.1 (112-115) and (110, 111)] suggest a role for SYT13 in development and cellular

differentiation, consistent with the idea that SYT13, directly or indirectly through induction of *WT1*, may be involved mesenchymal to epithelial differentiation.

Another putative target of the *WT1* transcription factor is the cholesterol/fatty acid synthetic pathways (130). A study which analyzed complementary overlap of genes which were differentially expressed in *WT1*-transfected and *WT1*-silenced cells identified this pathway as a target. Specifically, differential expression of *IDI1*, *LSS*, *FDFT1*, and *FDPS* was observed between *WT1*-positive and *WT1*-negative cells (130), and each of these genes (except *LSS* which was not measured) were similarly attenuated coordinate with increased *Wt1* expression in CX4 cells (FIGURE 3.26). The group additionally provided evidence that the effects of *WT1* were mediated by modifying (through protein-protein interaction) the transcriptional function of sterol responsive element-binding proteins (SREBPs), the proteins directly responsible for transcriptionally regulating the cholesterol biosynthesis pathway (130). It is interesting to note that another group has found that *SYT13* mRNA expression is affected by alterations in SREBP-1c function [TABLE 4.1, (117)].

Because our studies have provided supplementary evidence to suggest a role for *WT1* in the regulation of the cholesterol/mevalonate biosynthesis pathway, it is important to appreciate how this pathway may be important in both carcinogenesis and MET. The mevalonate pathway generates prenyl intermediates that are essential for the biological activity of signal transducing proteins, especially those of the Ras superfamily. These moieties covalently bind to ras and anchor it to the cell membrane where it is acted upon by surface receptors. Ras then transduces signals inside the cell to affect cytoskeleton organization, cell proliferation, and apoptosis (92, 131). Thus, aberrant expression of the mevalonate biosynthesis pathway corresponds to increased transforming activity of the ras

proto-oncogene. Another specific function of ras activation that may be important in SYT13-mediated effects is down-regulation of a prostate apoptosis response gene (*Par4*) through promoter hypermethylation (132). Not only is *Par4* a tumor suppressor gene via its pro-apoptotic functions, but it also modulates both the transcriptional and growth suppression functions of WT1 (133). Consistent with aberrant mevalonate synthesis inhibiting *Par4* (and by extrapolation from our data, elevated in cells expressing SYT13), mRNA levels were increased 7-fold by microarray or 30-fold by real-time RT-PCR in CX4 cells compared to GN6TF (FIGURES 3.25.C and D), and were also increased at least 10-fold in cells positive for the SYT13 dimer and *Wt1* (FIGURE 3.25.D). Another downstream effect of ras activation is induction of the powerful *CDH1* repressor *Snail* (134). Snail binds to E-boxes in the promoter of *CDH1* and represses its transcription (135). Thus, it is directly involved in epithelial to mesenchymal transition (EMT) which is essential for embryonic development and implicated in the progression of locally restricted cancers to metastatic disease (136). *Snail* mRNA expression was decreased >4-fold the suppressed CX4 cell line compared to GN6TF cells (FIGURE 3.25 E and F), and in each of the *SYT13*-transfected, dimer-positive cells (C2, E2, F3, and J1), *Snail* expression is decreased nearly 50% (FIGURE 3.25.F). These studies combine to suggest a pathway through which Wt1 may be effecting MET and tumor suppression in this experimental system.

The studies presented here suggest that the dimeric species of SYT13 is able to suppress the tumorigenic phenotype of GN6TF and induce differentiation of GN6TF cells to a normalized epithelial phenotype. The mechanisms of SYT13-mediated tumor suppression have not been directly assessed. However, several lines of evidence suggest different pathways/targets which may be directly or indirectly involved in this process. FIGURE 4.2

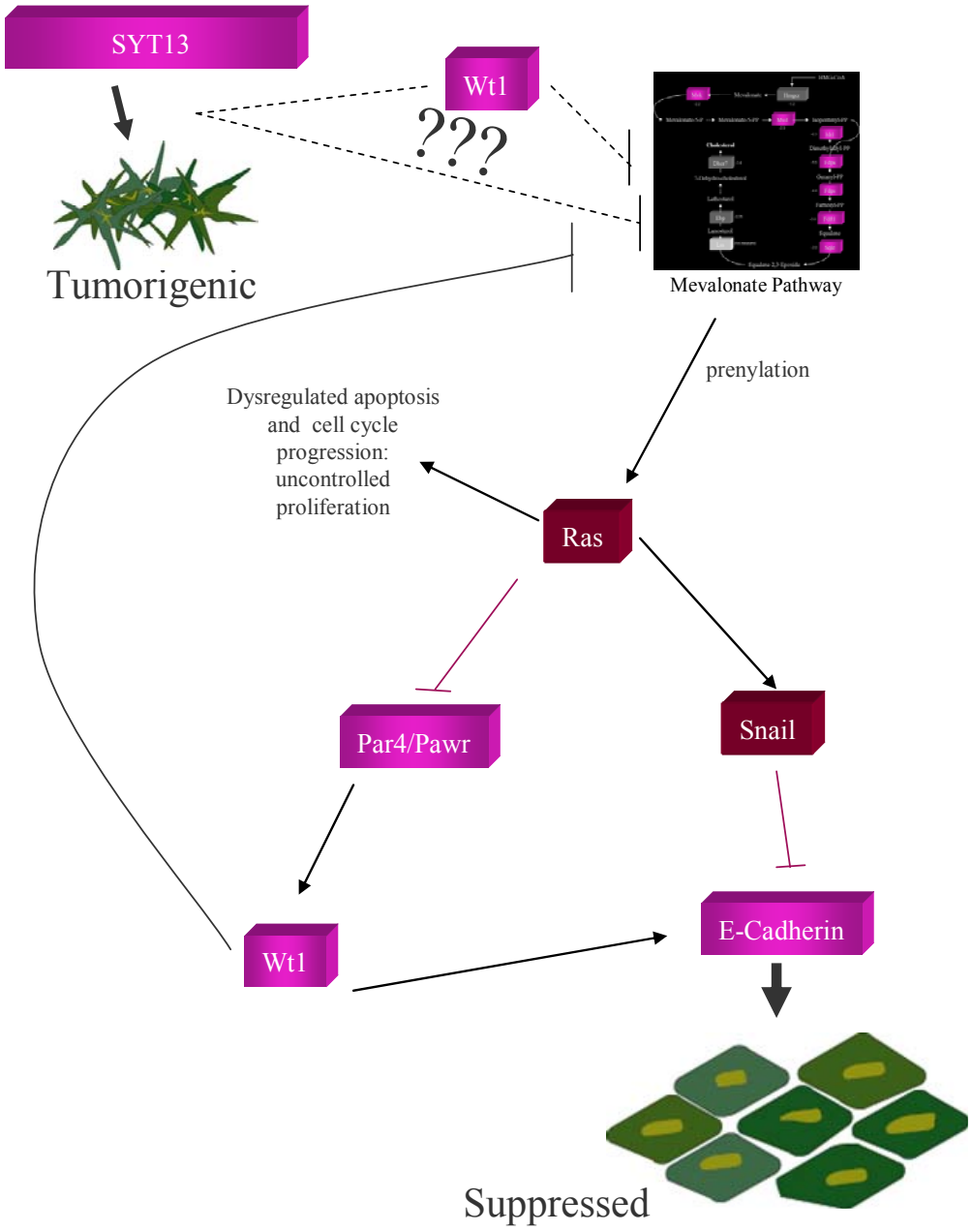

FIGURE 4.2. *Potential mechanisms of SYT13-mediated tumor suppression.* Several genes implicated in SYT13-mediated tumor suppression are shown. Genes in pink represent genes whose induction correspond to tumor suppression and epithelial differentiation, and in red are genes whose induction would promote a mesenchymal/tumorigenic phenotype. Question marks represent unknown pathways or mechanisms for regulation of expression.

illustrates several of the targets which have been implicated in SYT13-mediated tumor suppression.

POTENTIAL MECHANISMS OF SYT13 INACTIVATION

Several mechanisms of tumor suppressor gene inactivation have been recognized that contribute to neoplastic transformation of normal cells. These include gene deletion, mutation, epigenetic silencing, post-transcriptional modification, or post-translational modifications of tumor suppressor proteins (98). All of these mechanisms lead to loss of tumor suppressor function. The mechanism(s) of SYT13 inactivation is (are) not known, but various lines of evidence suggest potential mechanisms which could be experimentally examined. Mutation and/or deletion of a tumor suppressor gene represent potent mechanisms of inactivation. Given that *SYT13* has not been identified as a tumor suppressor gene through familial susceptibility segregation or otherwise detected in linkage and comparative genomic hybridization analyses, it is unlikely that *SYT13* is inactivated by these mechanisms in a significant subset of cancers. We have shown the potential for 5-aza-mediated induction of *SYT13* in HCC cell lines, suggesting that epigenetic regulation (specifically promoter hypermethylation) may directly or indirectly be responsible for gene inactivation in a subset of cancers. But considering the powerful suppressive ability of SYT13 in GN6TF tumor cells and the variety of microarray-based expression analyses available for all tumor types, it is conspicuous that *SYT13* has been implicated as a tumor suppressor-like gene in only two of these array-based experiments (84, 137). Importantly, one of these studies identified SYT13 through a proteomic approach and failed to implicate *SYT13* (mRNA) on their corresponding gene expression array (84). This corroborates the

studies presented here that fail to find a correlation between *SYT13* mRNA and the SYT13 protein. This observation is important because (i) it argues against the disqualification of *SYT13* as a tumor suppressor gene based on its lack of differential mRNA expression in normal compared to neoplastic tissue, and (ii) it suggests that the inactivation of SYT13 tumor suppressive function is regulated post-transcriptionally.

A number of post-transcriptional mechanisms of gene inactivation might affect *SYT13* regulation and expression. Interesting and perhaps relevant to SYT13 expression is the post-transcriptional silencing mediated by microRNAs (miRNAs). These non-coding mRNA transcripts form hairpin structures which hybridize to native mRNA (typically in the 3' UTR). Distinct from mechanisms of siRNA-mediated silencing, these molecules do not direct cleavage of target mRNA. Rather miRNAs direct sequestration of mRNA away from translational machinery resulting in an inhibition of protein synthesis (82). Several miRNAs have been implicated the progression of cancer (138, 139). The evolutionarily conserved 3' UTR of *SYT13* is among the longest recognized in the human genome, strongly implicating this region in SYT13 regulation. Additionally, temporal and spatial specificity of miRNA expression is important for gene regulation during differentiation and development (140). Since SYT13 has been implicated in development, miRNA expression may provide a mechanism by which SYT13 may be regulated during these events. It is also been shown the viruses are capable of producing miRNAs that work in *trans* to manipulate expression of proteins in the host (141). This is intriguing (i) because HCV and HBV are important etiologic factors for HCC and (ii) a BLAST search between *SYT13* and the HCV genome reveals several instances of sequence homology (FIGURE 4.3). A search for miRNA targets in *SYT13* using the miRBASE Target Database (http://microrna.sanger.ac.uk) identified at

FIGURE 4.3. *Sequence similarity between the coding sequences for* SYT13 *and* HCV. The coding sequence for SYT13 is shown. Sequence similarities between *SYT13* and *HCV* are highlighted in green.

least one potential miRNA target (and as many as 17) in each of the species (*SYT13* homologs) represented. Although translational control of SYT13 via this mechanism would have to be experimentally confirmed, it is quite possible that miRNA-mediated silencing is a potential post-transcriptional mode of SYT13 silencing. However, this mechanism is not responsible for *Syt13* inactivation in our model system. Expression of both *Syt13* and the monomeric form of the protein are detected, suggesting that endogenous transcription and translation machinery are functional. The endogenous *Syt13* gene found in GN6TF has not been sequenced. Therefore, the simplest explanation of *Syt13* inactivation in this cell line is a point mutation which inhibits the proper folding (thus function) of the protein. Our data strongly suggests that tumor suppression of GN6TF cells requires the dimeric form of SYT13. Since the native form of the protein is apparently unable to dimerize, this anomaly could provide evidence for alternative mechanisms of post-translational inactivation. Protein palmitoylation on conserved cysteine residues is required for dimerization (80). Therefore, if GN6TF cells lacked the capacity to execute this post-translational modification, the protein dimer would be absent. However, this does not appear to be the case because exogenously expressed proteins properly form SYT13 dimers. Another possibility is that a critical cysteine residue(s) has been mutated (80). Importantly, it appears that loss of endogenous Syt13 function in GN6TF cells is related to aberrant post-translational modification. Potential mechanisms of inactivation of SYT13 are summarized in FIGURE 4.4. This information and these cellular reagents provide an excellent background on which to further characterize and understand the biological function of Syt13.

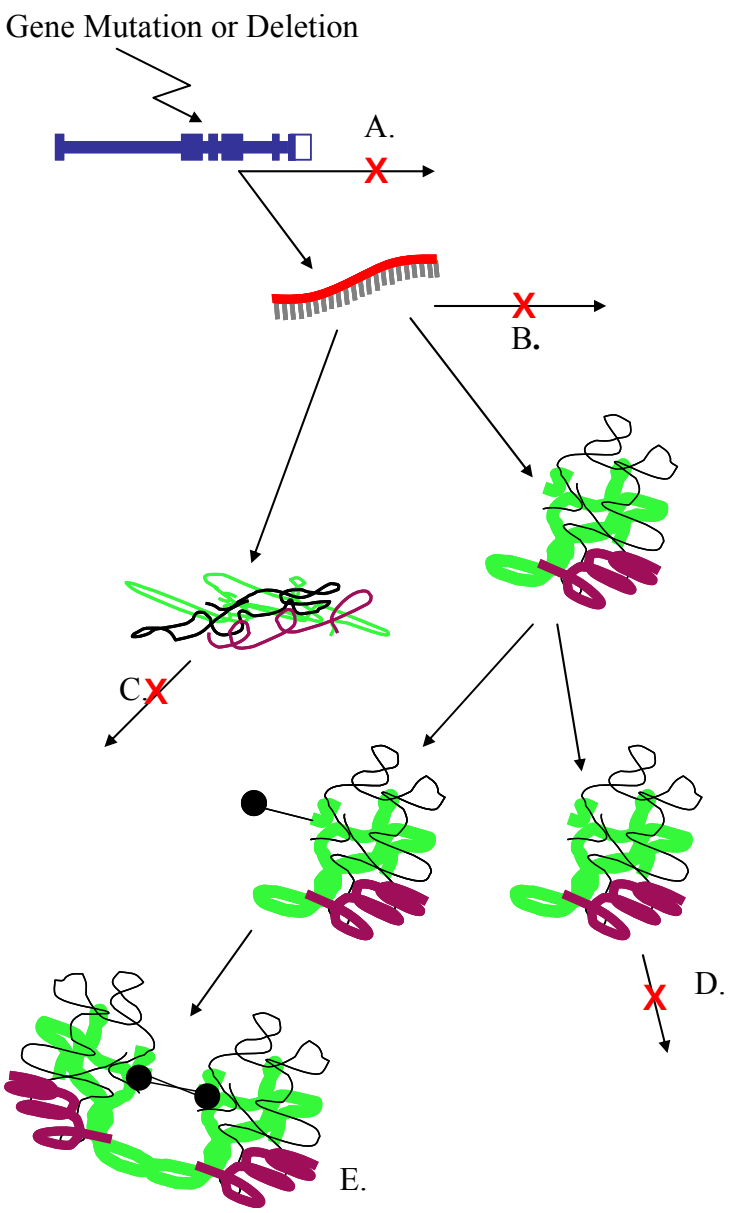

FIGURE 4.4. *Potential mechanisms of SYT13 inactivation.* Potential mechanisms for loss of function are shown. Initial insult to *SYT13* (shown in blue) could be caused by gene mutation or deletion. (A) *SYT13* is not properly transcribed. (B) Post-transcriptional silencing; the mRNA is not translated. (C) Improper folding of the protein leads to loss of function. (D) Deficient post-translational modification (such as palmitoylation) disables protein dimerization. (E) Functional SYT13 dimer.

SUMMARY AND PERSPECTIVES

The primary goals of this research project were (i) to identify the gene(s) responsible for suppression of the neoplastic phenotype of rat liver tumor cells, (ii) to characterize the involvement of this gene in tumor suppression, (iii) to determine the ability of this gene to individually express tumor suppressor activity *in vivo*, and (iv) to identify molecular targets and pathways in liver tumor cell lines that are subject to direct or indirect modification in response to the expression of the human chromosome 11p11.2 liver tumor suppressor gene. The results of the investigations described in this dissertation identified *SYT13* as the human 11p11.2 liver tumor suppressor gene and showed that this gene is required and sufficient for 11p11.2-mediated suppression of tumorigenicity in GN6TF cells. Furthermore, the results strongly suggest that the dimerized form of the SYT13 protein is necessary for tumor suppressor function and that tumor suppression may be affected through pathways implicated in epithelial to mesenchymal transition. Our observations also suggest that the deficit in GN6TF that leads to the tumorigenic phenotype involves loss of the ability of the endogenous Syt13 to dimerize, perhaps through protein misfolding or loss of palmitoylation. This research has not only answered several questions about human chromosome 11p11.2-mediated tumor suppression in rat liver tumor cells, but has raised new and intriguing questions regarding the biological function and regulation of SYT13 in tumor suppression, development, and the link between the two — epithelial to mesenchymal transition. Additional understanding of these phenomena may enable the development of effective strategies for prevention, detection, and/or molecular-based treatments of various developmental or neoplastic diseases.

REFERENCES

1. GLOBOCAN 2000: Cancer Incidence, Mortality, and Prevalence Worldwide. 1.0 edition. IARC CancerBase No. 5, Lyon: IARCPress, 2001.

2. Coleman, W. B. Mechanisms of human hepatocarcinogenesis. Curr Mol Med, *3:* 573-588, 2003.

3. Llovet, J. M., Burroughs, A., and Bruix, J. Hepatocellular carcinoma. Lancet, *362:* 1907-1917, 2003.

4. Colombo, M. and Sangiovanni, A. Etiology, natural history and treatment of hepatocellular carcinoma. Antiviral Res, *60:* 145-150, 2003.

5. Pawlotsky, J. M. Pathophysiology of hepatitis C virus infection and related liver disease. Trends Microbiol, *12:* 96-102, 2004.

6. Szabo, E., Paska, C., Kaposi Novak, P., Schaff, Z., and Kiss, A. Similarities and differences in hepatitis B and C virus induced hepatocarcinogenesis. Pathol Oncol Res, *10:* 5-11, 2004.

7. Kew, M. C. Synergistic interaction between aflatoxin B1 and hepatitis B virus in hepatocarcinogenesis. Liver Int, *23:* 405-409, 2003.

8. Grisham, J. W. Molecular genetic alterations in primary hepatocellular neoplasms. *In:* W. B. Coleman and G. J. Tsongalis (eds.), The Molecular Basis of Human Cancer, pp. 269-346. Totowa, N.J.: Humana Press, 2002.

9. Feitelson, M. A., Sun, B., Satiroglu Tufan, N. L., Liu, J., Pan, J., and Lian, Z. Genetic mechanisms of hepatocarcinogenesis. Oncogene, *21:* 2593-2604, 2002.

10. Thorgeirsson, S. S. and Grisham, J. W. Molecular pathogenesis of human hepatocellular carcinoma. Nat Genet, *31:* 339-346, 2002.

11. Boige, V., Laurent-Puig, P., Fouchet, P., Flejou, J. F., Monges, G., Bedossa, P., Bioulac-Sage, P., Capron, F., Schmitz, A., Olschwang, S., and Thomas, G. Concerted nonsyntenic allelic losses in hyperploid hepatocellular carcinoma as determined by a high-resolution allelotype. Cancer Res, *57:* 1986-1990, 1997.

12. Fujimori, M., Tokino, T., Hino, O., Kitagawa, T., Imamura, T., Okamoto, E., Mitsunobu, M., Ishikawa, T., Nakagama, H., and Harada, H. Allelotype study of primary hepatocellular carcinoma. Cancer Res, *51:* 89-93, 1991.

13. Nagai, H., Pineau, P., Tiollais, P., Buendia, M. A., and Dejean, A. Comprehensive allelotyping of human hepatocellular carcinoma. Oncogene, *14:* 2927-2933, 1997.

14. Piao, Z., Park, C., Park, J. H., and Kim, H. Allelotype analysis of hepatocellular carcinoma. Int J Cancer, *75:* 29-33, 1998.

15. Wang, H. P. and Rogler, C. E. Deletions in human chromosome arms 11p and 13q in primary hepatocellular carcinomas. Cytogenet Cell Genet, *48:* 72-78, 1988.

16. Walker, G. J., Hayward, N. K., Falvey, S., and Cooksley, W. G. Loss of somatic heterozygosity in hepatocellular carcinoma. Cancer Res, *51:* 4367-4370, 1991.

17. Sheu, J. C., Lin, Y. W., Chou, H. C., Huang, G. T., Lee, H. S., Lin, Y. H., Huang, S. Y., Chen, C. H., Wang, J. T., Lee, P. H., Lin, J. T., Lu, F. J., and Chen, D. S. Loss of heterozygosity and microsatellite instability in hepatocellular carcinoma in Taiwan. Br J Cancer, *80:* 468-476, 1999.

18. Buetow, K. H., Murray, J. C., Israel, J. L., London, W. T., Smith, M., Kew, M., Blanquet, V., Brechot, C., Redeker, A., and Govindarajah, S. Loss of heterozygosity suggests tumor suppressor gene responsible for primary hepatocellular carcinoma. Proc Natl Acad Sci U S A, *86:* 8852-8856, 1989.

19. Zhang, W. D., Hirohashi, S., Tsuda, H., Shimosato, Y., Yokota, J., Terada, M., and Sugimura, T. Frequent loss of heterozygosity on chromosomes 16 and 4 in human hepatocellular carcinoma. Jpn J Cancer Res, *81:* 108-111, 1990.

20. Nowell, P. C., Morris, H. P., and Potter, V. R. Chromosomes of "minimal deviation" hepatomas and some other transplantable rat tumors. Cancer Res, *27:* 1565-1579, 1967.

21. Wolman, S. R., Phillips, T. F., and Becker, F. F. Fluorescent banding patterns of rat chromosomes in normal cells and primary hepatocellular carcinomas. Science, *175:* 1267-1269, 1972.

22. Masuji, H. A non-random pattern in the initial chromosome aberrations in two diploid lines of rat liver cells. Gann, *65:* 429-438, 1974.

23. Becker, F. F., Wolman, S. R., Asofsky, R., and Sell, S. Sequential analysis of transplantable hepatocellular carcinomas. Cancer Res, *35:* 3021-3026, 1975.

24. Kovi, E. and Morris, H. P. Chromosome banding studies of several transplantable hepatomas. Adv Enzyme Regul, *14:* 139-162, 1976.

25. Mullen, N. T. and Barrett, C. A. Banded karyotypes of H-4-IIE-3C rat hepatoma cells grown *in vitro*. In Vitro Cell Mol. Miol, *12:* 658-664, 1976.

26. Olah, E. and Weber, G. Giemsa-banding karyotype of rat hepatomas of different growth rates. Cancer Res, *39:* 1708-1717, 1979.

27. Holecek, B. U., Kerler, R., and Rabes, H. M. Chromosomal analysis of a diethylnitrosamine-induced tumorigenic and a nontumorigenic rat liver cell line. Cancer Res, *49:* 3024-3028, 1989.

28. Iype, P. T., Malan-Shibley, L., and Raychaudhuri, R. Sequential chromosomal alterations in rat liver epithelial cells during aflatoxin-induced neoplastic transformation *in vivo*. J Toxicol-Toxin Rev, *8:* 195-216, 1989.

29. Herens, C., Alvarez Gonzalez, M. L., and Barbason, H. Cytogenetic changes in hepatocarcinomas from rats treated with chronic exposure to diethylnitrosamine. Cancer Genet Cytogenet, *60:* 45-52, 1992.

30. Sargent, L. M., Sattler, G. L., Roloff, B., Xu, Y. H., Sattler, C. A., Meisner, L., and Pitot, H. C. Ploidy and specific karyotypic changes during promotion with phenobarbital, 2,5,2',5'-tetrachlorobiphenyl, and/or 3,4,3'4'-tetrachlorobiphenyl in rat liver. Cancer Res, *52:* 955-962, 1992.

31. Steadman, J. S., Lee, L. W., Smith, G. J., and Grisham, J. W. DNA contents and chromosomes of clonal lines of transformed rat liver epithelial cells and of cells from their derived tumors. Carcinogenesis, *15:* 963-969, 1994.

32. Teeguarden, J. G., Newton, M. A., Dragan, Y. P., and Pitot, H. C. Genome-wide loss of heterozygosity analysis of chemically induced rat hepatocellular carcinomas reveals elevated frequency of allelic imbalances on chromosomes 1, 6, 8, 11, 15, 17, and 20. Mol Carcinog, *28:* 51-61, 2000.

33. Kovi, J., Kovi, E., Morris, H. P., and Rao, M. S. Chromosome banding patterns and breakpoints of three transplantable hepatomas induced in rats by aromatic amines. J Natl Cancer Inst, *61:* 495-506, 1978.

34. Grisham, J. W. Interspecies comparison of liver carcinogenesis: implications for cancer risk assessment. Carcinogenesis, *18:* 59-81, 1997.

35. Wu, Y., Renard, C. A., Apiou, F., Huerre, M., Tiollais, P., Dutrillaux, B., and Buendia, M. A. Recurrent allelic deletions at mouse chromosomes 4 and 14 in Myc-induced liver tumors. Oncogene, *21:* 1518-1526, 2002.

36. Sargent, L., Dragan, Y. P., Babcock, K., Wiley, J., Klaunig, J., and Pitot, H. C. Cytogenetic analysis of three rat liver epithelial cell lines (WBneo, WBHa-ras, and WBrasIIa) and correlation of an early chromosomal alteration with insulin-like growth factor II expression. Cancer Res, *56:* 2992-2997, 1996.

37. Sargent, L. M., Dragan, Y. P., Sattler, G., Xu, Y. H., Wiley, J., and Pitot, H. C. Specific chromosomal changes in albumin simian virus 40 T antigen transgenic rat liver neoplasms. Cancer Res, *57:* 3451-3456, 1997.

38. Davis, L. M., Caspary, W. J., Sakallah, S. A., Maronpot, R., Wiseman, R., Barrett, J. C., Elliott, R., and Hozier, J. C. Loss of heterozygosity in spontaneous and chemically induced tumors of the B6C3F1 mouse. Carcinogenesis, *15:* 1637-1645, 1994.

39. Doherty, A. M. and Fisher, E. M. Microcell-mediated chromosome transfer (MMCT): small cells with huge potential. Mamm Genome, *14:* 583-592, 2003.

40. Coleman, W. B., McCullough, K. D., Esch, G. L., Civalier, C. J., Livanos, E., Weissman, B. E., Grisham, J. W., and Smith, G. J. Suppression of the tumorigenic phenotype of a rat liver epithelial tumor cell line by the p11.2-p12 region of human chromosome 11. Mol Carcinog, *13:* 220-232, 1995.

41. Mahon, M. C., Driscoll, M. P., Glover, W. J., Borchert, K. M., Kelleher, Z. T., Smith, G. J., and Coleman, W. B. Suppression of tumorigenicity of rat liver epithelial tumor cell lines by a putative human 11p11.2-p12 liver tumor suppressor locus. Int J Oncol, *14:* 337-346, 1999.

42. Coleman, W. B., Esch, G. L., Borchert, K. M., McCullough, K. D., Reid, L. H., Weissman, B. E., Smith, G. J., and Grisham, J. W. Localization of a putative liver tumor suppressor locus to a 950-kb region of human 11p11.2-p12 using rat liver tumor microcell hybrid cell lines. Mol Carcinog, *19:* 267-272, 1997.

43. Coleman, W. B., Ricketts, S. L., Borchert, K. M., Presnell, S. C., Esch, G. L., McCullough, K. D., Weissman, B. E., Smith, G. J., and Grisham, J. W. Induction of rat WT1 gene expression correlates with human chromosome 11p11.2-p12-mediated suppression of tumorigenicity in rat liver epithelial tumor cell lines. Int J Oncol, *14:* 957-963, 1999.

44. Tsao, M. S. and Grisham, J. W. Phenotypic modulation during tumorigenesis by clones of transformed rat liver epithelial cells. Cancer Res, *47:* 1282-1286, 1987.

45. Tsao, M. S., Smith, J. D., Nelson, K. G., and Grisham, J. W. A diploid epithelial cell line from normal adult rat liver with phenotypic properties of 'oval' cells. Exp Cell Res, *154:* 38-52, 1984.

46. Tsao, M. S., Grisham, J. W., Chou, B. B., and Smith, J. D. Clonal isolation of populations of gamma-glutamyl transpeptidase-positive and -negative cells from rat liver epithelial cells chemically transformed in vitro. Cancer Res, *45:* 5134-5138, 1985.

47. Tsao, M. S., Grisham, J. W., Nelson, K. G., and Smith, J. D. Phenotypic and karyotypic changes induced in cultured rat hepatic epithelial cells that express the "oval" cell phenotype by exposure to N-methyl-N'-nitro-N-nitrosoguanidine. Am J Pathol, *118:* 306-315, 1985.

48. Lee, L. W., Raymond, V. W., Tsao, M. S., Lee, D. C., Earp, H. S., and Grisham, J. W. Clonal cosegregation of tumorigenicity with overexpression of c-myc and transforming growth factor alpha genes in chemically transformed rat liver epithelial cells. Cancer Res, *51:* 5238-5244, 1991.

49. Zimonjic, D. B., Keck, C. L., Thorgeirsson, S. S., and Popescu, N. C. Novel recurrent genetic imbalances in human hepatocellular carcinoma cell lines identified by comparative genomic hybridization. Hepatology, *29:* 1208-1214, 1999.

50. Inagaki, M., Moustakas, A., Lin, H. Y., Lodish, H. F., and Carr, B. I. Growth inhibition by transforming growth factor beta (TGF-beta) type I is restored in TGF-beta-resistant hepatoma cells after expression of TGF-beta receptor type II cDNA. Proc Natl Acad Sci U S A, *90:* 5359-5363, 1993.

51. Chang, R. S. Continuous subcultivation of epithelial-like cells from normal human tissues. Proc Soc Exp Biol Med, *87:* 440-443, 1954.

52. Gutierrez-Ruiz, M. C., Bucio, L., Souza, V., Gomez, J. J., Campos, C., and Carabez, A. Expression of some hepatocyte-like functional properties of WRL-68 cells in culture. In Vitro Cell Dev Biol Anim, *30A:* 366-371, 1994.

53. Tsao, M. S., Earp, H. S., and Grisham, J. W. Gradation of carcinogen-induced capacity for anchorage-independent growth in cultured rat liver epithelial cells. Cancer Res, *45:* 4428-4432, 1985.

54. Mosmann, T. Rapid colorimetric assay for cellular growth and survival: application to proliferation and cytotoxicity assays. J Immunol Methods, *65:* 55-63, 1983.

55. McCubbin, V. and Frank, M. B. Western Blot Protocol. *In:* M. Frank (ed.), Molecular Biology Protocols. (http://omrf.ouhsc.edu/~frank/western.html). Oklahoma City, 1997.

56. Paddison, P. J., Caudy, A. A., and Hannon, G. J. Stable suppression of gene expression by RNAi in mammalian cells. Proc Natl Acad Sci U S A, *99:* 1443-1448, 2002.

57. Sui, G., Soohoo, C., Affar el, B., Gay, F., Shi, Y., and Forrester, W. C. A DNA vector-based RNAi technology to suppress gene expression in mammalian cells. Proc Natl Acad Sci U S A, *99:* 5515-5520, 2002.

58. Brummelkamp, T. R., Bernards, R., and Agami, R. A system for stable expression of short interfering RNAs in mammalian cells. Science, *296:* 550-553, 2002.

59. Elbashir, S. M., Harborth, J., Lendeckel, W., Yalcin, A., Weber, K., and Tuschl, T. Duplexes of 21-nucleotide RNAs mediate RNA interference in cultured mammalian cells. Nature, *411:* 494-498, 2001.

60. Holen, T., Amarzguioui, M., Wiiger, M. T., Babaie, E., and Prydz, H. Positional effects of short interfering RNAs targeting the human coagulation trigger Tissue Factor. Nucleic Acids Res, *30:* 1757-1766, 2002.

61. Lee, N. S., Dohjima, T., Bauer, G., Li, H., Li, M. J., Ehsani, A., Salvaterra, P., and Rossi, J. Expression of small interfering RNAs targeted against HIV-1 rev transcripts in human cells. Nat Biotechnol, *20:* 500-505, 2002.

62. Yu, J. Y., DeRuiter, S. L., and Turner, D. L. RNA interference by expression of short-interfering RNAs and hairpin RNAs in mammalian cells. Proc Natl Acad Sci U S A, *99:* 6047-6052, 2002.

63. Connelly, J. C., Kirkham, L. A., and Leach, D. R. The SbcCD nuclease of Escherichia coli is a structural maintenance of chromosomes (SMC) family protein that cleaves hairpin DNA. Proc Natl Acad Sci U S A, *95:* 7969-7974, 1998.

64. Bolstad, B. M., Irizarry, R. A., Astrand, M., and Speed, T. P. A comparison of normalization methods for high density oligonucleotide array data based on variance and bias. Bioinformatics, *19:* 185-193, 2003.

65. Zhang, L., Miles, M. F., and Aldape, K. D. A model of molecular interactions on short oligonucleotide microarrays. Nat Biotechnol, *21:* 818-821, 2003.

66. Doniger, S. W., Salomonis, N., Dahlquist, K. D., Vranizan, K., Lawlor, S. C., and Conklin, B. R. MAPPFinder: using Gene Ontology and GenMAPP to create a global gene-expression profile from microarray data. Genome Biol, *4:* R7, 2003.

67. Dennis, G., Jr., Sherman, B. T., Hosack, D. A., Yang, J., Gao, W., Lane, H. C., and Lempicki, R. A. DAVID: Database for Annotation, Visualization, and Integrated Discovery. Genome Biol, *4:* P3, 2003.

68. Hosack, D. A., Dennis, G., Jr., Sherman, B. T., Lane, H. C., and Lempicki, R. A. Identifying biological themes within lists of genes with EASE. Genome Biol, *4:* R70, 2003.

69. Rogler, C. E., Sherman, M., Su, C. Y., Shafritz, D. A., Summers, J., Shows, T. B., Henderson, A., and Kew, M. Deletion in chromosome 11p associated with a hepatitis B integration site in hepatocellular carcinoma. Science, *230:* 319-322, 1985.

70. Fisher, J. H., Scoggin, C. H., and Rogler, C. E. Sequences which flank an 11p deletion observed in an hepatocellular carcinoma map to 11p13. Hum Genet, *75:* 66-69, 1987.

71. Ricketts, S. L., Garcia, N. F., Betz, B. L., and Coleman, W. B. Identification of candidate liver tumor suppressor genes from human 11p11.2-p12. Genes Chromosomes Cancer, *33:* 47-59, 2002.

72. Ricketts, S. L., Carter, J. C., and Coleman, W. B. Identification of three 11p11.2 candidate liver tumor suppressors through analysis of known human genes. Mol Carcinog, *36:* 90-99, 2003.

73. Jones, P. A. and Laird, P. W. Cancer epigenetics comes of age. Nat Genet, *21:* 163-167, 1999.

74. Baylin, S. B., Herman, J. G., Graff, J. R., Vertino, P. M., and Issa, J. P. Alterations in DNA methylation: a fundamental aspect of neoplasia. Adv Cancer Res, *72:* 141-196, 1998.

75. Esteller, M. Cancer epigenetics: DNA methylation and chromatin alterations in human cancer. Adv Exp Med Biol, *532:* 39-49, 2003.

76. Wagner, K. J., Cooper, W. N., Grundy, R. G., Caldwell, G., Jones, C., Wadey, R. B., Morton, D., Schofield, P. N., Reik, W., Latif, F., and Maher, E. R. Frequent RASSF1A tumour suppressor gene promoter methylation in Wilms' tumour and colorectal cancer. Oncogene, *21:* 7277-7282, 2002.

77. Yu, J., Zhang, H. Y., Ma, Z. Z., Lu, W., Wang, Y. F., and Zhu, J. D. Methylation profiling of twenty four genes and the concordant methylation behaviours of nineteen genes that may contribute to hepatocellular carcinogenesis. Cell Res, *13:* 319-333, 2003.

78. Fukuda, M. and Mikoshiba, K. Characterization of KIAA1427 protein as an atypical synaptotagmin (Syt XIII). Biochem J, *354:* 249-257, 2001.

79. von Poser, C. and Sudhof, T. C. Synaptotagmin 13: structure and expression of a novel synaptotagmin. Eur J Cell Biol, *80:* 41-47, 2001.

80. Fukuda, M., Kanno, E., Ogata, Y., and Mikoshiba, K. Mechanism of the SDS-resistant synaptotagmin clustering mediated by the cysteine cluster at the interface between the transmembrane and spacer domains. J Biol Chem, *276:* 40319-40325, 2001.

81. Gebauer, F. and Hentze, M. W. Molecular mechanisms of translational control. Nat Rev Mol Cell Biol, *5:* 827-835, 2004.

82. Liu, J., Valencia-Sanchez, M. A., Hannon, G. J., and Parker, R. MicroRNA-dependent localization of targeted mRNAs to mammalian P-bodies. Nat Cell Biol, *7:* 719-723, 2005.

83. Ambros, V. The functions of animal microRNAs. Nature, *431:* 350-355, 2004.

84. Gronborg, M., Kristiansen, T. Z., Iwahori, A., Chang, R., Reddy, R., Sato, N., Molina, H., Jensen, O. N., Hruban, R. H., Goggins, M. G., Maitra, A., and Pandey, A. Biomarker discovery from pancreatic cancer secretome using a differential proteomic approach. Mol Cell Proteomics, *5:* 157-171, 2006.

85. Scacheri, P. C., Rozenblatt-Rosen, O., Caplen, N. J., Wolfsberg, T. G., Umayam, L., Lee, J. C., Hughes, C. M., Shanmugam, K. S., Bhattacharjee, A., Meyerson, M., and Collins, F. S. Short interfering RNAs can induce unexpected and divergent changes in the levels of untargeted proteins in mammalian cells. Proc Natl Acad Sci U S A, *101:* 1892-1897, 2004.

86. Jackson, A. L. and Linsley, P. S. Noise amidst the silence: off-target effects of siRNAs? Trends Genet, *20:* 521-524, 2004.

87. Mise-Omata, S., Obata, Y., Iwase, S., Mise, N., and Doi, T. S. Transient strong reduction of PTEN expression by specific RNAi induces loss of adhesion of the cells. Biochem Biophys Res Commun, *328:* 1034-1042, 2005.

88. Bridge, A. J., Pebernard, S., Ducraux, A., Nicoulaz, A. L., and Iggo, R. Induction of an interferon response by RNAi vectors in mammalian cells. Nat Genet, *34:* 263-264, 2003.

89. Sledz, C. A., Holko, M., de Veer, M. J., Silverman, R. H., and Williams, B. R. Activation of the interferon system by short-interfering RNAs. Nat Cell Biol, *5:* 834-839, 2003.

90. Saxena, S., Jonsson, Z. O., and Dutta, A. Small RNAs with imperfect match to endogenous mRNA repress translation. Implications for off-target activity of small inhibitory RNA in mammalian cells. J Biol Chem, *278:* 44312-44319, 2003.

91. Koi, M., Shimizu, M., Morita, H., Yamada, H., and Oshimura, M. Construction of mouse A9 clones containing a single human chromosome tagged with neomycin-resistance gene via microcell fusion. Jpn J Cancer Res, *80:* 413-418, 1989.

92. Bifulco, M. Role of the isoprenoid pathway in ras transforming activity, cytoskeleton organization, cell proliferation and apoptosis. Life Sci, *77:* 1740-1749, 2005.

93. Singh, R. P., Kumar, R., and Kapur, N. Molecular regulation of cholesterol biosynthesis: implications in carcinogenesis. J Environ Pathol Toxicol Oncol, *22:* 75-92, 2003.

94. Lander, E. S., Linton, L. M., Birren, B., Nusbaum, C., Zody, M. C., Baldwin, J., Devon, K., Dewar, K., Doyle, M., FitzHugh, W., Funke, R., Gage, D., Harris, K., Heaford, A., Howland, J., Kann, L., Lehoczky, J., LeVine, R., McEwan, P., McKernan, K., Meldrim, J., Mesirov, J. P., Miranda, C., Morris, W., Naylor, J., Raymond, C., Rosetti, M., Santos, R., Sheridan, A., Sougnez, C., Stange-Thomann, N., Stojanovic, N., Subramanian, A., Wyman, D., Rogers, J., Sulston, J., Ainscough, R., Beck, S., Bentley, D., Burton, J., Clee, C., Carter, N., Coulson, A., Deadman, R., Deloukas, P., Dunham, A., Dunham, I., Durbin, R., French, L., Grafham, D., Gregory, S., Hubbard, T., Humphray, S., Hunt, A., Jones, M., Lloyd, C., McMurray, A., Matthews, L., Mercer, S., Milne, S., Mullikin, J. C., Mungall, A., Plumb, R., Ross, M., Shownkeen, R., Sims, S., Waterston, R. H., Wilson, R. K., Hillier, L. W., McPherson, J. D., Marra, M. A., Mardis, E. R., Fulton, L. A., Chinwalla, A. T., Pepin, K. H., Gish, W. R., Chissoe, S. L., Wendl, M. C., Delehaunty, K. D., Miner, T. L., Delehaunty, A., Kramer, J. B., Cook, L. L., Fulton, R. S., Johnson, D. L., Minx, P. J., Clifton, S. W., Hawkins, T., Branscomb, E., Predki, P., Richardson, P., Wenning, S., Slezak, T., Doggett, N., Cheng, J. F., Olsen, A., Lucas, S., Elkin, C., Uberbacher, E., Frazier, M., Gibbs, R. A., Muzny, D. M., Scherer, S. E., Bouck, J. B., Sodergren, E. J., Worley, K. C., Rives, C. M., Gorrell, J. H., Metzker, M. L., Naylor, S. L., Kucherlapati, R. S., Nelson, D. L., Weinstock, G. M., Sakaki, Y., Fujiyama, A., Hattori, M., Yada, T., Toyoda, A., Itoh, T., Kawagoe, C., Watanabe, H., Totoki, Y., Taylor, T., Weissenbach, J., Heilig, R., Saurin, W., Artiguenave, F., Brottier, P., Bruls, T., Pelletier, E., Robert, C., Wincker, P., Smith, D. R., Doucette-Stamm, L.,

Rubenfield, M., Weinstock, K., Lee, H. M., Dubois, J., Rosenthal, A., Platzer, M., Nyakatura, G., Taudien, S., Rump, A., Yang, H., Yu, J., Wang, J., Huang, G., Gu, J., Hood, L., Rowen, L., Madan, A., Qin, S., Davis, R. W., Federspiel, N. A., Abola, A. P., Proctor, M. J., Myers, R. M., Schmutz, J., Dickson, M., Grimwood, J., Cox, D. R., Olson, M. V., Kaul, R., Raymond, C., Shimizu, N., Kawasaki, K., Minoshima, S., Evans, G. A., Athanasiou, M., Schultz, R., Roe, B. A., Chen, F., Pan, H., Ramser, J., Lehrach, H., Reinhardt, R., McCombie, W. R., de la Bastide, M., Dedhia, N., Blocker, H., Hornischer, K., Nordsiek, G., Agarwala, R., Aravind, L., Bailey, J. A., Bateman, A., Batzoglou, S., Birney, E., Bork, P., Brown, D. G., Burge, C. B., Cerutti, L., Chen, H. C., Church, D., Clamp, M., Copley, R. R., Doerks, T., Eddy, S. R., Eichler, E. E., Furey, T. S., Galagan, J., Gilbert, J. G., Harmon, C., Hayashizaki, Y., Haussler, D., Hermjakob, H., Hokamp, K., Jang, W., Johnson, L. S., Jones, T. A., Kasif, S., Kaspryzk, A., Kennedy, S., Kent, W. J., Kitts, P., Koonin, E. V., Korf, I., Kulp, D., Lancet, D., Lowe, T. M., McLysaght, A., Mikkelsen, T., Moran, J. V., Mulder, N., Pollara, V. J., Ponting, C. P., Schuler, G., Schultz, J., Slater, G., Smit, A. F., Stupka, E., Szustakowski, J., Thierry-Mieg, D., Thierry-Mieg, J., Wagner, L., Wallis, J., Wheeler, R., Williams, A., Wolf, Y. I., Wolfe, K. H., Yang, S. P., Yeh, R. F., Collins, F., Guyer, M. S., Peterson, J., Felsenfeld, A., Wetterstrand, K. A., Patrinos, A., Morgan, M. J., de Jong, P., Catanese, J. J., Osoegawa, K., Shizuya, H., Choi, S. and Chen, Y. J. Initial sequencing and analysis of the human genome. Nature, *409:* 860-921, 2001.

95. Watson, J. D. and Crick, F. H. Molecular structure of nucleic acids; a structure for deoxyribose nucleic acid. Nature, *171:* 737-738, 1953.

96. Collins, F. S., Green, E. D., Guttmacher, A. E., and Guyer, M. S. A vision for the future of genomics research. Nature, *422:* 835-847, 2003.

97. Friederichs, J., Rosenberg, R., Mages, J., Janssen, K. P., Maeckl, C., Nekarda, H., Holzmann, B., and Siewert, J. R. Gene expression profiles of different clinical stages of colorectal carcinoma: toward a molecular genetic understanding of tumor progression. Int J Colorectal Dis, *20:* 391-402, 2005.

98. Hanahan, D. and Weinberg, R. A. The hallmarks of cancer. Cell, *100:* 57-70, 2000.

99. Fernandez-Chacon, R., Konigstorfer, A., Gerber, S. H., Garcia, J., Matos, M. F., Stevens, C. F., Brose, N., Rizo, J., Rosenmund, C., and Sudhof, T. C. Synaptotagmin I functions as a calcium regulator of release probability. Nature, *410:* 41-49, 2001.

100. Brose, N., Petrenko, A. G., Sudhof, T. C., and Jahn, R. Synaptotagmin: a calcium sensor on the synaptic vesicle surface. Science, *256:* 1021-1025, 1992.

101. Sutton, R. B., Davletov, B. A., Berghuis, A. M., Sudhof, T. C., and Sprang, S. R. Structure of the first C2 domain of synaptotagmin I: a novel Ca2+/phospholipid-binding fold. Cell, *80:* 929-938, 1995.

102. Rickman, C., Craxton, M., Osborne, S., and Davletov, B. Comparative analysis of tandem C2 domains from the mammalian synaptotagmin family. Biochem J, *378:* 681-686, 2004.

103. Ubach, J., Garcia, J., Nittler, M. P., Sudhof, T. C., and Rizo, J. Structure of the Janus-faced C2B domain of rabphilin. Nat Cell Biol, *1:* 106-112, 1999.

104. Perin, M. S. Mirror image motifs mediate the interaction of the COOH terminus of multiple synaptotagmins with the neurexins and calmodulin. Biochemistry, *35:* 13808-13816, 1996.

105. Tepass, U., Tanentzapf, G., Ward, R., and Fehon, R. Epithelial cell polarity and cell junctions in Drosophila. Annu Rev Genet, *35:* 747-784, 2001.

106. Fukuda, M. and Mikoshiba, K. Calcium-dependent and -independent hetero-oligomerization in the synaptotagmin family. J Biochem (Tokyo), *128:* 637-645, 2000.

107. Yanai, I., Benjamin, H., Shmoish, M., Chalifa-Caspi, V., Shklar, M., Ophir, R., Bar-Even, A., Horn-Saban, S., Safran, M., Domany, E., Lancet, D., and Shmueli, O. Genome-wide midrange transcription profiles reveal expression level relationships in human tissue specification. Bioinformatics, *21:* 650-659, 2005.

108. Thierry-Mieg, D. and Thierry-Mieg, J. AceView: a comprehensive cDNA-supported gene and transcripts annotation. Genome Biol, *7 Suppl 1:* S12 11-14, 2006.

109. Ashburner, M., Ball, C. A., Blake, J. A., Botstein, D., Butler, H., Cherry, J. M., Davis, A. P., Dolinski, K., Dwight, S. S., Eppig, J. T., Harris, M. A., Hill, D. P., Issel-Tarver, L., Kasarskis, A., Lewis, S., Matese, J. C., Richardson, J. E., Ringwald, M., Rubin, G. M., and Sherlock, G. Gene ontology: tool for the unification of biology. The Gene Ontology Consortium. Nat Genet, *25:* 25-29, 2000.

110. Wakui, K., Gregato, G., Ballif, B. C., Glotzbach, C. D., Bailey, K. A., Kuo, P. L., Sue, W. C., Sheffield, L. J., Irons, M., Gomez, E. G., Hecht, J. T., Potocki, L., and Shaffer, L. G. Construction of a natural panel of 11p11.2 deletions and further delineation of the critical region involved in Potocki-Shaffer syndrome. Eur J Hum Genet, *13:* 528-540, 2005.

111. Mavrogiannis, L. A., Taylor, I. B., Davies, S. J., Ramos, F. J., Olivares, J. L., and Wilkie, A. O. Enlarged parietal foramina caused by mutations in the homeobox genes ALX4 and MSX2: from genotype to phenotype. Eur J Hum Genet, *14:* 151-158, 2006.

112. Cristobal, R., Wackym, P. A., Cioffi, J. A., Erbe, C. B., Roche, J. P., and Popper, P. Assessment of differential gene expression in vestibular epithelial cell types using microarray analysis. Brain Res Mol Brain Res, *133:* 19-36, 2005.

113. Mu, X., Beremand, P. D., Zhao, S., Pershad, R., Sun, H., Scarpa, A., Liang, S., Thomas, T. L., and Klein, W. H. Discrete gene sets depend on POU domain transcription factor Brn3b/Brn-3.2/POU4f2 for their expression in the mouse embryonic retina. Development, *131:* 1197-1210, 2004.

114. Tropea, D., Kreiman, G., Lyckman, A., Mukherjee, S., Yu, H., Horng, S., and Sur, M. Gene expression changes and molecular pathways mediating activity-dependent plasticity in visual cortex. Nat Neurosci, *9:* 660-668, 2006.

115. Zhang, Z., Yuan, X. M., Li, L. H., and Xie, F. P. Transdifferentiation of neoplastic cells. Med Hypotheses, *57:* 655-666, 2001.

116. Impey, S., McCorkle, S. R., Cha-Molstad, H., Dwyer, J. M., Yochum, G. S., Boss, J. M., McWeeney, S., Dunn, J. J., Mandel, G., and Goodman, R. H. Defining the CREB regulon: a genome-wide analysis of transcription factor regulatory regions. Cell, *119:* 1041-1054, 2004.

117. Parton, L. E., McMillen, P. J., Shen, Y., Docherty, E., Sharpe, E., Diraison, F., Briscoe, C. P., and Rutter, G. A. Limited role for SREBP-1c in defective glucose-induced insulin secretion from Zucker diabetic fatty rat islets: a functional and gene profiling analysis. Am J Physiol Endocrinol Metab, *291:* E982-994, 2006.

118. Petri, A., Ahnfelt-Ronne, J., Frederiksen, K. S., Edwards, D. G., Madsen, D., Serup, P., Fleckner, J., and Heller, R. S. The effect of neurogenin3 deficiency on pancreatic gene expression in embryonic mice. J Mol Endocrinol, *37:* 301-316, 2006.

119. Clegg, N., Ferguson, C., True, L. D., Arnold, H., Moorman, A., Quinn, J. E., Vessella, R. L., and Nelson, P. S. Molecular characterization of prostatic small-cell neuroendocrine carcinoma. Prostate, *55:* 55-64, 2003.

120. Zhang, J., Moseley, A., Jegga, A. G., Gupta, A., Witte, D. P., Sartor, M., Medvedovic, M., Williams, S. S., Ley-Ebert, C., Coolen, L. M., Egnaczyk, G., Genter, M. B., Lehman, M., Lingrel, J., Maggio, J., Parysek, L., Walsh, R., Xu, M., and Aronow, B. J. Neural system-enriched gene expression: relationship to biological pathways and neurological diseases. Physiol Genomics, *18:* 167-183, 2004.

121. McGraw, D. W., Fogel, K. M., Kong, S., Litonjua, A. A., Kranias, E. G., Aronow, B. J., and Liggett, S. B. Transcriptional response to persistent beta2-adrenergic receptor signaling reveals regulation of phospholamban, which alters airway contractility. Physiol Genomics, *27:* 171-177, 2006.

122. Decraene, C., Brugg, B., Ruberg, M., Eveno, E., Matingou, C., Tahi, F., Mariani, J., Auffray, C., and Pietu, G. Identification of genes involved in ceramide-dependent neuronal apoptosis using cDNA arrays. Genome Biol, *3:* research0042, 2002.

123. Sequeira, A., Gwadry, F. G., Ffrench-Mullen, J. M., Canetti, L., Gingras, Y., Casero, R. A., Jr., Rouleau, G., Benkelfat, C., and Turecki, G. Implication of SSAT by gene expression and genetic variation in suicide and major depression. Arch Gen Psychiatry, *63:* 35-48, 2006.

124. Weng, T., Chen, Z., Jin, N., Gao, L., and Liu, L. Gene expression profiling identifies regulatory pathways involved in the late stage of rat fetal lung development. Am J Physiol Lung Cell Mol Physiol, *291:* L1027-1037, 2006.

125. Pritchard-Jones, K., Fleming, S., Davidson, D., Bickmore, W., Porteous, D., Gosden, C., Bard, J., Buckler, A., Pelletier, J., Housman, D., and et al. The candidate Wilms' tumour gene is involved in genitourinary development. Nature, *346:* 194-197, 1990.

126. Miwa, H., Tomlinson, G. E., Timmons, C. F., Huff, V., Cohn, S. L., Strong, L. C., and Saunders, G. F. RNA expression of the WT1 gene in Wilms' tumors in relation to histology. J Natl Cancer Inst, *84:* 181-187, 1992.

127. Hosono, S., Luo, X., Hyink, D. P., Schnapp, L. M., Wilson, P. D., Burrow, C. R., Reddy, J. C., Atweh, G. F., and Licht, J. D. WT1 expression induces features of renal epithelial differentiation in mesenchymal fibroblasts. Oncogene, *18:* 417-427, 1999.

128. Luo, X. N., Reddy, J. C., Yeyati, P. L., Idris, A. H., Hosono, S., Haber, D. A., Licht, J. D., and Atweh, G. F. The tumor suppressor gene WT1 inhibits ras-mediated transformation. Oncogene, *11:* 743-750, 1995.

129. Hosono, S., Gross, I., English, M. A., Hajra, K. M., Fearon, E. R., and Licht, J. D. E-cadherin is a WT1 target gene. J Biol Chem, *275:* 10943-10953, 2000.

130. Rae, F. K., Martinez, G., Gillinder, K. R., Smith, A., Shooter, G., Forrest, A. R., Grimmond, S. M., and Little, M. H. Anlaysis of complementary expression profiles following WT1 induction versus repression reveals the cholesterol/fatty acid synthetic pathways as a possible major target of WT1. Oncogene, *23:* 3067-3079, 2004.

131. Bourne, H. R., Wrischnik, L., and Kenyon, C. Ras proteins. Some signal developments. Nature, *348:* 678-679, 1990.

132. Pruitt, K., Ulku, A. S., Frantz, K., Rojas, R. J., Muniz-Medina, V. M., Rangnekar, V. M., Der, C. J., and Shields, J. M. Ras-mediated loss of the pro-apoptotic response protein Par-4 is mediated by DNA hypermethylation through Raf-independent and Raf-dependent signaling cascades in epithelial cells. J Biol Chem, *280:* 23363-23370, 2005.

133. Johnstone, R. W., See, R. H., Sells, S. F., Wang, J., Muthukkumar, S., Englert, C., Haber, D. A., Licht, J. D., Sugrue, S. P., Roberts, T., Rangnekar, V. M., and Shi, Y. A novel repressor, par-4, modulates transcription and growth suppression functions of the Wilms' tumor suppressor WT1. Mol Cell Biol, *16:* 6945-6956, 1996.

134. Schmidt, C. R., Gi, Y. J., Patel, T. A., Coffey, R. J., Beauchamp, R. D., and Pearson, A. S. E-cadherin is regulated by the transcriptional repressor SLUG during Ras-mediated transformation of intestinal epithelial cells. Surgery, *138:* 306-312, 2005.

135. Batlle, E., Sancho, E., Franci, C., Dominguez, D., Monfar, M., Baulida, J., and Garcia De Herreros, A. The transcription factor snail is a repressor of E-cadherin gene expression in epithelial tumour cells. Nat Cell Biol, *2:* 84-89, 2000.

136. Huber, M. A., Kraut, N., and Beug, H. Molecular requirements for epithelial-mesenchymal transition during tumor progression. Curr Opin Cell Biol, *17:* 548-558, 2005.

137. Baker, S. J., Markowitz, S., Fearon, E. R., Willson, J. K., and Vogelstein, B. Suppression of human colorectal carcinoma cell growth by wild-type p53. Science, *249:* 912-915, 1990.

138. Esquela-Kerscher, A. and Slack, F. J. Oncomirs - microRNAs with a role in cancer. Nat Rev Cancer, *6:* 259-269, 2006.

139. Dalmay, T. and Edwards, D. R. MicroRNAs and the hallmarks of cancer. Oncogene, *25:* 6170-6175, 2006.

140. Alvarez-Garcia, I. and Miska, E. A. MicroRNA functions in animal development and human disease. Development, *132:* 4653-4662, 2005.

141. Pfeffer, S. and Voinnet, O. Viruses, microRNAs and cancer. Oncogene, *25:* 6211-6219, 2006.

APPENDIX A

Transcripts ≥2-fold elevated in CX4 compared to GN6TF

AFFY ID	*GENE SYMBOL*	GENE DESCRIPTION
1383614_AT	*1200013B22RIK*	SNF1/AMP-ACTIVATED PROTEIN KINASE
1368081_AT	*ABCA2*	ATP-BINDING CASSETTE, SUB-FAMILY A (ABC1), MEMBER 2
1384603_AT	*ABCA4_PREDICTED*	ATP-BINDING CASSETTE, SUB-FAMILY A (ABC1), MEMBER 4 (PREDICTED)
1383229_AT	*ABCA7*	ATP-BINDING CASSETTE, SUB-FAMILY A, MEMBER 7
1387030_AT	*ABCC5*	ATP-BINDING CASSETTE, SUB-FAMILY C (CFTR/MRP), MEMBER 5
1382137_AT	*ABHD3_PREDICTED*	ABHYDROLASE DOMAIN CONTAINING 3 (PREDICTED)
1367958_AT	*ABI1*	ABL-INTERACTOR 1
1373215_AT	*ABR_PREDICTED*	ACTIVE BCR-RELATED GENE (PREDICTED)
1371793_AT	*ACHE*	GLYCOLIPID-ANCHORED FORM OF ACETYLCHOLINESTERASE
1397375_AT	*ACSL5*	ACYL-COA SYNTHETASE LONG-CHAIN FAMILY MEMBER 5
1373792_AT	*ACTR1B*	ARP1 ACTIN-RELATED PROTEIN 1 HOMOLOG B (YEAST)
1387135_AT	*ADAM15*	A DISINTEGRIN AND METALLOPROTEINASE DOMAIN 15 (METARGIDIN)
1382481_A_AT	*ADAM33_PREDICTED*	A DISINTEGRIN AND METALLOPROTEASE DOMAIN 33 (PREDICTED)
1375337_AT	*ADAM9_PREDICTED*	A DISINTEGRIN AND METALLOPROTEINASE DOMAIN 9 (MELTRIN GAMMA) (PREDICTED)
1387128_AT	*ADCY3*	ADENYLATE CYCLASE 3
1379598_AT	*ADCY7*	ADENYLATE CYCLASE 7
1388487_AT	*ADD1*	ADDUCIN 1 (ALPHA)
1387219_AT	*ADM*	ADRENOMEDULLIN
1372634_AT	*ADPRHL2_PREDICTED*	ADP-RIBOSYLHYDROLASE LIKE 2 (PREDICTED)
1376810_AT	*ADPRTL1*	ADP-RIBOSYLTRANSFERASE (NAD+; POLY (ADP-RIBOSE) POLYMERASE)-LIKE 1
1369115_AT	*ADRB2*	ADRENERGIC RECEPTOR, BETA 2
1376091_AT	*ADSL_PREDICTED*	ADENYLOSUCCINATE LYASE (PREDICTED)
1399050_AT	*ADSS2_PREDICTED*	ADENYLOSUCCINATE SYNTHETASE 2, NON MUSCLE (PREDICTED)
1370302_AT	*AF348365*	THYROID HORMONE-RESPONSE PROTEIN-1
1370307_AT	*AGRN*	AGRIN
1371703_AT	*AHNAK*	AHNAK NUCLEOPROTEIN (DESMOYOKIN)
1368869_AT	*AKAP12*	A KINASE (PRKA) ANCHOR PROTEIN (GRAVIN) 12
1390229_AT	*AKAP14*	A KINASE (PRKA) ANCHOR PROTEIN 14
1389496_AT	*AKAP7*	A KINASE (PRKA) ANCHOR PROTEIN 7
1370911_AT	*AKAP8*	A KINASE (PRKA) ANCHOR PROTEIN 8
1368121_AT	*AKR7A3*	ALDO-KETO REDUCTASE FAMILY 7, MEMBER A3 (AFLATOXIN ALDEHYDE REDUCTASE)
1367720_AT	*ALAD*	AMINOLEVULINATE, DELTA-, DEHYDRATASE
1367982_AT	*ALAS1*	AMINOLEVULINIC ACID SYNTHASE 1
1368130_AT	*ALDH3A1*	ALDEHYDE DEHYDROGENASE FAMILY 3, MEMBER A1
1368365_AT	*ALDH3A2*	ALDEHYDE DEHYDROGENASE FAMILY 3, SUBFAMILY A2
1382541_AT	*ALK*	ANAPLASTIC LYMPHOMA KINASE
1392689_AT	*ALOXE3_PREDICTED*	ARACHIDONATE LIPOXYGENASE 3 (PREDICTED)
1389363_AT	*ALP1*	ACI-REDUCTONE DIOXYGENASE (ARD)-LIKE PROTEIN 1
1377166_AT	*ALS2*	AMYOTROPHIC LATERAL SCLEROSIS 2 (JUVENILE)
1367933_AT	*AMD1*	S-ADENOSYLMETHIONINE DECARBOXYLASE 1
1389546_AT	*AMOTL2*	ANGIOMOTIN LIKE 2
1368342_AT	*AMPD3*	ADENOSINE MONOPHOSPHATE DEAMINASE 3
1367664_AT	*ANKRD1*	ANKYRIN REPEAT DOMAIN 1 (CARDIAC MUSCLE)
1373619_AT	*ANKRD10*	ANKYRIN REPEAT DOMAIN 10
1372069_AT	*ANKRD15*	ANKYRIN REPEAT DOMAIN 15
1371873_AT	*ANP32E*	ACIDIC (LEUCINE-RICH) NUCLEAR PHOSPHOPROTEIN 32 FAMILY, MEMBER E
1388445_AT	*ANXA11*	ANNEXIN A11
1389305_AT	*ANXA4*	ANNEXIN A4
1386862_AT	*ANXA5*	ANNEXIN A5
1373654_AT	*ANXA8*	ANNEXIN A8
1371493_AT	*AP2A2*	ADAPTOR PROTEIN COMPLEX AP-2, ALPHA 2 SUBUNIT
1371614_AT	*APG12L*	AUTOPHAGY 12-LIKE (S. CEREVISIAE)
1389273_AT	*APG4B*	APG4 (ATG4) AUTOPHAGY-RELATED HOMOLOG B (S. CEREVISIAE)
1390436_AT	*APG7L*	AUTOPHAGY 7-LIKE (S. CEREVISIAE)
1383193_AT	*APLP1*	AMYLOID BETA (A4) PRECURSOR-LIKE PROTEIN 1
1388121_AT	*APLP2*	AMYLOID BETA (A4) PRECURSOR-LIKE PROTEIN 2
1370862_AT	*APOE*	APOLIPOPROTEIN E
1387055_AT	*APPBP1*	AMYLOID BETA PRECURSOR PROTEIN BINDING PROTEIN 1
1392891_AT	*APRIN*	ANDROGEN-INDUCED PROLIFERATION INHIBITOR
1392891_AT	*APRIN_PREDICTED*	ANDROGEN-INDUCED PROLIFERATION INHIBITOR
1368621_AT	*AQP9*	AQUAPORIN 9
1380794_AT	*AQR_PREDICTED*	AQUARIUS (PREDICTED)
1388305_AT	*ARAF1*	V-RAF ONCOGENE HOMOLOG 1 (MURINE SARCOMA 3611 VIRUS)
1387068_AT	*ARC*	ACTIVITY REGULATED CYTOSKELETAL-ASSOCIATED PROTEIN
1369871_AT	*AREG*	AMPHIREGULIN
1388813_AT	*ARF2*	ADP-RIBOSYLATION FACTOR 2
1388997_AT	*ARF3*	ADP-RIBOSYLATION FACTOR 3
1368266_AT	*ARG1*	ARGINASE 1
1381296_AT	*ARG2*	ARGINASE 2
1377385_AT	*ARHGAP27*	RHO GTPASE ACTIVATING PROTEIN 27
1393666_AT	*ARHGAP5*	RHO GTPASE ACTIVATING PROTEIN 5
1376501_AT	*ARHGAP8*	RHO GTPASE ACTIVATING PROTEIN 8
1373881_AT	*ARHGDIB*	RHO, GDP DISSOCIATION INHIBITOR (GDI) BETA
1381100_AT	*ARHGEF12*	RHO GUANINE NUCLEOTIDE EXCHANGE FACTOR (GEF) 12
1383523_AT	*ARHGEF18_PREDICTED*	RHO/RAC GUANINE NUCLEOTIDE EXCHANGE FACTOR (GEF) 18 (PREDICTED)
1377750_AT	*ARHGEF3_PREDICTED*	RHO GUANINE NUCLEOTIDE EXCHANGE FACTOR (GEF) 3 (PREDICTED)
1382389_AT	*ARHGEF5*	RHO GUANINE NUCLEOTIDE EXCHANGE FACTOR (GEF) 5
1374823_AT	*ARIH1*	ARIADNE UBIQUITIN-CONJUGATING ENZYME E2 BINDING PROTEIN HOMOLOG 1 (DROSOPHILA)
1373141_AT	*ARIH2_PREDICTED*	ARIADNE HOMOLOG 2 (DROSOPHILA) (PREDICTED)
1389941_AT	*ARL2BP*	ADP-RIBOSYLATION FACTOR-LIKE 2 BINDING PROTEIN
1367960_AT	*ARL4*	ADP-RIBOSYLATION FACTOR-LIKE 4
1372557_AT	*ARL6_PREDICTED*	ADP-RIBOSYLATION FACTOR-LIKE 6 (PREDICTED)
1372470_AT	*ARVCF_PREDICTED*	ARMADILLO REPEAT GENE DELETED IN VELO-CARDIO-FACIAL SYNDROME (PREDICTED)
1382847_AT	*ASH1L_PREDICTED*	ASH1 (ABSENT, SMALL, OR HOMEOTIC)-LIKE (DROSOPHILA) (PREDICTED)

1389719_AT	*ASH2L_PREDICTED*	ASH2 (ABSENT, SMALL, OR HOMEOTIC)-LIKE (DROSOPHILA) (PREDICTED)
1370964_AT	*ASS*	ARGININOSUCCINATE SYNTHETASE
1376599_AT	*ATAD2_PREDICTED*	ATPASE FAMILY, AAA DOMAIN CONTAINING 2 (PREDICTED)
1389623_AT	*ATF1*	ACTIVATING TRANSCRIPTION FACTOR 1
1369268_AT	*ATF3*	ACTIVATING TRANSCRIPTION FACTOR 3
1376834_AT	*ATM_MAPPED*	ATAXIA TELANGIECTASIA MUTATED HOMOLOG (HUMAN) (MAPPED)
1373546_AT	*ATP11A_PREDICTED*	ATPASE, CLASS VI, TYPE 11A (PREDICTED)
1368108_AT	*ATP2A1*	ATPASE, CA++ TRANSPORTING, CARDIAC MUSCLE, FAST TWITCH 1
1372907_AT	*ATP6V0E2*	ATPASE, H+ TRANSPORTING, V0 SUBUNIT E ISOFORM 2
1371402_AT	*ATP6V1B2*	ATPASE, H+ TRANSPORTING, V1 SUBUNIT B, ISOFORM 2
1390429_AT	*AXIN2*	AXIN2
1398347_AT	*AXL_PREDICTED*	AXL RECEPTOR TYROSINE KINASE (PREDICTED)
1371440_AT	*B2M*	BETA-2 MICROGLOBULIN
1383689_AT	*B4GALT4*	UDP-GAL:BETAGLCNAC BETA 1,4-GALACTOSYLTRANSFERASE, POLYPEPTIDE 4
1374198_AT	*B7H3*	B7 HOMLOG 3
1377390_AT	*BACE2*	BETA-SITE APP-CLEAVING ENZYME 2
1392440_AT	*BARD1*	BRCA1 ASSOCIATED RING DOMAIN 1
1388158_AT	*BAT1A*	HLA-B-ASSOCIATED TRANSCRIPT 1A
1388536_AT	*BAT2*	HLA-B ASSOCIATED TRANSCRIPT 2
1372709_AT	*BCAP29*	B-CELL RECEPTOR-ASSOCIATED PROTEIN BAP29
1374947_AT	*BCAR3_PREDICTED*	BREAST CANCER ANTI-ESTROGEN RESISTANCE 3 (PREDICTED)
1368118_AT	*BCL10*	B-CELL CLL/LYMPHOMA 10
1398482_AT	*BCL3_PREDICTED*	B-CELL LEUKEMIA/LYMPHOMA 3 (PREDICTED)
1392933_A_AT	*BCL7A_PREDICTED*	B-CELL CLL/LYMPHOMA 7A (PREDICTED)
1373494_AT	*BCR_PREDICTED*	BREAKPOINT CLUSTER REGION (PREDICTED)
1383822_AT	*BICD2*	BICAUDAL D HOMOLOG 2 (DROSOPHILA)
1382236_AT	*BIRC6_PREDICTED*	BACULOVIRAL IAP REPEAT-CONTAINING 6 (PREDICTED)
1371808_AT	*BLMH*	BLEOMYCIN HYDROLASE
1379659_AT	*BMP2K*	BMP-2 INDUCIBLE KINASE
1390398_AT	*BMPR1A*	BONE MORPHOGENETIC PROTEIN RECEPTOR, TYPE 1A
1383201_AT	*BMPR2*	BONE MORPHOGENIC PROTEIN RECEPTOR, TYPE II (SERINE/THREONINE KINASE)
1386978_AT	*BNIP3L*	BCL2/ADENOVIRUS E1B 19 KDA-INTERACTING PROTEIN 3-LIKE
1392910_AT	*BOP1*	BLOCK OF PROLIFERATION 1
1374313_AT	*BPY2IP1_PREDICTED*	BPY2 INTERACTING PROTEIN 1 (PREDICTED)
1389029_AT	*BRD3_PREDICTED*	BROMODOMAIN CONTAINING 3 (PREDICTED)
1399055_AT	*BRD7_PREDICTED*	BROMODOMAIN CONTAINING 7 (PREDICTED)
1373599_AT	*BRF2*	BRF2, SUBUNIT OF RNA POLYMERASE III TRANSCRIPTION INITIATION FACTOR, BRF1-LIKE
1388690_AT	*BRMS1L_PREDICTED*	BREAST CANCER METASTASIS-SUPPRESSOR 1-LIKE (PREDICTED)
1372068_AT	*BS69*	BS69 PROTEIN
1367643_AT	*BSG*	BASIGIN
1390738_AT	*BST2*	BONE MARROW STROMAL CELL ANTIGEN 2
1372720_AT	*BTBD1*	BTB (POZ) DOMAIN CONTAINING 1
1380459_AT	*BTBD14A*	BTB (POZ) DOMAIN CONTAINING 14A
1387644_AT	*BTC*	BETACELLULIN
1386773_AT	*BTD*	BIOTINIDASE
1386994_AT	*BTG2*	B-CELL TRANSLOCATION GENE 2, ANTI-PROLIFERATIVE
1368072_AT	*BTG3*	B-CELL TRANSLOCATION GENE 3
1384050_AT	*BUB3*	BUDDING UNINHIBITED BY BENZIMIDAZOLES 3 HOMOLOG (S. CEREVISIAE)
1388554_AT	*BZW1*	BASIC LEUCINE ZIPPER AND W2 DOMAINS 1
1387043_AT	*C4.4A*	GPI-ANCHORED METASTASIS-ASSOCIATED PROTEIN HOMOLOG
1372244_AT	*CAB39_PREDICTED*	CALCIUM BINDING PROTEIN 39 (PREDICTED)
1370178_AT	*CACNB2*	CALCIUM CHANNEL, VOLTAGE-DEPENDENT, BETA 2 SUBUNIT
1393581_AT	*CALMBP1_PREDICTED*	CALMODULIN BINDING PROTEIN 1 (PREDICTED)
1371686_AT	*CANX*	CALNEXIN
1385851_AT	*CAPN5*	CALPAIN 5
1399091_AT	*CAPZB*	F-ACTIN CAPPING PROTEIN BETA SUBUNIT
1388659_AT	*CARHSP1*	CALCIUM REGULATED HEAT STABLE PROTEIN 1
1385639_AT	*CASP8AP2_PREDICTED*	CASPASE 8 ASSOCIATED PROTEIN 2 (PREDICTED)
1373466_AT	*CAST*	CALPASTATIN
1371921_AT	*CATNA1*	CATENIN (CADHERIN-ASSOCIATED PROTEIN), ALPHA 1, 102KDA
1398354_AT	*CATNAL1_PREDICTED*	CATENIN ALPHA-LIKE 1 (PREDICTED)
1376850_A_AT	*CCL27_PREDICTED*	CHEMOKINE (C-C MOTIF) LIGAND 27 (PREDICTED)
1370346_AT	*CCNB1*	CYCLIN B1
1390343_AT	*CCNC*	CYCLIN C
1367764_AT	*CCNG1*	CYCLIN G1
1368050_AT	*CCNL1*	CYCLIN L1
1385697_AT	*CCNT2_PREDICTED*	CYCLIN T2 (PREDICTED)
1371784_AT	*CCRP*	CYTOPLASMIC CAR RETENTION PROTEIN
1373784_AT	*CCT8_PREDICTED*	CHAPERONIN SUBUNIT 8 (THETA) (PREDICTED)
1368593_AT	*CD1D1*	CD1D1 ANTIGEN
1372036_AT	*CD2BP2_PREDICTED*	CD2 ANTIGEN (CYTOPLASMIC TAIL) BINDING PROTEIN 2 (PREDICTED)
1368518_AT	*CD53*	CD53 ANTIGEN
1367929_AT	*CD59*	CD59 ANTIGEN
1367716_AT	*CDA08*	T-CELL IMMUNOMODULATORY PROTEIN
1376782_AT	*CDC14A_PREDICTED*	CDC14 CELL DIVISION CYCLE 14 HOMOLOG A (S. CEREVISIAE) (PREDICTED)
1389145_AT	*CDC42EP2*	CDC42 EFFECTOR PROTEIN (RHO GTPASE BINDING) 2
1375910_AT	*CDC42EP3_PREDICTED*	CDC42 EFFECTOR PROTEIN (RHO GTPASE BINDING) 3 (PREDICTED)
1388730_AT	*CDC42EP4_PREDICTED*	CDC42 EFFECTOR PROTEIN (RHO GTPASE BINDING) 4 (PREDICTED)
1389378_AT	*CDC42EP5_PREDICTED*	CDC42 EFFECTOR PROTEIN (RHO GTPASE BINDING) 5 (PREDICTED)
1398793_AT	*CDC5L*	CELL DIVISION CYCLE 5-LIKE (S. POMBE)
1371928_AT	*CDCA8*	CELL DIVISION CYCLE ASSOCIATED 8
1386947_AT	*CDH1*	CADHERIN 1
1369224_AT	*CDH17*	CADHERIN 17
1373089_AT	*CDH3*	CADHERIN 3, TYPE 1, P-CADHERIN (PLACENTAL)
1381316_AT	*CDKAL1_PREDICTED*	CDK5 REGULATORY SUBUNIT ASSOCIATED PROTEIN 1-LIKE 1 (PREDICTED)
1368248_AT	*CDS1*	CDP-DIACYLGLYCEROL SYNTHASE 1
1398719_AT	*CDYL2_PREDICTED*	CHROMODOMAIN PROTEIN, Y CHROMOSOME-LIKE 2 (PREDICTED)
1379538_AT	*CENPJ_PREDICTED*	CENTROMERE PROTEIN J (PREDICTED)
1376030_AT	*CENTB1_PREDICTED*	CENTAURIN, BETA 1 (PREDICTED)
1375699_AT	*CENTB2*	CENTAURIN, BETA 2

1387871_AT	*CFL1*	COFILIN 1
1388928_AT	*CFL2_PREDICTED*	COFILIN 2, MUSCLE (PREDICTED)
1368545_AT	*CFLAR*	CASP8 AND FADD-LIKE APOPTOSIS REGULATOR
1371968_AT	*CGI119*	CGI-119 PROTEIN
1368692_A_AT	*CHKA*	CHOLINE KINASE ALPHA
1387388_AT	*CHP*	CALCIUM BINDING PROTEIN P22
1369091_AT	*CHRNB1*	CHOLINERGIC RECEPTOR, NICOTINIC, BETA POLYPEPTIDE 1 (MUSCLE)
1398726_AT	*CIAO1*	WD40 PROTEIN CIAO1
1367675_AT	*CIB1*	CALCIUM AND INTEGRIN BINDING 1 (CALMYRIN)
1382322_A_AT	*CIC_PREDICTED*	CAPICUA HOMOLOG (DROSOPHILA) (PREDICTED)
1384068_AT	*CKAP2_PREDICTED*	CYTOSKELETON ASSOCIATED PROTEIN 2 (PREDICTED)
1367740_AT	*CKB*	CREATINE KINASE, BRAIN
1372056_AT	*CKLFSF6*	CHEMOKINE-LIKE FACTOR SUPER FAMILY 6
1390566_A_AT	*CKMT1*	CREATINE KINASE, MITOCHONDRIAL 1, UBIQUITOUS
1375685_AT	*CLASP1*	CYTOPLASMIC LINKER ASSOCIATED PROTEIN 1
1368219_AT	*CLCN2*	CHLORIDE CHANNEL 2
1381993_AT	*CLIC2*	CHLORIDE INTRACELLULAR CHANNEL 2
1374630_AT	*CLIC3*	CHLORIDE INTRACELLULAR CHANNEL 3
1383121_AT	*CLN2*	CEROID-LIPOFUSCINOSIS, NEURONAL 2
1389791_AT	*CLN8*	CEROID-LIPOFUSCINOSIS, NEURONAL 8
1374846_AT	*CLP1*	CARDIAC LINEAGE PROTEIN 1
1391077_AT	*CLSPN_PREDICTED*	CLASPIN HOMOLOG (XENOPUS LAEVIS) (PREDICTED)
1371393_AT	*CLSTN1*	CALSYNTENIN 1
1367907_A_AT	*CLTB*	CLATHRIN, LIGHT POLYPEPTIDE (LCB)
1367784_A_AT	*CLU*	CLUSTERIN
1367940_AT	*CMKOR1*	CHEMOKINE ORPHAN RECEPTOR 1
1387856_AT	*CNN3*	CALPONIN 3, ACIDIC
1391270_AT	*CNNM3_PREDICTED*	CYCLIN M3 (PREDICTED)
1393619_AT	*CNOT6L_PREDICTED*	CCR4-NOT TRANSCRIPTION COMPLEX, SUBUNIT 6-LIKE (PREDICTED)
1368658_AT	*CNTF*	CILIARY NEUROTROPHIC FACTOR
1384834_AT	*COBL_PREDICTED*	CORDON-BLEU (PREDICTED)
1376868_AT	*COBLL1_PREDICTED*	COBL-LIKE 1 (PREDICTED)
1382310_AT	*COG5_PREDICTED*	COMPONENT OF OLIGOMERIC GOLGI COMPLEX 5 (PREDICTED)
1377254_A_AT	*COHH1_PREDICTED*	COHEN SYNDROME HOMOLOG 1 (PREDICTED)
1376105_AT	*COL14A1_PREDICTED*	COLLAGEN, TYPE XIV, ALPHA 1 (UNDULIN) (PREDICTED)
1383879_AT	*COL17A1_PREDICTED*	PROCOLLAGEN, TYPE XVII, ALPHA 1 (PREDICTED)
1371893_AT	*COL4A3BP_PREDICTED*	PROCOLLAGEN, TYPE IV, ALPHA 3 (GOODPASTURE ANTIGEN) BINDING PROTEIN (PREDICTED)
1393891_AT	*COL8A1_PREDICTED*	PROCOLLAGEN, TYPE VIII, ALPHA 1 (PREDICTED)
1368826_AT	*COMT*	CATECHOL-O-METHYLTRANSFERASE
1389271_AT	*CORO7*	CORONIN 7
1386921_AT	*CPE*	CARBOXYPEPTIDASE E
1377746_AT	*CPNE1_PREDICTED*	COPINE I (PREDICTED)
1374471_AT	*CPNE2_PREDICTED*	COPINE II (PREDICTED)
1371993_AT	*CPNE3_PREDICTED*	COPINE III (PREDICTED)
1377998_AT	*CPOX*	COPROPORPHYRINOGEN OXIDASE
1389293_AT	*CPSF2_PREDICTED*	CLEAVAGE AND POLYADENYLATION SPECIFIC FACTOR 2 (PREDICTED)
1398356_AT	*CPSF5*	CLEAVAGE AND POLYADENYLATION SPECIFIC FACTOR 5
1375033_AT	*CPT1C*	CARNITINE PALMITOYLTRANSFERASE 1C
1386927_AT	*CPT2*	CARNITINE PALMITOYLTRANSFERASE 2
1369994_AT	*CRCP*	CALCITONIN GENE-RELATED PEPTIDE-RECEPTOR COMPONENT PROTEIN
1393278_AT	*CREB3L4*	CAMP RESPONSIVE ELEMENT BINDING PROTEIN 3-LIKE 4
1381968_AT	*CREG_PREDICTED*	CELLULAR REPRESSOR OF E1A-STIMULATED GENES (PREDICTED)
1370026_AT	*CRYAB*	CRYSTALLIN, ALPHA B
1368685_AT	*CSPG4*	CHONDROITIN SULFATE PROTEOGLYCAN 4
1370057_AT	*CSRP1*	CYSTEINE AND GLYCINE-RICH PROTEIN 1
1376797_AT	*CSRP2BP_PREDICTED*	CYSTEINE AND GLYCINE-RICH PROTEIN 2 BINDING PROTEIN (PREDICTED)
1370855_AT	*CST3*	CYSTATIN C
1368162_AT	*CST6*	CYSTATIN E/M
1367631_AT	*CTGF*	CONNECTIVE TISSUE GROWTH FACTOR
1378127_AT	*CUL2_PREDICTED*	CULLIN 2 (PREDICTED)
1393343_AT	*CUL3_PREDICTED*	CULLIN 3 (PREDICTED)
1368200_AT	*CX3CL1*	CHEMOKINE (C-X3-C MOTIF) LIGAND 1
1372064_AT	*CXCL16*	SIMILAR TO CHEMOKINE (C-X-C MOTIF) LIGAND 16
1368192_AT	*CXCR3*	CHEMOKINE (C-X-C MOTIF) RECEPTOR 3
1386904_A_AT	*CYB5*	CYTOCHROME B-5
1398383_AT	*CYB561_PREDICTED*	CYTOCHROME B-561 (PREDICTED)
1368990_AT	*CYP1B1*	CYTOCHROME P450, FAMILY 1, SUBFAMILY B, POLYPEPTIDE 1
1390282_AT	*CYP2S1*	CYTOCHROME P450, FAMILY 2, SUBFAMILY S, POLYPEPTIDE 1
1370387_AT	*CYP3A13*	CYTOCHROME P450, FAMILY 3, SUBFAMILY A, POLYPEPTIDE 13
1368290_AT	*CYR61*	CYSTEINE RICH PROTEIN 61
1388159_AT	*CYTB*	CYTOCHROME B
1370990_AT	*CYTOR4*	SIMILAR TO CYTOKINE RECEPTOR RELATED PROTEIN 4
1368274_AT	*DBNL*	DREBRIN-LIKE
1398600_AT	*DCBLD2*	DISCOIDIN, CUB AND LCCL DOMAIN CONTAINING 2
1384041_AT	*DCK*	DEOXYCYTIDINE KINASE
1388904_AT	*DD25*	HYPOTHETICAL PROTEIN DD25
1394597_AT	*DDHD1*	DDHD DOMAIN CONTAINING 1
1375901_AT	*DDX21B*	DEAD (ASP-GLU-ALA-ASP) BOX POLYPEPTIDE 21B
1387912_AT	*DDX46*	RNA HELICASE
1372484_AT	*DDX5*	DDX5 GENE
1368588_AT	*DDX52*	ATP-DEPENDENT, RNA HELICASE
1398945_AT	*DDX6_MAPPED*	DEAD (ASP-GLU-ALA-ASP/HIS) BOX POLYPEPTIDE 6 (MAPPED)
1376914_AT	*DEPDC1_PREDICTED*	DEP DOMAIN CONTAINING 1 (PREDICTED)
1371806_AT	*DGCR8_PREDICTED*	DIGEORGE SYNDROME CRITICAL REGION GENE 8 (PREDICTED)
1395579_AT	*DHX32_PREDICTED*	DEAH (ASP-GLU-ALA-HIS) BOX POLYPEPTIDE 32 (PREDICTED)
1377763_AT	*DHX33_PREDICTED*	DEAH (ASP-GLU-ALA-HIS) BOX POLYPEPTIDE 33 (PREDICTED)
1393432_A_AT	*DHX36_PREDICTED*	DEAH (ASP-GLU-ALA-HIS) BOX POLYPEPTIDE 36 (PREDICTED)
1374299_AT	*DHX9_PREDICTED*	DEAH (ASP-GLU-ALA-HIS) BOX POLYPEPTIDE 9 (PREDICTED)
1373221_AT	*DIAPI_PREDICTED*	DIAPHANOUS HOMOLOG 1 (DROSOPHILA) (PREDICTED)
1388194_AT	*DLAT*	DIHYDROLIPOAMIDE S-ACETYLTRANSFERASE (E2 COMPONENT OF PYRUVATE

		DEHYDROGENASE COMPLEX)
1377121_AT	*DLG5_PREDICTED*	DISCS, LARGE HOMOLOG 5 (DROSOPHILA) (PREDICTED)
1380558_AT	*DLX3_PREDICTED*	DISTAL-LESS HOMEOBOX 3 (PREDICTED)
1368852_AT	*DNAJA1*	DNAJ-LIKE PROTEIN
1389308_AT	*DNAJB11*	DNAJ (HSP40) HOMOLOG, SUBFAMILY B, MEMBER 11
1372722_AT	*DNAJB4*	DNAJ (HSP40) HOMOLOG, SUBFAMILY B, MEMBER 4
1392598_AT	*DNAJB6*	DNAJ (HSP40) HOMOLOG, SUBFAMILY B, MEMBER 6
1387116_AT	*DNAJB9*	DNAJ (HSP40) HOMOLOG, SUBFAMILY B, MEMBER 9
1384305_AT	*DNB5*	PROTON-ASSOCIATED SUGAR TRANSPORTER A
1368402_AT	*DNCLI2*	DYNEIN, CYTOPLASMIC, LIGHT INTERMEDIATE POLYPEPTIDE 2
1373772_AT	*DNMT1*	DNA (CYTOSINE-5-)-METHYLTRANSFERASE 1
1384525_AT	*DOCK11*	DEDICATOR OF CYTOKINESIS 11
1372300_AT	*DOK4_PREDICTED*	DOCKING PROTEIN 4 (PREDICTED)
1376026_AT	*DONSON*	DOWNSTREAM NEIGHBOR OF SON
1388589_AT	*DOT1L_PREDICTED*	DOT1-LIKE, HISTONE H3 METHYLTRANSFERASE (S. CEREVISIAE) (PREDICTED)
1384400_AT	*DPDE1*	PHOSPHODIESTERASE 4C, CAMP-SPECIFIC
1388486_AT	*DPP8_PREDICTED*	DIPEPTIDYLPEPTIDASE 8 (PREDICTED)
1372453_AT	*DR1*	DOWN-REGULATOR OF TRANSCRIPTION 1
1388686_AT	*DSCR1*	DOWN SYNDROME CRITICAL REGION HOMOLOG 1 (HUMAN)
1388506_AT	*DSP*	DESMOPLAKIN
1376130_A_AT	*DTNB*	DYSTROBREVIN, BETA
1368983_AT	*DTR*	DIPHTHERIA TOXIN RECEPTOR
1394028_AT	*DUSP10_PREDICTED*	DUAL SPECIFICITY PHOSPHATASE 10 (PREDICTED)
1373324_AT	*DUSP14_PREDICTED*	DUAL SPECIFICITY PHOSPHATASE 14 (PREDICTED)
1372385_AT	*DUSP8_PREDICTED*	DUAL SPECIFICITY PHOSPHATASE 8 (PREDICTED)
1377424_AT	*DUTP*	DEOXYURIDINE TRIPHOSPHATASE
1388698_AT	*ECM1*	EXTRACELLULAR MATRIX PROTEIN 1
1383747_AT	*ECT2_PREDICTED*	ECT2 ONCOGENE (PREDICTED)
1369519_AT	*EDN1*	ENDOTHELIN 1
1369536_AT	*EDN2*	ENDOTHELIN 2
1373462_AT	*EED_PREDICTED*	EMBRYONIC ECTODERM DEVELOPMENT (PREDICTED)
1389328_AT	*EEF1A1*	EUKARYOTIC TRANSLATION ELONGATION FACTOR 1 ALPHA 1
1374388_AT	*EFHD2*	EF HAND DOMAIN CONTAINING 2
1387306_A_AT	*EGR2*	EARLY GROWTH RESPONSE 2
1387442_AT	*EGR4*	EARLY GROWTH RESPONSE 4
1376145_AT	*EIF2B5*	EUKARYOTIC TRANSLATION INITIATION FACTOR 2B, SUBUNIT 5 EPSILON
1385118_AT	*EIF2S1*	EUKARYOTIC TRANSLATION INITIATION FACTOR 2, SUBUNIT 1 ALPHA
1374721_AT	*EIF2S2*	EUKARYOTIC TRANSLATION INITIATION FACTOR 2, SUBUNIT 2 (BETA)
1371404_AT	*EIF4B*	EUKARYOTIC TRANSLATION INITIATION FACTOR 4B
1373364_AT	*EIF4G3_PREDICTED*	EUKARYOTIC TRANSLATION INITIATION FACTOR 4 GAMMA, 3 (PREDICTED)
1398845_AT	*EIF5*	EUKARYOTIC TRANSLATION INITIATION FACTOR 5
1396191_AT	*EIF5B*	EUKARYOTIC TRANSLATION INITIATION FACTOR 5B
1383736_AT	*ELAVL2*	ELAV (EMBRYONIC LETHAL, ABNORMAL VISION, DROSOPHILA)-LIKE 2 (HU ANTIGEN B)
1374119_AT	*ELF3*	E74-LIKE FACTOR 3
1388714_AT	*ELL_PREDICTED*	ELONGATION FACTOR RNA POLYMERASE II (PREDICTED)
1388111_AT	*ELN*	ELASTIN
1368541_AT	*EMB*	EMBIGIN
1368513_AT	*ENPEP*	GLUTAMYL AMINOPEPTIDASE
1388926_AT	*ENPP5*	ECTONUCLEOTIDE PYROPHOSPHATASE/PHOSPHODIESTERASE 5
1370845_AT	*ENTPD2*	ECTONUCLEOSIDE TRIPHOSPHATE DIPHOSPHOHYDROLASE 2
1374300_AT	*ENTPD4_PREDICTED*	ECTONUCLEOSIDE TRIPHOSPHATE DIPHOSPHOHYDROLASE 4 (PREDICTED)
1374984_AT	*EPB4.1L5*	ERYTHROCYTE PROTEIN BAND 4.1-LIKE 5
1378997_AT	*EPHB6*	EPH RECEPTOR B6
1373019_AT	*EPS15*	EPIDERMAL GROWTH FACTOR RECEPTOR PATHWAY SUBSTRATE 15
1372654_AT	*EPS8L2_PREDICTED*	EPS8-LIKE 2 (PREDICTED)
1387813_AT	*ERBB2*	V-ERB-B2 ERYTHROBLASTIC LEUKEMIA VIRAL ONCOGENE HOMOLOG 2,
1377821_AT	*ERBB3*	V-ERB-B2 ERYTHROBLASTIC LEUKEMIA VIRAL ONCOGENE HOMOLOG 3 (AVIAN)
1376866_AT	*ERCC1_PREDICTED*	EXCISION REPAIR CROSS-COMPLEMENTING RODENT REPAIR DEFICIENCY,
1391723_AT	*ERCC3*	EXCISION REPAIR CROSS-COMPLEMENTING RODENT REPAIR DEFICIENCY,
1374687_AT	*ESPL1_PREDICTED*	EXTRA SPINDLE POLES LIKE 1 (S. CEREVISIAE) (PREDICTED)
1372306_AT	*ETHE1_PREDICTED*	ETHYLMALONIC ENCEPHALOPATHY 1 (PREDICTED)
1371710_AT	*ETNK1_PREDICTED*	ETHANOLAMINE KINASE 1 (PREDICTED)
1368851_AT	*ETS1*	V-ETS ERYTHROBLASTOSIS VIRUS E26 ONCOGENE HOMOLOG 1 (AVIAN)
1375908_AT	*EVA_PREDICTED*	EPITHELIAL V-LIKE ANTIGEN (PREDICTED)
1376082_AT	*EVI1_PREDICTED*	ECOTROPIC VIRAL INTEGRATION SITE 1 (PREDICTED)
1389115_AT	*EVPL_PREDICTED*	ENVOPLAKIN (PREDICTED)
1387279_AT	*F11R*	JUNCTIONAL ADHESION MOLECULE 1
1367899_AT	*F2R*	COAGULATION FACTOR II (THROMBIN) RECEPTOR
1387596_AT	*F2RL1*	COAGULATION FACTOR II (THROMBIN) RECEPTOR-LIKE 1
1369182_AT	*F3*	COAGULATION FACTOR III
1391199_AT	*FADD*	FAS (TNFRSF6)-ASSOCIATED VIA DEATH DOMAIN
1368453_AT	*FADS2*	FATTY ACID DESATURASE 2
1389568_AT	*FAM26B*	FAMILY WITH SEQUENCE SIMILARITY 26, MEMBER B
1367654_AT	*FATH*	FAT TUMOR SUPPRESSOR HOMOLOG (DROSOPHILA)
1388528_AT	*FBL*	FIBRILLARIN
1389533_AT	*FBLN2*	FIBULIN 2
1368622_AT	*FBP2*	FRUCTOSE-1,6-BISPHOSPHATASE 2
1373147_AT	*FBXL3A*	F-BOX AND LEUCINE-RICH REPEAT PROTEIN 3A
1389333_AT	*FBXO3_PREDICTED*	F-BOX ONLY PROTEIN 3 (PREDICTED)
1392469_AT	*FBXW2_PREDICTED*	F-BOX AND WD-40 DOMAIN PROTEIN 2 (PREDICTED)
1367983_AT	*FEN1*	FLAP STRUCTURE-SPECIFIC ENDONUCLEASE 1
1388137_A_AT	*FEZ2*	FASCICULATION AND ELONGATION PROTEIN ZETA 2 (ZYGIN II)
1376042_AT	*FGD1*	FYVE, RHOGEF AND PH DOMAIN CONTAINING 1
1368114_AT	*FGF13*	FIBROBLAST GROWTH FACTOR 13
1387640_AT	*FGF15*	FIBROBLAST GROWTH FACTOR 15
1370106_AT	*FGF18*	FIBROBLAST GROWTH FACTOR 18
1392479_AT	*FKBP1A*	FK506 BINDING PROTEIN 1A
1390576_AT	*FLI1*	FRIEND LEUKEMIA INTEGRATION 1
1388401_AT	*FLNB_PREDICTED*	FILAMIN, BETA (PREDICTED)
1370234_AT	*FN1*	FIBRONECTIN 1

1382540_AT	*FNBP3_PREDICTED*	FORMIN BINDING PROTEIN 3 (PREDICTED)
1374726_AT	*FNDC1*	FIBRONECTIN TYPE III DOMAIN CONTAINING 1 (PREDICTED)
1370795_AT	*FOXC2*	FORKHEAD BOX C2
1377347_AT	*FOXJ3_PREDICTED*	FORKHEAD BOX J3 (PREDICTED)
1368550_AT	*FOXQ1*	FORKHEAD BOX Q1
1376249_AT	*FUCA2*	FUCOSIDASE, ALPHA-L- 2, PLASMA
1373195_AT	*FUS*	FUSION (INVOLVED IN T(12;16) IN MALIGNANT LIPOSARCOMA)
1388889_AT	*FXNA*	PUTATIVE AMINOPEPTIDASE FXNA
1378054_AT	*FXR1H*	FRAGILE X MENTAL RETARDATION GENE 1, AUTOSOMAL HOMOLOG
1368207_AT	*FXYD5*	FXYD DOMAIN-CONTAINING ION TRANSPORT REGULATOR 5
1373937_AT	*FYCO1_PREDICTED*	FYVE AND COILED-COIL DOMAIN CONTAINING 1 (PREDICTED)
1374530_AT	*FZD7_PREDICTED*	FRIZZLED HOMOLOG 7 (DROSOPHILA) (PREDICTED)
1382314_AT	*G1P2_PREDICTED*	INTERFERON, ALPHA-INDUCIBLE PROTEIN (CLONE IFI-15K) (PREDICTED)
1370976_AT	*G3BP*	RAS-GTPASE-ACTIVATING PROTEIN SH3-DOMAIN BINDING PROTEIN
1383377_AT	*GABPA_PREDICTED*	GA REPEAT BINDING PROTEIN, ALPHA (PREDICTED)
1372016_AT	*GADD45B*	GROWTH ARREST AND DNA-DAMAGE-INDUCIBLE 45 BETA
1388792_AT	*GADD45G*	GROWTH ARREST AND DNA-DAMAGE-INDUCIBLE 45 GAMMA
1376790_AT	*GALC*	GALACTOSYLCERAMIDASE
1378214_AT	*GALNAC4S6ST*	N-ACETYLGALACTOSAMINE 4-SULFATE 6-O-SULFOTRANSFERASE
1393651_AT	*GALNT10*	UDP-N-ACETYL-ALPHA-D-GALACTOSAMINE:
1384667_X_AT	*GALR2*	GALANIN RECEPTOR 2
1370963_AT	*GAS7*	GROWTH ARREST SPECIFIC 7
1387894_AT	*GATA4*	GATA BINDING PROTEIN 4
1368332_AT	*GBP2*	GUANYLATE NUCLEOTIDE BINDING PROTEIN 2
1368085_AT	*GCHFR*	GTP CYCLOHYDROLASE I FEEDBACK REGULATOR
1390517_AT	*GCN1L1_PREDICTED*	GCN1 GENERAL CONTROL OF AMINO-ACID SYNTHESIS 1-LIKE 1 (YEAST) (PREDICTED)
1368770_AT	*GCNT1*	GLUCOSAMINYL (N-ACETYL) TRANSFERASE 1, CORE 2
1382203_AT	*GDF1_PREDICTED*	GROWTH DIFFERENTIATION FACTOR 1 (PREDICTED)
1368307_AT	*GGTL3*	GAMMA-GLUTAMYLTRANSFERASE-LIKE 3
1369898_A_AT	*GIP*	GLUCOSE-DEPENDENT INSULINOTROPIC PEPTIDE
1370023_AT	*GJA4*	GAP JUNCTION MEMBRANE CHANNEL PROTEIN ALPHA 4
1368689_AT	*GJB5*	GAP JUNCTION MEMBRANE CHANNEL PROTEIN BETA 5
1376781_AT	*GLB1_MAPPED*	GALACTOSIDASE, BETA 1 (MAPPED)
1376427_A_AT	*GLDC_PREDICTED*	GLYCINE DEHYDROGENASE (DECARBOXYLATING; GLYCINE DECARBOXYLASE
1374690_AT	*GLE1L*	GLE1 RNA EXPORT MEDIATOR-LIKE (YEAST
1382077_AT	*GLI3*	GLI-KRUPPEL FAMILY MEMBER GLI3
1390121_AT	*GLIS2_PREDICTED*	GLIS FAMILY ZINC FINGER 2 (PREDICTED)
1373490_AT	*GMFG*	GLIA MATURATION FACTOR, GAMMA
1370423_AT	*GNA15*	GUANINE NUCLEOTIDE BINDING PROTEIN, ALPHA 15
1392471_AT	*GNG12*	GUANINE NUCLEOTIDE BINDING PROTEIN (G PROTEIN), GAMMA 12
1368117_AT	*GPHN*	GEPHYRIN
1387383_AT	*GPR51*	G PROTEIN-COUPLED RECEPTOR 51
1373693_AT	*GPRC5C*	G PROTEIN-COUPLED RECEPTOR, FAMILY C, GROUP 5, MEMBER C
1368408_AT	*GPRK5*	G PROTEIN-COUPLED RECEPTOR KINASE 5
1382232_AT	*GPT2_PREDICTED*	GLUTAMIC PYRUVATE TRANSAMINASE (ALANINE AMINOTRANSFERASE) 2 (PREDICTED)
1368386_AT	*GRB2*	GROWTH FACTOR RECEPTOR BOUND PROTEIN 2
1368334_AT	*GRB7*	GROWTH FACTOR RECEPTOR BOUND PROTEIN 7
1369128_AT	*GRIK5*	GLUTAMATE RECEPTOR, IONOTROPIC, KAINATE 5
1368690_A_AT	*GRM4*	GLUTAMATE RECEPTOR, METABOTROPIC 4
1385001_AT	*GSDMDC1_PREDICTED*	GASDERMIN DOMAIN CONTAINING 1 (PREDICTED)
1389714_AT	*GSK3A*	GLYCOGEN SYNTHASE KINASE 3 ALPHA
1371524_AT	*GTL3*	GENE TRAP LOCUS 3
1378166_AT	*GTL7_PREDICTED*	GENE TRAP LOCUS 7 (PREDICTED)
1398985_AT	*GTPBP1_PREDICTED*	GTP BINDING PROTEIN 1 (PREDICTED)
1376285_AT	*GULP1*	GULP, ENGULFMENT ADAPTOR PTB DOMAIN CONTAINING 1
1395652_AT	*GYLTL1B*	GLYCOSYLTRANSFERASE-LIKE 1B
1391280_AT	*H13_PREDICTED*	HISTOCOMPATIBILITY 13 (PREDICTED)
1371765_AT	*H2A*	HISTONE 2A
1370004_AT	*H2AFY*	H2A HISTONE FAMILY, MEMBER Y
1388428_AT	*HARS2_PREDICTED*	HISTIDYL TRNA SYNTHETASE 2 (PREDICTED)
1391731_AT	*HBP1*	HIGH MOBILITY GROUP BOX TRANSCRIPTION FACTOR 1
1395570_AT	*HDH*	HUNTINGTON DISEASE GENE HOMOLOG
1388918_AT	*HDLBP*	HIGH DENSITY LIPOPROTEIN BINDING PROTEIN
1383912_AT	*HECA_PREDICTED*	HEADCASE HOMOLOG (DROSOPHILA) (PREDICTED)
1374599_AT	*HERC1_PREDICTED*	HECT (HOMOLOGOUS TO THE E6-AP (UBE3A) CARBOXYL TERMINUS) DOMAIN AND RCC1
1367741_AT	*HERPUD1*	HOMOCYSTEINE-INDUCIBLE, ENDOPLASMIC RETICULUM STRESS-INDUCIBLE
1387036_AT	*HES1*	HAIRY AND ENHANCER OF SPLIT 1 (DROSOPHILA)
1372706_AT	*HEXB*	HEXOSAMINIDASE B
1399067_AT	*HFE*	HEMOCHROMATOSIS
1381006_AT	*HGFAC*	HEPATOCYTE GROWTH FACTOR ACTIVATOR
1374105_AT	*HIG1*	HYPOXIA INDUCED GENE 1
1389132_AT	*HIP1*	HUNTINGTIN INTERACTING PROTEIN 1
1370994_AT	*HIP1R*	HUNTINGTIN INTERACTING PROTEIN 1 RELATED
1385259_AT	*HIP2_PREDICTED*	HUNTINGTIN INTERACTING PROTEIN 2 (PREDICTED)
1392476_AT	*HIST1H4B*	GERMINAL HISTONE H4 GENE
1392476_AT	*HIST1H4M_PREDICTED*	GERMINAL HISTONE H4 GENE
1371959_AT	*HIST2H2AA_PREDICTED*	HISTONE 2, H2AA (PREDICTED)
1392476_AT	*HIST2H4_PREDICTED*	GERMINAL HISTONE H4 GENE
1392512_AT	*HIST3H2BA_PREDICTED*	HISTONE 3, H2BA (PREDICTED)
1383087_AT	*HMG20B_PREDICTED*	HIGH MOBILITY GROUP 20 B (PREDICTED)
1388309_AT	*HMGA1*	HIGH MOBILITY GROUP AT-HOOK 1
1367676_AT	*HMGB2*	HIGH MOBILITY GROUP BOX 2
1373927_AT	*HMGB2L1_PREDICTED*	HIGH MOBILITY GROUP BOX 2-LIKE 1 (PREDICTED)
1371352_AT	*HMGN2*	HIGH MOBILITY GROUP NUCLEOSOMAL BINDING DOMAIN 2
1388581_AT	*HN1*	HEMATOLOGICAL AND NEUROLOGICAL EXPRESSED SEQUENCE 1
1371333_AT	*HNRPDL*	HETEROGENEOUS NUCLEAR RIBONUCLEOPROTEIN D-LIKE
1398797_AT	*HNRPK*	HETEROGENEOUS NUCLEAR RIBONUCLEOPROTEIN K
1373905_AT	*HNRPR*	HETEROGENEOUS NUCLEAR RIBONUCLEOPROTEIN R
1370171_AT	*HNRPU*	HETEROGENEOUS NUCLEAR RIBONUCLEOPROTEIN U
1380824_AT	*HOOK3*	HOOK HOMOLOG 3

1368873_AT	*HOXA2*	HOMEO BOX A2
1392183_AT	*HOXC8_MAPPED*	HOMEO BOX C8 (MAPPED)
1382182_AT	*HOXC9_PREDICTED*	HOMEO BOX C9 (PREDICTED)
1371012_AT	*HPCL2*	2-HYDROXYPHYTANOYL-COENZYME A LYASE
1368407_AT	*HPSE*	HEPARANASE
1371490_AT	*HSBP1*	HEAT SHOCK FACTOR BINDING PROTEIN 1
1370433_AT	*HSD3B7*	CCA2 PROTEIN
1370344_AT	*HSPA4*	HEAT SHOCK PROTEIN 4
1383680_AT	*HSPA5BP1*	HEAT SHOCK 70KDA PROTEIN 5 BINDING PROTEIN 1
1368195_AT	*HSPBAP1*	HSPB ASSOCIATED PROTEIN 1
1387741_AT	*HTR1B*	5-HYDROXYTRYPTAMINE (SEROTONIN) RECEPTOR 1B
1367787_AT	*ICA1*	ISLET CELL AUTOANTIGEN 1
1387202_AT	*ICAM1*	INTERCELLULAR ADHESION MOLECULE 1
1387028_A_AT	*ID1*	INHIBITOR OF DNA BINDING 1, HELIX-LOOP-HELIX PROTEIN (SPLICE VARIATION)
1389355_AT	*IER5*	IMMEDIATE EARLY RESPONSE 5
1372070_AT	*IFI30*	INTERFERON GAMMA INDUCIBLE PROTEIN 30
1371357_AT	*IGFBP7*	INSULIN-LIKE GROWTH FACTOR BINDING PROTEIN 7
1378396_AT	*IGSF10*	IMMUNOGLOBULIN SUPERFAMILY, MEMBER 10
1376733_AT	*IGSF11*	IMMUNOGLOBULIN SUPERFAMILY, MEMBER 11
1368424_AT	*IKBKB*	INHIBITOR OF KAPPAB KINASE BETA
1370331_AT	*IL11RA1*	INTERLEUKIN 11 RECEPTOR, ALPHA CHAIN 1
1368210_AT	*IL24*	INTERLEUKIN 24
1386987_AT	*IL6R*	INTERLEUKIN 6 RECEPTOR
1372193_AT	*IMPACT*	IMPRINTED AND ANCIENT
1377163_AT	*INHBB*	INHIBIN BETA-B
1388697_AT	*INPP5A_PREDICTED*	INOSITOL POLYPHOSPHATE-5-PHOSPHATASE A (PREDICTED)
1368073_AT	*IRF1*	INTERFERON REGULATORY FACTOR 1
1387770_AT	*ISG12(A)*	PUTATIVE ISG12(A) PROTEIN
1389282_AT	*ITGA3_PREDICTED*	INTEGRIN ALPHA 3 (PREDICTED)
1383240_AT	*ITGA6*	INTEGRIN, ALPHA 6
1383398_AT	*ITGA8*	INTEGRIN ALPHA 8
1368612_AT	*ITGB4*	INTEGRIN BETA 4
1388507_AT	*ITGB4BP*	INTEGRIN BETA 4 BINDING PROTEIN
1371320_AT	*ITM2B*	INTEGRAL MEMBRANE PROTEIN 2B
1373623_AT	*ITPKC*	INOSITOL 1,4,5-TRISPHOSPHATE 3-KINASE C
1397161_A_AT	*ITSN*	INTERSECTIN 1
1368725_AT	*JAG1*	JAGGED 1
1387905_AT	*JDP1*	JUN DIMERIZATION PROTEIN 1
1387788_AT	*JUNB*	JUN-B ONCOGENE
1387762_S_AT	*JUND*	JUN D PROTO-ONCOGENE
1387061_AT	*JUP*	JUNCTION PLAKOGLOBIN
1397645_AT	*KA17*	TYPE I KERATIN KA17
1377246_AT	*KB40*	TYPE II KERATIN KB40
1379276_AT	*KCMF1*	POTASSIUM CHANNEL MODULATORY FACTOR 1
1398290_AT	*KCNK13*	POTASSIUM CHANNEL, SUBFAMILY K, MEMBER 13
1387264_AT	*KCNK6*	POTASSIUM CHANNEL, SUBFAMILY K, MEMBER 6
1368930_AT	*KCNN4*	POTASSIUM INTERMEDIATE/SMALL CONDUCTANCE CALCIUM-ACTIVATED CHANNEL, SUBFAMILY N, MEMBER 4
1385226_AT	*KCTD11_PREDICTED*	POTASSIUM CHANNEL TETRAMERISATION DOMAIN CONTAINING 11 (PREDICTED)
1373119_AT	*KCTD3*	POTASSIUM CHANNEL TETRAMERISATION DOMAIN CONTAINING 3
1374582_AT	*KCTD9_PREDICTED*	POTASSIUM CHANNEL TETRAMERISATION DOMAIN CONTAINING 9 (PREDICTED)
1398773_AT	*KHDRBS1*	SRC ASSOCIATED IN MITOSIS, 68 KDA
1387327_AT	*KHDRBS2*	KH DOMAIN CONTAINING, RNA BINDING, SIGNAL TRANSDUCTION ASSOCIATED 2
1387196_AT	*KHDRBS3*	ETOILE, SAM68-LIKE PROTEIN SLM-2
1370930_AT	*KIF1C*	KINESIN FAMILY MEMBER 1C
1389593_AT	*KIF2*	KINESIN HEAVY CHAIN FAMILY, MEMBER 2
1384828_AT	*KIF7_PREDICTED*	KINESIN FAMILY MEMBER 7 (PREDICTED)
1389374_AT	*KIFC3*	KINESIN FAMILY MEMBER C3
1388068_AT	*KLC3*	KINESIN LIGHT CHAIN 3
1387260_AT	*KLF4*	KRUPPEL-LIKE FACTOR 4 (GUT)
1383173_AT	*KLRC1*	KILLER CELL LECTIN-LIKE RECEPTOR SUBFAMILY C, MEMBER 1
1374794_AT	*KNSL7*	KINESIN-LIKE 7
1367683_AT	*KPNA2*	KARYOPHERIN (IMPORTIN) ALPHA 2
1373858_AT	*KPNB1*	KARYOPHERIN (IMPORTIN) BETA 1
1372355_AT	*KRAS2*	KIRSTEN RAT SARCOMA VIRAL ONCOGENE HOMOLOGUE 2 (ACTIVE)
1371895_AT	*KRT1-14*	KERATIN COMPLEX 1, ACIDIC, GENE 14
1388433_AT	*KRT1-19*	KERATIN COMPLEX 1, ACIDIC, GENE 19
1373900_AT	*KRT2-7*	KERATIN COMPLEX 2, BASIC, GENE 7 (PREDICTED)
1371530_AT	*KRT2-8*	KERATIN COMPLEX 2, BASIC, GENE 8
1374195_AT	*LAD1_PREDICTED*	LADININ (PREDICTED)
1370538_AT	*LAMA3*	LAMININ, ALPHA 3
1388932_AT	*LAMA5*	LAMININ, ALPHA 5
1367880_AT	*LAMB2*	LAMININ, BETA 2
1383080_AT	*LAMP2*	LYSOSOMAL MEMBRANE GLYCOPROTEIN 2
1376579_AT	*LAP3*	LEUCINE AMINOPEPTIDASE 3
1388728_AT	*LAPTM4B*	LYSOSOMAL-ASSOCIATED PROTEIN TRANSMEMBRANE 4B
1367650_AT	*LCN7*	LIPOCALIN 7
1388725_AT	*LEPROT*	LEPTIN RECEPTOR OVERLAPPING TRANSCRIPT
1388587_AT	*LER3*	IMMEDIATE EARLY RESPONSE 3
1389157_AT	*LGALS2*	LECTIN, GALACTOSIDE-BINDING, SOLUBLE 2
1369716_S_AT	*LGALS5*	LECTIN, GALACTOSE BINDING, SOLUBLE 5
1369716_S_AT	*LGALS9*	LECTIN, GALACTOSE BINDING, SOLUBLE 9
1368804_AT	*LIF*	LEUKEMIA INHIBITORY FACTOR
1387090_A_AT	*LIMK2*	LIM MOTIF-CONTAINING PROTEIN KINASE 2
1368368_A_AT	*LISCH7*	LIVER-SPECIFIC BHLH-ZIP TRANSCRIPTION FACTOR 7
1389500_AT	*LOC191574*	3-ALPHA-HYDROXYSTEROID DEHYDROGENASE
1370696_AT	*LOC207121*	MEMBRANE AND MICROFILAMENT-ASSOCIATED PROTEIN P58
1371091_AT	*LOC207125*	UNKNOWN PROTEIN
1383222_AT	*LOC257646*	FERM-DOMAIN-CONTAINING PROTEIN 163SCII
1397362_AT	*LOC257650*	HIPPYRAGRANIN

1391059_AT	*LOC259224*	PREPRO-NEUROPEPTIDE W POLYPEPTIDE
1370565_AT	*LOC286991*	PUTATIVE RETROVIRUS-RELATED GAG PROTEIN
1374991_AT	*LOC287938*	HYPOTHETICAL LOC287938
1389040_AT	*LOC288165*	SIMILAR TO PEST-CONTAINING NUCLEAR PROTEIN
1372809_AT	*LOC290595*	HYPOTHETICAL GENE SUPPORTED BY AF152002
1371817_AT	*LOC290651*	SIMILAR TO MYO-INOSITOL 1-PHOSPHATE SYNTHASE A1
1389918_AT	*LOC290704*	SIMILAR TO PALLADIN
1370925_AT	*LOC291411*	SIMILAR TO POTENTIAL PHOSPHOLIPID-TRANSPORTING ATPASE IIB
1393066_AT	*LOC292666*	SIMILAR TO PREGNANCY-SPECIFIC BETA 1-GLYCOPROTEIN
1374116_AT	*LOC295241*	SIMILAR TO METAXIN 1, ISOFORM 2
1398726_AT	*LOC296126*	SIMILAR TO U5 SNRNP-SPECIFIC PROTEIN, 200 KDA
1391491_A_AT	*LOC298012*	SIMILAR TO MHR23B
1388773_AT	*LOC299339*	SIMILAR TO [MOUSE PRIMARY RESPONSE GENE B94 MRNA, 3END.], GENE PRODUCT
1373393_AT	*LOC299907*	SIMILAR TO EXT1
1379422_AT	*LOC300284*	SIMILAR TO RIKEN CDNA 4833435D08
1398756_AT	*LOC300303*	SIMILAR TO NUCLEOPHOSMIN (NPM) (NUCLEOLAR PHOSPHOPROTEIN B23) (NUMATRIN)
1372629_AT	*LOC300768*	SIMILAR TO KIAA0925 PROTEIN
1389600_AT	*LOC301748*	SIMILAR TO RIKEN CDNA 1700001E04
1382146_AT	*LOC302313*	SIMILAR TO TRANSMEMBRANE 4 SUPERFAMILY MEMBER 6
1373335_AT	*LOC302808*	MEMBRANE-ASSOCIATED DHHC9 ZINC FINGER PROTEIN
1374181_AT	*LOC302855*	SIMILAR TO HETEROGENEOUS NUCLEAR RIBONUCLEOPROTEIN G - HUMAN
1372740_AT	*LOC303259*	SIMILAR TO MAP4K6-PENDING PROTEIN
1391022_AT	*LOC305078*	LAMININ CHAIN
1398988_AT	*LOC307347*	HYPOTHETICAL PROTEIN LOC307347
1383888_AT	*LOC307495*	SIMILAR TO BLVRB PROTEIN
1372989_AT	*LOC308081*	SIMILAR TO ZINC FINGER, DHHC DOMAIN CONTAINING 14
1386013_AT	*LOC308348*	SIMILAR TO CG17669-PA
1377869_AT	*LOC310395*	SIMILAR TO CARBON CATABOLITE REPRESSION 4 PROTEIN HOMOLOG
1374725_AT	*LOC310756*	SIMILAR TO MKIAA1631 PROTEIN
1388985_AT	*LOC310926*	HYPOTHETICAL PROTEIN LOC310926
1379748_AT	*LOC310968*	SIMILAR TO MINOR HISTOCOMPATIBILITY ANTIGEN PRECURSOR
1371468_AT	*LOC312502*	SIMILAR TO MKIAA0857 PROTEIN
1379244_AT	*LOC312777*	SIMILAR TO TEL PROTEIN
1381326_AT	*LOC313744*	SIMILAR TO RIKEN CDNA 4632412I24
1377903_AT	*LOC313934*	SIMILAR TO INTERSECTIN 2 (SH3 DOMAIN-CONTAINING PROTEIN 1B) (SH3P18)
1375862_AT	*LOC314016*	SIMILAR TO MKIAA0230 PROTEIN
1383932_AT	*LOC314964*	SIMILAR TO PHD FINGER PROTEIN 20-LIKE 1 ISOFORM 1
1391604_AT	*LOC315508*	SIMILAR TO MKIAA0056 PROTEIN
1390145_AT	*LOC315676*	SIMILAR TO DMX-LIKE 2
1372725_AT	*LOC315883*	SIMILAR TO PHOSPHOLIPID SCRAMBLASE 2
1389600_AT	*LOC316186*	SIMILAR TO RIKEN CDNA 1700001E04
1383906_AT	*LOC316326*	SIMILAR TO LUNG INDUCIBLE NEURALIZED-RELATED C3HC4 RING FINGER PROTEIN
1389911_AT	*LOC316842*	SIMILAR TO CDNA SEQUENCE BC019776
1373232_AT	*LOC317070*	SIMILAR TO NIDOGEN 2 PROTEIN
1382331_AT	*LOC317214*	SIMILAR TO RIKEN CDNA 0610038L10 GENE
1376861_AT	*LOC317312*	SIMILAR TO RIKEN CDNA 1810018L05
1398939_AT	*LOC360618*	SIMILAR TO ORM1-LIKE 3
1389600_AT	*LOC360998*	SIMILAR TO RIKEN CDNA 1700001E04
1396292_AT	*LOC361014*	SIMILAR TO PEPTIDE N-GLYCANASE
1390029_AT	*LOC361110*	HYPOTHETICAL PROTEIN
1389180_AT	*LOC361377*	SIMILAR TO PHOSPHORYLASE KINASE (EC 2.7.1.38) BETA CHAIN, NON-MUSCLE - RABBIT
1390058_AT	*LOC361990*	SIMILAR TO DKFZP547E1010 PROTEIN
1372448_AT	*LOC362156*	MEMBRANE-ASSOCIATED DHHC5 ZINC FINGER PROTEIN
1384565_AT	*LOC362557*	HYPOTHETICAL PROTEIN LOC362557
1371940_AT	*LOC362587*	SIMILAR TO MICROFILAMENT AND ACTIN FILAMENT CROSS-LINKER PROTEIN ISOFORM A
1399092_AT	*LOC362608*	SIMILAR TO HYPOTHETICAL PROTEIN FLJ10315
1389636_AT	*LOC362665*	SIMILAR TO KIAA0833 PROTEIN
1388709_AT	*LOC362703*	SIMILAR TO WD-REPEAT PROTEIN 43
1392655_AT	*LOC363269*	SIMILAR TO NUCLEAR AUTOANTIGEN SP-100 (SPECKLED 100 KDA)
1389600_AT	*LOC363306*	HYPOTHETICAL PROTEIN LOC363306
1389600_AT	*LOC363320*	SIMILAR TO RIKEN CDNA 1700001E04
1373489_AT	*LOC363333*	SIMILAR TO CHROMATIN ASSEMBLY FACTOR-I P150 SUBUNIT
1373232_AT	*LOC363405*	SIMILAR TO NIDOGEN 2 PROTEIN
1389600_AT	*LOC363433*	SIMILAR TO RIKEN CDNA 1700001E04
1397537_AT	*LOC363433*	SIMILAR TO RIKEN CDNA 1700001E04
1397537_AT	*LOC363434*	SIMILAR TO CDNA SEQUENCE AY358078
1382316_AT	*LOC363849*	SIMILAR TO HISTONE CELL CYCLE REGULATION DEFECTIVE HOMOLOG A ISOFORM 1
1384253_AT	*LOC364558*	SIMILAR TO PALLADIN; CGI-151 PROTEIN
1376160_AT	*LOC365510*	SIMILAR TO AVIAN RETICULOENDOTHELIOSIS VIRAL (V-REL) ONCOGENE RELATED B
1383287_AT	*LOC365960*	SIMILAR TO SEMAF CYTOPLASMIC DOMAIN ASSOCIATED PROTEIN 2
1372474_AT	*LOC366595*	SIMILAR TO SYNAPTOPHYSIN-LIKE PROTEIN; PANTOPHYSIN; PAN I; DNA SEGMENT,
1377653_AT	*LOC366669*	SIMILAR TO MKIAA1011 PROTEIN
1392901_AT	*LOC367113*	SIMILAR TO RIKEN CDNA A430093J20 GENE
1397537_AT	*LOC367381*	SIMILAR TO RIKEN CDNA 4930555G01
1373232_AT	*LOC367653*	SIMILAR TO NIDOGEN 2 PROTEIN
1379422_AT	*LOC367759*	SIMILAR TO GLYCOSYLTRANSFERASE 28 DOMAIN CONTAINING 1
1372406_AT	*LOC367976*	SIMILAR TO DNA REPLICATION LICENSING FACTOR MCM3
1389080_AT	*LOC474154*	ZINC RESPONSIVE PROTEIN ZD7
1387071_A_AT	*LOC497674*	HYPOTHETICAL GENE SUPPORTED BY NM_017212
1370517_AT	*LOC497675*	NEURONAL PENTRAXIN 1
1368550_AT	*LOC497713*	HYPOTHETICAL GENE SUPPORTED BY NM_022858
1368151_AT	*LOC497720*	MATRIN 3
1368812_AT	*LOC497722*	HYPOTHETICAL GENE SUPPORTED BY NM_053905
1367853_AT	*LOC497723*	HYPOTHETICAL GENE SUPPORTED BY NM_031798
1387264_AT	*LOC497732*	HYPOTHETICAL GENE SUPPORTED BY NM_053806
1383736_AT	*LOC497806*	HYPOTHETICAL GENE SUPPORTED BY NM_173309
1368174_AT	*LOC497816*	HYPOTHETICAL GENE SUPPORTED BY NM_019371
1373705_AT	*LOC497876*	SIMILAR TO MRPL28 PROTEIN
1378611_AT	*LOC498289*	SIMILAR TO ENCEPHALOPSIN
1374812_AT	*LOC498331*	PROTEIN TYROSINE PHOSPHATASE, NON-RECEPTOR TYPE 13

1389054_AT	*LOC498368*	SIMILAR TO RIKEN CDNA 0610040J01
1389600_AT	*LOC498374*	SIMILAR TO RIKEN CDNA 1700001E04
1389488_AT	*LOC498544*	HYPOTHETICAL PROTEIN LOC498544
1392644_S_AT	*LOC498662*	SIMILAR TO RIKEN CDNA 2610019F03
1377141_AT	*LOC498685*	SIMILAR TO RIKEN CDNA 1110018J18
1374170_AT	*LOC498749*	SIMILAR TO PUTATIVE TRAF AND TNF RECEPTOR ASSOCIATED PROTEIN
1393094_AT	*LOC498883*	SIMILAR TO METHYL-CPG BINDING PROTEIN MBD2
1388570_AT	*LOC498909*	SIMILAR TO RIKEN CDNA 2310005O14
1386823_AT	*LOC498918*	IROQUOIS HOMEOBOX PROTEIN 5
1374322_AT	*LOC499087*	SIMILAR TO MKIAA1064 PROTEIN
1382629_AT	*LOC499247*	SIMILAR TO MALE STERILITY DOMAIN CONTAINING 2
1382331_AT	*LOC499328*	SIMILAR TO RIKEN CDNA 0610038L10 GENE
1392494_AT	*LOC499331*	SIMILAR TO HYPOTHETICAL PROTEIN D030056L22
1398691_AT	*LOC499624*	SIMILAR TO KIAA0669 GENE PRODUCT
1371248_AT	*LOC499660*	SIMILAR TO CORNIFIN ALPHA (SMALL PROLINE-RICH PROTEIN 1) (SPRR1)
1373324_AT	*LOC499736*	SIMILAR TO DUAL SPECIFICITY PHOSPHATASE 14
1390602_A_AT	*LOC499749*	SIMILAR TO RIKEN CDNA C430004E15
1373100_AT	*LOC499779*	SIMILAR TO RIKEN CDNA 2900010J23
1372250_AT	*LOC499941*	SCF APOPTOSIS RESPONSE PROTEIN 1
1397537_AT	*LOC500070*	SIMILAR TO RIKEN CDNA 4930555G01
1372213_AT	*LOC500300*	SIMILAR TO HYPOTHETICAL PROTEIN MGC6835
1388838_AT	*LOC500373*	SIMILAR TO 2010012F05RIK PROTEIN
1393866_AT	*LOC500592*	SIMILAR TO WSL-1-LIKE PROTEIN
1377673_AT	*LOC500715*	SIMILAR TO CYCLIN K
1373819_AT	*LOC500855*	HYPOTHETICAL PROTEIN LOC500855
1374746_AT	*LOC500877*	AB1-152
1371479_AT	*LOC500939*	LOC500939
1389640_AT	*LOC501026*	SIMILAR TO SH3 DOMAIN BINDING GLUTAMIC ACID-RICH PROTEIN LIKE 2
1398342_AT	*LOC501052*	SIMILAR TO FUS1 PROTEIN
1389600_AT	*LOC501091*	SIMILAR TO RIKEN CDNA 1700001E04
1397537_AT	*LOC501091*	SIMILAR TO RIKEN CDNA 1700001E04
1389600_AT	*LOC501092*	SIMILAR TO RIKEN CDNA 4930555G01
1397537_AT	*LOC501092*	SIMILAR TO RIKEN CDNA 4930555G01
1389600_AT	*LOC501093*	SIMILAR TO RIKEN CDNA 2610042L04
1388985_AT	*LOC501211*	LOC501211
1389600_AT	*LOC501221*	SIMILAR TO CDNA SEQUENCE AY358078
1397537_AT	*LOC501221*	SIMILAR TO CDNA SEQUENCE AY358078
1397537_AT	*LOC501222*	SIMILAR TO RIKEN CDNA 4930555G01
1389600_AT	*LOC501225*	SIMILAR TO CDNA SEQUENCE AY358078
1389600_AT	*LOC501226*	SIMILAR TO RIKEN CDNA 1700001E04
1389600_AT	*LOC501245*	SIMILAR TO CDNA SEQUENCE AY358078
1389600_AT	*LOC501250*	SIMILAR TO RETICULOCALBIN 1 PRECURSOR
1389600_AT	*LOC501253*	SIMILAR TO RIKEN CDNA 4930555G01
1373232_AT	*LOC501271*	SIMILAR TO NIDOGEN 2 PROTEIN
1389600_AT	*LOC501393*	SIMILAR TO CDNA SEQUENCE AY358078
1389600_AT	*LOC501396*	HYPOTHETICAL PROTEIN LOC501396
1389600_AT	*LOC501399*	SIMILAR TO RIKEN CDNA 1700001E04
1397537_AT	*LOC501399*	SIMILAR TO RIKEN CDNA 1700001E04
1370684_S_AT	*LOC501546*	HYPOTHETICAL PROTEIN LOC501546
1376861_AT	*LOC501648*	SIMILAR TO RIKEN CDNA 1810018L05
1392257_AT	*LOC501706*	HYPOTHETICAL PROTEIN LOC501706
1391125_AT	*LOC501937*	SIMILAR TO CDNA SEQUENCE BC061212
1393177_AT	*LOC502020*	SIMILAR TO MKIAA1016 PROTEIN
1371816_AT	*LOC502684*	HYPOTHETICAL PROTEIN LOC502684
1374777_AT	*LOC502894*	HYPOTHETICAL PROTEIN LOC502894
1394889_AT	*LOC503215*	SIMILAR TO DEATH-ASSOCIATED PROTEIN KINASE 3 (DAP KINASE 3) (DAP-LIKE KINASE)
1387905_AT	*LOC619393*	JUN DIMERIZATION PROTEIN 1
1373830_AT	*LOC619574*	HYPOTHETICAL PROTEIN LOC619574
1375527_AT	*LOC65027*	BETA-CATENIN BINDING PROTEIN
1367952_AT	*LRP2*	LOW DENSITY LIPOPROTEIN RECEPTOR-RELATED PROTEIN 2
1371683_AT	*LSM4_PREDICTED*	LSM4 HOMOLOG, U6 SMALL NUCLEAR RNA ASSOCIATED (S. CEREVISIAE) (PREDICTED)
1367912_AT	*LTBP1*	LATENT TRANSFORMING GROWTH FACTOR BETA BINDING PROTEIN 1
1371500_AT	*LTBP4*	LATENT TRANSFORMING GROWTH FACTOR BETA BINDING PROTEIN 4
1369949_AT	*LU*	LUTHERAN BLOOD GROUP (AUBERGER B ANTIGEN INCLUDED)
1387003_AT	*LUZP1*	LEUCINE ZIPPER PROTEIN 1
1367768_AT	*LXN*	LATEXIN
1368679_A_AT	*LYN*	YAMAGUCHI SARCOMA VIRAL (V-YES-1) ONCOGENE HOMOLOG
1376184_AT	*LYNX1_PREDICTED*	LY6/NEUROTOXIN 1 (PREDICTED)
1376951_AT	*MAD2L1_PREDICTED*	MAD2 (MITOTIC ARREST DEFICIENT, HOMOLOG)-LIKE 1 (YEAST) (PREDICTED)
1387040_AT	*MAL*	MYELIN AND LYMPHOCYTE PROTEIN
1393053_AT	*MAN1C1_PREDICTED*	MANNOSIDASE, ALPHA, CLASS 1C, MEMBER 1 (PREDICTED)
1377621_AT	*MAP2K4*	MITOGEN ACTIVATED PROTEIN KINASE KINASE 4
1390372_AT	*MAP3K12*	MITOGEN ACTIVATED PROTEIN KINASE KINASE KINASE 12
1399075_AT	*MAP3K7_PREDICTED*	MITOGEN ACTIVATED PROTEIN KINASE KINASE KINASE 7 (PREDICTED)
1373719_AT	*MAP4K3*	MITOGEN-ACTIVATED PROTEIN KINASE KINASE KINASE KINASE 3
1376568_AT	*MAP4K4_PREDICTED*	MITOGEN-ACTIVATED PROTEIN KINASE KINASE KINASE KINASE 4 (PREDICTED)
1398297_AT	*MAPK12*	MITOGEN-ACTIVATED PROTEIN KINASE 12
1377007_AT	*MAPKAP1*	MITOGEN-ACTIVATED PROTEIN KINASE ASSOCIATED PROTEIN 1
1371446_AT	*MAPKAPK2*	MAP KINASE-ACTIVATED PROTEIN KINASE 2
1375525_AT	*MAPRE1*	MICROTUBULE-ASSOCIATED PROTEIN, RP/EB FAMILY, MEMBER 1
1387071_A_AT	*MAPT*	MICROTUBULE-ASSOCIATED PROTEIN TAU
1371031_AT	*MAT1A*	METHIONINE ADENOSYLTRANSFERASE I, ALPHA
1368151_AT	*MATR3*	MATRIN 3
1372406_AT	*MCM3_PREDICTED*	MINICHROMOSOME MAINTENANCE DEFICIENT 3 (S. CEREVISIAE) (PREDICTED)
1373557_AT	*MCM4*	MINICHROMOSOME MAINTENANCE DEFICIENT 4 HOMOLOG (S. CEREVISIAE)
1375382_AT	*MDC1*	MEDIATOR OF DNA DAMAGE CHECKPOINT 1
1398427_AT	*MEF2D*	MYOCYTE ENHANCER FACTOR 2D
1384308_AT	*MEIS1_PREDICTED*	MEIS1, MYELOID ECOTROPIC VIRAL INTEGRATION SITE 1 HOMOLOG (PREDICTED)
1399137_AT	*METAP1_PREDICTED*	METHIONYL AMINOPEPTIDASE 1 (PREDICTED)
1375035_AT	*MFN1*	MITOFUSIN 1

1367796_AT	*MGAT1*	ALPHA-1,3-MANNOSYL-GLYCOPROTEIN 2-BETA-N-ACETYLGLUCOSAMINYLTRANSFERASE
1369201_AT	*MGAT3*	MANNOSIDE ACETYL GLUCOSAMINYLTRANSFERASE 3
1392547_AT	*MGC105649*	HYPOTHETICAL LOC302884
1390944_AT	*MGC108776*	SNF7 HOMOLOGUE ASSOCIATED WITH ALIX 3
1398924_AT	*MGC109145*	SIMILAR TO MANNOSIDASE, BETA A, LYSOSOMAL-LIKE
1382113_AT	*MGC72612*	SIMILAR TO EXPRESSED SEQUENCE AI449175
1383623_AT	*MGC72984*	THYMOCYTE PROTEIN THY28
1383635_AT	*MGC93714*	SIMILAR TO RIKEN CDNA 1210002B07
1394491_AT	*MGC93975*	SIMILAR TO 2310044H10RIK PROTEIN
1371919_AT	*MGC94056*	SIMILAR TO RP2 PROTEIN, TESTOSTERONE-REGULATED - RICEFIELD MOUSE (MUS CAROLI)
1381591_AT	*MGC94145*	SIMILAR TO CDNA SEQUENCE BC026682
1371705_AT	*MGC94168*	SIMILAR TO VACUOLAR PROTEIN SORTING 26; VACUOLE PROTEIN SORTING 26; H BETA 58
1374509_AT	*MGC94226*	SIMILAR TO RIKEN CDNA 1110018O08
1390419_A_AT	*MGC94243*	SIMILAR TO N33 PROTEIN
1389407_AT	*MGC94370*	DEHYDROGENASE/REDUCTASE (SDR FAMILY) MEMBER 1
1390407_AT	*MGC94479*	SIMILAR TO PROTEIN C3ORF4 HOMOLOG
1374644_AT	*MGC94555*	INTIMAL THICKNESS-RELATED RECEPTOR
1372498_AT	*MGC94686*	SIMILAR TO RIKEN CDNA 2810413N20
1376106_AT	*MGC94782*	SIMILAR TO HYPOTHETICAL PROTEIN MGC33926
1373070_AT	*MGC94941*	SIMILAR TO MKRN1 PROTEIN
1397758_AT	*MGC95241*	SIMILAR TO CHOLINE PHOSPHOTRANSFERASE 1;
1398969_AT	*MGEA5*	MENINGIOMA EXPRESSED ANTIGEN 5 (HYALURONIDASE)
1368311_AT	*MGMT*	O-6-METHYLGUANINE-DNA METHYLTRANSFERASE
1386075_AT	*MINA*	MYC INDUCED NUCLEAR ANTIGEN
1398296_AT	*MIR16*	MEMBRANE INTERACTING PROTEIN OF RGS16
1374775_AT	*MKI67_PREDICTED*	ANTIGEN IDENTIFIED BY MONOCLONAL ANTIBODY KI-67 (PREDICTED)
1374618_AT	*MLLT2_PREDICTED*	MYELOID/LYMPHOID OR MIXED-LINEAGE LEUKEMIA
1385953_AT	*MLLT3*	MYELOID/LYMPHOID OR MIXED-LINEAGE LEUKEMIA,TRANSLOCATED TO, 3
1368595_AT	*MMP24*	MATRIX METALLOPEPTIDASE 24
1375966_AT	*MMRN2_PREDICTED*	MULTIMERIN 2 (PREDICTED)
1395604_AT	*MMS19L*	MMS19-LIKE (MET18 HOMOLOG, S. CEREVISIAE)
1385702_AT	*MNDA*	MYELOID CELL NUCLEAR DIFFERENTIATION ANTIGEN
1375929_AT	*MNT_PREDICTED*	MAX BINDING PROTEIN (PREDICTED)
1397949_AT	*MPP6_PREDICTED*	MEMBRANE PROTEIN, PALMITOYLATED 6 (MAGUK P55 SUBFAMILY MEMBER 6) (PREDICTED)
1382659_AT	*MRC2_PREDICTED*	MANNOSE RECEPTOR, C TYPE 2 (PREDICTED)
1369980_S_AT	*MRIP*	MYOSIN PHOSPHATASE-RHO INTERACTING PROTEIN
1386996_AT	*MRLCB*	MYOSIN LIGHT CHAIN, REGULATORY B
1382811_AT	*MRPL16*	MITOCHONDRIAL RIBOSOMAL PROTEIN L16
1371604_AT	*MRPL34*	MITOCHONDRIAL RIBOSOMAL PROTEIN L34
1371553_AT	*MRPL36_PREDICTED*	MITOCHONDRIAL RIBOSOMAL PROTEIN L36 (PREDICTED)
1388654_AT	*MRPL52_PREDICTED*	MITOCHONDRIAL RIBOSOMAL PROTEIN L52 (PREDICTED)
1377937_AT	*MRPS14_PREDICTED*	MITOCHONDRIAL RIBOSOMAL PROTEIN S14 (PREDICTED)
1396227_AT	*MRRF*	MITOCHONDRIAL RIBOSOME RECYCLING FACTOR
1381201_AT	*MRVLDC2_PREDICTED*	MARVEL (MEMBRANE-ASSOCIATING) DOMAIN CONTAINING 2 (PREDICTED)
1368441_AT	*MSLN*	MESOTHELIN
1388549_AT	*MSMB*	BETA-MICROSEMINOPROTEIN
1371237_A_AT	*MT1A*	METALLOTHIONEIN 1A
1368345_AT	*MTAP6*	MICROTUBULE-ASSOCIATED PROTEIN 6
1392916_AT	*MTAP7_PREDICTED*	MICROTUBULE-ASSOCIATED PROTEIN 7 (PREDICTED)
1372566_AT	*MTCH2_PREDICTED*	MITOCHONDRIAL CARRIER HOMOLOG 2 (C. ELEGANS) (PREDICTED)
1374214_AT	*MTDH*	METADHERIN
1368181_AT	*MTHFD1*	METHYLENETETRAHYDROFOLATE DEHYDROGENASE (NADP+ DEPENDENT), METHENYLTETRAHYDROFOLATE CYCLOHYDROLASE, FORMYLTETRAHYDROFOLATE SYNTHASE
1390878_AT	*MUC1*	MUCIN 1, TRANSMEMBRANE
1372580_AT	*MYBPC3_PREDICTED*	MYOSIN BINDING PROTEIN C, CARDIAC (PREDICTED)
1368308_AT	*MYC*	MYELOCYTOMATOSIS VIRAL ONCOGENE HOMOLOG (AVIAN)
1384264_AT	*MYH14*	MYOSIN, HEAVY POLYPEPTIDE 14
1371508_AT	*MYH4_PREDICTED*	CATENIN (CADHERIN-ASSOCIATED PROTEIN), BETA 1 (88KD)
1370933_AT	*MYO1E*	MYOSIN IE
1368355_AT	*MYO5B*	MYOSIN 5B
1391701_AT	*MYST3*	MYST HISTONE ACETYLTRANSFERASE (MONOCYTIC LEUKEMIA) 3
1374925_AT	*NAB2*	NGFI-A BINDING PROTEIN 2
1371872_AT	*NAP1L1*	NUCLEOSOME ASSEMBLY PROTEIN 1-LIKE 1
1374075_AT	*NAPG*	N-ETHYLMALEIMIDE-SENSITIVE FACTOR ATTACHMENT PROTEIN, GAMMA
1378264_AT	*NASP*	NUCLEAR AUTOANTIGENIC SPERM PROTEIN
1378175_AT	*NAT5_PREDICTED*	N-ACETYLTRANSFERASE 5 (ARD1 HOMOLOG, S. CEREVISIAE) (PREDICTED)
1381986_AT	*NAV1_PREDICTED*	NEURON NAVIGATOR 1 (PREDICTED)
1387004_AT	*NBL1*	NEUROBLASTOMA, SUPPRESSION OF TUMORIGENICITY 1
1387977_AT	*NBN*	NIBRIN
1378191_AT	*NCBP1*	NUCLEAR CAP BINDING PROTEIN SUBUNIT 1, 80KDA
1367956_AT	*NCDN*	NEUROCHONDRIN
1371407_AT	*NCKAP1*	NCK-ASSOCIATED PROTEIN 1
1382126_AT	*NCOR1*	NUCLEAR RECEPTOR CO-REPRESSOR 1
1370229_AT	*NDR4*	N-MYC DOWNSTREAM REGULATED 4
1376590_AT	*NDUFA5*	NADH DEHYDROGENASE (UBIQUINONE) 1 ALPHA SUBCOMPLEX 5
1395045_AT	*NDUFA7_PREDICTED*	NADH DEHYDROGENASE (UBIQUINONE) 1 ALPHA SUBCOMPLEX, 7 (B14.5A) (PREDICTED)
1389507_AT	*NEDD4L*	NEURAL PRECURSOR CELL EXPRESSED, DEVELOPMENTALLY DOWN-REGULATED 4-LIKE
1370815_AT	*NEFH*	NEUROFILAMENT, HEAVY POLYPEPTIDE
1372000_AT	*NET1*	NEUROEPITHELIAL CELL TRANSFORMING GENE 1
1378543_AT	*NFE2L3_PREDICTED*	NUCLEAR FACTOR, ERYTHROID DERIVED 2, LIKE 3 (PREDICTED)
1368488_AT	*NFIL3*	NUCLEAR FACTOR, INTERLEUKIN 3 REGULATED
1389538_AT	*NFKBIA*	NUCLEAR FACTOR OF KAPPA LIGHT CHAIN GENE ENHANCER IN B-CELLS INHIBITOR, ALPHA
1378637_AT	*NFX1*	NUCLEAR TRANSCRIPTION FACTOR, X-BOX BINDING 1
1382082_AT	*NFYB*	NUCLEAR TRANSCRIPTION FACTOR-Y BETA
1374098_AT	*NG3*	NG3 PROTEIN
1377091_AT	*NG5*	NG5 PROTEIN
1382214_AT	*NHLRC2_PREDICTED*	NHL REPEAT CONTAINING 2 (PREDICTED)
1388618_AT	*NID2*	NIDOGEN 2
1370408_AT	*NID67*	PUTATIVE SMALL MEMBRANE PROTEIN NID67

1384242_AT	*NLN*	NEUROLYSIN (METALLOPEPTIDASE M3 FAMILY)
1392473_AT	*NMT2*	N-MYRISTOYLTRANSFERASE 2
1368031_AT	*NOLC1*	NUCLEOLAR AND COILED-BODY PHOSPHOPROTEIN 1
1387311_AT	*NOX1*	NADPH OXIDASE 1
1396192_AT	*NPAT_PREDICTED*	NUCLEAR PROTEIN IN THE AT REGION (PREDICTED)
1398756_AT	*NPM1*	NUCLEOPHOSMIN 1
1367616_AT	*NPPB*	NATRIURETIC PEPTIDE PRECURSOR TYPE B
1370517_AT	*NPTX1*	NEURONAL PENTRAXIN 1
1370816_AT	*NR1D1*	NUCLEAR RECEPTOR SUBFAMILY 1, GROUP D, MEMBER 1
1398826_S_AT	*NR2F6*	NUCLEAR RECEPTOR SUBFAMILY 2, GROUP F, MEMBER 6
1372032_AT	*NRAS*	NEUROBLASTOMA RAS ONCOGENE
1371069_AT	*NRITP*	ION TRANSPORTER PROTEIN
1391413_AT	*NT5C2_PREDICTED*	5'-NUCLEOTIDASE, CYTOSOLIC II (PREDICTED)
1376112_A_AT	*NTF2*	NUCLEAR TRANSPORT FACTOR 2
1370180_AT	*NUDT4*	NUDIX (NUCLEOSIDE DIPHOSPHATE LINKED MOIETY X)-TYPE MOTIF 4
1375536_AT	*NUMB*	NUMB GENE HOMOLOG (DROSOPHILA)
1370934_AT	*NUP153*	NUCLEOPORIN 153KD
1393277_AT	*NUP155*	NUCLEOPORIN 155
1372519_AT	*NUP93*	NUCLEOPORIN 93
1367847_AT	*NUPR1*	NUCLEAR PROTEIN 1
1371908_AT	*NXT1_PREDICTED*	NTF2-RELATED EXPORT PROTEIN 1 (PREDICTED)
1370191_AT	*OAZIN*	ORNITHINE DECARBOXYLASE ANTIZYME INHIBITOR
1370163_AT	*ODC1*	ORNITHINE DECARBOXYLASE 1
1368496_AT	*ODF1*	OUTER DENSE FIBER OF SPERM TAILS 1
1397492_AT	*OLR1733_PREDICTED*	OLFACTORY RECEPTOR 1733 (PREDICTED)
1388432_AT	*OPTN*	OPTINEURIN
1385522_AT	*ORC1L*	ORIGIN RECOGNITION COMPLEX, SUBUNIT 1-LIKE (S.CEREVIAIAE)
1378010_AT	*ORC4*	ORIGIN RECOGNITION COMPLEX, SUBUNIT 4
1367519_AT	*OSBPL2*	OXYSTEROL BINDING PROTEIN-LIKE 2
1393368_AT	*OSBPL5*	OXYSTEROL BINDING PROTEIN-LIKE 5
1378002_AT	*OSP94_PREDICTED*	OSMOTIC STRESS PROTEIN 94 KDA (PREDICTED)
1380133_AT	*OSR2*	ODD-SKIPPED RELATED 2 (DROSOPHILA)
1370606_AT	*P2RY1*	PURINERGIC RECEPTOR P2Y, G-PROTEIN COUPLED 1
1372610_AT	*P4HA2_PREDICTED*	PROCOLLAGEN-PROLINE, 2-OXOGLUTARATE 4-DIOXYGENASE (PROLINE 4-HYDROXYLASE),
1372857_AT	*PACSIN2*	PROTEIN KINASE C AND CASEIN KINASE SUBSTRATE IN NEURONS 2
1379335_AT	*PAIP1_PREDICTED*	POLYADENYLATE BINDING PROTEIN-INTERACTING PROTEIN 1 (PREDICTED)
1389153_AT	*PAIRBP1*	PAI-1 MRNA-BINDING PROTEIN
1393184_AT	*PAK2*	P21 (CDKN1A)-ACTIVATED KINASE 2
1378380_AT	*PAK4_PREDICTED*	P21 (CDKN1A)-ACTIVATED KINASE 4 (PREDICTED)
1367687_A_AT	*PAM*	PEPTIDYLGLYCINE ALPHA-AMIDATING MONOOXYGENASE
1387581_AT	*PAMCI*	PEPTIDYLGLYCINE ALPHA-AMIDATING MONOOXYGENASE COOH-TERMINAL INTERACTOR
1374753_AT	*PAPD4*	PAP ASSOCIATED DOMAIN CONTAINING 4
1374612_AT	*PAPD5_PREDICTED*	PAP ASSOCIATED DOMAIN CONTAINING 5 (PREDICTED)
1380101_AT	*PAPOLG_PREDICTED*	POLY(A) POLYMERASE GAMMA (PREDICTED)
1392927_AT	*PAQR4*	PROGESTIN AND ADIPOQ RECEPTOR FAMILY MEMBER IV
1373642_AT	*PAQR6_PREDICTED*	PROGESTIN AND ADIPOQ RECEPTOR FAMILY MEMBER VI (PREDICTED)
1383224_AT	*PARD6B_PREDICTED*	PAR-6 (PARTITIONING DEFECTIVE 6) HOMOLOG BETA (C. ELEGANS) (PREDICTED)
1370354_AT	*PARG*	POLY (ADP-RIBOSE) GLYCOHYDROLASE
1368702_AT	*PAWR*	PRKC, APOPTOSIS, WT1, REGULATOR
1374503_AT	*PBX3_PREDICTED*	PRE B-CELL LEUKEMIA TRANSCRIPTION FACTOR 3 (PREDICTED)
1374266_AT	*PCDH1_PREDICTED*	PROTOCADHERIN 1 (CADHERIN-LIKE 1) (PREDICTED)
1367888_AT	*PCDH21*	MT-PROTOCADHERIN
1371966_AT	*PCMT1*	PROTEIN-L-ISOASPARTATE (D-ASPARTATE) O-METHYLTRANSFERASE 1
1390650_AT	*PCNT1*	PERICENTRIN 1
1379047_AT	*PDAP1*	PDGFA ASSOCIATED PROTEIN 1
1375367_AT	*PDLIM2*	PDZ AND LIM DOMAIN 2
1380045_AT	*PDP2*	PYRUVATE DEHYDROGENASE PHOSPHATASE ISOENZYME 2
1373748_AT	*PDZRN3_PREDICTED*	PDZ DOMAIN CONTAINING RING FINGER 3 (PREDICTED)
1390814_AT	*PELI1*	PELLINO HOMOLOG 1 (DROSOPHILA)
1368303_AT	*PER2*	PERIOD HOMOLOG 2 (DROSOPHILA)
1372294_AT	*PERC64*	PE RESPONSIVE PROTEIN C64
1368526_AT	*PEX3*	PEROXISOMAL BIOGENESIS FACTOR 3
1389654_AT	*PGEA1*	PKD2 INTERACTOR, GOLGI AND ENDOPLASMIC RETICULUM ASSOCIATED 1
1373769_AT	*PGM1_PREDICTED*	PHOSPHOGLUCOMUTASE 1 (PREDICTED)
1388180_AT	*PHAX*	PHOSPHORYLATED ADAPTOR FOR RNA EXPORT
1389201_AT	*PHF10*	PHD FINGER PROTEIN 10
1386974_AT	*PHLDB1*	PLECKSTRIN HOMOLOGY-LIKE DOMAIN, FAMILY B, MEMBER 1
1372863_AT	*PHR1_PREDICTED*	PAM, HIGHWIRE, RPM 1 (PREDICTED)
1369042_AT	*PIGM*	PHOSPHATIDYLINOSITOL GLYCAN, CLASS M
1387847_AT	*PIK3CB*	PHOSPHATIDYLINOSITOL 3-KINASE, CATALYTIC, BETA POLYPEPTIDE
1373528_AT	*PIK3CD_PREDICTED*	PHOSPHATIDYLINOSITOL 3-KINASE CATALYTIC DELTA POLYPEPTIDE (PREDICTED)
1370318_AT	*PIK4CA*	PHOSPHATIDYLINOSITOL 4-KINASE, CATALYTIC, ALPHA POLYPEPTIDE
1374429_AT	*PIM1*	PROVIRAL INTEGRATION SITE 1
1392560_AT	*PIP5K1B_PREDICTED*	PHOSPHATIDYLINOSITOL-4-PHOSPHATE 5-KINASE, TYPE 1 BETA (PREDICTED)
1372861_AT	*PIP5K1C*	PHOSPHATIDYLINOSITOL-4-PHOSPHATE 5-KINASE, TYPE I, GAMMA
1373082_AT	*PKIA*	PROTEIN KINASE INHIBITOR, ALPHA
1385182_AT	*PKP1_PREDICTED*	PLAKOPHILIN 1 (PREDICTED)
1388539_AT	*PKP2*	PLAKOPHILIN 2
1381056_AT	*PKP3_PREDICTED*	PLAKOPHILIN 3 (PREDICTED)
1373091_AT	*PLAGL2_PREDICTED*	PLEIOMORPHIC ADENOMA GENE-LIKE 2 (PREDICTED)
1367800_AT	*PLAT*	PLASMINOGEN ACTIVATOR, TISSUE
1389628_AT	*PLCD3_PREDICTED*	PHOSPHOLIPASE C, DELTA 3 (PREDICTED)
1368700_AT	*PLCL1*	PHOSPHOLIPASE C-LIKE 1
1383286_AT	*PLEK2_PREDICTED*	PLECKSTRIN 2 (PREDICTED)
1398327_AT	*PLEKHC1*	PLECKSTRIN HOMOLOGY DOMAIN CONTAINING, FAMILY C (WITH FERM DOMAIN) MEMBER 1
1372824_AT	*PLEKHF2_PREDICTED*	PLECKSTRIN HOMOLOGY DOMAIN CONTAINING, FAMILY F (WITH FYVE DOMAIN) MEMBER 2
1368106_AT	*PLK2*	POLO-LIKE KINASE 2 (DROSOPHILA)
1369029_AT	*PLSCR1*	PHOSPHOLIPID SCRAMBLASE 1
1371411_AT	*PLXNB2*	PLEXIN B2
1376312_A_AT	*PNAS-4*	CGI-146 PROTEIN

1370381_AT	*PNRC1*	PROLINE RICH 2
1387795_AT	*POLA2*	POLYMERASE (DNA DIRECTED), ALPHA 2
1387142_AT	*POLB*	POLYMERASE (DNA DIRECTED), BETA
1388808_AT	*POLR2A_MAPPED*	POLYMERASE (RNA) II (DNA DIRECTED) POLYPEPTIDE A (MAPPED)
1398899_AT	*POLR2C*	POLYMERASE (RNA) II (DNA DIRECTED) POLYPEPTIDE C
1379832_AT	*POLR2D_PREDICTED*	POLYMERASE (RNA) II (DNA DIRECTED) POLYPEPTIDE D (PREDICTED)
1367471_AT	*POLR2E_PREDICTED*	POLYMERASE (RNA) II (DNA DIRECTED) POLYPEPTIDE E (PREDICTED)
1367919_AT	*POM210*	NUCLEAR PORE MEMBRANE GLYCOPROTEIN 210
1375848_AT	*PON2*	PARAOXONASE 2
1373083_AT	*PPAPDC2*	PHOSPHATIDIC ACID PHOSPHATASE TYPE 2 DOMAIN CONTAINING 2
1369785_AT	*PPAT*	PHOSPHORIBOSYL PYROPHOSPHATE AMIDOTRANSFERASE
1373444_AT	*PPFIA1_PREDICTED*	PROTEIN TYROSINE PHOSPHATASE, RECEPTOR TYPE, F POLYPEPTIDE (PTPRF)
1372531_AT	*PPFIBP2*	PROTEIN TYROSINE PHOSPHATASE, RECEPTOR-TYPE, F INTERACTING PROTEIN
1370319_AT	*PPIF*	PEPTIDYLPROLYL ISOMERASE F (CYCLOPHILIN F)
1387229_AT	*PPIG*	PEPTIDYLPROLYL ISOMERASE G
1372517_AT	*PPIL1*	PEPTIDYLPROLYL ISOMERASE (CYCLOPHILIN)-LIKE 1
1391187_AT	*PPL_PREDICTED*	PERIPLAKIN (PREDICTED)
1383475_AT	*PPM1A*	PROTEIN PHOSPHATASE 1A, MAGNESIUM DEPENDENT, ALPHA ISOFORM
1371136_AT	*PPM1B*	PROTEIN PHOSPHATASE 1B, MAGNESIUM DEPENDENT, BETA ISOFORM
1374884_AT	*PPM1D_PREDICTED*	PROTEIN PHOSPHATASE 1D MAGNESIUM-DEPENDENT, DELTA ISOFORM (PREDICTED)
1376060_AT	*PPM1H*	PROTEIN PHOSPHATASE 1H (PP2C DOMAIN CONTAINING)
1390990_AT	*PPP1CB*	PROTEIN PHOSPHATASE 1, CATALYTIC SUBUNIT, BETA ISOFORM
1386971_AT	*PPP1R10*	PROTEIN PHOSPHATASE 1, REGULATORY SUBUNIT 10
1376662_AT	*PPP1R12A*	PROTEIN PHOSPHATASE 1, REGULATORY (INHIBITOR) SUBUNIT 12A
1373301_AT	*PPP1R13B_PREDICTED*	PROTEIN PHOSPHATASE 1, REGULATORY (INHIBITOR) SUBUNIT 13B (PREDICTED)
1372446_AT	*PPP1R2*	PROTEIN PHOSPHATASE 1, REGULATORY (INHIBITOR) SUBUNIT 2
1376728_AT	*PPP1R8_PREDICTED*	PROTEIN PHOSPHATASE 1, REGULATORY (INHIBITOR) SUBUNIT 8 (PREDICTED)
1367827_AT	*PPP2CB*	PROTEIN PHOSPHATASE 2A, CATALYTIC SUBUNIT, BETA ISOFORM
1369297_AT	*PPP2R2C*	PROTEIN PHOSPHATASE 2 (FORMERLY 2A), REGULATORY SUBUNIT B (PR 52), GAMMA ISOFORM
1373384_AT	*PPP2R5C_PREDICTED*	PROTEIN PHOSPHATASE 2, REGULATORY SUBUNIT B (B56), GAMMA ISOFORM (PREDICTED)
1379314_AT	*PPP3CB*	PROTEIN PHOSPHATASE 3, CATALYTIC SUBUNIT, BETA ISOFORM
1388103_AT	*PR1*	PROTEIN DISTANTLY RELATED TO TO THE GAMMA SUBUNIT FAMILY
1392899_AT	*PRC1_PREDICTED*	PROTEIN REGULATOR OF CYTOKINESIS 1 (PREDICTED)
1390202_AT	*PRDM2_MAPPED*	PR DOMAIN CONTAINING 2, WITH ZNF DOMAIN (MAPPED)
1388182_AT	*PRIM1*	DNA PRIMASE, P49 SUBUNIT
1386945_A_AT	*PRKAB1*	PROTEIN KINASE, AMP-ACTIVATED, BETA 1 NON-CATALYTIC SUBUNIT
1389463_AT	*PRKAR1B*	PROTEIN KINASE, CAMP DEPENDENT REGULATORY, TYPE I, BETA
1372176_AT	*PRKCA*	PROTEIN KINASE C, ALPHA
1368169_AT	*PRKCABP*	PROTEIN KINASE C, ALPHA BINDING PROTEIN
1374466_AT	*PRKCE*	PROTEIN KINASE C, EPSILON
1379912_AT	*PRKCM*	PROTEIN KINASE C, MU
1370197_A_AT	*PRKCZ*	PROTEIN KINASE C, ZETA
1389662_AT	*PRKWNK4*	PROTEIN KINASE, LYSINE DEFICIENT 4
1398867_AT	*PRP19*	NEURONAL DIFFERENTIATION-RELATED GENE
1384329_AT	*PRSS22_PREDICTED*	PROTEASE, SERINE, 22 (PREDICTED)
1373152_AT	*PRSS23*	PROTEASE, SERINE, 23
1370064_AT	*PSEN2*	PRESENILIN 2
1394047_AT	*PSG4*	PREGNANCY SPECIFIC BETA-1-GLYCOPROTEIN 4
1373350_AT	*PSIP1*	PC4 AND SFRS1 INTERACTING PROTEIN 1
1368508_AT	*PSMA3*	PROTEASOME (PROSOME, MACROPAIN) SUBUNIT, ALPHA TYPE 3
1368508_AT	*PSMA3L*	PROTEASOME (PROSOME, MACROPAIN) SUBUNIT, ALPHA TYPE 3
1376069_AT	*PSMD11_PREDICTED*	PROTEASOME (PROSOME, MACROPAIN) 26S SUBUNIT, NON-ATPASE, 11 (PREDICTED)
1392983_AT	*PSMD12*	PROTEASOME 26S NON-ATPASE SUBUNIT 12
1367663_AT	*PSME1*	PROTEASE (PROSOME, MACROPAIN) 28 SUBUNIT, ALPHA
1368818_AT	*PSME4*	PROTEASOME (PROSOME, MACROPAIN) ACTIVATOR SUBUNIT 4
1384465_AT	*PSPC1*	PARASPECKLE PROTEIN 1
1370445_AT	*PSPLA1*	PHOSPHATIDYLSERINE-SPECIFIC PHOSPHOLIPASE A1
1393638_AT	*PTGER4*	PROSTAGLANDIN E RECEPTOR 4 (SUBTYPE EP4)
1367986_AT	*PTGFRN*	PROSTAGLANDIN F2 RECEPTOR NEGATIVE REGULATOR
1369688_S_AT	*PTK2B*	PROTEIN TYROSINE KINASE 2 BETA
1369496_AT	*PTPN12*	PROTEIN TYROSINE PHOSPHATASE, NON-RECEPTOR TYPE 12
1373065_AT	*PTPN18*	PROTEIN TYROSINE PHOSPHATASE, NON-RECEPTOR TYPE 18
1371261_AT	*PTPN2*	PROTEIN TYROSINE PHOSPHATASE, NON-RECEPTOR TYPE 2
1368087_A_AT	*PTPN21*	PROTEIN TYROSINE PHOSPHATASE 2E
1368010_AT	*PTPN6*	PROTEIN TYROSINE PHOSPHATASE, NON-RECEPTOR TYPE 6
1391669_AT	*PTPRB_PREDICTED*	PROTEIN TYROSINE PHOSPHATASE, RECEPTOR TYPE, B (PREDICTED)
1373419_AT	*PTPRG*	PROTEIN TYROSINE PHOSPHATASE, RECEPTOR TYPE, G
1383017_AT	*PTPRM*	PROTEIN TYROSINE PHOSPHATASE, RECEPTOR TYPE, M
1368358_A_AT	*PTPRR*	PROTEIN TYROSINE PHOSPHATASE, RECEPTOR TYPE, R
1370177_AT	*PVR*	POLIOVIRUS RECEPTOR
1368674_AT	*PYGL*	LIVER GLYCOGEN PHOSPHORYLASE
1373022_AT	*RAB1*	RAB1, MEMBER RAS ONCOGENE FAMILY
1375338_AT	*RAB10*	RAB10, MEMBER RAS ONCOGENE FAMILY
1374069_AT	*RAB11A*	RAB11A, MEMBER RAS ONCOGENE FAMILY
1398825_AT	*RAB11B*	RAB11B, MEMBER RAS ONCOGENE FAMILY
1373646_AT	*RAB15*	RAB15, MEMBER RAS ONOCOGENE FAMILY
1392681_AT	*RAB2*	RAB2, MEMBER RAS ONCOGENE FAMILY
1389331_AT	*RAB21*	RAB21, MEMBER RAS ONCOGENE FAMILY
1376029_AT	*RAB2L*	RAB2, MEMBER RAS ONCOGENE FAMILY-LIKE
1387821_AT	*RAB3IP*	RAB3A INTERACTING PROTEIN
1370001_AT	*RAB8A*	RAB8A, MEMBER RAS ONCOGENE FAMILY
1373658_AT	*RACGAP1_PREDICTED*	RAC GTPASE-ACTIVATING PROTEIN 1 (PREDICTED)
1397642_AT	*RAD50*	RAD50 HOMOLOG (S. CEREVISIAE)
1376828_AT	*RAI3*	RETINOIC ACID INDUCED 3
1387001_AT	*RALB*	V-RAL SIMIAN LEUKEMIA VIRAL ONCOGENE HOMOLOG B
1368217_AT	*RALBP1*	RALA BINDING PROTEIN 1
1388363_AT	*RALY*	HNRNP-ASSOCIATED WITH LETHAL YELLOW
1367701_AT	*RAMP2*	RECEPTOR (CALCITONIN) ACTIVITY MODIFYING PROTEIN 2
1389279_AT	*RAN*	RAN, MEMBER RAS ONCOGENE FAMILY
1373933_AT	*RAPGEF2_PREDICTED*	RAP GUANINE NUCLEOTIDE EXCHANGE FACTOR (GEF) 2 (PREDICTED)

1389181_AT	*RAPGEF6_PREDICTED*	RAP GUANINE NUCLEOTIDE EXCHANGE FACTOR (GEF) 6 (PREDICTED)
1370415_AT	*RASSF5*	RAS ASSOCIATION (RALGDS/AF-6) DOMAIN FAMILY 5
1379449_AT	*RB1CC1_PREDICTED*	RB1-INDUCIBLE COILED-COIL 1 (PREDICTED)
1369896_S_AT	*RBM16*	RNA BINDING MOTIF PROTEIN 16
1388751_AT	*RBM24_PREDICTED*	RNA BINDING MOTIF PROTEIN 24 (PREDICTED)
1388886_AT	*RBM25_PREDICTED*	RNA BINDING MOTIF PROTEIN 25 (PREDICTED)
1389981_AT	*RBM27_PREDICTED*	RNA BINDING MOTIF PROTEIN 27 (PREDICTED)
1384751_AT	*RBM8_PREDICTED*	RNA BINDING MOTIF PROTEIN 8 (PREDICTED)
1388538_AT	*RBX1*	RING-BOX 1
1384391_AT	*RDH10*	RETINOL DEHYDROGENASE 10 (ALL-TRANS)
1389304_AT	*REST*	RE1-SILENCING TRANSCRIPTION FACTOR
1385504_AT	*RFFL*	FRING
1374936_AT	*RGD1304601*	SIMILAR TO RIKEN CDNA 5730457F11
1389107_AT	*RGD1304623_PREDICTED*	SIMILAR TO KIAA1749 PROTEIN (PREDICTED)
1380243_AT	*RGD1304693_PREDICTED*	SIMILAR TO CG14803-PA (PREDICTED)
1367510_AT	*RGD1304696*	SIMILAR TO HYPOTHETICAL PROTEIN FLJ22625
1373903_AT	*RGD1304715_PREDICTED*	SIMILAR TO HYPOTHETICAL PROTEIN MGC32399 (PREDICTED)
1382945_AT	*RGD1304748*	SIMILAR TO CDNA SEQUENCE BC006662
1390403_AT	*RGD1304790*	SIMILAR TO CG8312-PA
1394468_AT	*RGD1304792_PREDICTED*	SIMILAR TO CHROMOSOME 2 OPEN READING FRAME 3; TRANSCRIPTION FACTOR 9
1390526_AT	*RGD1304814_PREDICTED*	SIMILAR TO HYPOTHETICAL PROTEIN KIAA1354 (PREDICTED)
1376260_AT	*RGD1304822_PREDICTED*	SIMILAR TO KIAA1627 PROTEIN (PREDICTED)
1390387_AT	*RGD1304885_PREDICTED*	SIMILAR TO SH3 DOMAIN PROTEIN D19 (PREDICTED)
1377899_AT	*RGD1304982_PREDICTED*	SIMILAR TO RIKEN CDNA 2810025M15 (PREDICTED)
1373447_AT	*RGD1305117*	SIMILAR TO HN1-LIKE PROTEIN
1367518_AT	*RGD1305121_PREDICTED*	SIMILAR TO FATSO (PREDICTED)
1374159_AT	*RGD1305208_PREDICTED*	SIMILAR TO RN49018 (PREDICTED)
1388987_AT	*RGD1305215*	SIMILAR TO EXPRESSED SEQUENCE AA960436
1393394_AT	*RGD1305240_PREDICTED*	SIMILAR TO PM5 PROTEIN; DNA SEGMENT, CHR 7, ERATO DOI 156, EXPRESSED (PREDICTED)
1383308_A_AT	*RGD1305243_PREDICTED*	SIMILAR TO HYPOTHETICAL PROTEIN FLJ34389 (PREDICTED)
1371730_AT	*RGD1305466*	SIMILAR TO RIKEN CDNA 1300002A08
1398385_AT	*RGD1305475_PREDICTED*	SIMILAR TO RIKEN CDNA 1500006O09 (PREDICTED)
1373870_AT	*RGD1305486*	SIMILAR TO RIKEN CDNA 2810405J04
1375563_AT	*RGD1305506_PREDICTED*	SIMILAR TO DENDRITIC CELL-DERIVED UBIQUITIN-LIKE PROTEIN (PREDICTED)
1389782_AT	*RGD1305587_PREDICTED*	SIMILAR TO RIKEN CDNA 2010107G23 (PREDICTED)
1374438_AT	*RGD1305606*	SIMILAR TO MKIAA1046 PROTEIN
1382220_AT	*RGD1305614_PREDICTED*	SIMILAR TO IGF-II MRNA-BINDING PROTEIN 2 (PREDICTED)
1388930_AT	*RGD1305625*	SIMILAR TO RIKEN CDNA 2310075C12
1372136_AT	*RGD1305714_PREDICTED*	SIMILAR TO TETRASPANIN SIMILAR TO TM4SF9 (PREDICTED)
1374699_AT	*RGD1305779_PREDICTED*	SIMILAR TO NSE1 (PREDICTED)
1372164_AT	*RGD1305793*	SIMILAR TO HYPOTHETICAL PROTEIN FLJ20154
1372957_AT	*RGD1305846_PREDICTED*	SIMILAR TO HYPOTHETICAL PROTEIN A730008H23 (PREDICTED)
1391475_AT	*RGD1305861_PREDICTED*	SIMILAR TO 2810036L13RIK PROTEIN (PREDICTED)
1382178_AT	*RGD1305866_PREDICTED*	SIMILAR TO HYPOTHETICAL PROTEIN FLJ20200 (PREDICTED)
1376100_AT	*RGD1305887*	SIMILAR TO RIKEN CDNA 2310057H16
1383841_AT	*RGD1305891_PREDICTED*	SIMILAR TO DNA (CYTOSINE-5)-METHYLTRANSFERASE 3A (DNMT3A)
1377737_AT	*RGD1306051_PREDICTED*	SIMILAR TO HYPOTHETICAL PROTEIN MGC5466 (PREDICTED)
1399150_AT	*RGD1306064_PREDICTED*	SIMILAR TO RIKEN CDNA A630054L15; HYPOTHETICAL PROTEIN MGC38041 (PREDICTED)
1378007_AT	*RGD1306148_PREDICTED*	SIMILAR TO KIAA0368 (PREDICTED)
1377877_AT	*RGD1306152_PREDICTED*	SIMILAR TO KIAA0980 PROTEIN (PREDICTED)
1398397_AT	*RGD1306185*	SIMILAR TO PARG1-PENDING PROTEIN
1376263_AT	*RGD1306222*	SIMILAR TO 1810034B16RIK PROTEIN
1379315_AT	*RGD1306244_PREDICTED*	SIMILAR TO RIKEN CDNA 2400009B11 GENE (PREDICTED)
1389197_AT	*RGD1306248*	SIMILAR TO RIKEN CDNA 9630046K23
1373924_AT	*RGD1306568*	SIMILAR TO C530044N13RIK PROTEIN
1383267_AT	*RGD1306577*	SIMILAR TO RIKEN CDNA 2210404D11
1388648_AT	*RGD1306614*	SIMILAR TO D7WSU128E PROTEIN
1391157_AT	*RGD1306651_PREDICTED*	SIMILAR TO CG7744-PA (PREDICTED)
1392579_AT	*RGD1306658*	SIMILAR TO 5830411E10RIK PROTEIN
1393832_AT	*RGD1306676*	SIMILAR TO RIKEN CDNA 0610033I05 (PREDICTED)
1388579_AT	*RGD1306691_PREDICTED*	SIMILAR TO HYPOTHETICAL GENE MGC19595 (PREDICTED)
1373060_AT	*RGD1306781_PREDICTED*	SIMILAR TO CGI-84 PROTEIN (PREDICTED)
1381091_AT	*RGD1306802*	SIMILAR TO HYPOTHETICAL PROTEIN BC008207
1372917_AT	*RGD1306819*	SIMILAR TO A230072I16RIK PROTEIN
1388321_AT	*RGD1306825_PREDICTED*	SIMILAR TO RIKEN CDNA 1190002L16 (PREDICTED)
1377190_AT	*RGD1306939*	SIMILAR TO MKIAA0386 PROTEIN
1377011_AT	*RGD1307034_PREDICTED*	SIMILAR TO HYPOTHETICAL PROTEIN CG003 (PREDICTED)
1372922_AT	*RGD1307036_PREDICTED*	HYPOTHETICAL LOC287306 (PREDICTED)
1388408_AT	*RGD1307129*	SIMILAR TO RIKEN CDNA 1110020C13
1375037_AT	*RGD1307145_PREDICTED*	SIMILAR TO SPORULATION-INDUCED TRANSCRIPT 4-ASSOCIATED PROTEIN (PREDICTED)
1372192_AT	*RGD1307374_PREDICTED*	SIMILAR TO HYPOTHETICAL PROTEIN MGC36325 (PREDICTED)
1374124_AT	*RGD1307381*	SIMILAR TO RIKEN CDNA 2610003J06
1372913_AT	*RGD1307433*	SIMILAR TO RIKEN CDNA 2310065K24
1372748_AT	*RGD1307436*	SIMILAR TO KIAA1055 PROTEIN
1378104_AT	*RGD1307465*	SIMILAR TO RIKEN CDNA 8430406I07
1388471_AT	*RGD1307494*	SIMILAR TO RIKEN CDNA E430026E19
1389007_AT	*RGD1307524_PREDICTED*	SIMILAR TO FRIEDREICH ATAXIA REGION GENE X123 (PREDICTED)
1376144_AT	*RGD1307534_PREDICTED*	SIMILAR TO B AGGRESSIVE LYMPHOMA (PREDICTED)
1371347_AT	*RGD1307561*	SIMILAR TO RIKEN CDNA B230114J08
1390336_AT	*RGD1307569_PREDICTED*	SIMILAR TO PROTEIN C21ORF63 HOMOLOG PRECURSOR (PREDICTED)
1373093_AT	*RGD1307599*	SIMILAR TO MITOGEN-INDUCIBLE GENE 6 PROTEIN HOMOLOG (MIG-6) (GENE 33 POLYPEPTIDE)
1384388_AT	*RGD1307627*	SIMILAR TO GP25L2 PROTEIN
1393085_AT	*RGD1307700*	SIMILAR TO HYPOTHETICAL PROTEIN BC018453
1384185_AT	*RGD1307704_PREDICTED*	SIMILAR TO RIKEN CDNA 2410016O06 (PREDICTED)
1385481_AT	*RGD1307724_PREDICTED*	SIMILAR TO NCAG1 (PREDICTED)
1383186_AT	*RGD1307749_PREDICTED*	SIMILAR TO RIKEN CDNA 1600013K19 (PREDICTED)
1388881_AT	*RGD1307773_PREDICTED*	SIMILAR TO RIKEN CDNA 1700012G19 GENE (PREDICTED)
1398517_AT	*RGD1307854*	SIMILAR TO HSPC182 PROTEIN
1372763_AT	*RGD1307879_PREDICTED*	SIMILAR TO HYPOTHETICAL PROTEIN D10ERTD438E (PREDICTED)
1389171_AT	*RGD1307901_PREDICTED*	SIMILAR TO RIKEN CDNA 1110001E17 (PREDICTED)

1379682_AT	*RGD1307927_PREDICTED*	SIMILAR TO RIKEN CDNA 6030446I19 GENE (PREDICTED)
1379778_AT	*RGD1307983_PREDICTED*	SIMILAR TO HSPC043 PROTEIN (PREDICTED)
1398951_AT	*RGD1308009*	SIMILAR TO KIAA1007 PROTEIN; ADRENAL GLAND PROTEIN AD-005
1391166_AT	*RGD1308015_PREDICTED*	SIMILAR TO RIKEN CDNA 1700025B16 (PREDICTED)
1372420_AT	*RGD1308064_PREDICTED*	SIMILAR TO FKSG24 (PREDICTED)
1375767_AT	*RGD1308089_PREDICTED*	SIMILAR TO COMMON-SITE LYMPHOMA LEUKEMIA GUANINE NUCLEOTIDE EXCHANGE FACTOR
1372563_AT	*RGD1308143*	SIMILAR TO D330021B20 PROTEIN
1389393_AT	*RGD1308210*	SIMILAR TO RIKEN CDNA 2210412D01
1395796_AT	*RGD1308257*	SIMILAR TO INTERMEDIATE FILAMENT-LIKE PROTEIN MGC:2625 ISOFORM 2;
1393898_AT	*RGD1308268_PREDICTED*	SIMILAR TO KIAA0460 PROTEIN (PREDICTED)
1379027_AT	*RGD1308329_PREDICTED*	SIMILAR TO KIAA0869 PROTEIN (PREDICTED)
1393775_AT	*RGD1308356*	SIMILAR TO HYPOTHETICAL PROTEIN KIAA0341
1392508_AT	*RGD1308378*	SIMILAR TO RIKEN CDNA 3110010F15
1391595_AT	*RGD1308414_PREDICTED*	SIMILAR TO ACHERON; DEATH-ASSOCIATED LA MOTIF PROTEIN (PREDICTED)
1388577_AT	*RGD1308433*	SIMILAR TO STEROID DEHYDROGENASE-LIKE
1375941_AT	*RGD1308452*	SIMILAR TO RIKEN CDNA 1300006M19
1379407_AT	*RGD1308463*	SIMILAR TO IMP4
1382428_AT	*RGD1308591_PREDICTED*	SIMILAR TO 4930485D02RIK PROTEIN (PREDICTED)
1373493_AT	*RGD1308768_PREDICTED*	SIMILAR TO ARS COMPONENT B PRECURSOR (PREDICTED)
1374418_AT	*RGD1308816_PREDICTED*	SIMILAR TO CG8009-PA (PREDICTED)
1373852_AT	*RGD1308828*	SIMILAR TO SRD5A2L
1377021_AT	*RGD1308877_PREDICTED*	SIMILAR TO CGI-09 PROTEIN (PREDICTED)
1376376_AT	*RGD1308984*	SIMILAR TO RIKEN CDNA 6030404E16
1372488_AT	*RGD1309016*	SIMILAR TO RIKEN CDNA 2310057D15
1373521_AT	*RGD1309038*	SIMILAR TO RIKEN CDNA D430044G18
1371697_AT	*RGD1309044_PREDICTED*	SIMILAR TO RIKEN CDNA 0610039C21 (PREDICTED)
1383738_AT	*RGD1309101_PREDICTED*	SIMILAR TO KIAA0582 PROTEIN (PREDICTED)
1372781_AT	*RGD1309181*	SIMILAR TO RIKEN CDNA 1810073M12
1374408_AT	*RGD1309199*	SIMILAR TO CBF1 INTERACTING COREPRESSOR
1372288_AT	*RGD1309256*	SIMILAR TO D11BWG0280E PROTEIN
1376680_AT	*RGD1309258_PREDICTED*	SIMILAR TO RIKEN CDNA 5730409F24 (PREDICTED)
1372554_AT	*RGD1309266_PREDICTED*	SIMILAR TO RW1 PROTEIN (PREDICTED)
1393009_AT	*RGD1309326*	SIMILAR TO RIKEN CDNA 2410002F23
1383975_AT	*RGD1309383*	SIMILAR TO RIKEN CDNA G630055P03 GENE
1372003_AT	*RGD1309417_PREDICTED*	SIMILAR TO CG17660-PA (PREDICTED)
1372059_AT	*RGD1309437*	SIMILAR TO RIKEN CDNA 2610528E23
1380309_AT	*RGD1309443_PREDICTED*	SIMILAR TO MKIAA0804 PROTEIN (PREDICTED)
1374568_AT	*RGD1309492_PREDICTED*	SIMILAR TO MKIAA1737 PROTEIN (PREDICTED)
1375974_AT	*RGD1309571*	SIMILAR TO RNA-BINDING PROTEIN ISOFORM G3BP-2A
1390392_AT	*RGD1309602_PREDICTED*	SIMILAR TO RIKEN CDNA 2500001K11 (PREDICTED)
1372641_AT	*RGD1309860_PREDICTED*	SIMILAR TO MYOCYTIC INDUCTION/DIFFERENTIATION ORIGINATOR (PREDICTED)
1395973_AT	*RGD1309871_PREDICTED*	SIMILAR TO RIKEN CDNA 5730596K20 (PREDICTED)
1377829_AT	*RGD1309884*	SIMILAR TO TRANSLOKIN
1393043_AT	*RGD1309957_PREDICTED*	SIMILAR TO HYPOTHETICAL WD-REPEAT PROTEIN CGI-48 (PREDICTED)
1373407_AT	*RGD1309983_PREDICTED*	SIMILAR TO HYPOTHETICAL PROTEIN 9930016O13 (PREDICTED)
1389708_AT	*RGD1310006*	SIMILAR TO RIKEN CDNA 5730421E18
1376780_AT	*RGD1310022*	SIMILAR TO RIKEN CDNA 2610204K14
1391419_AT	*RGD1310031_PREDICTED*	SIMILAR TO HYPOTHETICAL PROTEIN MGC29331 (PREDICTED)
1373035_AT	*RGD1310127*	SIMILAR TO CDNA SEQUENCE BC017158
1375182_AT	*RGD1310143*	SIMILAR TO RIKEN CDNA D030028O16
1384219_AT	*RGD1310144*	SIMILAR TO EAP30 SUBUNIT OF ELL COMPLEX
1384788_AT	*RGD1310193_PREDICTED*	SIMILAR TO KCCR13L (PREDICTED)
1372433_AT	*RGD1310211_PREDICTED*	SIMILAR TO CG11030-PA (PREDICTED)
1375060_AT	*RGD1310244_PREDICTED*	SIMILAR TO CC2-27 (PREDICTED)
1393701_AT	*RGD1310265_PREDICTED*	SIMILAR TO ALPHA-1,4-N-ACETYLGLUCOSAMINYLTRANSFERASE (ALPHA4GNT) (PREDICTED)
1373588_AT	*RGD1310323*	SIMILAR TO RIKEN CDNA 1200004M23
1372903_AT	*RGD1310360*	SIMILAR TO 3000004C01RIK PROTEIN
1378947_AT	*RGD1310402*	SIMILAR TO C-TERMINAL TENSIN-LIKE
1390218_AT	*RGD1310440_PREDICTED*	SIMILAR TO HYPOTHETICAL PROTEIN (PREDICTED)
1372805_AT	*RGD1310444_PREDICTED*	LOC363015 (PREDICTED)
1374042_AT	*RGD1310453_PREDICTED*	SIMILAR TO HYPOTHETICAL PROTEIN FLJ23451 (PREDICTED)
1392556_AT	*RGD1310470*	SIMILAR TO PDZ DOMAIN ACTIN BINDING PROTEIN SHROOM
1382765_AT	*RGD1310493_PREDICTED*	SIMILAR TO RIKEN CDNA 2410007P03 (PREDICTED)
1375943_AT	*RGD1310509_PREDICTED*	SIMILAR TO HYPOTHETICAL PROTEIN KIAA0419 (PREDICTED)
1372202_AT	*RGD1310553*	SIMILAR TO EXPRESSED SEQUENCE AI597479
1372851_AT	*RGD1310570_PREDICTED*	SIMILAR TO HYPOTHETICAL PROTEIN (PREDICTED)
1393015_AT	*RGD1310587*	SIMILAR TO HYPOTHETICAL PROTEIN FLJ14146
1374359_AT	*RGD1310592_PREDICTED*	SIMILAR TO RIKEN CDNA 2810013E07 (PREDICTED)
1389793_AT	*RGD1310596*	SIMILAR TO P66 ALPHA HOMOLOG
1386266_AT	*RGD1310606*	SIMILAR TO RIKEN CDNA 1200009B18; EST AA408438
1377016_AT	*RGD1310614*	SIMILAR TO RIKEN CDNA 5730592L21
1372814_AT	*RGD1310623*	SIMILAR TO RIKEN CDNA 2010005O13
1371747_AT	*RGD1310660*	SIMILAR TO RIKEN CDNA 2700038C09
1394612_AT	*RGD1310781_PREDICTED*	SIMILAR TO RIKEN CDNA 1810020G14 (PREDICTED)
1373576_AT	*RGD1310783*	SIMILAR TO CCR4
1376328_AT	*RGD1310819_PREDICTED*	SIMILAR TO PUTATIVE PROTEIN (5S487) (PREDICTED)
1378032_AT	*RGD1310834_PREDICTED*	SIMILAR TO MOLECULE POSSESSING ANKYRIN-REPEATS INDUCED BY LIPOPOLYSACCHARIDE
1383531_AT	*RGD1310862_PREDICTED*	SIMILAR TO ADULT RETINA PROTEIN (PREDICTED)
1373965_AT	*RGD1310931_PREDICTED*	SIMILAR TO HYPOTHETICAL PROTEIN BC013949 (PREDICTED)
1395856_AT	*RGD1311021_PREDICTED*	HYPOTHETICAL LOC308765 (PREDICTED)
1383794_AT	*RGD1311080_PREDICTED*	SIMILAR TO RIKEN CDNA A930038C07 (PREDICTED)
1398442_AT	*RGD1311091_PREDICTED*	SIMILAR TO CHROMOSOME 14 OPEN READING FRAME 80 (PREDICTED)
1378288_AT	*RGD1311100_PREDICTED*	SIMILAR TO RIKEN CDNA D630035O19 (PREDICTED)
1374265_AT	*RGD1311104_PREDICTED*	SIMILAR TO ARYLACETAMIDE DEACETYLASE (ESTERASE) (PREDICTED)
1373971_AT	*RGD1311177_PREDICTED*	SIMILAR TO PCPD PROTEIN (PREDICTED)
1377210_AT	*RGD1311203*	SIMILAR TO HGFL PROTEIN
1380134_AT	*RGD1311204*	SIMILAR TO B7S1
1371740_AT	*RGD1311316*	SIMILAR TO RIKEN CDNA 5730470L24
1397346_AT	*RGD1311320_PREDICTED*	SIMILAR TO MGC31683 PROTEIN (PREDICTED)
1383461_AT	*RGD1311362*	SIMILAR TO HYPOTHETICAL PROTEIN FLJ10204

1392337_AT	*RGD1311424_PREDICTED*	SIMILAR TO HYPOTHETICAL PROTEIN FLJ38348 (PREDICTED)
1374562_AT	*RGD1311429_PREDICTED*	SIMILAR TO KIAA1267 PROTEIN (PREDICTED)
1385369_AT	*RGD1311430*	SIMILAR TO HYPOTHETICAL PROTEIN FLJ32844
1391126_AT	*RGD1311462_PREDICTED*	SIMILAR TO RIKEN CDNA 2410011G03 (PREDICTED)
1398380_AT	*RGD1311476*	SIMILAR TO VON WILLEBRAND FACTOR A-DOMAIN CONTAINING 1
1380981_AT	*RGD1311502_PREDICTED*	SIMILAR TO STONIN 2; HOMOLOG OF STONED B (DROSOPHILA) (PREDICTED)
1373171_AT	*RGD1311520*	SIMILAR TO HYPOTHETICAL PROTEIN DKFZP434L0117
1377287_AT	*RGD1311527_PREDICTED*	SIMILAR TO HYPOTHETICAL PROTEIN BC009115 (PREDICTED)
1388909_AT	*RGD1311534_PREDICTED*	SIMILAR TO CDNA SEQUENCE BC019806 (PREDICTED)
1390876_AT	*RGD1311552_PREDICTED*	SIMILAR TO KIAA0377-LIKE PROTEIN (PREDICTED)
1382630_AT	*RGD1311558_PREDICTED*	SIMILAR TO 4930506M07RIK PROTEIN (PREDICTED)
1374142_AT	*RGD1311589_PREDICTED*	SIMILAR TO RIKEN CDNA E130201N16 (PREDICTED)
1373186_AT	*RGD1311593_PREDICTED*	SIMILAR TO RIKEN CDNA 5033405K12 (PREDICTED)
1371923_AT	*RGD1311599_PREDICTED*	SIMILAR TO HYPOTHETICAL PROTEIN FLJ20481 (PREDICTED)
1393718_AT	*RGD1311704_PREDICTED*	SIMILAR TO DKFZP564P1916 PROTEIN (PREDICTED)
1378120_AT	*RGD1311709_PREDICTED*	SIMILAR TO RIBOSOMAL PROTEIN P0-LIKE PROTEIN
1383548_AT	*RGD1311759_PREDICTED*	SIMILAR TO HYPOTHETICAL PROTEIN FLJ20189 (PREDICTED)
1381390_AT	*RGD1311768_PREDICTED*	SIMILAR TO HYPOTHETICAL PROTEIN FLJ32001 (PREDICTED)
1391121_AT	*RGD1311793_PREDICTED*	SIMILAR TO DNA SEGMENT, CHR 8, ERATO DOI 82, EXPRESSED (PREDICTED)
1374609_AT	*RGD1311857_PREDICTED*	SIMILAR TO HYPOTHETICAL PROTEIN FLJ10326 (PREDICTED)
1384296_AT	*RGD1311909_PREDICTED*	HYPOTHETICAL LOC312654 (PREDICTED)
1389656_AT	*RGD1312037*	SIMILAR TO RIKEN CDNA 1700023M09
1397579_X_AT	*RGD1359127*	SIMILAR TO RIKEN CDNA 2310011J03
1373866_AT	*RGD1359509*	SIMILAR TO HYPOTHETICAL PROTEIN FLJ13448
1380334_AT	*RGD1359713*	HYPOTHETICAL RNA BINDING PROTEIN RGD1359713
1385783_AT	*RGD1559427_PREDICTED*	SIMILAR TO BH3-ONLY MEMBER B PROTEIN
1390865_AT	*RGD1559440_PREDICTED*	SIMILAR TO CA2+-DEPENDENT ACTIVATOR FOR SECRETION PROTEIN 2
1373584_AT	*RGD1559643_PREDICTED*	SIMILAR TO HYPOTHETICAL PROTEIN A430031N04
1378906_AT	*RGD1559690_PREDICTED*	SIMILAR TO HYPOTHETICAL PROTEIN FLJ25416
1388842_AT	*RGD1559787_PREDICTED*	SIMILAR TO SERUM RESPONSE FACTOR
1391443_AT	*RGD1559923_PREDICTED*	SIMILAR TO CHROMOSOME 14 OPEN READING FRAME 35
1398432_AT	*RGD1559931_PREDICTED*	SIMILAR TO ANKYRIN REPEAT DOMAIN PROTEIN 28
1367676_AT	*RGD1559962_PREDICTED*	SIMILAR TO HIGH MOBILITY GROUP PROTEIN 2 (HMG-2)
1379108_AT	*RGD1559968_PREDICTED*	SIMILAR TO ADP-RIBOSYLATION FACTOR GUANINE NUCLEOTIDE FACTOR 6 ISOFORM A
1372403_AT	*RGD1560011_PREDICTED*	SIMILAR TO NUCLEAR MEMBRANE BINDING PROTEIN NUCLING
1389050_AT	*RGD1560049_PREDICTED*	SIMILAR TO DUAL SPECIFICITY PROTEIN PHOSPHATASE 3 (T-DSP11)
1389425_AT	*RGD1560091_PREDICTED*	SIMILAR TO 5(3)-DEOXYRIBONUCLEOTIDASE
1372840_AT	*RGD1560093_PREDICTED*	SIMILAR TO ZBED4 PROTEIN
1388957_AT	*RGD1560152_PREDICTED*	SIMILAR TO HYPOTHETICAL PROTEIN D10ERTD641E
1384886_AT	*RGD1560157_PREDICTED*	SIMILAR TO HYPOTHETICAL PROTEIN LOC168850
1391474_AT	*RGD1560170_PREDICTED*	SIMILAR TO COFACTOR REQUIRED FOR SP1 TRANSCRIPTIONAL ACTIVATION, SUBUNIT 2, 150KDA
1379029_AT	*RGD1560191_PREDICTED*	SIMILAR TO ZINC FINGER PROTEIN 62 HOMOLOG (ZFP-62) (ZT3)
1377961_AT	*RGD1560268_PREDICTED*	SIMILAR TO AT MOTIF-BINDING FACTOR
1373321_AT	*RGD1560328_PREDICTED*	SIMILAR TO UPF0197 PROTEIN C11ORF10 HOMOLOG
1383616_AT	*RGD1560373_PREDICTED*	SIMILAR TO CLASS II CYTOKINE RECEPTOR 4
1392930_AT	*RGD1560393_PREDICTED*	SIMILAR TO ARMADILLO REPEAT-CONTAINING PROTEIN
1377675_AT	*RGD1560441_PREDICTED*	LOC498261
1390586_AT	*RGD1560601_PREDICTED*	SIMILAR TO JUMONJI/ARID DOMAIN-CONTAINING PROTEIN 1C (SMCX PROTEIN) (XE169 PROTEIN)
1371382_AT	*RGD1560614_PREDICTED*	SIMILAR TO FILAMIN A (ALPHA-FILAMIN) (FILAMIN 1) (ENDOTHELIAL ACTIN-BINDING PROTEIN)
1373906_AT	*RGD1560629_PREDICTED*	SIMILAR TO RIKEN CDNA A930016P21
1375859_A_AT	*RGD1560682_PREDICTED*	SIMILAR TO ZINC FINGER PROTEIN 565
1391269_AT	*RGD1560759_PREDICTED*	SIMILAR TO SERINE-THREONINE PROTEIN KINASE PIM-2 ISOFORM 1
1374003_AT	*RGD1560835_PREDICTED*	LOC498007
1389440_AT	*RGD1560863_PREDICTED*	SIMILAR TO CELL DIVISION CYCLE ASSOCIATED 5
1383095_AT	*RGD1560873_PREDICTED*	SIMILAR TO RIKEN CDNA E230015L20 GENE
1380449_AT	*RGD1560924_PREDICTED*	SIMILAR TO C230080I20RIK PROTEIN
1374375_AT	*RGD1560925_PREDICTED*	SIMILAR TO 2610034M16RIK PROTEIN
1382331_AT	*RGD1560961_PREDICTED*	SIMILAR TO RIKEN CDNA 0610038L10 GENE
1380318_AT	*RGD1560976_PREDICTED*	LOC499196
1372373_AT	*RGD1560982_PREDICTED*	SIMILAR TO PUTATIVE WD-REPEAT PROTEIN
1372460_AT	*RGD1561000_PREDICTED*	LOC499767
1376177_AT	*RGD1561062_PREDICTED*	SIMILAR TO RIKEN CDNA 5730593F17
1377819_AT	*RGD1561065_PREDICTED*	SIMILAR TO MKIAA1111 PROTEIN
1399041_AT	*RGD1561117_PREDICTED*	SIMILAR TO OPA3 PROTEIN
1396379_AT	*RGD1561121_PREDICTED*	SIMILAR TO PLECKSTRIN HOMOLOGY-LIKE DOMAIN, FAMILY B, MEMBER 3
1375873_AT	*RGD1561149_PREDICTED*	SIMILAR TO MKIAA1522 PROTEIN
1376087_AT	*RGD1561189_PREDICTED*	SIMILAR TO RIKEN CDNA 1300010M03
1389307_AT	*RGD1561211_PREDICTED*	SIMILAR TO AMYLOID BETA (A4) PRECURSOR-LIKE PROTEIN 1
1385558_AT	*RGD1561304_PREDICTED*	SIMILAR TO HYPOTHETICAL PROTEIN D930024E11
1379603_AT	*RGD1561386_PREDICTED*	SIMILAR TO CBL E3 UBIQUITIN PROTEIN LIGASE (SIGNAL TRANSDUCTION PROTEIN CBL)
1393170_AT	*RGD1561431_PREDICTED*	SIMILAR TO HOMEOBOX-CONTAINING TRANSCRIPTION FACTOR
1392128_AT	*RGD1561464_PREDICTED*	SIMILAR TO NOVEL PROTEIN
1383312_AT	*RGD1561596_PREDICTED*	SIMILAR TO JM11 PROTEIN
1392987_AT	*RGD1561605_PREDICTED*	SIMILAR TO HYPOTHETICAL PROTEIN
1383743_AT	*RGD1561607_PREDICTED*	SIMILAR TO RP23-462P2.7
1384457_AT	*RGD1561663_PREDICTED*	SIMILAR TO FBXW17 PROTEIN
1393346_AT	*RGD1561673_PREDICTED*	SIMILAR TO RIKEN CDNA 5830436D01
1367676_AT	*RGD1561694_PREDICTED*	SIMILAR TO HIGH MOBILITY GROUP PROTEIN 2 (HMG-2)
1389580_AT	*RGD1561695_PREDICTED*	LOC499580
1372292_AT	*RGD1561742_PREDICTED*	SIMILAR TO SERINE/THREONINE PROTEIN KINASE 24
1389242_AT	*RGD1561784_PREDICTED*	SIMILAR TO LRRGT00194
1380100_AT	*RGD1561817_PREDICTED*	SIMILAR TO TRAF2 AND NCK INTERACTING KINASE, SPLICE VARIANT 4
1379085_AT	*RGD1561878_PREDICTED*	SIMILAR TO MKIAA0978 PROTEIN
1373616_AT	*RGD1561936_PREDICTED*	LOC499369
1371544_AT	*RGD1561971_PREDICTED*	SIMILAR TO ENHANCER OF RUDIMENTARY HOMOLOG
1373183_AT	*RGD1561982_PREDICTED*	LOC500713
1380619_AT	*RGD1561986_PREDICTED*	SIMILAR TO RIKEN CDNA 3110001I22
1393713_AT	*RGD1561989_PREDICTED*	SIMILAR TO GDP-MANNOSE 4, 6-DEHYDRATASE
1371823_AT	*RGD1562042_PREDICTED*	SIMILAR TO STROMAL ANTIGEN 2
1373761_AT	*RGD1562072_PREDICTED*	SIMILAR TO IMMUNOGLOBULIN LIGHT CHAIN

1382406_AT	*RGD1562149_PREDICTED*	SIMILAR TO MIXED-LINEAGE PROTEIN KINASE 1
1391603_AT	*RGD1562161_PREDICTED*	SIMILAR TO CHROMOSOME X OPEN READING FRAME 23
1390808_AT	*RGD1562232_PREDICTED*	SIMILAR TO MICROFIBRILLAR-ASSOCIATED PROTEIN 1
1389907_AT	*RGD1562249_PREDICTED*	SIMILAR TO ARCHEASE
1380118_AT	*RGD1562252_PREDICTED*	SIMILAR TO HYPOTHETICAL GENE SUPPORTED BY AK085276
1382750_AT	*RGD1562274_PREDICTED*	LOC500687
1399025_AT	*RGD1562337_PREDICTED*	SIMILAR TO MESODERM INDUCTION EARLY RESPONSE 1 (MI-ER1)
1392476_AT	*RGD1562378_PREDICTED*	GERMINAL HISTONE H4 GENE
1381937_AT	*RGD1562446_PREDICTED*	SIMILAR TO 60S RIBOSOMAL PROTEIN L7A
1398943_AT	*RGD1562476_PREDICTED*	SIMILAR TO ESO3 PROTEIN
1391595_AT	*RGD1562514_PREDICTED*	SIMILAR TO RIBOSOMAL PROTEIN L21
1392109_AT	*RGD1562529_PREDICTED*	SIMILAR TO HYPOTHETICAL PROTEIN FLJ21439
1390226_AT	*RGD1562552_PREDICTED*	SIMILAR TO HYPOTHETICAL PROTEIN LOC340061
1392758_AT	*RGD1562563_PREDICTED*	SIMILAR TO RIKEN CDNA G430041M01
1374536_AT	*RGD1562568_PREDICTED*	LOC499569
1383146_AT	*RGD1562629_PREDICTED*	SIMILAR TO NEUROBEACHIN
1385551_AT	*RGD1562652_PREDICTED*	SIMILAR TO CLASS I HISTOCOMPATIBILITY ANTIGEN ALPHA CHAIN - COTTON-TOP TAMARIN
1385592_AT	*RGD1562735_PREDICTED*	SIMILAR TO BCOR PROTEIN (BCL-6 COREPRESSOR)
1383991_AT	*RGD1562754_PREDICTED*	SIMILAR TO 1810049O03RIK PROTEIN
1375429_AT	*RGD1562784_PREDICTED*	SIMILAR TO HYPOTHETICAL PROTEIN
1379104_AT	*RGD1562845_PREDICTED*	SIMILAR TO ZINC FINGER PROTEIN 120 ISOFORM 1
1378860_AT	*RGD1562973_PREDICTED*	SIMILAR TO HYPOTHETICAL PROTEIN D930020E02
1382084_AT	*RGD1562988_PREDICTED*	SIMILAR TO EHM2
1375362_AT	*RGD1563001_PREDICTED*	SIMILAR TO RIKEN CDNA 2010106G01
1385876_AT	*RGD1563063_PREDICTED*	SIMILAR TO GPC6 PROTEIN
1372262_AT	*RGD1563087_PREDICTED*	LOC500344
1379475_AT	*RGD1563120_PREDICTED*	SIMILAR TO RIKEN CDNA 2210009G21
1394789_AT	*RGD1563160_PREDICTED*	LOC499812
1380226_AT	*RGD1563203_PREDICTED*	SIMILAR TO STERILE ALPHA MOTIF DOMAIN CONTAINING 10
1382331_AT	*RGD1563242_PREDICTED*	SIMILAR TO RIKEN CDNA 0610038L10 GENE
1391518_AT	*RGD1563264_PREDICTED*	SIMILAR TO 60S RIBOSOMAL PROTEIN L7A
1370802_AT	*RGD1563276_PREDICTED*	SIMILAR TO INTEGRIN BETA-5
1385687_AT	*RGD1563327_PREDICTED*	SIMILAR TO RIKEN CDNA 2200001I15
1384254_AT	*RGD1563344_PREDICTED*	SIMILAR TO OTU DOMAIN CONTAINING 1
1377670_AT	*RGD1563397_PREDICTED*	SIMILAR TO MKIAA0824 PROTEIN
1378003_AT	*RGD1563429_PREDICTED*	SIMILAR TO T-CELL ACTIVATION LEUCINE REPEAT-RICH PROTEIN
1377818_AT	*RGD1563506_PREDICTED*	SIMILAR TO JUNCTION-MEDIATING AND REGULATORY PROTEIN
1377155_AT	*RGD1563507_PREDICTED*	SIMILAR TO RIKEN CDNA 1700019G17
1372830_AT	*RGD1563508_PREDICTED*	SIMILAR TO PI-3-KINASE-RELATED KINASE SMG-1 ISOFORM 2
1395428_AT	*RGD1563533_PREDICTED*	SIMILAR TO NOVEL PROTEIN
1373088_AT	*RGD1563661_PREDICTED*	HYPOTHETICAL LOC291665
1388446_AT	*RGD1563684_PREDICTED*	SIMILAR TO HETEROGENEOUS NUCLEAR RIBONUCLEOPROTEIN A0
1372545_AT	*RGD1563727_PREDICTED*	SIMILAR TO GENE MODEL 609
1391296_AT	*RGD1563762_PREDICTED*	SIMILAR TO COX11 HOMOLOG, CYTOCHROME C OXIDASE ASSEMBLY PROTEIN
1376018_AT	*RGD1563803_PREDICTED*	SIMILAR TO LMNB2 PROTEIN
1372530_AT	*RGD1563804_PREDICTED*	SIMILAR TO HCF
1374433_AT	*RGD1563902_PREDICTED*	SIMILAR TO FERRITIN LIGHT CHAIN (FERRITIN L SUBUNIT)
1389412_AT	*RGD1563919_PREDICTED*	LOC499414
1373557_AT	*RGD1563943_PREDICTED*	SIMILAR TO MCDC21 PROTEIN
1375041_AT	*RGD1563982_PREDICTED*	SIMILAR TO F-BOX ONLY PROTEIN 27
1388720_AT	*RGD1564045_PREDICTED*	HYPOTHETICAL LOC361225
1390808_AT	*RGD1564148_PREDICTED*	SIMILAR TO MICROFIBRILLAR-ASSOCIATED PROTEIN 1
1375857_AT	*RGD1564216_PREDICTED*	SIMILAR TO MYOFERLIN (FER-1 LIKE PROTEIN 3)
1374586_AT	*RGD1564269_PREDICTED*	SIMILAR TO ADP-RIBOSYLATION FACTOR RELATED PROTEIN 2
1390474_AT	*RGD1564315_PREDICTED*	SIMILAR TO RIKEN CDNA 9330161F08
1372626_AT	*RGD1564417_PREDICTED*	SIMILAR TO TUMOR PROTEIN D53
1382940_AT	*RGD1564436_PREDICTED*	SIMILAR TO HYPOTHETICAL PROTEIN MGC47419
1393186_AT	*RGD1564454_PREDICTED*	SIMILAR TO RIKEN CDNA 2010200O16
1367676_AT	*RGD1564519_PREDICTED*	HIGH MOBILITY GROUP BOX 2
1367479_AT	*RGD1564529_PREDICTED*	SIMILAR TO NUCLEAR PROTEIN IN TESTIS
1380185_AT	*RGD1564541_PREDICTED*	SIMILAR TO HYPOTHETICAL PROTEIN FLJ22965
1396219_AT	*RGD1564559_PREDICTED*	SIMILAR TO MIC2L1
1399081_AT	*RGD1564594_PREDICTED*	SIMILAR TO PELLINO PROTEIN
1389400_AT	*RGD1564662_PREDICTED*	SIMILAR TO MSX-2 INTERACTING NUCLEAR TARGET PROTEIN
1374766_AT	*RGD1564703_PREDICTED*	SIMILAR TO MKIAA0493 PROTEIN
1384956_AT	*RGD1564714_PREDICTED*	SIMILAR TO BC021442 PROTEIN
1383012_AT	*RGD1564719_PREDICTED*	SIMILAR TO RIKEN CDNA C230052I12
1383299_AT	*RGD1564793_PREDICTED*	SIMILAR TO KIAA0965 PROTEIN
1374775_AT	*RGD1564824_PREDICTED*	SIMILAR TO MKI67 PROTEIN
1379310_AT	*RGD1564862_PREDICTED*	SIMILAR TO HYPOTHETICAL PROTEIN MGC51082
1383428_AT	*RGD1564871_PREDICTED*	SIMILAR TO THIOREDOXIN DOMAIN CONTAINING PROTEIN 6 (THIOREDOXIN-LIKE PROTEIN 2)
1371984_AT	*RGD1564875_PREDICTED*	SIMILAR TO MKIAA0613 PROTEIN
1371771_AT	*RGD1564888_PREDICTED*	SIMILAR TO NOVEL PROTEIN
1374175_AT	*RGD1564947_PREDICTED*	SIMILAR TO PORCUPINE-D
1387388_AT	*RGD1564956_PREDICTED*	SIMILAR TO CALCIUM BINDING PROTEIN P22
1392476_AT	*RGD1565073_PREDICTED*	SIMILAR TO GERMINAL HISTONE H4 GENE
1376885_AT	*RGD1565098_PREDICTED*	SIMILAR TO CHEMOKINE-LIKE FACTOR SUPER FAMILY 4
1374718_AT	*RGD1565144_PREDICTED*	SIMILAR TO DELTEX 3-LIKE
1397855_AT	*RGD1565145_PREDICTED*	SIMILAR TO CYSTEINE SULFINIC ACID DECARBOXYLASE
1390122_AT	*RGD1565175_PREDICTED*	SIMILAR TO TRIGGERING RECEPTOR EXPRESSED ON MYELOID CELLS-LIKE 1
1383056_A_AT	*RGD1565210_PREDICTED*	LOC499072
1383538_AT	*RGD1565257_PREDICTED*	SIMILAR TO ZINC FINGER PROTEIN 650
1390891_AT	*RGD1565333_PREDICTED*	SIMILAR TO KINESIN FAMILY MEMBER 11
1389639_AT	*RGD1565350_PREDICTED*	SIMILAR TO SHB PROTEIN
1382130_AT	*RGD1565392_PREDICTED*	SIMILAR TO PROTOCADHERIN 19 PRECURSOR
1391537_AT	*RGD1565408_PREDICTED*	SIMILAR TO SERTA DOMAIN CONTAINING 4
1372767_AT	*RGD1565461_PREDICTED*	SIMILAR TO CDNA SEQUENCE BC043098
1392936_AT	*RGD1565486_PREDICTED*	SIMILAR TO RNA BINDING MOTIF PROTEIN 25
1383581_AT	*RGD1565520_PREDICTED*	SIMILAR TO 60S RIBOSOMAL PROTEIN L7A
1382776_AT	*RGD1565561_PREDICTED*	SIMILAR TO O-ACYLTRANSFERASE (MEMBRANE BOUND) DOMAIN CONTAINING 1

1384070_AT	*RGD1565577_PREDICTED*	SIMILAR TO GEM-INTERACTING PROTEIN
1387388_AT	*RGD1565588_PREDICTED*	SIMILAR TO CALCIUM BINDING PROTEIN P22
1374294_AT	*RGD1565594_PREDICTED*	HYPOTHETICAL LOC293513
1397196_AT	*RGD1565595_PREDICTED*	LOC498009
1372604_AT	*RGD1565597_PREDICTED*	SIMILAR TO RIKEN CDNA 2210421G13
1378390_AT	*RGD1565635_PREDICTED*	SIMILAR TO ZINC FINGER PROTEIN 124
1380619_AT	*RGD1565661_PREDICTED*	SIMILAR TO RIKEN CDNA 3110001I22
1373639_AT	*RGD1565675_PREDICTED*	SIMILAR TO RIKEN CDNA 2410022L05
1372395_AT	*RGD1565757_PREDICTED*	SIMILAR TO KIAA0597 PROTEIN
1373248_AT	*RGD1565800_PREDICTED*	SIMILAR TO HYPOTHETICAL PROTEIN FLJ20674
1393247_AT	*RGD1565847_PREDICTED*	SIMILAR TO ZINC FINGER PROTEIN 560
1376937_AT	*RGD1565927_PREDICTED*	SIMILAR TO 4631422O05RIK PROTEIN
1381759_AT	*RGD1565975_PREDICTED*	HYPOTHETICAL LOC291903
1376013_AT	*RGD1565985_PREDICTED*	SIMILAR TO MKIAA0227 PROTEIN
1383361_AT	*RGD1565996_PREDICTED*	SIMILAR TO DNAJ HOMOLOG SUBFAMILY B MEMBER 6 (HEAT SHOCK PROTEIN J2) (HSJ-2) (MRJ)
1367527_AT	*RGD1565998_PREDICTED*	SIMILAR TO RIBOSOMAL PROTEIN L34
1391062_AT	*RGD1566052_PREDICTED*	SIMILAR TO ELONGATION PROTEIN 4 HOMOLOG
1378155_AT	*RGD1566064_PREDICTED*	SIMILAR TO KIAA1096 PROTEIN
1389102_AT	*RGD1566072_PREDICTED*	SIMILAR TO DOCK1 PROTEIN
1373232_AT	*RGD1566091_PREDICTED*	SIMILAR TO NIDOGEN 2
1393214_AT	*RGD1566144_PREDICTED*	SIMILAR TO HYPOTHETICAL PROTEIN A230042K10
1388903_AT	*RGD1566162_PREDICTED*	T-COMPLEX ASSOCIATED-TESTIS-EXPRESSED 1-LIKE (PROTEIN 91/23)
1374775_AT	*RGD1566252_PREDICTED*	SIMILAR TO KI-67
1372585_AT	*RGD1566254_PREDICTED*	LOC499318
1371755_AT	*RGD1566359_PREDICTED*	SIMILAR TO RIKEN CDNA B230219D22
1371959_AT	*RGD1566374_PREDICTED*	SIMILAR TO HIST2H2AA1 PROTEIN
1374328_AT	*RGD1566393_PREDICTED*	SIMILAR TO HYPOTHETICAL PROTEIN
1392754_AT	*RGD1566394_PREDICTED*	SIMILAR TO CYSTEINE-RICH GLYCOPROTEIN
1389794_AT	*RGD1566403_PREDICTED*	SIMILAR TO OTTHUMP00000040081
1368226_AT	*RGD620382*	NUCLEOSIDE 2-DEOXYRIBOSYLTRANSFERASE DOMAIN CONTAINING PROTEIN RGD620382
1395960_AT	*RHBDL7_PREDICTED*	RHOMBOID, VEINLET-LIKE 7 (DROSOPHILA) (PREDICTED)
1369958_AT	*RHOB*	RHOB GENE
1371659_AT	*RHOC_PREDICTED*	RAS HOMOLOG GENE FAMILY, MEMBER C (PREDICTED)
1382197_AT	*RHOD_PREDICTED*	RAS HOMOLOG GENE FAMILY, MEMBER D (PREDICTED)
1374534_AT	*RHOT2*	MIRO2 PROTEIN
1387153_AT	*RIL*	REVERSION INDUCED LIM GENE
1375020_AT	*RIN3_PREDICTED*	RAS AND RAB INTERACTOR 3 (PREDICTED)
1370422_AT	*RIPK3*	RECEPTOR-INTERACTING SERINE-THREONINE KINASE 3
1374545_AT	*RKHD2_PREDICTED*	RING FINGER AND KH DOMAIN CONTAINING 2 (PREDICTED)
1381386_AT	*RNF10*	RING FINGER PROTEIN 10
1383139_AT	*RNF141*	RING FINGER PROTEIN 141
1395820_AT	*RNF150_PREDICTED*	RING FINGER PROTEIN 150 (PREDICTED)
1388937_AT	*RNF19_PREDICTED*	RING FINGER PROTEIN (C3HC4 TYPE) 19 (PREDICTED)
1376805_AT	*RNF2*	RING FINGER PROTEIN 2
1368662_AT	*RNF39*	RING FINGER PROTEIN 39
1371489_AT	*RNF4*	RING FINGER PROTEIN 4
1372867_AT	*RNMT*	RNA (GUANINE-7-) METHYLTRANSFERASE
1399101_AT	*RNPC2*	RNA-BINDING REGION (RNP1, RRM) CONTAINING 2
1372181_AT	*RPA1*	REPLICATION PROTEIN A1
1388135_AT	*RPA2*	REPLICATION PROTEIN A2
1389202_AT	*RPE_PREDICTED*	RIBULOSE-5-PHOSPHATE-3-EPIMERASE (PREDICTED)
1387176_AT	*RPH3AL*	RABPHILIN 3A-LIKE (WITHOUT C2 DOMAINS)
1374990_AT	*RPL22*	RIBOSOMAL PROTEIN L22
1376110_AT	*RPP25*	RIBONUCLEASE P 25 SUBUNIT (HUMAN)
1392473_AT	*RPP38*	RIBONUCLEASE P/MRP 38KDA SUBUNIT
1398617_AT	*RPS27A*	RIBOSOMAL PROTEIN S27A
1391211_AT	*RPS6KA4_PREDICTED*	RIBOSOMAL PROTEIN S6 KINASE, POLYPEPTIDE 4 (PREDICTED)
1374331_AT	*RQCD1*	RCD1 (REQUIRED FOR CELL DIFFERENTIATION) HOMOLOG 1 (S. POMBE)
1371862_AT	*RRM1_MAPPED*	RIBONUCLEOTIDE REDUCTASE M1 (MAPPED)
1376065_AT	*RRS1_PREDICTED*	RRS1 RIBOSOME BIOGENESIS REGULATOR HOMOLOG (S. CEREVISIAE) (PREDICTED)
1370400_AT	*RT1-N1*	RT1 CLASS IB GENE, H2-TL-LIKE, GRC REGION (N1)
1370400_AT	*RT1-N2*	RT1 CLASS IB GENE, H2-TL-LIKE, GRC REGION(N2)
1370400_AT	*RT1-N3*	RT1 CLASS IB GENE, H2-TL-LIKE, GRC REGION (N3)
1385551_AT	*RT1-O*	RT1 CLASS IB, LOCUS H2-Q-LIKE, GRC REGION
1373571_AT	*RTN3*	RETICULON 3
1389480_AT	*RWDD4A*	RWD DOMAIN CONTAINING 4A
1374077_AT	*RXRA*	RETINOID X RECEPTOR ALPHA
1375170_AT	*S100A11_PREDICTED*	S100 CALCIUM BINDING PROTEIN A11 (CALIZZARIN) (PREDICTED)
1388356_AT	*S100A16_PREDICTED*	S100 CALCIUM BINDING PROTEIN A16 (PREDICTED)
1371774_AT	*SAT_MAPPED*	SPERMIDINE/SPERMINE N1-ACETYL TRANSFERASE (MAPPED)
1372968_AT	*SBF1_PREDICTED*	SET BINDING FACTOR 1 (PREDICTED)
1388819_AT	*SCAMP1*	SECRETORY CARRIER MEMBRANE PROTEIN 1
1367688_AT	*SCAMP4*	SECRETORY CARRIER MEMBRANE PROTEIN 4
1377198_AT	*SCAP2*	SRC FAMILY ASSOCIATED PHOSPHOPROTEIN 2
1391279_AT	*SCIN*	SCINDERIN
1377647_AT	*SCMH1_PREDICTED*	SEX COMB ON MIDLEG HOMOLOG 1 (PREDICTED)
1387896_AT	*SCP2*	STEROL CARRIER PROTEIN 2
1367721_AT	*SDC4*	SYNDECAN 4
1376973_AT	*SDCBP2*	SYNDECAN BINDING PROTEIN (SYNTENIN) 2
1372874_AT	*SDCCAG8*	SLINKY
1373043_AT	*SDF2L1*	STROMAL CELL-DERIVED FACTOR 2-LIKE 1
1378160_AT	*SDFR2_PREDICTED*	STROMAL CELL DERIVED FACTOR RECEPTOR 2 (PREDICTED)
1381981_AT	*SEC10L1*	SEC10-LIKE 1 (S. CEREVISIAE)
1387369_AT	*SEC15L1*	SEC15-LIKE 1 (S. CEREVISIAE)
1388857_AT	*SEC23B_PREDICTED*	SEC23B (S. CEREVISIAE) (PREDICTED)
1397765_AT	*SEC61A2_PREDICTED*	SEC61, ALPHA SUBUNIT 2 (S. CEREVISIAE) (PREDICTED)
1390115_AT	*SEC63_PREDICTED*	SEC63-LIKE (S. CEREVISIAE) (PREDICTED)
1377336_AT	*SEMA3B_PREDICTED*	(SEMAPHORIN) 3B (PREDICTED)
1374678_AT	*SEMA4B*	SEMA DOMAIN, IMMUNOGLOBULIN DOMAIN (IG),
1368926_AT	*SEMA4F*	SEMAPHORIN 4F

1372594_AT	*SENP5_PREDICTED*	SUMO/SENTRIN SPECIFIC PROTEASE 5 (PREDICTED)
1372417_AT	*SERTAD1*	SERTA DOMAIN CONTAINING 1
1388132_AT	*SFPQ*	SPLICING FACTOR PROLINE/GLUTAMINE RICH
1370189_AT	*SFRS10*	SPLICING FACTOR, ARGININE/SERINE-RICH 10 (TRANSFORMER 2 HOMOLOG, DROSOPHILA)
1383520_AT	*SFRS12*	SPLICING FACTOR, ARGININE/SERINE-RICH 12
1368992_A_AT	*SFRS5*	SPLICING FACTOR, ARGININE/SERINE-RICH 5
1387008_AT	*SFXN3*	SIDEROFLEXIN 3
1367802_AT	*SGK*	SERUM/GLUCOCORTICOID REGULATED KINASE
1373874_AT	*SGPP1*	SPHINGOSINE-1-PHOSPHATE PHOSPHATASE 1
1387106_AT	*SH3BP4*	SH3-DOMAIN BINDING PROTEIN 4
1387294_AT	*SH3BP5*	SH3-DOMAIN BINDING PROTEIN 5 (BTK-ASSOCIATED)
1371485_AT	*SH3MD1_PREDICTED*	SH3 MULTIPLE DOMAINS 1 (PREDICTED)
1393617_AT	*SH3RF2*	SH3 DOMAIN CONTAINING RING FINGER 2
1392301_AT	*SH3TC1_PREDICTED*	SH3 DOMAIN AND TETRATRICOPEPTIDE REPEATS 1 (PREDICTED)
1387266_AT	*SIAH1A*	SEVEN IN ABSENTIA 1A
1392012_AT	*SIAHBP1*	SIAH BINDING PROTEIN 1; FBP INTERACTING REPRESSOR
1379390_AT	*SIAT7B*	ALPHA-N-ACETYLGALACTOSAMINIDE ALPHA-2,6-SIALYLTRANSFERASE II ()
1377690_AT	*SIPA1L3*	SIGNAL-INDUCED PROLIFERATION-ASSOCIATED 1 LIKE 3
1383962_AT	*SIVA_PREDICTED*	CD27 BINDING PROTEIN (HINDU GOD OF DESTRUCTION)
1381253_AT	*SLC12A2*	SOLUTE CARRIER FAMILY 12, MEMBER 2
1371525_AT	*SLC12A7*	SOLUTE CARRIER FAMILY 12 (POTASSIUM/CHLORIDE TRANSPORTERS), MEMBER 7
1368965_AT	*SLC16A3*	MONOCARBOXYLATE TRANSPORTER
1368564_AT	*SLC17A6*	SOLUTE CARRIER FAMILY 17, MEMBER 6
1371040_AT	*SLC1A5*	SOLUTE CARRIER FAMILY 1, MEMBER 7
1374652_AT	*SLC25A26_PREDICTED*	SOLUTE CARRIER FAMILY 25, MEMBER 26 (PREDICTED)
1368193_AT	*SLC26A4*	SOLUTE CARRIER FAMILY 26, MEMBER 4
1367789_AT	*SLC27A1*	SOLUTE CARRIER FAMILY 27 (FATTY ACID TRANSPORTER), MEMBER 1
1398295_AT	*SLC29A1*	SOLUTE CARRIER FAMILY 29 (NUCLEOSIDE TRANSPORTERS), MEMBER 1
1388534_AT	*SLC31A1*	SOLUTE CARRIER FAMILY 31 (COPPER TRANSPORTERS), MEMBER 1
1383996_AT	*SLC35E1_PREDICTED*	SOLUTE CARRIER FAMILY 35, MEMBER E1 (PREDICTED)
1387942_AT	*SLC35E4*	SOLUTE CARRIER FAMILY 35, MEMBER E4
1398531_AT	*SLC36A4_PREDICTED*	SOLUTE CARRIER FAMILY 36 (PROTON/AMINO ACID SYMPORTER), MEMBER 4 (PREDICTED)
1376709_AT	*SLC39A8*	SOLUTE CARRIER FAMILY 39 (METAL ION TRANSPORTER), MEMBER 8
1390412_AT	*SLC40A1*	SOLUTE CARRIER FAMILY 39 (IRON-REGULATED TRANSPORTER), MEMBER 1
1391613_AT	*SLC8A3*	SOLUTE CARRIER FAMILY 8 (SODIUM/CALCIUM EXCHANGER), MEMBER 3
1387793_AT	*SLC9A3R1*	ERM-BINDING PHOSPHOPROTEIN
1395986_AT	*SLIT2*	SLIT HOMOLOG 2 (DROSOPHILA)
1372489_AT	*SLMAP_PREDICTED*	SARCOLEMMA ASSOCIATED PROTEIN (PREDICTED)
1390534_AT	*SMC5L1_PREDICTED*	SMC5 STRUCTURAL MAINTENANCE OF CHROMOSOMES 5-LIKE 1 (YEAST) (PREDICTED)
1377202_AT	*SMC6L1_PREDICTED*	SMC6 STRUCTURAL MAINTENANCE OF CHROMOSOMES 6-LIKE 1 (YEAST) (PREDICTED)
1368991_AT	*SMPD3*	SPHINGOMYELIN PHOSPHODIESTERASE 3, NEUTRAL
1373850_AT	*SMPDL3B*	SPHINGOMYELIN PHOSPHODIESTERASE, ACID-LIKE 3B
1373213_AT	*SNAP29*	SYNAPTOSOMAL-ASSOCIATED PROTEIN 29
1397294_AT	*SNRPB*	SMALL NUCLEAR RIBONUCLEOPROTEIN POLYPEPTIDES B AND B1
1372743_AT	*SNX5_PREDICTED*	SORTING NEXIN 5 (PREDICTED)
1372727_AT	*SOCS2*	SUPPRESSOR OF CYTOKINE SIGNALING 2
1370173_AT	*SOD2*	SUPEROXIDE DISMUTASE 2, MITOCHONDRIAL
1391557_AT	*SOX15_PREDICTED*	SRY-BOX CONTAINING GENE 15 (PREDICTED)
1392990_AT	*SOX17_PREDICTED*	SRY-BOX CONTAINING GENE 17 (PREDICTED)
1392180_AT	*SP1*	SP1 TRANSCRIPTION FACTOR
1397734_AT	*SP3*	SP3 TRANSCRIPTION FACTOR
1388520_AT	*SPAG9_PREDICTED*	SPERM ASSOCIATED ANTIGEN 9 (PREDICTED)
1391885_AT	*SPATA9_PREDICTED*	SPERMATOGENESIS ASSOCIATED 9 (PREDICTED)
1383192_AT	*SPG4_PREDICTED*	SPASTIC PARAPLEGIA 4 (AUTOSOMAL DOMINANT; SPASTIN) (PREDICTED)
1368254_A_AT	*SPHK1*	SPHINGOSINE KINASE 1
1383290_AT	*SPINT1*	HEPATOCYTE GROWTH FACTOR ACTIVATOR INHIBITOR 1
1388320_AT	*SPINT2*	SERINE PROTEASE INHIBITOR, KUNITZ TYPE 2
1370838_S_AT	*SPNA2*	ALPHA-SPECTRIN 2
1389008_AT	*SPRED2*	SPROUTY-RELATED, EVH1 DOMAIN CONTAINING 2
1370420_AT	*SRD5A1*	STEROID 5 ALPHA-REDUCTASE 1
1391773_AT	*SRP54*	SIGNAL RECOGNITION PARTICLE 54
1371714_AT	*SRPK1*	SERINE/ARGININE-RICH PROTEIN SPECIFIC KINASE 1
1370228_AT	*SRPRB*	SIGNAL RECOGNITION PARTICLE RECEPTOR, B SUBUNIT
1375895_AT	*SRR*	SERINE RACEMASE
1371425_AT	*SRRM1_PREDICTED*	SERINE/ARGININE REPETITIVE MATRIX 1 (PREDICTED)
1383138_AT	*SSH3*	SLINGSHOT HOMOLOG 3 (DROSOPHILA)
1398409_AT	*ST13*	SUPPRESSION OF TUMORIGENICITY 13
1387195_AT	*ST14*	SUPPRESSION OF TUMORIGENICITY 14
1373288_AT	*ST5_PREDICTED*	SUPPRESSION OF TUMORIGENICITY 5 (PREDICTED)
1389226_AT	*STAG1_PREDICTED*	STROMAL ANTIGEN 1 (PREDICTED)
1389420_AT	*STAP2*	SIGNAL-TRANSDUCING ADAPTOR PROTEIN-2
1398063_X_AT	*STFA3_PREDICTED*	STEFIN A3 (PREDICTED)
1376024_AT	*STIM1_PREDICTED*	STROMAL INTERACTION MOLECULE 1 (PREDICTED)
1379279_AT	*STIM2_PREDICTED*	STROMAL INTERACTION MOLECULE 2 (PREDICTED)
1369712_AT	*STK3*	SERINE/THREONINE KINASE 3 (STE20 HOMOLOG, YEAST)
1392231_AT	*STK4_PREDICTED*	SERINE/THREONINE KINASE 4 (PREDICTED)
1372078_AT	*STRAP*	SERINE/THREONINE KINASE RECEPTOR ASSOCIATED PROTEIN
1379732_AT	*STX11*	SYNTAXIN 11
1390447_AT	*STX3*	SYNTAXIN 3
1388753_AT	*SULF2*	SULFATASE 2
1370019_AT	*SULT1A1*	SULFOTRANSFERASE FAMILY 1A, PHENOL-PREFERRING, MEMBER 1
1377281_AT	*SUPT16H_PREDICTED*	SUPPRESSOR OF TY 16 HOMOLOG (S. CEREVISIAE) (PREDICTED)
1384849_AT	*SUSD1_PREDICTED*	SUSHI DOMAIN CONTAINING 1 (PREDICTED)
1388586_AT	*SYNJ1*	SYNAPTOJANIN 1
1395678_AT	*SYT15*	SYNAPTOTAGMIN 15
1388199_AT	*TACSTD1*	TUMOR-ASSOCIATED CALCIUM SIGNAL TRANSDUCER 1
1391509_AT	*TACSTD2*	TUMOR-ASSOCIATED CALCIUM SIGNAL TRANSDUCER 2
1367570_AT	*TAGLN*	TRANSGELIN
1373922_AT	*TANC*	TPR DOMAIN, ANKYRIN-REPEAT AND COILED-COIL-CONTAINING
1388392_AT	*TAX1BP3*	TAX1 (HUMAN T-CELL LEUKEMIA VIRUS TYPE I) BINDING PROTEIN 3

1374972_AT	*TBC1D2_PREDICTED*	TBC1 DOMAIN FAMILY, MEMBER 2 (PREDICTED)
1373242_AT	*TBPL1_PREDICTED*	TATA BOX BINDING PROTEIN-LIKE 1 (PREDICTED)
1371787_AT	*TCEB3*	TRANSCRIPTION ELONGATION FACTOR B (SIII), POLYPEPTIDE 3
1379914_AT	*TCFCP2L2*	TRANSCRIPTION FACTOR CP2-LIKE 2
1388903_AT	*TCTE1L*	T-COMPLEX ASSOCIATED-TESTIS-EXPRESSED 1-LIKE (PROTEIN 91/23)
1374697_AT	*TECH*	NEURONAL RHOA GEF PROTEIN
1393681_AT	*TESSP5*	TESTIS-SPECIFIC SERINE PROTEASE-5
1370453_AT	*TEX101*	TESTIS EXPRESSED GENE 101
1382487_AT	*TEX14_PREDICTED*	TESTIS EXPRESSED GENE 14 (PREDICTED)
1370228_AT	*TF*	TRANSFERRIN
1383171_AT	*TFB2M*	TRANSCRIPTION FACTOR B2, MITOCHONDRIAL
1387450_AT	*TGFA*	TRANSFORMING GROWTH FACTOR ALPHA
1370887_AT	*TGFB1I1*	TRANSFORMING GROWTH FACTOR BETA 1 INDUCED TRANSCRIPT 1
1398759_AT	*TGFB1I4*	TRANSFORMING GROWTH FACTOR BETA 1 INDUCED TRANSCRIPT 4
1373421_AT	*TGIF*	TG INTERACTING FACTOR
1370051_AT	*TGM1*	TRANSGLUTAMINASE 1
1378447_AT	*THRAP1_PREDICTED*	THYROID HORMONE RECEPTOR ASSOCIATED PROTEIN 1 (PREDICTED)
1382536_AT	*THRAP2_PREDICTED*	THYROID HORMONE RECEPTOR ASSOCIATED PROTEIN 2 (PREDICTED)
1367525_AT	*THRAP3*	THYROID HORMONE RECEPTOR ASSOCIATED PROTEIN 3
1370474_AT	*THRB*	THYROID HORMONE RECEPTOR BETA
1388567_AT	*THUMPD1*	THUMP DOMAIN CONTAINING 1
1381985_AT	*TIA1*	CYTOTOXIC GRANULE-ASSOCIATED RNA BINDING PROTEIN 1
1368650_AT	*TIEG*	TGFB INDUCIBLE EARLY GROWTH RESPONSE
1368522_AT	*TIMELESS*	TIMELESS HOMOLOG (DROSOPHILA)
1390237_AT	*TIMM8A*	TRANSLOCASE OF INNER MITOCHONDRIAL MEMBRANE 8 HOMOLOG A (YEAST)
1372473_AT	*TJP1_PREDICTED*	TIGHT JUNCTION PROTEIN 1 (PREDICTED)
1370940_AT	*TJP2*	TIGHT JUNCTION PROTEIN 2
1378567_AT	*TJP3_PREDICTED*	TIGHT JUNCTION PROTEIN 3 (PREDICTED)
1376635_AT	*TKT*	TRANSKETOLASE
1374425_AT	*TLE1_PREDICTED*	TRANSDUCIN-LIKE ENHANCER OF SPLIT 1, HOMOLOG OF DROSOPHILA E(SPL) (PREDICTED)
1387169_AT	*TLE3*	TRANSDUCIN-LIKE ENHANCER OF SPLIT 3, E(SPL) HOMOLOG (DROSOPHILA)
1392280_AT	*TLR2*	TOLL-LIKE RECEPTOR 2
1386943_AT	*TM4SF11*	TRANSMEMBRANE 4 SUPERFAMILY MEMBER 11
1391684_AT	*TMEM14A_PREDICTED*	TRANSMEMBRANE PROTEIN 14A (PREDICTED)
1382387_AT	*TMEM16A_PREDICTED*	TRANSMEMBRANE PROTEIN 16A (PREDICTED)
1372624_AT	*TMEM16F_PREDICTED*	TRANSMEMBRANE PROTEIN 16F (PREDICTED)
1394160_AT	*TMEM2_PREDICTED*	TRANSMEMBRANE PROTEIN 2 (PREDICTED)
1392534_AT	*TMEPAI_PREDICTED*	TRANSMEMBRANE, PROSTATE ANDROGEN INDUCED RNA (PREDICTED)
1399015_AT	*TMP21*	TRANSMEMBRANE TRAFFICKING PROTEIN 21
1371796_AT	*TMX2*	THIOREDOXIN-RELATED TRANSMEMBRANE PROTEIN 2
1371911_AT	*TNFAIP1*	TUMOR NECROSIS FACTOR, ALPHA-INDUCED PROTEIN 1 (ENDOTHELIAL)
1371785_AT	*TNFRSF12A*	TUMOR NECROSIS FACTOR RECEPTOR SUPERFAMILY, MEMBER 12A
1388492_AT	*TNIP1_PREDICTED*	TNFAIP3 INTERACTING PROTEIN 1 (PREDICTED)
1371610_AT	*TNKS_PREDICTED*	TANKYRASE, TRF1-INTERACTING ANKYRIN-RELATED ADP-RIBOSE POLYMERASE (PREDICTED)
1393095_AT	*TNKS1BP1_PREDICTED*	TANKYRASE 1 BINDING PROTEIN 1 (PREDICTED)
1388145_AT	*TNXA*	TENASCIN XA
1373039_AT	*TOMM70A*	TRANSLOCASE OF OUTER MITOCHONDRIAL MEMBRANE 70 HOMOLOG A
1399046_AT	*TOP1*	TOPOISOMERASE (DNA) I
1368540_AT	*TPBG*	TROPHOBLAST GLYCOPROTEIN
1387617_AT	*TPM3*	TROPOMYOSIN 3, GAMMA
1386979_AT	*TPO1*	DEVELOPMENTALLY REGULATED PROTEIN TPO1
1367976_AT	*TPP2*	TRIPEPTIDYL PEPTIDASE II
1382939_AT	*TPR*	TRANSLOCATED PROMOTER REGION
1377052_AT	*TRIM26*	TRIPARTITE MOTIF PROTEIN 26
1377234_AT	*TRIM27_PREDICTED*	TRIPARTITE MOTIF PROTEIN 27 (PREDICTED)
1389058_AT	*TRIM29_PREDICTED*	TRIPARTITE MOTIF PROTEIN 29 (PREDICTED)
1373398_AT	*TRIM37_PREDICTED*	TRIPARTITE MOTIF PROTEIN 37 (PREDICTED)
1390415_AT	*TRIP13*	THYROID HORMONE RECEPTOR INTERACTOR 13
1398521_AT	*TRPV6*	TRANSIENT RECEPTOR POTENTIAL CATION CHANNEL, SUBFAMILY V, MEMBER 6
1398953_AT	*TSTA3_PREDICTED*	TISSUE SPECIFIC TRANSPLANTATION ANTIGEN P35B (PREDICTED)
1376974_AT	*TTC7*	TETRATRICOPEPTIDE REPEAT DOMAIN 7
1376035_AT	*TTC7B_PREDICTED*	TETRATRICOPEPTIDE REPEAT DOMAIN 7B (PREDICTED)
1371542_AT	*TUBA4*	TUBULIN, ALPHA 4
1371390_AT	*TUBB2*	TUBULIN, BETA, 2
1371618_S_AT	*TUBB3*	TUBULIN, BETA 3
1398624_X_AT	*TUBB4*	TUBULIN, BETA 4
1384143_AT	*TUFT1_PREDICTED*	TUFTELIN 1 (PREDICTED)
1376712_AT	*TXNDC4*	THIOREDOXIN DOMAIN CONTAINING 4 (ENDOPLASMIC RETICULUM)
1371131_A_AT	*TXNIP*	UPREGULATED BY 1,25-DIHYDROXYVITAMIN D-3
1388862_AT	*TXNL1*	THIOREDOXIN-LIKE (32KD)
1388656_AT	*UBC2E*	UBIQUITIN-CONJUGATING ENZYME E2D 2
1388656_AT	*UBE2D2*	UBIQUITIN-CONJUGATING ENZYME E2D 2
1398802_AT	*UBE2D3*	UBIQUITIN-CONJUGATING ENZYME E2D 3 (UBC4/5 HOMOLOG, YEAST)
1383408_AT	*UBE2G1*	UBIQUITIN-CONJUGATING ENZYME E2G 1 (UBC7 HOMOLOG, C. ELEGANS)
1388474_AT	*UBE2I*	UBIQUITIN-CONJUGATING ENZYME E2I
1371945_AT	*UBE2L3_PREDICTED*	UBIQUITIN-CONJUGATING ENZYME E2L 3 (PREDICTED)
1398897_AT	*UBE2V1_PREDICTED*	UBIQUITIN-CONJUGATING ENZYME E2 VARIANT 1 (PREDICTED)
1381878_AT	*UBN1_PREDICTED*	UBINUCLEIN 1 (PREDICTED)
1388719_AT	*UBQLN1*	UBIQUILIN 1
1383477_AT	*UCHL5*	UBIQUITIN CARBOXYL-TERMINAL HYDROLASE L5
1368669_AT	*UCP2*	UNCOUPLING PROTEIN 2
1388696_AT	*UFD1L*	UBIQUITIN FUSION DEGRADATION 1-LIKE
1387975_AT	*UGCG*	UDP-GLUCOSE CERAMIDE GLUCOSYLTRANSFERASE
1389218_AT	*UGCGL1*	UDP-GLUCOSE CERAMIDE GLUCOSYLTRANSFERASE-LIKE 1
1389587_AT	*UMPS*	URIDINE MONOPHOSPHATE SYNTHETASE
1383875_AT	*UPK1B*	UROPLAKIN 1B
1377004_AT	*USP15*	UBIQUITIN SPECIFIC PROTEASE 15
1389427_AT	*USP3*	UBIQUITIN SPECIFIC PROTEASE 3
1374940_AT	*USP36_PREDICTED*	UBIQUITIN SPECIFIC PROTEASE 36 (PREDICTED)
1399029_AT	*USP48*	UBIQUITIN SPECIFIC PROTEASE 48

1379341_AT	*USP6NL_PREDICTED*	USP6 N-TERMINAL LIKE (PREDICTED)
1394435_AT	*VANGL1_PREDICTED*	VANG, VAN GOGH-LIKE 1 (DROSOPHILA) (PREDICTED)
1386745_AT	*VCIP135*	VALOSIN-CONTAINING PROTEIN (P97)/P47 COMPLEX-INTERACTING PROTEIN 135
1368463_AT	*VEGFC*	VASCULAR ENDOTHELIAL GROWTH FACTOR C
1374072_AT	*VEZF1_PREDICTED*	VASCULAR ENDOTHELIAL ZINC FINGER 1 (PREDICTED)
1375533_AT	*VGLL4*	VESTIGIAL LIKE 4 (DROSOPHILA)
1370875_AT	*VIL2*	VILLIN 2
1389253_AT	*VNN1*	VANIN 1
1389560_AT	*VPS24*	VACUOLAR PROTEIN SORTING 24 (YEAST)
1372806_AT	*VPS35_MAPPED*	VACUOLAR PROTEIN SORTING 35 (MAPPED)
1389369_AT	*VPS52*	VACUOLAR PROTEIN SORTING 52 (YEAST)
1380009_AT	*VRK1*	VACCINIA RELATED KINASE 1
1368854_AT	*VSNL1*	VISININ-LIKE 1
1379980_AT	*VTI1A*	VESICLE TRANSPORT THROUGH INTERACTION WITH T-SNARES HOMOLOG 1A (YEAST)
1376448_AT	*WDFY1*	WD REPEAT AND FYVE DOMAIN CONTAINING 1
1389128_AT	*WDFY3_PREDICTED*	WD REPEAT AND FYVE DOMAIN CONTAINING 3 (PREDICTED)
1391201_AT	*WDHD1_PREDICTED*	WD REPEAT AND HMG-BOX DNA BINDING PROTEIN 1 (PREDICTED)
1389993_AT	*WDR33_PREDICTED*	WD REPEAT DOMAIN 33 (PREDICTED)
1380499_AT	*WDR9_PREDICTED*	WD REPEAT DOMAIN 9 (PREDICTED)
1380148_AT	*WHSC1_PREDICTED*	WOLF-HIRSCHHORN SYNDROME CANDIDATE 1 (PREDICTED)
1392806_AT	*WHSC1L1_PREDICTED*	WOLF-HIRSCHHORN SYNDROME CANDIDATE 1-LIKE 1 (PREDICTED)
1387021_AT	*WIG1*	WILD-TYPE P53-INDUCED GENE 1
1381034_AT	*WNT10A_PREDICTED*	WINGLESS RELATED MMTV INTEGRATION SITE 10A (PREDICTED)
1389090_AT	*WRNIP1*	WERNER HELICASE INTERACTING PROTEIN 1
1374204_AT	*WSB1*	WD REPEAT AND SOCS BOX-CONTAINING 1
1369695_AT	*WT1*	WILMS TUMOR 1
1374395_AT	*XPO1*	EXPORTIN 1, CRM1 HOMOLOG (YEAST)
1383296_A_AT	*XPO4_PREDICTED*	EXPORTIN 4 (PREDICTED)
1367498_AT	*YTHDF1*	YTH DOMAIN FAMILY 1
1389524_AT	*YTHDF3_PREDICTED*	YTH DOMAIN FAMILY 3 (PREDICTED)
1398800_AT	*YWHAB*	TYROSINE 3-MONOOXYGENASE/TRYPTOPHAN 5-MONOOXYGENASE ACTIVATION PROTEIN
1395901_AT	*YY1*	YY1 TRANSCRIPTION FACTOR
1393652_AT	*ZBTB1*	ZINC FINGER AND BTB DOMAIN CONTAINING 1
1376125_AT	*ZBTB10*	ZINC FINGER AND BTB DOMAIN CONTAINING 10
1390142_AT	*ZCWCC3_PREDICTED*	ZINC FINGER, CW-TYPE WITH COILED-COIL DOMAIN 3 (PREDICTED)
1370828_AT	*ZDHHC2*	ZINC FINGER, DHHC DOMAIN CONTAINING 2
1393388_AT	*ZDHHC3*	ZINC FINGER, DHHC DOMAIN CONTAINING 3 (PREDICTED)
1398339_AT	*ZFP162*	ZINC FINGER PROTEIN 162
1394591_AT	*ZFP207*	ZINC FINGER PROTEIN 207
1389252_AT	*ZFP238*	ZINC FINGER PROTEIN 238
1382223_AT	*ZFP262_PREDICTED*	ZINC FINGER PROTEIN 262 (PREDICTED)
1368228_AT	*ZFP265*	ZINC FINGER PROTEIN 265
1379441_AT	*ZFP294*	ZINC FINGER PROTEIN 294
1373763_AT	*ZFP297B*	ZINC FINGER PROTEIN 297B
1372865_AT	*ZFP364_PREDICTED*	ZINC FINGER PROTEIN 364 (PREDICTED)
1379967_AT	*ZFP367*	ZINC FINGER PROTEIN 367
1387105_AT	*ZFP422*	ZINC FINGER PROTEIN 422
1387105_AT	*ZFP422_PREDICTED*	ZINC FINGER PROTEIN 422 (PREDICTED)
1375148_AT	*ZFPM1_PREDICTED*	ZINC FINGER PROTEIN, MULTITYPE 1 (PREDICTED)
1372319_AT	*ZHX3*	ZINC FINGERS AND HOMEOBOXES 3
1379264_AT	*ZNRF1_PREDICTED*	ZINC AND RING FINGER 1 (PREDICTED)
1376113_AT	*ZSWIM1_PREDICTED*	ZINC FINGER, SWIM DOMAIN CONTAINING 1 (PREDICTED)

APPENDIX B

Transcripts ≥2-fold decreased in CX4 compared to GN6TF

AFFY ID	*GENE SYMBOL*	GENE DESCRIPTION
1373660_AT	*AFG3L1_PREDICTED*	AFG3(ATPASE FAMILY GENE 3)-LIKE 1 (YEAST) (PREDICTED)
1370137_AT	*AGPS*	ALKYLGLYCERONE PHOSPHATE SYNTHASE
1380746_AT	*AHRR*	ARYL-HYDROCARBON RECEPTOR REPRESSOR
1371493_AT	*AP2A2*	ADAPTOR PROTEIN COMPLEX AP-2, ALPHA 2 SUBUNIT
1371497_AT	*ASB6*	ANKYRIN REPEAT AND SOCS BOX-CONTAINING PROTEIN 6
1379741_AT	*ATP6V0A4_PREDICTED*	ATPASE, H+ TRANSPORTING, LYSOSOMAL V0 SUBUNIT A ISOFORM 4 (PREDICTED)
1369248_A_AT	*BIRC4*	BACULOVIRAL IAP REPEAT-CONTAINING 4
1390873_AT	*BTBD11_PREDICTED*	BTB (POZ) DOMAIN CONTAINING 11 (PREDICTED)
1387446_AT	*C1GALT1*	CORE 1 UDP-GALACTOSE:N-ACETYLGALACTOSAMINE-ALPHA-R
1387893_AT	*C1S*	COMPLEMENT COMPONENT 1, S SUBCOMPONENT
1387726_AT	*CDX2*	CAUDAL TYPE HOMEO BOX 2
1385827_AT	*CLC*	CARDIOTROPHIN-LIKE CYTOKINE
1374190_AT	*CLYBL*	CITRATE LYASE BETA LIKE
1390846_AT	*COL16A1*	PROCOLLAGEN, TYPE XVI, ALPHA 1
1368347_AT	*COL5A3*	COLLAGEN, TYPE V, ALPHA 3
1389340_AT	*CRIP3_PREDICTED*	CYSTEINE-RICH PROTEIN 3 (PREDICTED)
1371847_AT	*CRTAP_PREDICTED*	CARTILAGE ASSOCIATED PROTEIN (PREDICTED)
1376051_AT	*CRYL1*	CRYSTALLIN, LAMDA 1
1378377_AT	*DAPP1_PREDICTED*	DUAL ADAPTOR FOR PHOSPHOTYROSINE AND 3-PHOSPHOINOSITIDES 1 (PREDICTED)
1395316_AT	*DDX21A*	DEAD (ASP-GLU-ALA-ASP) BOX POLYPEPTIDE 21A
1382024_AT	*DNAJB6*	DNAJ (HSP40) HOMOLOG, SUBFAMILY B, MEMBER 6
1385210_AT	*DOCK5_PREDICTED*	DEDICATOR OF CYTOKINESIS 5 (PREDICTED)
1368315_AT	*ENTPD6*	ECTONUCLEOSIDE TRIPHOSPHATE DIPHOSPHOHYDROLASE 6
1398466_AT	*EPS15*	EPIDERMAL GROWTH FACTOR RECEPTOR PATHWAY SUBSTRATE 15
1383213_AT	*EPS8_PREDICTED*	EPIDERMAL GROWTH FACTOR RECEPTOR PATHWAY SUBSTRATE 8 (PREDICTED)
1369587_AT	*EREG*	EPIREGULIN
1393808_AT	*FA2H_PREDICTED*	FATTY ACID 2-HYDROXYLASE (PREDICTED)
1381193_AT	*FAM34A_PREDICTED*	FAMILY WITH SEQUENCE SIMILARITY 34, MEMBER A (PREDICTED)
1389106_AT	*FBXW9*	F-BOX AND WD-40 DOMAIN PROTEIN 9
1378046_AT	*FUK_PREDICTED*	FUCOKINASE (PREDICTED)
1382325_AT	*GCAT*	GLYCINE C-ACETYLTRANSFERASE (2-AMINO-3-KETOBUTYRATE-COENZYME A LIGASE)
1382351_AT	*GEM_PREDICTED*	GTP BINDING PROTEIN (GENE OVEREXPRESSED IN SKELETAL MUSCLE) (PREDICTED)
1378079_AT	*GOLGA3_PREDICTED*	GOLGI AUTOANTIGEN, GOLGIN SUBFAMILY A, 3 (PREDICTED)
1376650_AT	*GOLGA5*	GOLGI AUTOANTIGEN, GOLGIN SUBFAMILY A, 5
1369571_AT	*GOLPH3*	GOLGI PHOSPHOPROTEIN 3
1387182_AT	*GPR37*	G PROTEIN-COUPLED RECEPTOR 37
RC_AI235747_AT	*GSTA2*	GLUTATHIONE-S-TRANSFERASE, ALPHA TYPE2
1382779_AT	*HACE1_PREDICTED*	HECT DOMAIN AND ANKYRIN REPEAT CONTAINING, E3 UBIQUITIN PROTEIN LIGASE 1
1392089_AT	*HCFC2*	HOST CELL FACTOR C2
1393629_AT	*HLX1_PREDICTED*	H2.0-LIKE HOMEO BOX 1 (DROSOPHILA) (PREDICTED)
1392616_AT	*IAG2*	IMPLANTATION-ASSOCIATED PROTEIN
AF008554_AT	*IAG2*	IMPLANTATION-ASSOCIATED PROTEIN
1391133_AT	*IL17RC_PREDICTED*	INTERLEUKIN 17 RECEPTOR C (PREDICTED)
1387642_AT	*IL23A*	INTERLEUKIN 23, ALPHA SUBUNIT P19
1385649_AT	*ITGA5_MAPPED*	INTEGRIN ALPHA 5 (MAPPED)
1369038_AT	*ITGAD*	INTEGRIN, ALPHA D
1388329_AT	*KA13*	TYPE I KERATIN KA13
1372153_AT	*KA15*	TYPE I KERATIN KA15
RC_AA859966_I_AT	*KCTD13*	POTASSIUM CHANNEL TETRAMERISATION DOMAIN CONTAINING 13
1395966_AT	*KCTD14_PREDICTED*	POTASSIUM CHANNEL TETRAMERISATION DOMAIN CONTAINING 14 (PREDICTED)
1392292_AT	*KCTD5_PREDICTED*	POTASSIUM CHANNEL TETRAMERISATION DOMAIN CONTAINING 5 (PREDICTED)
1369253_AT	*KREMEN*	KRINGLE CONTAINING TRANSMEMBRANE PROTEIN
1388747_AT	*LCMT1*	LEUCINE CARBOXYL METHYLTRANSFERASE 1
1372469_AT	*LOC292322*	SIMILAR TO STRESS-INDUCED-PHOSPHOPROTEIN 1
1396034_AT	*LOC307660*	CARBOXYLESTERASE 615
1381162_AT	*LOC309891*	SIMILAR TO SEPTIN 10 ISOFORM 1
1383673_AT	*LOC317247*	SIMILAR TO NAP1L2
1394537_AT	*LOC317380*	SIMILAR TO LMO6 PROTEIN
1378985_AT	*LOC362681*	SIMILAR TO PSEUDOURIDYLATE SYNTHASE-LIKE 1
1383213_AT	*LOC365516*	SIMILAR TO EPS8
1386282_X_AT	*LOC367880*	HYPOTHETICAL GENE SUPPORTED BY NM_138833
RC_AI235747_AT	*LOC494499*	LOC494499 PROTEIN
AF008554_AT	*LOC497846*	HYPOTHETICAL GENE SUPPORTED BY NM_053946
1392839_AT	*LOC498176*	SIMILAR TO BRI3-BINDING PROTEIN
1375552_AT	*LOC498351*	SIMILAR TO SIGNAL RECOGNITION PARTICLE,72 KDA SUBUNIT
1372291_AT	*LOC498512*	SIMILAR TO OXA1L PROTEIN
1376011_AT	*LOC501789*	SIMILAR TO MITOGEN-ACTIVATED PROTEIN KINASE KINASE KINASE 13
RC_AI102539_AT	*LOC502605*	SIMILAR TO LIPOPROTEIN RECEPTOR-RELATED PROTEIN
1369866_AT	*LOC56825*	PROCHYMOSIN
RC_AI102539_AT	*LRP1*	LOW DENSITY LIPOPROTEIN RECEPTOR-RELATED PROTEIN 1
1382277_AT	*LY96*	LYMPHOCYTE ANTIGEN 96
1395316_AT	*MAGEH1*	MELANOMA ANTIGEN, FAMILY H, 1
1397556_AT	*MAK3_PREDICTED*	MAK3 HOMOLOG (S. CEREVISIAE) (PREDICTED)
RC_AI235753_AT	*MAPK3*	MITOGEN ACTIVATED PROTEIN KINASE 3
1387330_AT	*MEPE*	MATRIX EXTRACELLULAR PHOSPHOGLYCOPROTEIN WITH ASARM MOTIF (BONE)
1381388_AT	*MGC116217*	SIMILAR TO NASOPHARYNGEAL EPITHELIUM SPECIFIC PROTEIN 1
1387500_AT	*MID1*	MIDLINE 1
1391095_AT	*MMP19_PREDICTED*	MATRIX METALLOPROTEINASE 19 (PREDICTED)
1397372_AT	*MOBK1B_PREDICTED*	SIMILAR TO MOB4B PROTEIN
1387745_AT	*MOX2R*	ANTIGEN IDENTIFIED BY MONOCLONAL ANTIBODY MRC OX-2 RECEPTOR
1387732_AT	*MTERF*	MITOCHONDRIAL TRANSCRIPTION TERMINATION FACTOR 1
RC_AI011922_AT	*NAP1L1*	NUCLEOSOME ASSEMBLY PROTEIN 1-LIKE 1
1393689_AT	*NDUFAF1_PREDICTED*	NADH DEHYDROGENASE (UBIQUINONE) 1 ALPHA SUBCOMPLEX, ASSEMBLY FACTOR 1
1387454_AT	*NIBAN*	NIBAN PROTEIN

1394851_AT	*NKX2-3_PREDICTED*	NK2 TRANSCRIPTION FACTOR RELATED, LOCUS 3 (DROSOPHILA) (PREDICTED)
RC_AA850885_S_AT	*NOL3*	NUCLEOLAR PROTEIN 3 (APOPTOSIS REPRESSOR WITH CARD DOMAIN)
1396173_AT	*NRIP3_PREDICTED*	NUCLEAR RECEPTOR INTERACTING PROTEIN 3 (PREDICTED)
1379560_AT	*NSD1_PREDICTED*	NUCLEAR RECEPTOR BINDING SET DOMAIN PROTEIN 1 (PREDICTED)
1370000_AT	*NUCB2*	NUCLEOBINDIN 2
1396909_AT	*PANK2_PREDICTED*	PANTOTHENATE KINASE 2 (HALLERVORDEN-SPATZ SYNDROME) (PREDICTED)
1385974_AT	*PARD6G_PREDICTED*	PAR-6 PARTITIONING DEFECTIVE 6 HOMOLOG GAMMA (C. ELEGANS) (PREDICTED)
1384824_AT	*PCDH18_PREDICTED*	PROTOCADHERIN 18 (PREDICTED)
RC_AI232135_AT	*PFKL*	PHOSPHOFRUCTOKINASE, LIVER, B-TYPE
1367841_A_AT	*PRLPC2*	PROLACTIN-LIKE PROTEIN C 2
1397686_AT	*PSMD9*	PROTEASOME (PROSOME, MACROPAIN) 26S SUBUNIT, NON-ATPASE, 9
1394486_AT	*RAB43*	RAS-RELATED PROTEIN RAB43
1377338_AT	*RAD1_PREDICTED*	RAD1 HOMOLOG (S. POMBE) (PREDICTED)
1378740_AT	*RASAL2_PREDICTED*	RAS PROTEIN ACTIVATOR LIKE 2 (PREDICTED)
1391776_AT	*RGD1305283_PREDICTED*	SIMILAR TO RIKEN CDNA 2010110K16 (PREDICTED)
1378948_AT	*RGD1306164_PREDICTED*	SIMILAR TO HYPOTHETICAL PROTEIN FLJ90798 (PREDICTED)
1377872_AT	*RGD1306936_PREDICTED*	SIMILAR TO CHROMOSOME 7 OPEN READING FRAME 30 (PREDICTED)
1394392_AT	*RGD1307696_PREDICTED*	SIMILAR TO DJ881L22.2 (NOVEL PROTEIN) (PREDICTED)
1379059_AT	*RGD1307875_PREDICTED*	SIMILAR TO FLJ23471 PROTEIN (PREDICTED)
1383118_AT	*RGD1309682*	SIMILAR TO HYPOTHETICAL PROTEIN FLJ14803
1374120_AT	*RGD1309971_PREDICTED*	SIMILAR TO KIAA1126 PROTEIN (PREDICTED)
1385801_AT	*RGD1310237*	SIMILAR TO RIKEN CDNA 2700075B01
1378587_AT	*RGD1310602_PREDICTED*	SIMILAR TO HYPOTHETICAL PROTEIN MGC15396 (PREDICTED)
1373230_AT	*RGD1311802*	SIMILAR TO CDNA SEQUENCE BC036718
1375080_AT	*RGD1311842_PREDICTED*	SIMILAR TO EXPRESSED SEQUENCE AW491445 (PREDICTED)
1389720_AT	*RGD1559577_PREDICTED*	SIMILAR TO RIKEN CDNA 1700020L24
1389037_AT	*RGD1559874_PREDICTED*	SIMILAR TO RIT
1376897_AT	*RGD1560022_PREDICTED*	SIMILAR TO HYPOTHETICAL PROTEIN 4832420M10
1382552_AT	*RGD1560155_PREDICTED*	SIMILAR TO MKIAA0934 PROTEIN
1393547_AT	*RGD1560399_PREDICTED*	SIMILAR TO HYPOTHETICAL PROTEIN C630023L15
RC_AI011922_AT	*RGD1560617_PREDICTED*	HYPOTHETICAL GENE SUPPORTED BY NM_053561; AF062594
1393653_AT	*RGD1560766_PREDICTED*	SIMILAR TO PUTATIVE PROTEIN PRODUCT OF HMFN2073
RC_AI171982_AT	*RGD1560916_PREDICTED*	SIMILAR TO FUN14 DOMAIN CONTAINING 2
1374643_AT	*RGD1560944_PREDICTED*	SIMILAR TO 6030410K14RIK PROTEIN
1384437_AT	*RGD1561046_PREDICTED*	SIMILAR TO SMARCA1 PROTEIN
1377718_AT	*RGD1561555_PREDICTED*	SIMILAR TO CDNA SEQUENCE BC022692
1387893_AT	*RGD1561715_PREDICTED*	SIMILAR TO COMPLEMENT COMPONENT 1, S SUBCOMPONENT
1375928_AT	*RGD1561853_PREDICTED*	SIMILAR TO SET DOMAIN-CONTAINING PROTEIN
1372236_AT	*RGD1562269_PREDICTED*	SIMILAR TO CASPASE RECRUITMENT DOMAIN PROTEIN 4
1373000_AT	*RGD1562444_PREDICTED*	SIMILAR TO SUSHI-REPEAT CONTAINING PROTEIN
1397372_AT	*RGD1562445_PREDICTED*	SIMILAR TO MOB4B PROTEIN
1382024_AT	*RGD1562684_PREDICTED*	SIMILAR TO MDJ4
1385912_AT	*RGD1562711_PREDICTED*	SIMILAR TO INTERFERON REGULATORY FACTOR 10
1384752_AT	*RGD1563033_PREDICTED*	SIMILAR TO OSTEOCLAST INHIBITORY LECTIN
AF036761_G_AT	*RGD1563648_PREDICTED*	SIMILAR TO STEAROYL-COA DESATURASE-4
1390652_AT	*RGD1563662_PREDICTED*	SIMILAR TO LOC283514 PROTEIN
1378587_AT	*RGD1563810_PREDICTED*	SIMILAR TO RIKEN CDNA 5530600A18
1383528_AT	*RGD1563945_PREDICTED*	SIMILAR TO MKIAA0215 PROTEIN
1391262_AT	*RGD1564247_PREDICTED*	SIMILAR TO SUMO/SENTRIN SPECIFIC PROTEASE 5
1373020_AT	*RGD1564452_PREDICTED*	MITOCHONDRIA-ASSOCIATED GRANULOCYTE MACROPHAGE
1392856_AT	*RGD1565105_PREDICTED*	SIMILAR TO SMALL EDRK-RICH FACTOR 1
1371847_AT	*RGD1565180_PREDICTED*	SIMILAR TO CARTILAGE-ASSOCIATED PROTEIN PRECURSOR
1382024_AT	*RGD1565241_PREDICTED*	SIMILAR TO DNAJ HOMOLOG SUBFAMILY B MEMBER 6
1378079_AT	*RGD1565361_PREDICTED*	SIMILAR TO MALE-ENHANCED ANTIGEN-2
RC_AI235753_AT	*RGD1565506_PREDICTED*	SIMILAR TO EXTRACELLULAR SIGNAL-RELATED KINASE 1C
1389504_AT	*RGD1566181_PREDICTED*	SIMILAR TO DELTEX3
1380682_AT	*RKHD3_PREDICTED*	RING FINGER AND KH DOMAIN CONTAINING 3 (PREDICTED)
1390524_AT	*RNF12*	RING FINGER PROTEIN 12
1395571_AT	*RNF3_PREDICTED*	RING FINGER PROTEIN 3 (PREDICTED)
AF036761_G_AT	*SCD1*	STEAROYL-COENZYME A DESATURASE 1
RC_AA963858_AT	*SCD1*	STEAROYL-COENZYME A DESATURASE 1
AF036761_G_AT	*SCD2*	STEAROYL-COENZYME A DESATURASE 2
1391262_AT	*SENP5_PREDICTED*	SUMO/SENTRIN SPECIFIC PROTEASE 5 (PREDICTED)
1397866_AT	*SERPINB6B*	SERINE (OR CYSTEINE) PROTEINASE INHIBITOR, CLADE B, MEMBER 6B
1369547_AT	*SERPINB7*	SERINE (OR CYSTEINE) PROTEINASE INHIBITOR, CLADE B, MEMBER 7
1398435_AT	*SLC22A15_PREDICTED*	SOLUTE CARRIER FAMILY 22 (ORGANIC CATION TRANSPORTER), MEMBER 15 ()
1379805_AT	*SLC41A2_PREDICTED*	SOLUTE CARRIER FAMILY 41, MEMBER 2 (PREDICTED)
1369160_A_AT	*SLC4A7*	SOLUTE CARRIER FAMILY 4, SODIUM BICARBONATE COTRANSPORTER, MEMBER 7
1387134_AT	*SLFN3*	SCHLAFEN 3
1386282_X_AT	*SNRK*	SNF RELATED KINASE
1395405_AT	*SNX26_PREDICTED*	SORTING NEXIN 26 (PREDICTED)
1368620_AT	*SPAG4*	SPERM ASSOCIATED ANTIGEN 4
1393706_AT	*STEAP_PREDICTED*	SIX TRANSMEMBRANE EPITHELIAL ANTIGEN OF THE PROSTATE (PREDICTED)
1375084_AT	*TDE2L*	TUMOR DIFFERENTIALLY EXPRESSED 2-LIKE
1381196_AT	*TM6SF2_PREDICTED*	TRANSMEMBRANE 6 SUPERFAMILY MEMBER 2 (PREDICTED)
1376450_AT	*TMEM5*	TRANSMEMBRANE PROTEIN 5
RC_AI010612_AT	*TNC*	TENASCIN C
1395635_AT	*TNFRSF26_PREDICTED*	TUMOR NECROSIS FACTOR RECEPTOR SUPERFAMILY, MEMBER 26 (PREDICTED)
1385227_AT	*TRPS1_PREDICTED*	TRICHORHINOPHALANGEAL SYNDROME I (PREDICTED)
1373274_AT	*TXNRD3_PREDICTED*	THIOREDOXIN REDUCTASE 3 (PREDICTED)
1388938_AT	*USP5_PREDICTED*	UBIQUITIN SPECIFIC PROTEASE 5 (ISOPEPTIDASE T) (PREDICTED)
1372837_AT	*WDFY2_PREDICTED*	WD REPEAT AND FYVE DOMAIN CONTAINING 2 (PREDICTED)
1385275_AT	*WNT16*	WINGLESS-RELATED MMTV INTEGRATION SITE 16
1389340_AT	*ZNF318_PREDICTED*	ZINC FINGER PROTEIN 318 (PREDICTED)

APPENDIX C

Significant biological themes associated with genes decreased in CX4 compared to GN6TF

Gene Ontology Term	*P*Value
cellular lipid metabolism	2.6E-06
lipid biosynthesis	8.7E-06
lipid synthesis	1.2E-05
cytoplasm	2.1E-05
nadp	2.6E-05
biosynthesis of steroids	3.2E-05
lipid metabolism	4.7E-05
Golgi-associated vesicle	9.0E-05
coenzyme metabolism	1.0E-04
extracellular matrix (sensu Metazoa)	1.1E-04
cholesterol biosynthesis	1.1E-04
organelle membrane	1.3E-04
cofactor metabolism	1.3E-04
extracellular matrix	1.4E-04
catalytic activity	1.6E-04
cholesterol metabolism	1.7E-04
isoprenoid biosynthesis	2.5E-04
sterol biosynthesis	2.5E-04
oxidoreductase activity, acting on the CH-OH group of donors, NAD or NADP as acceptor	2.6E-04
fatty acid metabolism	2.6E-04
Golgi apparatus	2.8E-04
oxidoreductase activity, acting on CH-OH group of donors	3.0E-04
integrin binding	3.1E-04
cell adhesion	3.1E-04
oxidoreductase activity	3.5E-04
organic acid metabolism	3.6E-04
Golgi membrane	3.7E-04
sterol metabolism	4.0E-04
cholesterol biosynthesis	4.5E-04
organ morphogenesis	4.7E-04
endoplasmic reticulum	5.7E-04
peroxisome	6.3E-04
collagen	7.0E-04
microbody	7.1E-04
peroxisome	7.1E-04
sterol biosynthesis	7.6E-04
carboxylic acid metabolism	7.9E-04
homophilic cell adhesion	7.9E-04
alcohol metabolism	8.0E-04
lipid metabolism	8.8E-04
endomembrane system	0.001
Golgi vesicle transport	0.001
steroid biosynthesis	0.001
isoprenoid metabolism	0.001
coated membrane	0.002
membrane coat	0.002
coenzyme A metabolism	0.002
vesicle-mediated transport	0.002
antioxidant activity	0.002
vesicle coat	0.002
intracellular transport	0.002
glutathione transferase activity	0.003
Fibrillar collagen, C-terminal	0.003
oxidoreductase	0.003
coated vesicle membrane	0.003
cellular localization	0.003
cellular carbohydrate metabolism	0.003
Golgi stack	0.003
oxidoreductase activity, acting on the CH-CH group of donors	0.004
establishment of cellular localization	0.004
calcium ion binding	0.004
transferase activity, transferring alkyl or aryl (other than methyl) groups	0.004
COPI vesicle coat	0.004
COPI coated vesicle membrane	0.004
extracellular matrix	0.004
RAB protein domain	0.004
calcium	0.004
COLFI protein domain	0.005
steroid biosynthesis	0.005
carbohydrate metabolism	0.005
coenzyme A biosynthesis	0.006
oxidoreductase activity, acting on the CH-CH group of donors, NAD or NADP as acceptor	0.006
antigen	0.006
membrane	0.006
thiolester hydrolase activity	0.007
blood vessel morphogenesis	0.007
intracellular protein transport	0.007
vacuole	0.007
peroxidase activity	0.007
oxidoreductase activity, acting on peroxide as acceptor	0.007
protein localization	0.008
Endoplasmic reticulum	0.008
organ development	0.008
cytoplasmic vesicle membrane	0.009

ER-Golgi intermediate compartment	0.010
steroid metabolism	0.011
skeletal development	0.011
prenylation	0.012
vesicle membrane	0.012
ADP-ribosylation factor	0.012
reproductive organismal physiological process	0.012
protein transport	0.013
vasculogenesis	0.014
dimer	0.014
reproductive physiological process	0.014
vasculature development	0.014
coated vesicle	0.014
Collagen helix repeat	0.015
ECM-RECEPTOR INTERACTION	0.015
NICOTINATE AND NICOTINAMIDE METABOLISM	0.015
glycosaminoglycan binding	0.015
GLUTATHIONE METABOLISM	0.016
ER to Golgi vesicle-mediated transport	0.016
cytosol	0.017
polysaccharide binding	0.017
coenzyme biosynthesis	0.017
fibrillar collagen	0.018
COPI-coated vesicle	0.018
microtubule	0.018
protein amino acid O-linked glycosylation	0.019
Peptidylprolyl isomerase, FKBP-type	0.019
fatty acid metabolism	0.019
transport vesicle	0.019
Ras small GTPase, Rab type	0.020
blood vessel development	0.021
lysosome	0.021
alternative promoter usage	0.021
heparin-binding	0.022
establishment of protein localization	0.022
coenzyme A	0.022
Nucleotide transport and metabolism	0.022
collagen	0.022
cell-cell adhesion	0.023
lytic vacuole	0.023
peroxidase	0.023
Rotamase	0.024
pattern binding	0.024
transit peptide	0.024
Ras GTPase	0.025
endoplasmic reticulum	0.027
electron transporter activity	0.027
female sex differentiation	0.028
female gonad development	0.028
development of primary female sexual characteristics	0.028
acetyl-CoA metabolism	0.029
signal sequence binding	0.029
heparin binding	0.029
IB protein domain	0.029
BRLZ protein domain	0.029
transcription cofactor activity	0.030
Small GTP-binding protein domain	0.030
vesicle	0.030
homotetramer	0.030
hydroxylation	0.030
Collagen triple helix repeat	0.031
golgi stack	0.031
cytoplasmic vesicle	0.031
localization	0.032
HUNTINGTON'S DISEASE	0.033
carbohydrate binding	0.034
collagen type V	0.034
membrane-bound vesicle	0.035
transcription corepressor activity	0.035
glutathione transferase	0.035
secretory pathway	0.037
GTP-binding nuclear protein Ran	0.037
protein transporter activity	0.037
isoprene biosynthesis	0.037
cytoplasmic membrane-bound vesicle	0.039
Basic-leucine zipper (bZIP) transcription factor	0.039
menstrual cycle	0.040
coated pit	0.041
establishment of localization	0.042
ABC transporter, transmembrane region	0.043
cell-substrate adhesion	0.043
cell-matrix adhesion	0.043
ubiquitin thiolesterase activity	0.044
nucleotide phosphate-binding region:NADP	0.047
angiogenesis	0.049
embryonic pattern specification	0.050

APPENDIX D

Significant biological themes associated with genes elevated in CX4 compared to GN6TF

Gene Ontology Term	*P*Value
nucleus	2.5E-08
intracellular	1.4E-07
nuclear protein	2.7E-07
cell	1.1E-06
cell junction	1.2E-06
cell organization and biogenesis	2.2E-06
intercellular jnction	2.5E-06
rna-binding	3.8E-06
intracellular signaling cascade	6.6E-06
cellular localization	7.3E-06
establishment of cellular localization	7.8E-06
intracellular transport	8.9E-06
cytoskeleton	1.1E-05
protein binding	2.0E-05
phosphorylation	2.8E-05
RNA-binding region RNP-1 (RNA recognition motif)	7.5E-05
apical part of cell	9.3E-05
organelle	1.0E-04
intracellular organelle	1.1E-04
cytoskeletal protein binding	1.2E-04
adherens junction	1.2E-04
protein amino acid dephosphorylation	1.4E-04
non-membrane-bound organelle	1.5E-04
intracellular non-membrane-bound organelle	1.5E-04
Nucleotide-binding, alpha-beta plait	1.5E-04
actin binding	1.5E-04
RRM domain	1.8E-04
dephosphorylation	2.1E-04
cell-cell adherens junction	2.4E-04
regulation of cellular physiological process	2.4E-04
regulation of biological process	2.4E-04
adherens junction	2.6E-04
transforming protein	2.7E-04
positive regulation of apoptosis	3.8E-04
tight junction	4.4E-04
positive regulation of programmed cell death	4.9E-04
focal adhesion	5.1E-04
regulation of physiological process	5.2E-04
programmed cell death	5.2E-04
cell death	6.0E-04
regulation of cellular process	6.3E-04
zinc-finger	6.4E-04
apicolateral plasma membrane	6.4E-04
apical junction complex	6.4E-04
proto-oncogene	6.8E-04
biopolymer metabolism	6.9E-04
mRNA processing	7.0E-04
establishment of protein localization	7.1E-04
apoptosis	7.4E-04
nucleic acid binding	7.5E-04
DNA binding	7.7E-04
GTP binding	8.0E-04
guanyl nucleotide binding	8.5E-04
death	9.7E-04
Tyrosine specific protein phosphatase	0.001
chromosome	0.001
protein transport	0.001
phosphoprotein phosphatase activity	0.001
actin filament binding	0.001
regulation of programmed cell death	0.001
small GTPase mediated signal transduction	0.001
induction of programmed cell death	0.002
induction of apoptosis	0.002
mRNA metabolism	0.002
RNA transport	0.002
establishment of RNA localization	0.002
nucleic acid transport	0.002
basolateral plasma membrane	0.002
FERM	0.002
protein localization	0.002
prenylation	0.002
sh3 domain	0.002
zinc	0.002
regulation of apoptosis	0.002
zinc finger region:C2H2-type 2	0.002
cytoskeleton organization and biogenesis	0.002
nucleocytoplasmic transport	0.003
regulation of actin cytoskeleton	0.003
cytoskeleton	0.003
RNA localization	0.003
protein transport	0.003
zinc finger region:C2H2-type 1	0.003
RNA splicing	0.003
basement membrane	0.004

protein tyrosine phosphatase activity	0.004
glycosphingolipid metabolism	0.004
transition metal ion homeostasis	0.004
GTPase activity	0.004
tyrosine-specific phosphatase	0.005
antigen presentation, endogenous antigen	0.005
microtubule-based process	0.005
enzyme binding	0.005
cytoskeleton-dependent intracellular transport	0.005
Rho protein signal transduction	0.005
membrane-bound organelle	0.005
intracellular membrane-bound organelle	0.005
dna-binding	0.006
nucleobase, nucleoside, nucleotide and nucleic acid transport	0.006
RNA processing	0.006
protein kinase cascade	0.006
Heat shock protein DnaJ	0.006
cell cycle	0.007
mRNA transport	0.007
phosphoric monoester hydrolase activity	0.007
Tyrosine specific protein phosphatase and dual specificity protein phosphatase	0.007
protein ubiquitination	0.007
EGF_Lam	0.007
organelle organization and biogenesis	0.007
glucuronosyltransferase	0.007
nucleotide binding	0.007
nucleotide phosphate-binding region:GTP	0.007
PTPc	0.007
protein metabolism	0.008
microtubule-based movement	0.008
IPR001452:Src homology-3	0.008
negative regulation of biological process	0.008
zinc finger region:C2H2-type 3	0.008
biopolymer modification	0.008
DNA replication	0.008
protein phosphatase	0.009
gtp-binding	0.009
nuclear transport	0.009
RNA splicing, via transesterification reactions with bulged adenosine as nucleophile	0.009
RNA splicing, via transesterification reactions	0.009
nuclear mRNA splicing, via spliceosome	0.009
PTPc_motif	0.009
prenylated cysteine	0.009
cross-link:Glycyl lysine isopeptide (Lys-Gly) (interchain with G-Cter in ubiquitin)	0.009
regulation of metabolism	0.009
Heat shock protein DnaJ, N-terminal	0.009
manganese ion binding	0.010
iron ion homeostasis	0.010
cell communication	0.010
Band 4.1	0.010
GTP binding	0.010
mhc i	0.010
epidermis development	0.011
cellular morphogenesis	0.012
calcium-dependent phospholipid binding	0.012
cellular process	0.012
regulation of progression through cell cycle	0.012
protein modification	0.013
transcription regulation	0.013
regulation of cell cycle	0.013
Protein tyrosine phosphatase, catalytic region	0.013
regulation of DNA replication	0.014
regulation of protein metabolism	0.014
coated pit	0.014
transcription	0.014
IPR001464:Annexin	0.014
IPR006212:Furin-like repeat	0.014
intracellular protein transport	0.014
IPR002213:UDP-glucuronosyl/UDP-glucosyltransferase	0.014
MHC class I receptor activity	0.015
RNA helicase activity	0.015
RNO04512:ECM-RECEPTOR INTERACTION	0.015
phosphoric monoester hydrolase	0.015
nucleobase, nucleoside, nucleotide and nucleic acid metabolism	0.015
pyrophosphatase activity	0.015
signal transduction	0.015
negative regulation of cellular physiological process	0.016
RNA metabolism	0.016
domain:J	0.016
metal ion-binding site:Manganese 2	0.016
metal ion-binding site:Manganese 1	0.016
SF002359:annexin I	0.016
SF001710:Rab protein	0.016
IPR003577:Ras small GTPase, Ras type	0.017
regulation of cellular metabolism	0.017
IPR002041:GTP-binding nuclear protein Ran	0.017
hydrolase activity, acting on acid anhydrides, in phosphorus-containing anhydrides	0.017
IPR003579:Ras small GTPase, Rab type	0.017
cellular physiological process	0.017
ubiquitin-protein ligase activity	0.018

manganese	0.018
morphogenesis	0.018
hydrolase activity, acting on acid anhydrides	0.018
annexin	0.018
negative regulation of cellular process	0.019
tight junction	0.019
apical plasma membrane	0.019
ectoderm development	0.019
DNA replication, recombination, and repair	0.020
negative regulation of physiological process	0.020
kinase binding	0.021
RNO04320:DORSO-VENTRAL AXIS FORMATION	0.022
SM00261:FU	0.022
IPR003578:Ras small GTPase, Rho type	0.022
Rac GTPase activator activity	0.023
structural constituent of cytoskeleton	0.023
antigen processing, endogenous antigen via MHC class I	0.024
protein phosphatase type 2A activity	0.024
regulation of mRNA processing	0.024
response to DNA damage stimulus	0.024
IPR003118:Sterile alpha motif/pointed	0.024
transcription	0.024
IPR004088:KH, type 1	0.024
IPR004087:KH	0.024
RNO04662:B CELL RECEPTOR SIGNALING PATHWAY	0.025
ligase activity, forming carbon-nitrogen bonds	0.025
IPR001806:Ras GTPase	0.025
primary metabolism	0.025
RNO00220:UREA CYCLE AND METABOLISM OF AMINO GROUPS	0.026
regulation of axonogenesis	0.026
methylation	0.026
cellular protein metabolism	0.027
cell cycle	0.028
magnesium-dependent protein serine/threonine phosphatase activity	0.028
nucleotide binding	0.028
SM00251:SAM_PNT	0.028
phosphoric ester hydrolase activity	0.029
nuclear chromosome	0.029
positive regulation of axonogenesis	0.029
cellular macromolecule metabolism	0.030
phosphoprotein	0.030
RNA export from nucleus	0.030
protein kinase CK2 activity	0.031
metal-binding	0.031
endocytic vesicle	0.032
basal lamina	0.032
regulation of transcription	0.032
SH3 domain binding	0.033
protein polymerization	0.033
SM00335:ANX	0.033
regulation of nucleobase, nucleoside, nucleotide and nucleic acid metabolism	0.034
RNO04010:MAPK SIGNALING PATHWAY	0.034
domain:SH3	0.035
DNA-dependent DNA replication	0.035
enzyme regulator activity	0.035
negative regulation of metabolism	0.035
protein targeting	0.035
transferase activity, transferring hexosyl groups	0.036
P-loop	0.036
protein serine/threonine kinase activity	0.037
lamellipodium	0.038
repeat:Annexin 4	0.039
repeat:Annexin 3	0.039
repeat:Annexin 2	0.039
repeat:Annexin 1	0.039
site:Stutter	0.039
induction of apoptosis by intracellular signals	0.040
nuclear export	0.040
desmosome	0.040
regulation of transcription, DNA-dependent	0.040
T CELL RECEPTOR SIGNALING PATHWAY	0.041
RNA recognition, region 1	0.041
urea cycle	0.042
macromolecule metabolism	0.043
Chaperone DnaJ, C-terminal	0.044
jun transforming protein	0.044
CTD phosphatase activity	0.044
myosin phosphatase activity	0.044
cell adhesion	0.044
Ets	0.045
protein domain specific binding	0.045
enzyme linked receptor protein signaling pathway	0.046
translation initiation factor activity	0.047
kinase activity	0.047
Neutrophil cytosol factor 2	0.047
negative regulation of progression through cell cycle	0.047
CIRCADIAN RHYTHM	0.049
transcription from RNA polymerase II promoter	0.049